5-2017

Synthesis of 20S-Hydroxyvitamin D3 Analogs and Their 1α-Hydroxyl Derivatives as Potent Anti-inflammatory Agents

Zongtao Lin
University of Tennessee Health Science Center

Synthesis of 20S-Hydroxyvitamin D3 Analogs and Their 1α-Hydroxyl Derivatives as Potent Anti-inflammatory Agents

ORCID
http://orcid.org/0000-0002-6017-338X

DOI
10.21007/etd.cghs.2017.0433

Synthesis of 20S-Hydroxyvitamin D3 Analogs and Their 1α-Hydroxyl Derivatives as Potent Anti-inflammatory Agents

A Dissertation
Presented for
The Graduate Studies Council
The University of Tennessee
Health Science Center

In Partial Fulfillment
Of the Requirements for the Degree
Doctor of Philosophy
From The University of Tennessee

By
Zongtao Lin
May 2017

DEDICATION

This work is dedicated to my parents, Rongjun Lin and Defang Zhu,
and my fiancée, Xian Han.

Thank you for all of your love and support along the way.

ACKNOWLEDGEMENTS

First of all, I would like to express my thankfulness to my advisor, Dr. Wei Li, who has been extremely supportive to not only my research as a teacher but also my career as a friend. His patient guidance and high-standard commitment to research have deeply inspired me during the past five years, when I can always think, choose and conduct experiments freely for my projects. Besides, his hard-working attitude and pure pursuit of research have enlightened me how to become a good scientist in the future.

I really appreciate the guidance and support of my committee members, Dr. Andrzej T. Slominski (University of Alabama at Birmingham, UAB), Dr. Tomoko Fujiwara (University of Memphis), Dr. Sarka Beranova-Giorgianni and Dr. Duane D. Miller. I would like to additionally thank the people in Dr. Miller's group for their discussion and comments on my projects in our routine joint group meetings.

I am grateful to all the present members of the Li lab, Dr. Dejian Ma, Dr. Jim Zhongzhi Wu, Dr. Yi Xue, Dr. Hao Chen, Mr. Qinghui Wang, Ms. Kinsie Arnst and Ms. Shanshan Deng, and past lab members, Dr. Srinivasa R. Marepally, Dr. Jianjun Chen, Dr. Min Xiao, Dr. Jin Wang, Dr. Dajun Chen, Ms. Georgina Masoud, Mr. Xiaoxin Wu and Ms. Rachel A. Ness. It has been such a pleasant time to work with a group of experienced and talented scientists. I have to thank Dr. Srinivasa R. Marepally for his detailed teaching on synthetic procedures, without him I don't think it is possible for me to work out all the compounds reported in this dissertation. I am appreciative to our collaborators, Dr. Robert Tuckey (University of Western Australia), Dr. Natacha Rochel (IGBMC, France), Dr. Junming Yue, Dr. Arnold E. Postlethwaite, Dr. Liang Hong, Dr. Tae-Kang Kim (UAB) and Dr. Zorica Janjetovic (UAB) for their proof-of-concept contributions to my projects. I would like to thank people in Dr. Slominski's group for their kind assistance during the development of biological assays, Dr. Hong Wang's group (Peking University) and Dr. Shizhong Chen's group (Peking University) for their continuous support for my research and career development.

I acknowledge the Alma and Hal Reagan Fellowship from UTHSC for generous financial support during the academic year 2016-2017. I also thank the scholarship received from China Scholarship Council for financial support. Thanks to the University of Tennessee Health Science Center for offering me such an opportunity and excellent academic environment for carrying out research. I am deeply indebted to everyone who helped and participated my research, as well as to unnamed family/friends and anonymous donors who financially supported me personally during my tough days.

Finally, my heartful thankfulness goes to my parents, Rongjun Lin and Defang Zhu, and my fiancée Ms. Xian Han currently studying in UTHSC. Without their love and support, I could never have completed my study.

ABSTRACT

Rheumatoid arthritis (RA) is one of the autoimmune diseases, and is affecting 2.5 million Americans in total. Among the treatment options of RA, 1α,25-dihydroxyvitamin D3 [1,25(OH)2D3] is the only steroidal drug used clinically for anti-inflammatory and immune diseases. However, long-term use of 1,25(OH)2D3 (625 μg/day) in human would result in hypercalcemia (toxicity), and 1,25(OH)2D3 has substantial hypercalcemic effects (toxicity) in mice at a dose as low as only 2 μg/kg. Fortunately, during the investigation of novel metabolic pathway of vitamin D3 by cytochrome P450 enzymes, we found 20S-hydroxyvitamin D3 [20*S*(OH)D3] as a good lead compound. 20*S*(OH)D3 suppressed disease symptoms at 2 μg/kg in collagen-induced arthritis model, and high doses of 20*S*(OH)D3 (up to 30 μg/kg) do not cause hypercalcemia in rats or mice. Thus 20*S*(OH)D3 has the potential to be structurally optimized for providing anti-inflammatory agents without toxicity. In this study, four series of 20*S*(OH)D3 analogs have been synthesized and studied, they are C20 Gemini analogs, C24-hydroxlated analogs, C23-hydroxlated analogs and C24 modified analogs together with their 1α-hydroxylated derivatives.

Since D3 analogs with two symmetric side chains (Gemini analogs) result in potent activation of the vitamin D receptor (VDR), we hypothesized that the chain length and composition of these types of analogs also containing a 20-hydroxyl group would affect their biological activities. In this study, we designed and synthesized a series of Gemini 20S(OH)D3 analogs. Biological tests showed that some of these analogs are partial VDR activators and can significantly stimulate the expression of mRNA for *VDR* and VDR-regulated genes including *CYP24A1* and transient receptor potential cation channel V6 (*TRPV6*). These analogs inhibited the proliferation of melanoma cells with potency comparable to that of 1α,25-dihydroxyvitamin D3. Moreover, these analogs reduced the level of interferon γ and up-regulated the expression of leukocyte associated immunoglobulin-like receptor 1 in splenocytes, indicating that they have potent anti-inflammatory activities. There are no clear correlations between the Gemini chain length and their VDR activation or biological activities, consistent with the high flexibility of the ligand-binding pocket of the VDR.

Bioactive vitamin D3 metabolites 20*S*,24*S*-dihydroxyvitamin D3 [20*S*,24*S*(OH)2D3] and 20*S*,24*R*-dihydroxyvitamin D3 [20*S*,24R(OH)2D3] were chemically synthesized and confirmed to be identical to their enzymatically generated counterparts. The absolute configurations at C24 and its influence on the kinetics of 1α-hydroxylation by CYP27B1 were determined. Their corresponding 1α-hydroxyl derivatives were subsequently produced. Biological comparisons of these products showed different properties with respect to vitamin D3 receptor activation, anti-inflammatory activity, and anti-proliferative activity, with 1α,20S,24R(OH)2D3 being the most potent compound.

The vitamin D3 metabolite, 20*S*,23*S*-dihydroxyvitamin D3, was chemically synthesized for the first time, and identified to be the same as the enzymatically produced

metabolite. The C23 absolute configurations of both 20*S*,23*S/R*-dihydroxyvitamin D3 epimers were unambiguously assigned by NMR and Mosher ester analysis. Their kinetics of CYP27B1 metabolism were investigated during the production of their 1α-hydroxylated derivatives. Bioactivities of these products were compared in terms of vitamin D3 receptor activation, anti-inflammatory and anti-proliferative activities.

Four C24 modified analogs of 20S(OH)D3 were chemically synthesized and comprehensively tested against different activities together with their 1α-hydroxyl derivatives. Metabolism of 20S(OH)D3 analogs against cytochrome P450 27B1 (CYP27B1, activation enzyme) and CYP24A1 (catabolism enzyme) suggested that they are better substrates of both enzymes than 20S(OH)D3, and can be activated (1α-hydroxylated) by CYP27B1 except 23-amide which is not a substrate but an inhibitor of CYP27B1. Their 1α-OH derivatives were potent vitamin D receptor (VDR) agonists comparable with 1,25(OH)2D3 although they themselves showed weak or none VDR stimulation activity in three cell lines. To understand the molecular interactions between these analog and VDR, two analogs together with 20S(OH)D3 and 1,25(OH)2D3 were co-crystalized with human VDR. These analogs and 1α-OH derivatives significantly upregulated the mRNA expression of VDR target genes, suggesting their actions via VDR, at least partially. In addition, their anti-inflammatory activities have been investigated in aspect of IFNγ inhibition in splenocytes. This study demonstrates the mechanisms of action of 20S(OH)D3 anlogs, is of great importance for future drug development of anti-inflammatory agents.

From the above-mentioned studies, we learned that the introduction of 1α-hydroxy could potentiate the anti-inflammatory activities of 20S(OH)D3 and its anlogs. Thus it would be beneficial to further investigate the 1α,20*S*-Dihydroxyvitamin D3 [1,20*S*(OH)2D3] analogs. 1,20*S*(OH)2D3 was chemically synthesized for the first time. A semi-reduced intermediate of the Birch reduction for 1α-OH formation was obtained for the first time, and thus was used to propose the reaction mechanism. X-ray crystallography analysis of the key intermediate confirmed the formation of 1α-OH. 1,20*S*(OH)2D3 binds efficiently in vitamin D receptor (VDR), being similar with its native ligand 1α,25-dihydroxyvitamin D3 [1,25(OH)2D3]. However, their co-crystal structures revealed differential molecular interactions of 20*S*-OH and 25-OH in VDR, which may help understand their biological activities. In addition, 1,20*S*(OH)2D3 functions as a VDR agonist with stronger/comparable activities than/with 1,25(OH)2D3 in aspects of VDR stimulation and regulating VDR downstream genes, and inhibition of inflammatory markers. This study offers a convenient synthetic route using a novel intermediate 1α,3β-diacetoxypregn-5-en-20-one, and provides molecular basis of design for drug development of 1,20*S*(OH)2D3 and its analogs.

Overall, we have synthesized and biologically evaluated four series of 20S(OH)D3 analogs for their potential applications in anti-inflammatory diseases such as RA. The synthetic scheme of 1,20*S*(OH)2D3 could pioneer future development of its analogs. These findings will provide important guidance for the development of next generation anti-RA agents using 20*S*(OH)2D3 scaffold.

TABLE OF CONTENTS

LIST OF TABLES

LIST OF FIGURES

LIST OF ABBREVIATIONS

1,24,25(OH)3D3	1α,24,25-Trihydroxyvitamin D3
1,20S(OH)2D3	1α,20S-Dihydroxyvitamin D3
1,25(OH)2D3	1α,25-Dihydroxyvitamin D3
20,24(OH)2D3	20S,24-Dihydroxyvitamin D3
20S(OH)D3	20S-Hydroxyvitamin D3
20S,23(OH)2D3	20S,23-Dihydroxyvitamin D3
20S,24R(OH)2D3	20S,24R-Dihydroxyvitamin D3
20S,24S(OH)2D3	20S,24S-Dihydroxyvitamin D3
22-Oxa	22-Oxa-1α-25-dihydroxyvitamin D3
24,25(OH)2D3	24,25-Dihydroxyvitamin D3
25(OH)D3	25-Hydroxyvitamin D3
7DHC	7-Dehydrocholesterol
9-BBN	9-Borabicyclo[3.3.1]nonane
9cRA	9-cis-Retinoic Acid
AIBN	Azobisisobutyronitrile
APC	Antigen-presenting Cell
CBP	CREB Binding Protein
CD	Crohn's Disease
COSY	1H-1H Correlation Spectroscopy
COX	Cyclooxygenase
CSA	Camphorsulfonic Acid
CyA	Cyclosporine A
CYP	Cytochrome P450
CYP	Cytochrome P450
CYP11A1	Cytochrome P450scc
CYP27B1	Cytochrome P450 27B1
D3	Vitamin D3
DAST	Diethylaminosulfur Trifluoride
DC	Dendritic Cells
Dibromantin	1,3-Dibromo-5,5-dimethylhydantoin
DIPEA	Diisopropylethylamine
DMAP	4-Dimethylaminopyridine
DMEM	Dulbecco's modified Eagle's medium
DMF	Dimethylformamide
EMEM	Eagle's Minimal Essential Medium
EOMCl	Chloromethyl Ethyl Ether
ESI	Electrospray Ionization
HMBC	1H-13C Heteronuclear Multiple Bond Correlation Spectroscopy
HPLC	High Performance Liquid Chromatography
HRMS	High-resolution Mass Spectrometry
HSQC	1H-13C Heteronuclear Single Quantum Correlation Spectroscopy
IBD	Inflammatory Bowel Disease
IFNγ	Interferon γ

INF-γ	Interferon-γ
LAIR1	Leukocyte-associated Immunoglobulin-like Receptor 1
LPS	Lipopolysaccharide
MeCN	Acetonitrile
MHC2	Class II Major Histocompatibility Complex
MTD	Maximum Tolerated Dose
NCo-A-62	Nuclear Receptor Coactivator-62
NFκB	Nuclear Factor Kappa Light-chain-enhancer of Activated B Cells
NK	Natural Killer
NMR	Nuclear Magnetic Resonance
NSAID	Nonsteroidal Anti-inflammatory Drug
OCT	22-Oxacalcitriol
PBAF	Polybromo-associated BAF
PBMC	Peripheral Blood Mononuclear Cell
PCR	Polymerase Chain Reaction
PDC	Pyridinium Dichromate
PG	Prostaglandin
PTH	Parathyroid Hormone
PyBOP	Benzotriazol-1-yl-oxytripyrrolidinophosphonium Hexafluorophosphate
RA	Rheumatoid Arthritis
RXR	9-cis-Retinoic acid (9cRA) Receptor
SKIP	Ski-interaction Protein
SLE	Systemic Lupus Erythematosus
SRC	Steroid Receptor Coactivator
T1D	Type 1 Diabetes
TBAB	Tetra-n-butylammonium Bromide
TBAF	Tetra-n-butylammonium Fluoride
TBSCl	Tert-butyldimethylsilyl Chloride
TGF-β	Transforming Growth Factor-β
Th1	T Helper 1
TLC	Thin Layer Chromatography
TLR	Toll-like Receptor
TNBS	2,4,6-Trinitrobenzene Sulfonic Acid
TNF-α	Tumor Necrosis Factor-α
TOCSY	1H-1H Total Correlation Spectroscopy
TOCSY	1H-1H Total Correlation Spectroscopy
Treg	T Regulatory Cell
TRIP1	Thyroid Hormone Receptor Interacting Protein 1
TRPV6	Transient Receptor Potential Cation Channel V6
UC	Ulcerative Colitis
UVB	Ultraviolet B
VD3	Vitamin D3
VDR	Vitamin D Receptor
VDRE	Vitamin D Response Element

CHAPTER 1. THE ROLES OF VITAMIN D AND ITS ANALOGS IN INFLAMMATORY DISEASES*

Introduction

The discovery of nonclassical actions, other than mineral homeostasis, of 1α,25-dihydroxyvitamin D3 [1,25(OH)2D3] has expanded its applications. Among these, its anti-inflammation activity has drawn more and more attention of researchers to investigate its role in regulating the progression of inflammatory diseases. The expression of many inflammation-related genes is regulated by 1,25(OH)2D3 through vitamin D receptor (VDR) in a large variety of cells including immune cells such as, but not limited to, macrophages, dendritic cells, T helper cells, and B cells. Studies of 1,25(OH)2D3 in these immune cells have shown both direct and indirect immunomodulatory activities affecting innate and adaptive immune responses. Moreover, 1,25(OH)2D3 can also exert its anti-inflammation effects through regulating the biosynthesis of pro-inflammatory molecules in the prostaglandin pathway or through nuclear factor kappa light-chain-enhancer of activated B cells (NFκB) by affecting cytokine production and inflammatory responses. These actions of 1,25(OH)2D3 may explain the associations between vitamin D levels and inflammatory diseases such as rheumatoid arthritis, inflammatory bowel disease, multiple sclerosis, asthma, type 1 diabetes, and systemic lupus erythematosus. Although several analogs of 1,25(OH)2D3 have shown potent immunomodulatory or anti-inflammatory activity on immune cell cultures or in animal models, no vitamin D analog has been used in clinical research to treat inflammatory diseases. Here, we review the relationship between vitamin D analogs and inflammation based on observations of immune cells, prostaglandin and NFκB pathways, as well as common inflammatory diseases.

Production and Metabolism Pathway of Active Vitamin D3

As a hormone precursor, vitamin D can be either produced endogenously in humans or ingested from food and supplements. Vitamin D has two major functional forms: vitamin D2 and vitamin D3. Vitamin D2 (or ergocalciferol) is a fungal-derived form of vitamin D that can be absorbed from dietary sources [1] such as mushrooms or plants. In contrast, vitamin D3 (cholecalciferol) comes mainly from the photoconversion reaction with assistance of ultraviolet (UV) light [2]; however, it can also be obtained directly from animal sources (e.g., meat and milk). In the skin epidermis, 7-DHC is firstly irradiated by UV light from the sun to begin a ring-opening reaction and forms previtamin D3, which is then automatically isomerized to vitamin D3 (**Figure 1-1**). This precursor is further diffused into body fluids and binds to vitamin D binding protein (DBP) as part of the circulation system. After being transported to the liver [3], vitamin D3 undergoes its first hydroxylation reaction by cytochrome P450 (CYP), CYP2R1 [3, 4], or

---

*Adapted with permission. Lin Z, Li W. The roles of vitamin D and its analogs in inflammatory diseases. *Curr. Top. Med. Chem.* 2016(11), 16, 1242-1261.

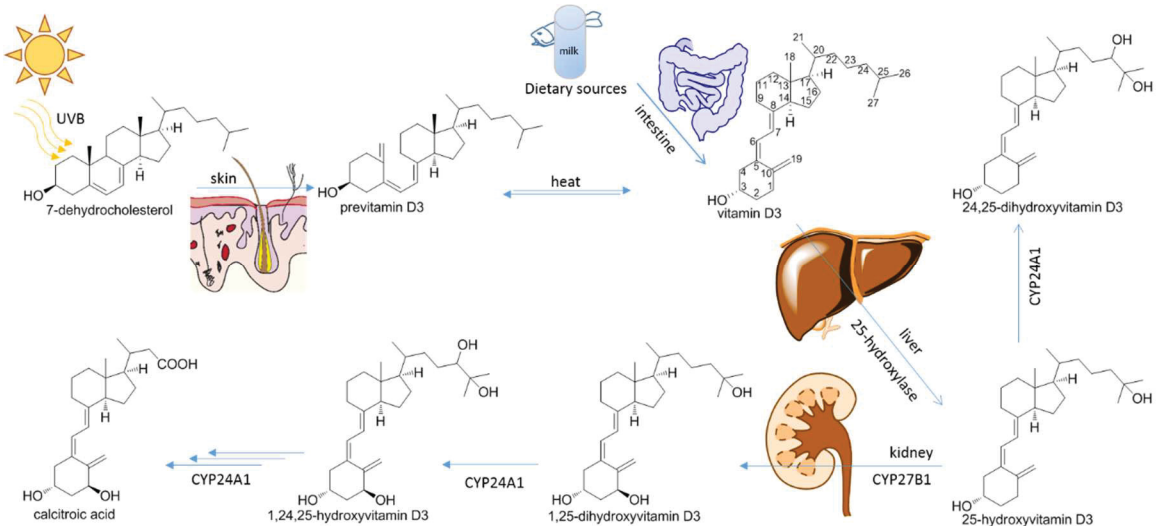

Figure 1-1. Metabolism of vitamin D3.
Vitamin D can be obtained endogenously from photochemical conversion of 7DHC, or from dietary sources such as meat, fish, and milk. The formed Vitamin D is diffused into the circulatory system and carried by vitamin D-binding protein (DBP), then transported to the liver where it is hydroxylated into 25(OH)D3 by 25-hydroxylase. 25(OH)D3, as the circulating form of vitamin D3, is further hydroxylated into the active secosteroid, 1,25(OH)2D3, by 1α-hydroxylase in the kidney or other targeted cells and tissues. This active form can induce its inactivation enzyme, 24-hydroxylase, to produce 1,24, 25(OH)3D3, which can then be successively oxidized into calcitroic acid for excretion.

CYP27A1 [5] as 25-hydroxylase at the C-25 position to form the circulation form of vitamin D3: 25-hydroxyvitamin D3 or calcidiol [25(OH)D3]. The final activation step of vitamin D is carried out by the proximal convoluted tubule cells in the kidney [6], where 25(OH)D3 is further hydroxylated by mitochondrial 1α-hydroxylase (CYP27B1) at the C-1 position to give 1α,25-dihydroxyvitamin D3 or calcitriol, the hormonal form of vitamin D. 1,25(OH)2D3 can induce expression of CYP24A1, which acts as 24-hydroxylase to inactivate 1,25(OH)2D3 to produce 1α,24,25-trihydroxyvitamin D3 [1,24,25(OH)3D3] [7], which further undergoes a series of oxidations and hydroxylations to produce calcitroic acid, resulting from cleavage of side chains between C-23 and C-24 for excretion [8, 9]. It is well known that liver cytochrome P450 is the enzyme family for 25-hydroxylation for vitamin D; however, it is still uncertain what enzyme combinations are responsible for this step. Recently, evidence [3] has shown that CYP2R1$^{-/-}$ mice had more than a 50% reduction in 25(OH)D3, suggesting that CYP2R1 is the major, but not exclusive, enzyme for 25-hydroxylation of vitamin D. Other than CYP2R1, five other P450 enzymes (CYP27A1, CYP2J2/3, CYP3A4, CYP2D25 and CYP2C11) can also catalyze 25-hydroxylation step [3, 10]. The renal expression level of CYP27B1 is regulated by several factors. Parathyroid hormone (PTH), hypocalcemia, and a hypophosphatemia are major stimuli for CYP27B1 expression, which generates more 1,25(OH)2D3 to satisfy the need for mineral ion homeostasis [11]. In turn, excess production of 1,25(OH)2D3 can negatively inhibit the expression of CYP27B1 to limit the production of 1,25(OH)2D3 [12] and positively promote the expression and bone release of fibroblast-growth factor 23 [13] (FGF23) to suppress the CYP27B1 gene in response to elevated 1,25(OH)2D3 [14]. In addition, 25(OH)D3 can be converted to 24,25-dihydroxyvitamin D3 [24,25(OH)2D3] under hypercalcemia, low PTH level, or high FGF23 expression level [15]. Although having less activity on calcemic effects, 24,25(OH)2D3 was still proven to play a role in regulation of intestinal calcium absorption [16, 17].

1,25(OH)2D3 Exerts Its Effects Through Downstream Genes of Vitamin D Receptor

The active hormone 1,25(OH)2D3 stays inactive until it binds specifically to the VDR, which is a member of the nuclear receptor superfamily of transcription factors [18]. In humans, cells express a basal level of VDR as either membrane VDR (memVDR) or cytosolic VDR (cVDR). After binding with either form of VDR, 1,25(OH)2D3 is then translocated into the nucleus, where 9-*cis*-retinoic acid (9cRA) receptor (RXR) binds tightly to the liganded VDR to form a VDR-RXR heterodimer [19]. Before binding to vitamin D response element (VDRE) adjacent to the target genes, this heterodimer requires many other co-activators for the transcriptional activation step. VDR-RXR firstly undergoes hormone-dependent phosphorylation [20], and further binds to steroid receptor coactivators (SRC), nuclear receptor coactivator-62 (NCoA-62), Ski-interaction protein (SKIP), histone acetyltransferase (HAT), CREB binding protein (CBP)/p300 and polybromo-associated BAF (PBAF) to remodel chromatin, acetylate histone and attract the heterodimer closer to the controlled genes. Then autoacetylation occurs to SRC resulting in the dissociation of SRC-CBP/p300-PBAF moiety from the VDRE-bound VDR-RXR- NCoA-62-SKIP-SRC-CBP/p300-PBAF complex. This dissociation facilitates the binding of vitamin D receptor-interacting protein 205 (DRIP205) to the

activation function 2 (AF2) on VDR and successively attracts a series of DRIPs for the bridge formation between VDRE-VDR-RXR-NCoA-62-SKIP-DRIP205 complex and transcriptional factor IIB (TFIIB) attached with RNA polymerase II (RNA Pol II) transcription machine to initiate the gene transcription including CYP24A1 [9, 21]. Once the RNA Pol II is moving forward from the 5'- to the 3'-end of the DNA, dissociation from the VDR-RXR coregulator complex occurs to the NCoA-62/SKIP and DRIP205, the latter of which is replaced by thyroid hormone receptor interacting protein 1 (TRIP1) to facilitate ubiquitination (U) of VDR for preparation of degradation. This complex (VDRE-VDR-RXR-TRIP1-U) can get transformed to the VDRE-bound VDR-RXR-NCoA-62-SKIP-SRC-CBP/p300-PBAF complex for rapid transcription initiation through dissociation of TRIP1-U and re-association of corresponding coactivators such as NCoA-62, SRC, and CBP/p300. Meanwhile, the VDRE-VDR-RXR-TRIP1-U complex can also get decomposed by losing its ligand, 1,25(OH)2D3, through the catabolic enzyme CYP24A1 generated from the above-mentioned gene transcription, further resulting in dissociated VDR, RXR, and TRIP1, as the termination of VDR transcription cycle (**Figure 1-2**).

1,25(OH)2D3 Regulates Inflammatory System Via Immnue Cells, Prostaglandin Pathway and NFκB Pathway

Vitamin D and the inflammatory system were first linked after observations of VDR expression in activated lymphocytes [22, 23], which are essential for the vertebrate immune system. Additional studies have focused on the role of vitamin D in immune responses. VDR is expressed in almost all immune cells of innate and adaptive immunity, including activated $CD4^+$ and $CD8^+$ T cells, B cells, neutrophils [24], and antigen-presenting cells (APC) including macrophages and dendritic cells [23]. The effects of 1,25(OH)2D3 on individual immune cells are listed in **Table 1-1**.

The Regulatory Effects of 1,25(OH)2D3 on Macrophages

As a critical part of the innate immunity, macrophages are differentiated from monocytes and play an important anti-inflammatory role during immune response. In addition to decreasing immune responses by releasing cytokines, macrophages also can help initiate adaptive immunity by recruiting corresponding lymphocytes. Several studies have demonstrated that 1,25(OH)2D3 is able to induce the differentiation of monocytes and monocyte-related cells to macrophages [25, 26]. Disease-associated macrophages can also increase the level of 1,25(OH)2D3 in patients under granulomatous conditions [27, 28]. 1,25(OH)2D3 can prevent macrophages from producing inflammatory cytokines and chemokines [29] and can stimulate production of prostaglandin E2 (suppressive cytokine) while suppressing the granulocyte-macrophage colony stimulating factor (GM-CSF) by binding VDR to the promotor region of the GM-CSF gene [30]. Moreover, addition of 1,25(OH)2D3 can increase the expression of macrophage-specific surface antigens and lysosomal enzyme acid phosphatase to stimulate H_2O_2 production, which is essential for

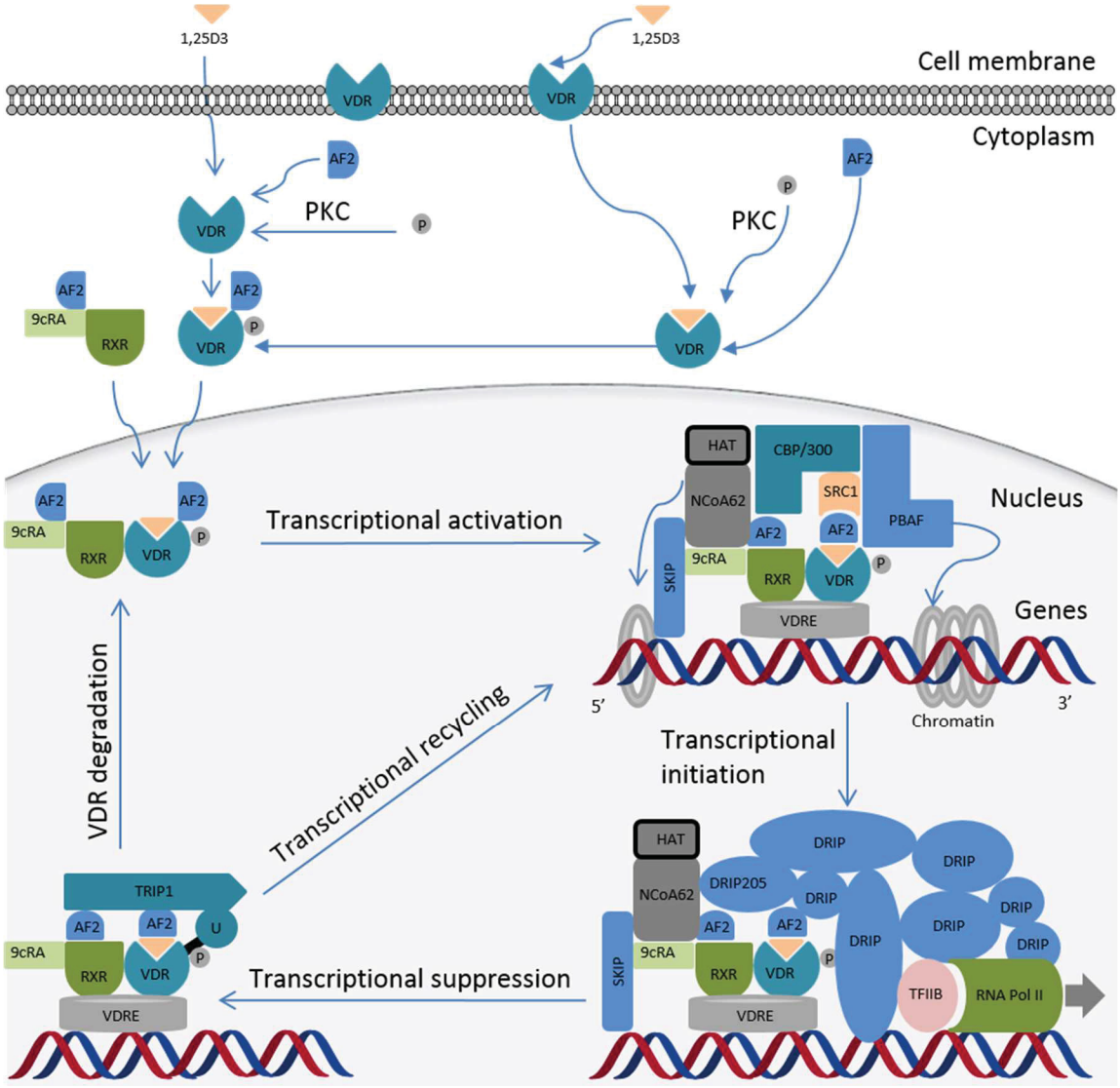

Figure 1-2. The transcriptional cycle of VDR regulated by 1,25(OH)2D3.
The generated 1,25(OH)2D3 can bind to either membrane VDR or cytosolic VDR to form a 1,25(OH)2D3-bound VDR-RXR heterodimer after being translocated into the nucleus. This dimer is then bound to VDRE with assistance from many other co-activators to initiate the transcription cycle, which includes transcriptional activation, transcriptional initiation, transcriptional suppression, transcriptional recycling, and VDR degradation.

Table 1-1. Effects of 1,25(OH)2D3 on different immune cells.

Cell	Effects of 1,25(OH)2D3	Reference
Macrophages	Increase monocyte-to-macrophage differentiation.	[25, 26]
	Stimulate PGE2.	[30]
	Suppress GM-CSF.	[30]
	Down-regulate TLRs.	[33]
	Reduce MHC2.	[34]
	Decrease IL-6 and IL-23.	[33]
	Decrease TNF-α and IL-1.	[37]
	Increase cathelicidin, phagocytosis, and chemotaxis.	[29]
	Stimulate antimicrobial response.	[34]
	Upregulate VDR, CYP27B1, and CYP24A1.	[38]
Dendritic cells	Impede T-cell/DCs interaction.	[39, 40]
	Decrease IL-1, IL-2, TNF-α, and INF-γ.	See above.
	Increase IL-10 and TGF-β.	See above.
	Diminish T cell activation.	See above.
	Inhibit differentiation, maturation, activation, and survival.	[41-43]
	Decrease MHC2 (CD40, CD80, and CD86).	See above.
	Reduce IL-12.	See above.
	Upregulate ILT3 and ILT4.	[44]
	Inhibit Th1 response indirectly.	[45]
	Inhibit Th17 cell induction.	[37]
	Affect chemokine production (increase CCL2,	[43]
	CCL18, and CCL22, and decrease CCL17 and	See above.
	CCL20).	[43]
	Increase maturation-induced apoptosis.	
T cells: $CD4^+$	Inhibit proliferation.	[48]
	Inhibit INF-γ.	[49]
	Increase IL-4, IL-5, and IL-10.	[50]
	Decrease IL-17, IL-6, and IL-23.	[51, 52]
	Inhibit Th17 activity.	[53]
T cells: $CD8^+$	Express high level of VDR.	[54]
	Express 1α-hydroxylase.	[55]
	Reduce INF-γ and TNF-α.	[57]
	Increase IL-5 and TGF-β.	[57]
T cells: T_{reg}	Promote induction.	[52, 59, 60]
T cells: γδ T	Inhibit expansion.	[61, 62]
	Inhibit INF-γ production.	[64]
	Downregulate CD25.	See above.
	Potentiate cell death.	See above.
T cells: memory	Suppress IL-17A, IL-17F, TNF-α, and IL-22.	See above.
T cells: NK	Attenuate NK activity.	[65]
	Stimulate NK activity.	[66, 67]

Table 1-1. Continued.

Cell	Effects of 1,25(OH)2D3	Reference
B cells	Inhibit proliferation.	[69]
	Upregulate p27 gene.	See above.
	Inhibit plasma cell generation.	See above.
	Inhibit memory B cell generation.	See above.
	Inhibit IgG and IgM secretion.	[68, 69]
	Induce apoptosis.	[69]
	Induce CYP27B1, CYP24A1, VDR, and TRPV6.	[69, 70]
	Induce IL-10 and CCR10.	[70, 71]

antimicrobial activity [31, 32] and can inhibit the expression level of toll-like receptors (TLR) such as innate immunity receptors TLR2, TLR4, and TLR9 required for the production of interleukin-6 (IL-6) [33]. In addition, 1,25(OH)2D3 can reduce the expression of class II major histocompatibility complex (MHC2) molecules on cell surface, thereby reducing the antigen-presenting function of macrophages to lymphocytes [34]. It was also reported that 1α-hydroxylase (CYP27B1) presented in macrophages is identical to the renal enzyme and is regulated primarily by immune signals such as interferon-γ (INF-γ), lipopolysaccharide (LPS), and viral infection [35, 36]. In addition, 1,25(OH)2D3 can decrease the levels of TNF-α and IL-1 [37], as well as upregulate VDR, CYP27B1, and CYP24A1 [38].

The Regulatory Effects of 1,25(OH)2D3 on Dendritic Cells

Dendritic cells (DC) are a specific kind of APCs of the human immune system. DCs are called the "messengers" between the innate and adaptive immune systems, since they can process antigens and then "send" (present) them to T cells via cell-surface interactions. The T cell/DCs interaction can be impeded by 1,25(OH)2D3, resulting in decreased production of pro-inflammatory cytokines such as IL-1, IL-2, tumor necrosis factor-α (TNF-α), and INF-γ and increased production of IL-10 and transforming growth factor-β (TGF-β) [39, 40]. Many studies have shown that 1,25(OH)2D3 is able to inhibit the differentiation, maturation, activation, and survival of DCs. Human monocyte-derived or mouse bone marrow-derived DCs treated with 1,25(OH)2D3 show a decreased expression level of MHC2 molecules CD40, CD80, and CD86, as well as reduced IL-12 and increased IL-10, suggesting diminished T cell activation and possible induction of type 1 regulatory cells producing IL-10 [41-43]. In another study, VDR ligands were proven to upregulate the inhibition receptor IL-T3 and IL-T4, both of which are related to tolerance induction [44]. In addition, indirect inhibition of T helper 1 (Th1) response by 1,25(OH)2D3 can be achieved by IL-12 inhibition of DCs, involving direct binding of 1,25(OH)2D3 to both VDR and NFκB cells resulting in downregulation of IL-12 transcription [45]. DCs have also been reported to increase the expression of CYP27B1 *in vitro* for the production of 1,25(OH)2D3 [46], suggesting that 1,25(OH)2D3 may control immune responses locally in DCs.

The Regulatory Effects of 1,25(OH)2D3 on T Cells

T cells, also called T lymphocytes, mature in the thymus, express T cell receptor (TCR) on their surface, and are central for cell-mediated immunity. There are several types of T cells: T helper cells ($CD4^+$ T cells), cytotoxic T cells ($CD8^+$ T cells), regulatory T cells, memory T cells, natural killer T cells, and γδ T cells, which are potential targets of 1,25(OH)2D3 .

The Regulatory Effects of 1,25(OH)2D3 on Helper T Cells. A 5-fold increase of the VDR expression level was observed after the activation of $CD4^+$ cells, in which 102 genes have been identified as targets of 1,25(OH)2D3 [47]. In 1985, Lemire and co-

authors reported vitamin D responses in $CD4^+$ cells, whose proliferation and cytokine production are regulated by 1,25(OH)2D3 [48]. [^{3}H]thymidine assay showed a 56% reduced incorporation in $CD4^+$ cells, suggesting the antiproliferative activity of 1,25(OH)2D3 on $CD4^+$ cells. Once presented with antigen by MHC2 molecules of APCs, $CD4^+$ cells are activated and divided into different subtypes (such as Th1 and Th2 cells) secreting various cytokines, which can regulate or help immune responses. *In vitro* tests suggested that 1,25(OH)2D3 can directly inhibit cytokine secretion (INF-γ) [49], while it can directly augment Th2 cell development by promoting IL-4, IL-5, and IL-10 production [50]. In recent studies [51, 52], significantly decreased production of INF-γ, IL-17, IL-6, and IL-23 was observed in Th17 cells, suggesting that Th17 cells are also the targets of vitamin D. This was confirmed by another study showing that antiretinal autoimmunity can be suppressed by inhibiting Th17 activity by 1,25(OH)2D3 [53].

The Regulatory Effects of 1,25(OH)2D3 on Cytotoxic T Cells. $CD8^+$ T cells are also the targets for 1,25(OH)2D3 since they express higher level of VDR than other immune cells [54], and express the 1α-hydroxylase for activation of vitamin D in mice $CD8^+$ cells [55]. $CD8^+$ cells are reported to mediate the suppressive effects of 1,25(OH)2D3 in murine multiple sclerosis (MS), and experimental autoimmune encephalomyelitis (EAE) [56]. However, more recent study has revealed $CD8^+$ cells secreted less INF-γ and TNF-α, and increased IL-5 and TGF-β after treatment of 1,25(OH)2D3 [57], suggesting 1,25(OH)2D3 act directly on $CD8^+$ cells. Another study has also reported the role of vitamin D in CD8αα cells, which is a variant of $CD8^+$ cells [58]. VDR knockout mouse showed reduced number of CD8αα cells with low expressed IL-10 level.

The Regulatory Effects of 1,25(OH)2D3 on Regulatory T Cells. Regulatory T cells (T_{reg}), also called suppressor T cells, suppress the action and proliferation of effector T cells and are important in treating autoimmune diseases and organ transplantation. A previous study demonstrated that 1,25(OH)2D3 can promote the induction of $CD4^+/CD25^+$ T_{reg} through APC DCs [59]. In addition, 1,25(OH)2D3 can increase the expression levels of Fox2 and IL-10, which are essential for T_{reg} induction [52]. However, later studies have revealed direct effects of 1,25(OH)2D3 on T_{reg} cells. Jeffery and co-authors [60] reported the effects of 1,25(OH)2D3 treatment on T cells to produce adaptive T_{reg} cells. In addition, an increased number of circulating T_{reg} cells has been observed in patients with systemic administration of 1,25(OH)2D3 [61]. Moreover, topical use of 1,25(OH)2D3 in mice can also increase the number of T_{reg} cells [62]. Interestingly, data from a recent study [63] showed that biologically active non-DBP-bound 25(OH)D3 promotes the production of T_{reg} in the presence of DCs in which CYP27B1 and VDR are expressed. These T_{reg} induction effects of 1,25(OH)2D3 suggest its immunosuppression actions in autoimmune and inflammatory diseases.

The Regulatory Effects of 1,25(OH)2D3 on γδ T Cells, Memory T Cells, and Natural Killer Cells. In other types of T cells, 1,25(OH)2D3 also plays an important role in adaptive immunity. Chen and co-authors [64] reported that 1,25(OH)2D3 significantly inhibited γδ T cell expansion and INF-γ production and downregulates CD25 expression. In addition, 1,25(OH)2D3 regulates signaling of γδ T cells through the Akt and ERK pathways and potentiates Ag-induced cell death at high concentrations (100 nM).

Interestingly, another study [65] showed suppressive effects of 1,25(OH)2D3 on IL-17A, IL-17F, TNF-α, and IL-22 production by memory T cells in an early rheumatoid arthritis (RA) patient. Currently, little is known about the effect between 1,25(OH)2D3 and natural killer (NK) cells. Early data have shown attenuated NK activity after addition of 1,25(OH)2D3, which did not directly inhibit NK cell cytotoxicity [66]. Conversely, more recent results from Balogh and co-authors [67] suggested a stimulation role of 1,25(OH)2D3 of NK activity through a pathway involving protein kinase C (PKC) and extracellular calcium. Until now, unfortunately, no direct interactions between NK cells and vitamin D have been established.

The Regulatory Effects of 1,25(OH)2D3 on B Cells

B cells, originating from bone marrow as an important type of lymphocyte of the adaptive immune system, express B cell receptor (BCR) on their outer surface, which allows B cells to recognize and bind to antigen. The major functions of B cells are secreting antibodies, performing the role of APCs, developing into memory B cells, and secreting cytokines. Many studies have revealed the influence of 1,25(OH)2D3 on various aspects of B. 1,25(OH)2D3 inhibits the ongoing proliferation of activated B cells, possibly through upregulation of the p27 gene expression, generation of plasma cells and memory B cells, immunoglobulin secretion (IgG and IgM) indirectly [68] or directly [69]. In addition, exposing B cells to 1,25(OH)2D3 induces their apoptosis [69]. Importantly, expression of CYP27B1, CYP24A1, VDR, and TRPV6 (encoding a calcium selective channel protein) involving metabolism and function of vitamin D were detected and induced by adding 1,25(OH)2D3 [69, 70]. In some other studies, 3-fold expression of activated B cell IL-10 [70] and induced expression of CCR10 in terminally differentiating B cells [71] were also observed after treatment with 1,25(OH)2D3 . These observations suggest a comprehensive effect of 1,25(OH)2D3 on the regulation of B cells.

1,25(OH)2D3 Modulates Inflammatory Responses via Prostaglandin Pathway

Other than the innate and adaptive immune systems, 1,25(OH)2D3 can also exert its anti-inflammatory effects through the prostaglandin (PG) pathway [72]. PGs are a type of active lipids biosynthesized by cyclooxygenase (COX) from arachidonic acid (AA). PGs are pro-inflammatory molecules and mediate homeostatic functions, as well as pathogenic mechanisms including an inflammation response [73]. There are two types of COX: COX-1 and COX-2: COX-1 is constitutively expressed in almost all cells to sustain the basal level of prostaglandins, while COX-2 is induced for prostaglandin production through stimulation. COX-2 is the key target for the selective, nonsteroidal anti-inflammatory drugs (NSAID), although many NSAIDs inhibit both COX-1 and COX-2. Many studies have demonstrated the effects of 1,25(OH)2D3 in the regulation of PGs, as discussed below.

1,25(OH)2D3 is capable of significantly inhibiting the expression of COX-2, as well as promoting the expression of 15-prostaglandin dehydrogenase [74, 75], which

inactivates PGs and downregulates PG receptor expression. The result is a reduced level of prostacyclins, which are derived from PGs and are involved in inflammation. In addition, 1,25(OH)2D3 upregulates the expression of mitogen-activated protein kinase phosphatase-5 (MKP5), resulting in inactivation of p38 and reduced downstream inflammation responses such as decreased IL-6 production [76]. Moreover, data from Krishnan and co-authors [77] have shown that 1,25(OH)2D3 induced the downregulation of PG receptors, leading to attenuation of PG-related inflammation responses. A detailed mechanism of the anti-inflammatory actions of 1,25(OH)2D3 through PG pathway has been summarized and proposed in several reports [73, 77, 78].

1,25(OH)2D3 Modulates Inflammatory Responses via NFκB Pathway

NFκB is a family of protein found ubiquitously in almost all cell types, and is involved in cellular responses to various stimuli such as cytokines and is important regulators for innate immune system and inflammation process. In basal level, specific inhibitory proteins named IκB are bound to NFκB dimers which can be activated by pro-inflammatory cytokines mainly through phosphorylation and degradation of IκB proteins. The obtained free NFκB can then be translocated into nucleus to activate the expression of pro-inflammatory cytokines and other genes. Of these pro-inflammatory cytokines, IL-8 is a key for NFκB-mediated immune responses and inflammation, since IL-8 is a potent chemotactic factor of neutrophils and associated in many ways with the progression of inflammatory responses [79, 80].

Many inflammation-related cells including human lymphocytes and peripheral blood mononuclear cells (PBMC) are the targets of 1,25(OH)2D3 [78]. 1,25(OH)2D3 and its analogs TX527 blocked NFκB activation through increased expression of IκBα in PBMCs and macrophages [80, 81]. In addition, activated NFκB is linked together with the production of pro-inflammatory cytokine IL-8, the level of which can be decreased through addition of 1,25(OH)2D3 in several cell lines [82, 83]. It was reported that 1,25(OH)2D3 could reduce the nuclear translocation of NFκB through its subunit p65, resulting in suppression of NFκB activation as well as its downstream genes including IL-8 [83]. Thus, 1,25(OH)2D3 can be an effective modulator in the progression of immune responses and inflammation through NFκB-mediated pathway.

Correlations Between Vitamin D and Inflammatory Diseases

Inflammatory diseases in different tissues result from complex biological responses to harmful stimuli. These stimuli include pathogens, cell debris, and irritants and so on [84]. Immune cells from both innate immunity and adaptive immunity, such as macrophages, dendritic cells, T cells and B cells, are involved in such protective responses together with blood vessels and molecular mediators [85]. The progression of acute inflammation is usually initiated by cells from innate immunity such as monocytes, neutrophils and macrophages, while cells from innate and adaptive immunities (monocytes, macrophages, T cells) are involved in inflammation [86]. Moreover, cytokines

such as INF-γ, IL-17 and IL-13 excreted from these immune cells are considered as major molecular regulators for inflammatory diseases [86]. Since these immune cells and cytokines are targets of vitamin D, exploration of correlation between vitamin D and inflammatory disease is of great importance to explain the immunomodulatory roles of vitamin D in related diseases.

Vitamin D Mediates Immunomodulatory Effects in Rheumatoid Arthritis

RA is a chronic, systemic, inflammatory, autoimmune disorder. RA affects primarily joints on both sides of the body equally, beginning with a few joints and then progressing into more joints including wrists, hands, elbows, shoulders, knees, and ankles. RA may also develop into joint and tissue damage, which leads to severe disability and increased mortality [87].

The genetic VDR polymorphisms were first linked to RA when BsmI polymorphisms were found to be involved in the progression of osteoporosis in RA patients [88]. A higher prevalence of RA and lower 25(OH)D3 level [plasma 25(OH)D3 < 40 nmol/L] are observed in patients from northern Europe compared with those in southern Europe [89]. Another study including 1191 RA patients, investigated the relationship between 25(OH)D3 and RA [90]. In a subgroup of patients not taking vitamin D supplements, PTH levels were much higher in patients with erosive arthritis; however, no difference in 25(OH)D3 concentrations was seen. Another hypothesis from the Iowa Women's Health Study concluded that vitamin D intake for older women is associated with a lower risk of RA [91], while an evaluation by means of a semiquantitative food frequency questionnaire in the Nurse's Health Study including 722 patients with RA found no correlation between vitamin D intake and the risk of RA [92]. In addition, a serum-bank, case-control study commented negatively on results from the Iowa Women's Health Study, since no correlation between serum 25(OH)D3 level and progression of RA was found [93]. Interestingly, in early inflammatory polyarthritis (IP) patients, an inverse relationship between 25(OH)D3 level and disease activity was observed, suggesting that vitamin D plays an immunomodulatory role in inflammatory arthritis [94]. In an interventional pilot study in a small group of RA patients, supplementation with active vitamin D metabolites showed no significant effect in regulating inflammatory processes, indicating a very limited effect of vitamin D in RA [95], while a high dose of vitamin D analogues showed positive effects on disease activity and decreased pain [96].

Further evidence linking vitamin D and RA has come from recent studies. In a cross-sectional study, serum vitamin D insufficiency (less than 75 nM) was found in 94% patients with RA, whereas vitamin D deficiency (less than 25 nM) was found in only 39% patients with RA. Additional data suggested an association between high prevalence of serum vitamin D insufficiency/deficiency and rheumatic patients, regardless of type of arthritis [97]. Another study examined 101 patients with early inflammatory arthritis and found that severe vitamin D deficiency was associated with RA while no difference was found between the occurrence of vitamin D deficiency in RA patients and that of

controls [98]. In addition, vitamin D concentration in 170 patients was found to be inversely associated with RA disease activity, severity, and physical disability after investigating the relationship between 25(OH)D3 and RA [99].

Vitamin D Mediates Immunomodulatory Effects in Inflammatory Bowel Disease

Inflammatory bowel disease (IBD), a type of autoimmune diseases characterized by the body's own immune system attacking the digestive system, is a series of inflammation conditions of the colon and small intestine. Two primary types are Crohn's disease (CD) and ulcerative colitis (UC). In an early study on 40 CD patients, data suggested that CD patients with higher levels of disease activity are at higher risk of vitamin D deficiency [100]. Another study found vitamin D deficiency in a high proportion (19%) of Australian children with IBD [101]. Studies conducted in Ireland (high latitude) on 58 CD patients found that the percentages of patients with vitamin D deficiency (serum 25(OH)D3 level less than 50 nM) during winter and summer months were 50% and 19%, respectively [102]. However, the same data were not given for Irish people without CD; thus, the relationship between vitamin D deficiency and CD was uncertain in this study. In addition, vitamin D deficiency was found to be highly prevalent among children and young adults with IBD (34.6%). This may due to their dark-skin complexion, limited exposure to the sun, lack of vitamin D supplementation, and decreased gastrointestinal absorption [103]. Nevertheless, newly diagnosed patients with IBD already have lower 25(OH)D3 levels compared with controls [104]. In a recent study, 28% and 42% of IBD patients were found to be vitamin D deficient (less than 20 ng/mL) during summer/autumn and winter/spring periods, respectively. Data has also shown that health related quality of life was the highest in in UC/CD patients with serum vitamin D concentrations of 50-59 ng/mL during either the summer/autumn period or the winter/spring period, suggesting a positive association between higher vitamin D serum levels and the quality of life of IBD patients [105]. In experimental IBD, vitamin D deficiency led to severe progression of diarrhea in IL-10 knockout mice which is the spontaneously IBD model [106]. Treating IL-10 knockout mice with 1,25(OH)2D3 significantly ameliorated the progression of the IBD symptoms, and 2 weeks' treatment with 1,25(OH)2D3 suppressed the development of experimental IBD.

Vitamin D Mediates Immunomodulatory Effects in Multiple Sclerosis

MS, an inflammatory neurodegenerative disease, is characterized by damaged insulating covers of nerve cells in brain and spinal cord. This damage may result in the loss of communication ability of the nervous system, sensory loss, muscle weakness, dizziness, and even mental problems [107, 108]. A strong correlation exists between vitamin D level and incidence of MS. In animal model, 1,25(OH)2D3 supplementation has also shown impressive protective effects in a mouse model for MS [109, 110]. Importantly, in White Americans (148 patients and 296 controls), a 41% decrease in MS risk was found for every 50-nmol/L increase in serum 25(OH)D3 levels, and there was no significant difference between men and women (95% confidence interval, $p = 0.90$ for interaction),

suggesting a strong positive association between high circulating levels of 25(OH)D3 and lower risk of MS [111]. Several studies have established a correlation between outdoor activities and a decreased risk of developing MS in Norwegian, Tasmanian, and North American children and adolescents, which might be explained by the fact that the increased exposure to the sun from outdoor activities can increase the 25(OH)D3 level [112-114]. Indeed, vitamin D deficiency is common in patients with MS [115], and serum 25(OH)D3 levels are correlated with clinical MS parameters while 1,25(OH)2D3 levels are not directly associated with relapse rate or disease activity of MS [116]. A protective effect from vitamin D has been proposed relative to the risk of MS [117]: women with a high-dose intake of vitamin D (more than 400 IU/day) were 40% less risky of developing MS than those who had no supplemental vitamin D. The same study also suggested that a dose of 1000-4000 IUs of vitamin D daily can increase the serum level of 25(OH)D3 to a concentration higher than 99 nM, which may reduce the risk of developing MS by 62% [117].

Vitamin D Mediates Immunomodulatory Effects in Asthma

Asthma, a chronic inflammatory disease of the airways, is characterized by recurring symptoms including wheezing, coughing, breathlessness, and chest tightness [118]. Although the role of vitamin D in asthma is not currently well understood, some putative correlations between vitamin D and asthma have been reported. For example, high prevalence of vitamin D insufficiency was seen in North American and Costa Rican children with asthma [119, 120]. In addition, vitamin D insufficiency exacerbated the progression of severe asthma [121]. Other studies have observed a vitamin D deficiency in children [122-125], adolescents [126, 127], and adults [127-129] with asthma higher than in controls. Moreover, a reduced level of vitamin D metabolites was revealed by metabolomic analysis in asthmatic children [130]. Interestingly, an age-dependent association between vitamin D level and prevalence in asthmatic children was described by Van Oeffelen and co-authors [131]. These data together with a previous report [132], collectively, suggest a role of vitamin D in the development of asthma. Potential mechanisms of the action of vitamin D might include promoting lung immunity, decreasing inflammation, slowing cell cycling, reducing hyperplasia, and enhancing the effects of exogenous steroids [132].

Conversely, numerous studies have argued that there was no correlation between serum vitamin D level and the occurrence of asthma. Although a high prevalence of vitamin D insufficiency was found in Puerto Rican children with asthma, this prevalence was comparable with that of healthy children without asthma [133]. Another study including 74 children concluded that there was no significant difference between vitamin D level in asthma patients and in a control group [134]. In addition, 25(OH)D3 insufficiency was found not to be associated with airway obstruction in most asthma adults [135]. In a randomized, double-blind, placebo-controlled study on children with asthma age 6-18 years, oral administration of 14,000 units of vitamin D once weekly showed no difference on the disease parameters compared with those in a control group Interestingly, some

other studies [136, 137] have revealed an increased risk of asthma in association with high-dose vitamin D supplementation (or high vitamin D levels).

Vitamin D Mediates Immunomodulatory Effects in Type 1 Diabetes

Type 1 diabetes (T1D), also called diabetes mellitus type 1, is an autoimmune disease involving $CD4^+$ and $CD8^+$ T cells and specific antibodies of insulin-producing β-cells in pancreatic islets [138]. Although the cause of T1D is still unknown, many studies have shown clear associations between vitamin D and T1D [138-141]. Recent studies have shown a similar relationship between the vitamin D level and T1D. Evidence has shown that an increased serum 25(OH)D3 level is associated with a leveling incidence of T1D in Finnish children [142], a trend that may due to increased vitamin D intake in the country since 2003. Similarly, a higher prevalence of 25(OH)D3 deficiency was observed in T1D patients compared to controls in different populations [143-146].
Although vitamin D repletion did not affect the inflammatory markers [144], its metabolites, 25(OH)D3 and 1,25(OH)2D3, have shown some immunomodulatory effects in T1D. In animal models, by reducing effector T cells and chemokine production of islet cells, a high dose of 1,25(OH)2D3 successfully reduced the incidence of diabetes [147]. Moreover, 25(OH)D3 showed inhibitory effect on dendritic cells differentiation in T1D patients, suggesting its immunosuppresive role in the progression of T1D. In another prospective study, T1D patients with vitamin D deficiency (or insufficiency) displayed a high level of inflammatory markers as expected; these markers were found to be negatively associated with serum 25(OH)D3 levels. Interestingly, after 1,25(OH)2D3 supplementation for 6 months, all inflammatory markers in serum and urine decreased significantly, suggesting an inflammation suppressive role of 1,25(OH)2D3 in T1D patients [148].

Vitamin D Mediates Immunomodulatory Effects in Systemic Lupus Erythematosus

Systemic lupus erythematosus (SLE) is a common autoimmune disease in which the body's immune system produces antibodies against its own healthy tissues. Numerous studies have linked vitamin D with SLE. A recent study of 67 women with SLE found a 30.7% prevalence of 25(OH)D3 deficiency (less than 20 ng/mL), which was a level higher than that of the control group [149]. Similarly, another cross-sectional study found a 55% prevalence of 25(OH)D3 insufficiency in SLE patients, while the prevalence was only 8% in the control participants [150]. Interestingly, higher levels of IL-6 were associated with insufficient 25(OH)D3 in these patients, suggesting an immunosuppressive role for vitamin D in the inflammation process of SLE. These statistical data are consistent with studies that have reported a vitamin D insufficiency prevalence ranging from 38% to 96%, while the vitamin D deficiency prevalence varied from 8% to 30% [151-153]. Other than vitamin D levels, VDR gene polymorphism may also play a role in the risk of SLE. A recent meta-analysis concluded that BsmI B may be a risk factor for SLE onset for the overall populations and that the FokI FF genotype is a risk factor in Asians for SLE susceptibility [154]. This was further confirmed by a recent follow-up study, which found a

positive association between VDR polymorphisms and SLE severity, especially for the FokI CT and TaqI TT genotypes [155], in 170 SLE patients.

Representatives of Anti-inflammatory Vitamin D Analogs

A large amount of vitamin D analogs have been synthesized during the years, however, only a limited number of analogs have been focusing on the anti-inflammation effects. Of these analogs that have been produced, the activities by which they are more or less effective than the native hormone [1,25(OH)2D3] are not always known. These analogs have largely appeared by synthetic design as well as from metabolism studies of parent compounds. Detailed activities (compared with 1,25(OH)2D3 or not) of representative analogs with promising anti-inflammatory potential are summarized in **Table 1-2**.

BXL-62 (2)

After 6-h stimulation with LPS of peripheral blood mononuclear cells (PBMC) from IBD patients, BXL-62 (**Figure 1-3**) significantly inhibited the transcription of some key pro-inflammatory cytokines including TNF-α (IC50 = 4.0×10^{-12} M), IL-6 (IC50 = 7.1×10^{-12} M), and IL-12/23p40 (IC50 = 5.5×10^{-12} M) at lower concentrations than 1,25(OH)2D3 (compound **1**, **Figure 1-3**), which showed IC50s at 1.9×10^{-9} M, 9.6×10^{-10} M, and 7.9×10^{-9} M, respectively. At the protein level in culture supernatants, BXL-62 inhibited secretion levels of TNF-α (IC50 < 1.0×10^{-12} M), IL- 6 (IC50 = 9.0×10^{-12} M), and IL-12/23p40 (IC50 < 1.0×10^{-12} M) with a significantly higher potency than 1,25(OH)2D3 with IC50s = 2.0×10^{-9} M, > 1.0×10^{-8} M, and = 6.4×10^{-10} M, respectively. This regulatory effect of BXL-62 on the innate immune system was further confirmed by TLR agonist-stimulated PBMCs, in which the production of TNF-α, IL-12/23p40, and IL-6 was significantly inhibited by BXL-62 at 1.0×10^{-8} M. In addition, BXL-62 treatment in unstimulated PBMCs showed greater potency on transcription of CYP24A1 (EC50 = 8.2×10^{-12} M) and cathelicidin antimicrobial peptide (CAMP) (EC50 = 1.7×10^{-11} M) than 1,25(OH)2D3 (EC50 = 4.1×10^{-10} M, 2.9×10^{-10} M, separately). Moreover, 50% INF-γ and 60% TNF-α production in lamina propria mononuclear cells (LPMCs) from IBD tissue was inhibited by BXL-62 at 1.0×10^{-8} M. BXL-62 also had fewer hypercalcemic effects than did 1,25(OH)2D3, and showed good efficacy on dextran sodium sulfate (DSS)-induced colitis, suggesting a promising future for IBD treatment [156]. Moreover, BXL-62 showed a maximum tolerated dose (MTD) at 3.0 μg/kg while 1,25(OH)2D3 showed a MTD of 0.3 μg/kg in an *in vivo* assay for calcemic activity [157].

1α,25-Dihydroxy-16-ene-20-cyclopropyl-vitamin D3 (3)

As the parent compound of BXL-62, compound **3** was identified as the most potent anti-inflammatory compound among a series of analogs in the 16-ene-20-

Table 1-2. Summary of the anti-inflammatory efficacies of representative vitamin D analogues.

Compound	Models	Effects	Activity	Activity (1,25D3)	References
2	PBMCs	Inhibit TNF-α transcription	IC50 = 4.0×10^{-12} M	IC50 = 1.9×10^{-9} M	[156]
		Inhibit IL-6 transcription	IC50 = 7.1×10^{-12} M	IC50 = 9.6×10^{-10} M	See above.
		Inhibit IL-12/23p40 transcription	IC50 = 5.5×10^{-12} M	IC50 = 7.9×10^{-9} M	See above.
		Inhibit TNF-α production	IC50 < 1.0×10^{-12} M	IC50 = 2.0×10^{-9} M	See above.
		Inhibit IL-6 production	IC50 = 9.0×10^{-12} M	IC50 = > 1.0×10^{-8} M	See above.
		Inhibit IL-12/23p40 production	IC50 < 1.0×10^{-12} M	IC50 = 6.4×10^{-10} M	See above.
	LPMCs	Inhibit 50% INF-γ production	1.0×10^{-8} M	-	See above.
		Inhibit 60% TNF-α production	1.0×10^{-8} M	-	See above.
	DSS-induced colitis in mice	Prevent body weight loss	Better than 1,25D3	Effective at 0.3 μg/kg	See above.
		Ameliorate the bloody stool score	Better than 1,25D3	Effective at 0.3 μg/kg	See above.
		Ameliorate disease symptoms	Better than 1,25D3	Effective at 0.3 μg/kg	See above.
		Inhibit colon lesions	Better than 1,25D3	Effective at 1 μg/kg	See above.
		Calcemic effect	MTD = 3 μg/kg	Effective at 0.3 μg/kg	[157]
3	lymphocytes	Inhibit INF-γ production	IC50 < 1.0×10^{-17} M	IC50 = 2.9×10^{-11} M	[157]
	PBMCs	Inhibit TNF-α production	IC50 = 2.0×10^{-16} M	IC50 = 8×10^{-9} M	See above.
	Healthy mice	Calcemic effect	MTD = 1 μg/kg	MTD = = 0.3 μg/kg	See above.
4	PBMCs	Inhibit INF-γ production	IC50 = 7.0×10^{-9} M	IC50 = 1.0×10^{-6} M	[160]
		Inhibit TNF-α secretion	IC50 > 1.0×10^{-6}	IC50 = 9.0×10^{-8} M	See above.
		Inhibit IL-1β secretion	IC50 = 9.0×10^{-7} M	IC50 < 9.0×10^{-7} M	See above.
		Increase IL-10	Weaker than 1,25D3 at 1.0×10^{-9} M	Effective at 1.0×10^{-10} M	See above.
		Increase IL-4	Weaker than 1,25D3 at 1.0×10^{-10} M	Effective at 1.0×10^{-10} M	See above.
		Decrease ICAM-1 and LFA-1	Effective at 1.0×10^{-6} M	-	[161]
		Decrease MMP-9 and MMP-2	Effective at 1.0×10^{-6} M	-	See above.
		Decrease TNF-α	Effective at 1.0×10^{-6} M	-	See above.
		Lactate dehydrogenase activity	Non-toxicity	Non-toxicity	[160]
		Induce cell death	No apoptosis induction up to 1.0×10^{-5} M	No apoptosis induction up to 1.0×10^{-5} M	See above.
	TNBS-induced colitis in mice	Ameliorate the colitis-associated symptoms	Comparable to 1,25D3	Effective at 0.2 μg/kg	[162]
		MPO activity	Comparable to 1,25D3	Effective at 0.2 μg/kg	See above.

Table 1-2. Continued.

Compound	Models	Effects	Activity	Activity (1,25D3)	References
		Downregulate TNF-α and INF-γ	Comparable to 1,25D3	Effective at 0.2 μg/kg	See above.
		Upregulate IL-4 and IL-10	Comparable to 1,25D3	Effective at 0.2 μg/kg	See above.
		Calcemic effect	No effect at 2.0 μg/kg	induce calcemic effect at 0.2 μg/kg	See above.
		Serum creatinine level	Not changed at 2.0 μg/kg	Not changed at 0.2 μg/kg	See above.
5	DCs	Impair DC differentiation and maturation	More potent than 1,25D3	Effective at 1.0×10^{-8} M	[166]
		Block INF-γ, IL-10 but not IL-13 production	More potent than 1,25D3	Effective at 1.0×10^{-8} M	See above.
		Inhibit T cell proliferation	More potent than 1,25D3	Effective at 1.0×10^{-8} M	See above.
		Modulate surface phenotype	More potent than 1,25D3	Effective at 1.0×10^{-8} M	[169]
		Induce cell survival	No effect up to 1.0×10^{-7} M	No effect up to 1.0×10^{-8} M	See above.
	PBMCs	Inhibit TNF-α production and downregulate NFκB	Effective at 1.0×10^{-10} M	-	[81]
	T cell	Suppress proliferation	Effective at 1.0×10^{-8} M	-	[170]
		Decrease INF-γ, IL-4 and IL-17	Effective at 1.0×10^{-8} M	-	See above.
		Suppress cell activation	Effective at 1.0×10^{-8} M	-	See above.
		Affect global protein expression	Effective at 1.0×10^{-8} M	-	[171]
	T1D mice	Prevent T1D	Effective at 12.5 μg/kg	-	[167]
		Delay T1D recurrence	Effective at 10 μg/kg	-	[172]
	DSS-induced colitis in mice	Attenuate disease severity	Effective at 3 μg/kg	Effective at 0.5 μg/kg	[173]
		Calcemic level	Not elevated at 3 μg/kg	Elevated at 0.5 μg/kg	See above.
6	Mouse T cells	Inhibit proliferation	Comparable to 1,25D3	Effective at 1.0×10^{-12} M	[175]
	keratinocytes	Suppress IL-8 production	Comparable to 1,25D3	Effective at 1.0×10^{-6} M	See above.
		Inhibit IL-6 production	Effective at 1.0×10^{-11} M	Effective at 1.0×10^{-10} M	See above.
	Jurkat cells	Inhibit Ap-1 transcription	Slightly stronger than 1,25D3	Effective at ~ 1.0×10^{-7} M	See above.
		Inhibit NFκB transcription	Effective at ~ 1.0×10^{-8} M	Effective at ~ 1.0×10^{-7} M	See above.
	Rats	Suppress carrageenin-induced inflammation	Effective at 7 μg/kg	-	[174]
	Mice	inhibit NFκB activation	Effective at 2.0 μg/kg	-	[176]

Table 1-2. Continued.

Compound	Models	Effects	Activity	Activity (1,25D3)	References
		reduce infiltration by macrophages and other TGF-β-expressing cells	Effective at 2.0 μg/kg	-	See above.
		reduce phosphorylated Smad2/3 and MCP-1	Effective at 2.0 μg/kg	-	See above.
		Calcemic level	Not elevated	Elevated at 1.0 μg/kg	[177]
7	COX-2	Inhibit COX-2	IC50 = 5.8×10^{-9} M	IC50 > 1.0×10^{-6} M	[178]
	COX-1	Inhibit COX-1	No effect up to 1.0×10^{-6} M	No effect up to 1.0×10^{-6} M	See above.
	Macrophages	Inhibit the growth	IC50 = 1.0×10^{-8} M	-	See above.
		Inhibit expression of COX-2, iNOS and IL-2	Effective at 1.0×10^{-8} M	-	See above.
	Rats	Inhibit inflammation	Effective at 10 μg/kg	-	See above.
		Inhibit expression of COX-2, iNOS and IL-2	Effective at 10 μg/kg	-	See above.
	Chick	Stimulate calcium uptake in intestinal epithelium	No effect up to 1.0×10^{-8} M	Effective at 1.0×10^{-9} M	[179]
	Human	Calcemic effect	No hypercalcemia at 45 $\mu g/m^2$/day	-	[180]
8	PBMC	Inhibit ICAM-1, MAdCAM-1 and MMP-2, MMP-9 and MMP-3	Effective at 1.0×10^{-6} M	Effective at 1.0×10^{-7} M	[183]
		Inhibit proliferation	IC50 = 4.3×10^{-8} M	IC50 = 8.0×10^{-9} M	[181]
		Downregulate HLA-DR	IC50 = 1.9×10^{-9} M	IC50 = 9.6×10^{-10} M	See above.
		Upregulate CD14	EC50 = 3.8×10^{-9} M	EC50 = 1.4×10^{-9} M	See above.
		Downregulate ICAM-1	IC50 = 5.4×10^{-10} M	IC50 = 4.8×10^{-10} M	See above.
		Downregulate B7.1	IC50 = 3.7×10^{-10} M	IC50 = 9.2×10^{-10} M	See above.
		Inhibit IL-12	IC50 = 4.2×10^{-9} M	IC50 = 5.8×10^{-9} M	See above.
		Inhibit TNF-α	IC50 = 2.2×10^{-9} M	IC50 = 9.1×10^{-10} M	See above.
		Inhibit IL-10	IC50 = 1.4×10^{-7} M	IC50 = 1.5×10^{-8} M	See above.
	T cell	Inhibit proliferation	IC50 = 4.2×10^{-8} M	IC50 = 1.5×10^{-8} M	See above.
	Mice	Calcemic effect	No effect up to 200 μg/kg/d	effective at 0.03 μg/kg/d	See above.
	DCs	Inhibit INF-γ, TNF-α, IL-12, CD40, CD80 and CD86	Effective at 1.0×10^{-6} M	-	[182]
	DSS-induced colitis in mice	Ameliorate disease activity	Effective at 100 μg/kg/d	-	See above.
		Inhibit the production of INF-γ and IL-10	Effective at 100 μg/kg/d	-	See above.

Table 1-2. Continued.

Compound	Models	Effects	Activity	Activity (1,25D3)	References
9	Rat cardiac transplantation	Prolong survival	Effective at 0.1 μg/kg/d	-	[184]
		Prolong graft survival	Effective at 0.1 μg/kg	-	[185]
	Rat bone marrow transplantation	Decrease CD4, CD8, MHC-II, IL-2 receptor, nitric oxide 2, and NKR-P1A	Effective at 0.1 μg/kg/2d	-	[186]
		Prevent graft-versus-host disease	Effective at 0.1 μg/kg/2d	-	See above.
	Rat aortic allografts	Prolong survival	Effective at 0.1 μg/kg/2d	-	[187]
10	DCs	Inhibit MHC2, B7-1, B7-2 and CD40	Effective at 1.0×10^{-12} M	Effective at 1.0×10^{-10} M	[189]
		Inhibit maturation	Effective at 1.0×10^{-10} M	Effective at 1.0×10^{-10} M	[45]
11	Lukemic cells	Inhibit proliferation	IC50 = 1.0×10^{-10} M	IC50 = 1.5×10^{-9} M	[159]
		Induce differentiation	EC50 < 3.2×10^{-10} M	EC50 = 3.2×10^{-10} M	See above.
12	Rats	Prevent autoimmune symptoms	Effective at 0.03 μg/kg/d	Effective at 0.1 μg/kg/d	[190]
	T cells	Inhibit proliferation	Comparable to 1,25D3	Effective at 1.0×10^{-8} M	[191]
	Lymphoma cells	Inhibit growth and differentiation	IC50 = 1.0×10^{-12} M	IC50 = 1.4×10^{-8} M	[193]

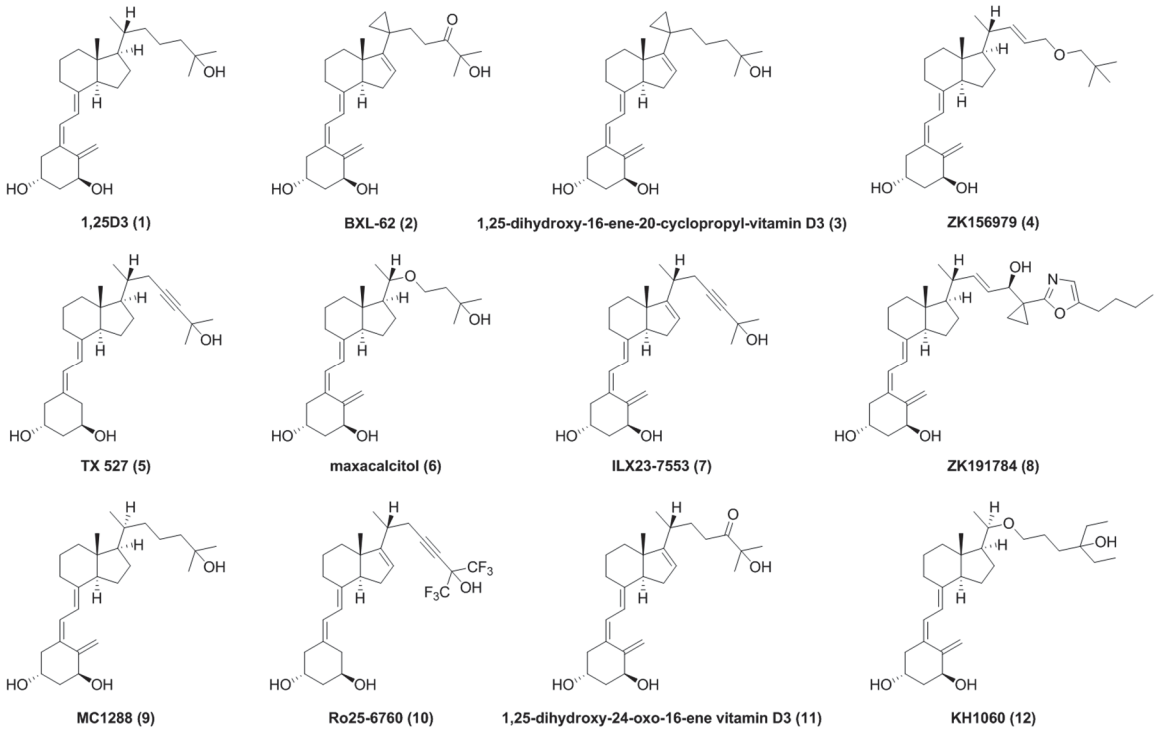

Figure 1-3. Representatives of developed vitamin D3 analogs with anti-inflammatory activities.

cyclopropyl-vitamin D3 family [157], optimized from two classes of analogues with 16-ene or 20-cyclopropyl modification [158, 159]. By assessing its ability to inhibit production of TNF-α and INF-γ, compound **3** showed much stronger anti-inflammatory potency, with an IC50 < 1.0×10^{-17} M against INF-γ production and 2.0×10^{-16} M against LPS TNF-α production, than that of 1,25(OH)2D3 (2.9×10^{-11} M and 8×10^{-9} M, respectively).

ZK156979 (4)

The inhibitory effect of ZK156979 (22-ene-25-oxa vitamin D) against INF-γ in PBMCs showed an IC50 of 7.0×10^{-9} M with a maximum inhibition at 81% of control values, while the IC50 of 1,25(OH)2D3 was 1.0×10^{-6} M with a maximum inhibition rate of 70%. However, the suppressive effects of 1,25(OH)2D3 on TNF-α and IL-1β secretion were slightly stronger than those of ZK156979. The IC50 of 1,25(OH)2D3 on TNF-α was 9.0×10^{-8} M (maximum inhibition: 76% of control value), while the IC50 for ZK156979 was > 1.0×10^{-6} M. As for IL-1β secretion at the same concentration (1.0×10^{-5} M), 1,25(OH)2D3 gave an 82% inhibition rate, while only 60% was inhibited by ZK156979, which gave an IC50 of 9.0×10^{-7} M. In contrast, both 1,25(OH)2D3 and ZK156979 showed strong stimulatory effects on the anti-inflammatory cytokines IL-4 and IL-10. 1,25(OH)2D3 at 1.0×10^{-10} M increased 35% while ZK156979 at 1.0×10^{-9} M increased 14% of IL-10 production. Interestingly, these two compounds showed comparable effects at high concentration (1.0×10^{-5} M): 1,25(OH)2D3 and ZK156979 increased 77% and 66% of IL-10 production, respectively. Similarly, 1,25(OH)2D3 and ZK156979 at a concentration of 1.0×10^{-10} M could also increase 34% and 18% secretion of IL-4, separately, and at 1.0×10^{-5} M the increase for 1,25(OH)2D3 and ZK156979 was 80% and 64%, respectively [160]. In addition, ZK156979 was able to decrease ICAM-1 and LFA-1 at 1 μM [161].

Additional anti-inflammatory effects of ZK156979 were evaluated on a 2,4,6-trinitrobenzene sulfonic acid (TNBS)-induced colitis model in mice [162]. Data showed that ZK156979 was able to remarkably ameliorate the colitis-associated symptoms. This compound reduced colitis-associated weight loss, improved clinical activity score of colitis, and reduced the extent of the TNBS-related colon shortening, as well as colitis-mediated increase of colon weight significantly and dose dependently. In addition, after ZK156979 treatment, mice colons showed a massive reduction of colitis-associated hyperemia, necrosis, inflammation, and ulceration compared with those of ethanol-treated controls. Moreover, ZK156979 also reduced the local production of inflammatory mediator, myeloperoxidase (MPO), in colon at low and high concentrations (25% and 65% reduction at 0.2 μg/kg and 2.0 μg/kg, respectively). ZK156979 was also proven to exert its anti-inflammatory effects through upregulation of anti-inflammatory cytokines IL-4 and IL-10 and downregulation of key inflammatory cytokines INF-γ and TNF-α expression, further confirmed by rapid and specific induction of Th1-relevant transcription factor T-beta in Th1-differentiated lymphocytes.

TX527 (5)

TX527 (inecalcitol), together with its C20 epimer (KS532), was initially reported to be active on growth inhibition of human breast cancer cells *in vitro* and *in vivo*, as a potent anticancer agent [163]. Successive studies have focusing mainly on its anti-inflammatory activity assessed on different immune systems and inflammatory disease models. At different concentrations (0.01, 0.1 and 1 nM), TX527 can exert anti-proliferation activity and TNF-α inhibitory effect mediated via NFκB and IκB upregulation on PBMCs from CD patients [81]. In an islet transplantation survival study, synergistic immunomodulatory effects of TX527 were proved when it was combined with cyclosporine A (CyA) or IFN-β [164]. Later studies have also shown similar synergistic effects in T1D mice; but, in addition, increased IL-10 transcripts and decreased mRNA of IL-2, INF-γ, and IL-12 were seen in TX527-treated mice [165]. Continuous treatment of TX 527 could impair the differentiation, maturation and function of DCs, whose cytokine profiles can be changed significantly such as down-regulated INF-γ and IL-10 [166]. The same group further confirmed the immunomodulation potential of this compound and observed its activity to prevent T1D in mouse model, and to extend lifetime of mice after syngeneic islets grafts [167]. Latter investigations were focused on its anti-inflammation properties applying DCs [168, 169], T cells [170, 171], mouse diabetes model [172] and IBD mouse model [173].

Maxacalcitol (6)

Although 22-oxacalcitriol (OCT, **6**) has been approved recently as either monotherapy or in combination with other steroids to treat psoriasis, its anti-inflammatory activity was found ever since 1994. In rats with carrageenin-induced inflammation, administering OCT significantly suppressed the formation of granulation tissue and the weight of exudates in both early and late phases of inflammation [174]. In addition, OCT inhibited the proliferation of lymphocytes, the production of IL-8 and IL-6 in keratinocytes, and expression of AP-1-dependent and NFκB-dependent genes [175]. In a recent study, OCT inhibited the activation of NFκB, reduced infiltration by macrophages and a number of cells expressing TGF-β, and phosphorylated Smad2/3 and MCP-1, which are inflammatory mediators [176]. In addition, OCT did not elevate the calcemic level in mice as compared with 1,25(OH)2D3 [177]. The results suggest a suppressive action in inflammatory processes.

ILX23-7553 (7)

ILX23-7553 (1α,25-dihydroxy-16-ene-23-yne-vitamin D3) was first found to inhibit COX-2 activity selectively with an IC50 of 5.8 nM, and then it was proved to inhibit the proliferation of macrophage cells whose COX-2 and inflammatory mediators like inducible nitric oxide synthase (iNOS) and IL-2 were downregulated. In an air pouch of a rat model, it can also inhibit carrageen-induced inflammation effectively with reduced expressions of COX-2, iNOS, and IL-2 in the tissues of the air pouch.

Importantly, this compound did not affect the expression of COX-1, suggesting that ILX23-7553 is a selective COX-2 inhibitor and may exert its potent anti-inflammatory effects through the prostaglandin pathway [178]. In chick, ILX23-7553 was not effective to stimulate calcium uptake in intestinal epithelium up to 10 nM [179]. And in human, it was not hypercalcemic at 45 μg/m^2/day [180].

ZK191784 (8)

ZK191784, a non-calcemic analog of 1,25(OH)2D3, exhibited potent immunosuppressive activity in an animal model. It inhibited proliferation of lymphocytes and the production of TNF-α and IL-12 in monocytes. Meanwhile, treatment of monocytes with ZK191784 significantly reduced gene expression of MHC2, B7.1, and intercellular adhesion molecule-1 (ICAM1) [181]. In a DSS-induced colitis model, this compound significantly ameliorated disease symptoms. It inhibited the secretion of pro-inflammatory cytokines INF-γ and IL-6 in isolated mesenteric lymph node cells and increased of IL-10 expression 1.4-fold in colonic tissue, whereas a decrease of 81.6% was observed for the expression of Th1-specific transcription factor T-beta. In addition, reduced numbers of activated CD11c$^+$ DCs infiltrated the colon, and decreased production of pro-inflammatory cytokines in primary mucosal DCs were found in mice after treatment with ZK191784 [182]. According to a recent study [183], increased expression of ICAM-1, MAdCAM-1 and MMP-2, -9 and -3 were found in tissues and PMBCs from IBD patients cultured with ZK191784, suggesting a therapeutic role of ZK191784 in IBD patients.

MC1288 (9)

MC1288, 20-epi-1α,25-dihydroxyvitamin D3, was tested for immunosuppressive effects in different transplantation models. It was able to prolong survival and significantly delay the cardiac allograft rejection [184, 185] and showed similar immunosuppressive effects on rejection in small bowel transplantation [184], as well as a bone marrow transplantation model [186]. In a rat aortic allograft model, MC1288 alone or in combination with CsA suppressed the rejection as evidenced by decreased adventitial inflammation and intimal thickening. In addition, it inhibited proliferation of T cells and suppression of immune cells expressing IL-2 receptor [187], affecting antibody production and macrophage effector function via T cells [188]. The immunomodulatory effects of MC1288 treatment were further confirmed by decreased expression of CD4, MHC2, IL-2 receptor, nitric oxide 2, and NKR-P1A in the liver and skin of bone marrow transplantation rats [186].

Ro25-6760 (10)

1α,25-dihydroxy-16-ene-23-yne-26,27-hexafluoro-19-nor-D3 (**10**) was proven to be 100-fold more potent than 1,25(OH)2D3 as an immunosuppressor in several ways. It

inhibited the expression levels of MHC2 and costimulatory ligands, B7-1, B7-2, and CD40, in murine DCs without inhibiting the proliferation of DCs, but it could affect the differentiation of DCs by reducing DC yield. Meanwhile, adding Ro25-6760 could reduce the proliferation-induction capacity of DCs on allogeneic T cells. In contrast, no inhibition effect was observed in cell cultures from VDR knockout mice, suggesting the ability of Ro25-6760 to reduce DC function as VDR-dependent [189]. Further investigations revealed that treatment of Ro25-6760 on bone marrow cultures resulted in accumulated immature DCs characterized by reduced IL-12 production and unchanged TGF-β1. In addition, these immature DCs had a poor response to maturing stimuli such as CD40, macrophage products, or even LPS, indicating an inhibition effect of Ro25-6760 against DC maturity [45].

1α,25-Dihydroxy-24-oxo-16-ene vitamin D3 (11)

1α,25-dihydroxy-24-oxo-16-ene vitamin D3 is an accumulated intermediary metabolite of its parent compound, 1α,25-dihydroxy-16-ene vitamin D3. The accumulation of this compound is due to its resistance to further metabolism, conferring on this compound a slower clearance compared with 1,25(OH)2D3 . In addition, both compounds showed promising immunosuppressive effects such as growth inhibition and differentiation stimulation of human myeloid leukemic cell line (RWLeu-4). These activities were several-folds more potent than 1,25(OH)2D3 [159].

KH1060 (12)

In mercuric chloride-induced Brown Norway (BN) rats, adding KH1060 partially prevented autoimmune symptoms including proteinuria and serum IgE and antilaminin antibodies in a concentration-dependent manner; however, when given together with CyA, an additive effect leading to complete prevention of proteinuria was seen. In addition, a combination of KH1060 and CyA significantly reduced serum IgE and antilaminin levels [190]. It was also reported that KH1060 significantly inhibited proliferation of T cells from UC patients, and the highest inhibition was always obtained in the presence of KH1060 other than 1,25(OH)2D3 or EB1089 [191]. In an animal study, KH1060 was shown to effectively prevent T1D. KH1060-treated mice gave only an 11% incidence of T1D, while the incidence of 1,25(OH)2D3 -treated and control groups were 18% and 55%, respectively [192]. Together, these data suggest the immunosuppressive activity of this noncalcemic compound, which should be further studied for its promising potential for treating inflammatory diseases. In lymphoma cells, KH1060 inhibited cell growth and differentiation with an IC50 of 1.0 pM, while 1,25(OH)2D3 showed its IC50 of 14 nM [193].

Concluding Remarks

Vitamin D and its key endogenous metabolites, 25(OH)D3 and 1,25(OH)2D3, are associated with a variety of inflammatory diseases (**Figure 1-4**). Vitamin D deficiency is a risk factor for autoimmune and inflammatory diseases, and elevated serum 25(OH)D3 level, either through vitamin D supplementation or endogenous conversion, appears to exert anti-inflammation actions in related diseases. The relationship of vitamin D and inflammatory diseases is associated in several ways, and administering vitamin D and its analogs is beneficial for ameliorating the symptoms of these diseases. 1,25(OH)2D3, as the active form of vitamin D, exerts its immunomodulatory activities and affects inflammatory responses not only by regulating cell function at a cellular level but also by modulating cytokine profiles on a molecular level of various cells. These cells, including macrophages, dendritic cells, T cells, and B cells, either belonging to innate or adaptive immunity, are essential for the immune system. Other than regulating immunity-mediated inflammation responses, 1,25(OH)2D3 can also be an effective modulator for inflammation through the prostaglandin and NFκB pathways, of which the prostaglandin pathway is the major targets of NSAIDs, emphasizing the diversity of the anti-inflammatory potential of 1,25(OH)2D3 and its analogs. Currently, it is short of 1,25(OH)2D3 analogs concentrating on their anti-inflammatory activities, which can be seen from limited reporting analogs and numbered literature reports. However, some analogs have been proven to be potent anti-inflammatory VDR agonists by a series of positive efficacies such as inhibiting pro-inflammatory cytokine profiles, suppressing immune cell-mediated inflammatory responses, and ameliorating symptoms in inflammatory diseases. Moreover, it is beneficial to apply the combination therapy strategy, vitamin D analogs and other effective therapies, since this may enhance the efficacy or reduce the side effects of standard therapies. Therefore, we believe that there is still promising potential for 1,25(OH)2D3 analogs awaiting more investigation for future treatments of inflammatory diseases.

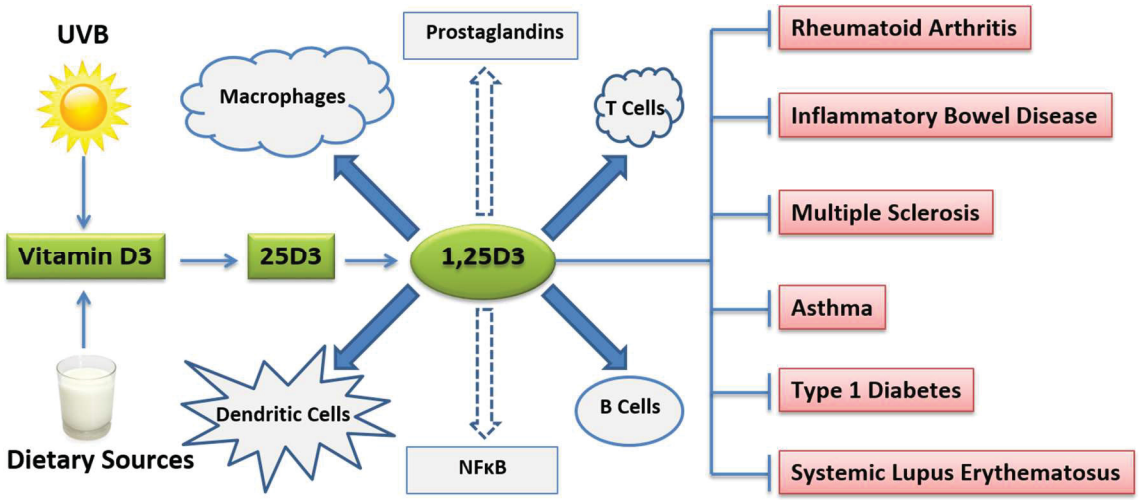

Figure 1-4. Summary of the associations between 1,25(OH)2D3 and inflammatory diseases.

CHAPTER 2. DESIGN, SYNTHESIS AND BIOLOGICAL ACTIVITIES OF NOVEL GEMINI 20S-HYDROXYVITAMIN D3 ANALOGS*

Vitamin D3 (D3) can be metabolized by cytochrome P450scc (CYP11A1) into 20*S*-hydroxyvitamin D3 [20S(OH)D3]as a major metabolite. This bioactive metabolite has shown strong antiproliferative, antifibrotic, pro-differentiation and anti-inflammatory effects while being non-toxic (non-calcemic) at high concentrations. Since D3 analogs with two symmetric side chains (Gemini analogs) result in potent activation of the vitamin D receptor (VDR), we hypothesized that the chain length and composition of these types of analogs also containing a 20-hydroxyl group would affect their biological activities. In this study, we designed and synthesized a series of Gemini 20S(OH)D3 analogs. Biological tests showed that some of these analogs are partial VDR activators and can significantly stimulate the expression of mRNA for *VDR* and VDR-regulated genes including *CYP24A1* and transient receptor potential cation channel V6 (*TRPV6*). These analogs inhibited the proliferation of melanoma cells with potency comparable to that of 1α,25-dihydroxyvitamin D3. Moreover, these analogs reduced the level of interferon γ and up-regulated the expression of leukocyte associated immunoglobulin-like receptor 1 in splenocytes, indicating that they have potent anti-inflammatory activities. There are no clear correlations between the Gemini chain length and their VDR activation or biological activities, consistent with the high flexibility of the ligand-binding pocket of the VDR.

Introduction

The production, activation and metabolism of vitamin D3 (D3) involves the participation of a variety of tissues and organs [20]. In the epidermis of the skin, D3 is produced from ultraviolet (UV) irradiation causing photoconvesion of 7-dehydrocholesterol (7DHC) to pre-D3, which undergoes thermal isomerization to D3. On the systemic level, activation of D3 involves initial hydroxylation in the liver by a 25-hydroxylase [cytochrome P450 2R1 (CYP2R1) or cytochrome P450 (CYP27A1)] followed by 1α-hydroxylation by CYP27B1 in the kidney to form its biological active form, 1α,25-dihydroxyvitamin D3 [1,25(OH)2D3, **Figure 2-1**]. 1,25(OH)2D3 acts through the vitamin D receptor (VDR) and regulates the expression of a variety of genes involved in immunomodulation, anti-inflammation, anti-proliferation, pro-differentiation, anti-angiogenesis, pro-apoptosis, mineral homeostasis and vitamin D catabolism [194, 195]. One of these genes, *CYP24A1*, encodes D3 24-hydroxylase which sequentially oxidizes the side chain of 1,25(OH)2D3 producing 1α,24*R*,25-trihydroxyvitamin D3 [1,24,25(OH)3D3], 24-oxo-1,25(OH)2D3, 24-oxo-1α,23,25-trihydroxyvitamin D3, 23-oxo-24,25,26,27-tetranor-1α,-hydroxyvitamin D3, and finally calcitroic acid for excretion [9, 196].

---

*Adapted with permission. Lin Z, Marepally, SR, et al. Design, Synthesis and Biological Activities of Novel Gemini 20S-Hydroxyvitamin D3 Analogs. *Anticancer. Res.* 2016, 36(3), 877-886.

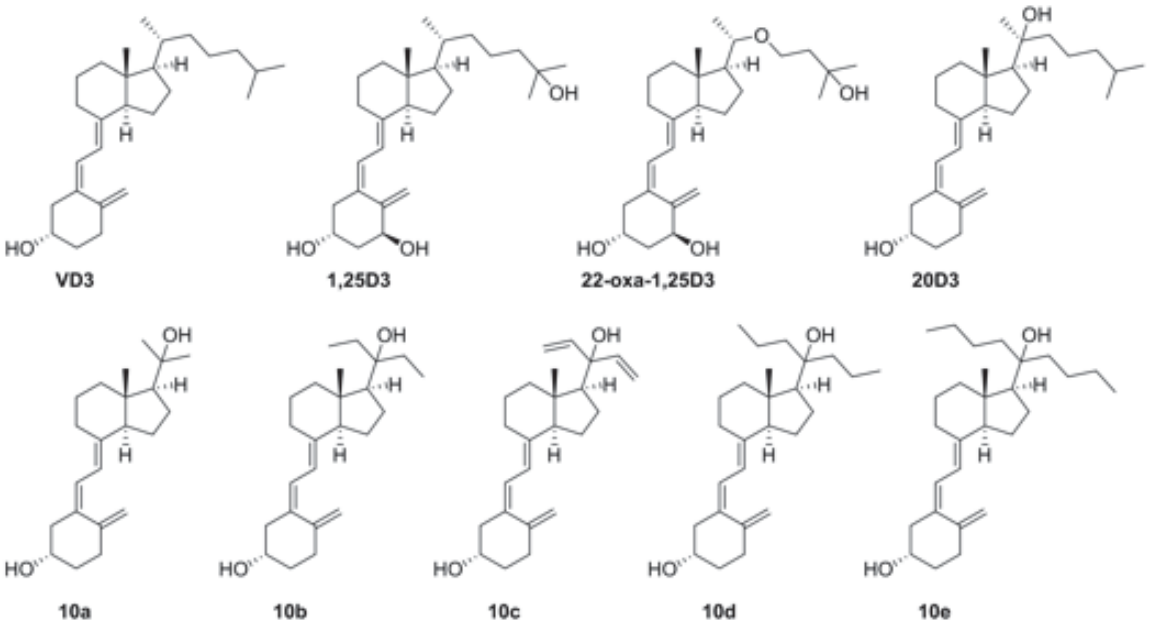

Figure 2-1. Chemical structures of vitamin D_3 (D_3), 1α,25-dihydroxyvitamin D_3 [1,25(OH)2D3], 22-oxa-1α,25-dihydroxyvitamin D_3 (22-oxa), 20*S*-hydroxyvitamin D_3 [20S(OH)D3] and its five Gemini analogs (10a-10e).

We previously reported the identification and characterization of a new metabolic pathway, in addition to the classical pathway described above, for activation of D3 [9, 197-199]. This pathway is initiated by mammalian CYP11A1 (also known as cytochrome P450scc) acting on D3 to produce 20*S*-hydroxyvitamin D3 [20S(OH)D3] as the major product [198, 200], which can be further metabolized into di- and tri-hydroxy products by CYP11A1 and other vitamin D-metabolizing enzymes such as CYP24A1, CYP27A1 and CYP27B1 [9, 198, 201]. Importantly, 20S(OH)D3 and its di- and tri-hydroxymetabolites accumulate *in vivo* in the human epidermis and serum [202]. 20S(OH)D3 produces a number of biological effects similar to those of 1,25(OH)2D3, acting as a biased agonist on the VDR [198, 203], but lacks the calcemic effect. High doses of 20S(OH)D3 (up to 30 μg/kg) do not cause hypercalcemia in rats or mice, while 1,25(OH)2D3 has substantial hypercalcemic effects (toxicity) at a dose as low as only 2 μg/kg [204, 205]. Thus 20S(OH)D3 has the potential to be used at therapeutic doses without toxicity. 20S(OH)D3 displays antiproliferative, pro-differentiation and anti-inflammatory properties in many cell lines [198, 206]. In addition, 20S(OH)D3 is able to inhibit the growth of solid tumors [207] and leukemia [204], indicating its tumorostatic activities, and it has shown antifibrotic activity *in vitro* and *in vivo* [205, 208, 209].

Gemini analogs of D3 are characterized by having two symmetric side chains at C20. Many Gemini D3 analogs have been synthesized to investigate the contribution of the extra side chain to their drug-like properties [210, 211]. To determine the effects of chain length and composition in the Gemini analogs also possessing a 20-hydroxyl group, we designed and synthesized a series of 20S(OH)D3 Gemini analogs (**Figure 2-2**) based on our established synthetic route [206]. Biological activities including VDR activation, expression of VDR-regulated genes, and inhibition of proliferation and inflammation were investigated for these Gemini analogs by comparison of their properties with those of positive controls.

Materials and Methods

Chemicals

The starting material pregnenolone acetate was purchased from Bosche Scientific LLC (New Brunswick, NJ, USA) with a purity above 98% as determined by high-performance liquid chromatography (HPLC). HPLC-grade acetonitrile was purchased from Fisher Scientific (Hampton, NH, USA). De-ionized water was prepared by a Milli-Q purification system for the HPLC mobile phases. Vitamin D3 (Sigma-Aldrich, St. Louis, MO, USA) was used as standard reference to generate HPLC standard curves to quantify small aliquots of vitamin D3 analogs.

Chemistry

All reagents and solvents for the synthesis and separation were purchased from commercial sources and were used as received. Reactions of 5,7-diene compounds were carried out in the dark by wrapping the flasks with aluminum foils. Moisture- or air-

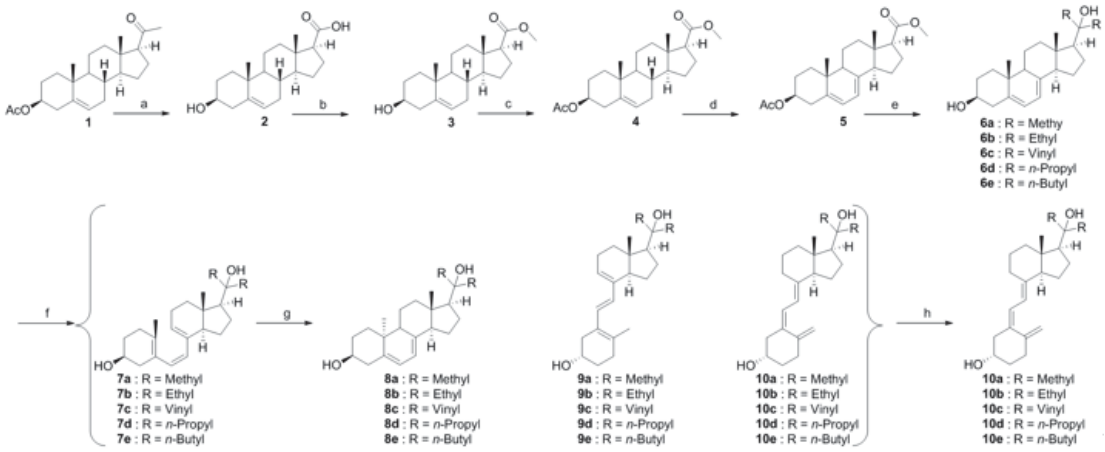

Figure 2-2. Synthetic route for producing Gemini analogs of 20-hdroxyvitamin D_3.

Reagents and conditions: (a) NaOH, Br_2, 0°C then warmed up to r.t., overnight. (b) H_2SO_4, methanol, reflux 2 h. (c) Acetic anhydride, pyridine, 4-dimethylaminopyridine (DMAP), 6 h. (d) Dibromantin, azobisisobutyronitrile (AIBN), benzene: hexane (1:1), reflux 20 min; tetra-*n*-butylammonium bromide (TBAB), tetrahydrofuran (THF), r.t., 75 min, then tetra-*n*-butylammonium fluoride (TBAF), r.t., 50 min. (e) Grignard reagent in THF, THF, 0 °C then warmed up to r.t., 8 h (**6c**: vinyl magnesium bromide, $CeCl_3$, −78°C then warmed up to r.t., 24 h). (f) Ultraviolet B (UVB), diethyl ether, 15 min. (g) Ethanol, reflux, 3 h. (h) High-performance liquid chromatography, acetonitrile:H_2O.

sensitive reactions were performed under an argon atmosphere. All reactions were routinely monitored by thin layer chromatography (TLC) on silica gel using ethyl acetate and hexane as mobile phases, and visualized by 5% phosphomolybdic acid in ethanol or UV lights. Mass spectra of all compounds were obtained by a Bruker ESQUIRE-LC/MS system (Bruker Corporation, Billerica, MA, USA) equipped with an electrospray ionization (ESI) source. Nuclear magnetic resonance (NMR) spectra were recorded by either a Bruker Avance III 400 MHz or an Agilent Unity Inova 500 MHz spectrometer. High-resolution mass spectrometry (HRMS) was carried out based on our previous methods [212, 213] by a Waters Acquity™ ultra-performance liquid chromatography system (Milford, MA, USA) equipped with a Waters Xevo™ G2-S quadrupole time-of-flight mass spectrometer and an ESI source in positive mode. Ethyl acetate was used for extraction of reaction mixtures and then dried over anhydrous Na_2SO_4, filtered and removed using a rotary evaporator under reduced pressure.

Synthesis of (3S,8S,10R,13S,14S,17S)-3-hydroxy-10,13-dimethyl-2,3,4,7,8,9,10,11,12,13,14,15,16,17-tetradecahydro-1H-cyclopenta[a]phenanthrene-17-carboxylic acid (**2**). Bromine (2.9 g, 18 mmol, 4.5 equiv.) was added dropwise to a vigorously stirred solution of NaOH (2.1 g, 54 mmol, 13.5 equiv.) in 18 mL H_2O at 0ºC. The mixture was stirred until all the bromine was dissolved and then diluted with 12 mL of cold 1,4-dioxane. The resulting hypobromite solution was added slowly to a stirred solution of 1.4 g (4.0 mmol, 1 equiv.) of pregnenolone acetate (**1**) in 56 mL of 1,4-dioxane and 16 mL H_2O. The reaction was monitored by TLC (ethyl acetate: hexanes=1:4) until all pregnenolone acetate was converted to one more polar spot. After stirring overnight, sodium sulfite (0.7 g, 18 mmol, 4.5 equiv.) solution was added to destroy the remaining oxidizing agent. The resulting mixture was then heated to reflux until all solid material dissolved. Acidification of the solution with concentrated HCl furnished a white precipitate which was filtered, washed with water and dried to yield 1.2 g product (3.9 mmol, 96 %). [214] ^{1}H NMR (400 MHz, Chloroform-*d*) δ 5.19 (dd, *J* = 4.9, 2.2 Hz, 1H), 3.31 (tt, *J* = 10.7, 4.8 Hz, 1H), 3.20 (p, *J* = 1.6 Hz, 2H), 2.19 (t, *J* = 9.3 Hz, 1H), 2.09 (qdd, *J* = 13.1, 9.0, 4.0 Hz, 2H), 1.99 – 1.79 (m, 3H), 1.72 (t, *J* = 3.6 Hz, 1H), 1.55 (tdd, *J* = 12.2, 6.9, 3.6 Hz, 1H), 1.42 (ddt, *J* = 16.5, 12.7, 3.0 Hz, 2H), 1.37 – 1.23 (m, 3H), 1.12 (tdd, *J* = 12.0, 7.8, 5.1 Hz, 2H), 1.03 – 0.88 (m, 2H), 0.86 (s, 3H), 0.84 – 0.77 (m, 1H), 0.57 (s, 3H). MS (ESI) *m/z* 317.1 $[M-H]^-$.

Synthesis of (3S,8S,10R,13S,14S,17S)-methyl 3-hydroxy-10,13-dimethyl-2,3,4,7,8,9,10,11,12,13,14,15,16,17-tetradecahydro-1H-cyclopenta[a]phenanthrene-17-carboxylate (**3**). To the carboxylic acid **2** (1.2 g, 3.9 mmol) in methanol (50 mL) was added concentrated sulfuric acid (0.5 mL). The mixture was heated to reflux for 4 h, cooled to room temperature and 20 mL of saturated Na_2CO_3 added. After removing methanol under reduced pressure, the residue was extracted with ethyl acetate (2 × 20 mL). The combined organic layer was washed with water (50 mL), dried over anhydrous Na_2SO_4. Removal of ethyl acetate gave ester (**3**) as a white powder (1.2 g, 3.7 mmol, 97%). ^{1}H NMR (400 MHz, Chloroform-*d*) δ 5.36 (dt, *J* = 5.4, 2.0 Hz, 1H), 3.68 (s, 3H), 3.53 (tt, *J* = 11.2, 4.7 Hz, 1H), 2.36 (t, *J* = 9.3 Hz, 1H), 2.33 – 2.17 (m, 2H), 2.17 – 2.08 (m, 1H), 2.00 (ddt, *J* = 7.5, 4.9, 2.7 Hz, 1H), 1.84 (dddd, *J* = 19.4, 13.8, 7.1, 3.3 Hz, 3H), 1.77 – 1.65 (m, 1H), 1.65 – 1.56 (m, 2H), 1.56 – 1.45 (m, 2H), 1.45 – 1.38 (m, 1H), 1.36

– 1.21 (m, 2H), 1.17 – 1.04 (m, 2H), 1.02 (s, 3H), 1.00 – 0.93 (m, 1H), 0.92 – 0.80 (m, 1H), 0.68 (s, 3H). MS (ESI) *m/z* 355.4 $[M+Na]^+$.

Synthesis of (3S,8S,10R,13S,14S,17S)-methyl 3-acetoxy-10,13-dimethyl-2,3,4,7,8,9,10,11,12,13,14,15,16,17-tetradecahydro-1H-cyclopenta[a]phenanthrene-17-carboxylate (**4**). To a solution of **3** (1.2 g, 3.7 mmol) in pyridine (30 mL) acetic anhydride (1.1 g, 11.1 mmol, 3 equiv.) and catalytic DMAP (0.05 equiv.) were added. The reaction mixture was stirred at room temperature for 6 h, quenched with 1 N HCl (50 mL), and filtered. The solid residue was washed with water, dried, collected to afford **4** as a white powder (1.3 g, 3.5 mmol, 91%). ^{1}H NMR (400 MHz, Chloroform-*d*) δ 5.37 (dt, *J* = 5.1, 1.6 Hz, 1H), 4.71 – 4.50 (m, 1H), 3.67 (s, 3H), 2.40 – 2.32 (m, 2H), 2.32 – 2.25 (m, 1H), 2.22 – 2.08 (m, 1H), 2.05 (s, 1H), 2.04 (s, 1H), 2.02 – 1.95 (m, 1H), 1.92 – 1.83 (m, 2H), 1.83 – 1.75 (m, 1H), 1.75 – 1.67 (m, 1H), 1.67 – 1.63 (m, 1H), 1.63 – 1.53 (m, 2H), 1.53 – 1.37 (m, 2H), 1.35 – 1.21 (m, 3H), 1.20 – 1.06 (m, 2H), 1.02 (s, 3H), 1.01 – 0.94 (m, 1H), 0.92 – 0.77 (m, 1H), 0.67 (s, 3H). MS (ESI) *m/z* 397.4 $[M+Na]^+$.

Synthesis of (3S,10R,13S,14R,17S)-methyl 3-acetoxy-10,13-dimethyl-2,3,4,9,10,11,12,13,14,15,16,17-dodecahydro-1H-cyclopenta[a]phenanthrene-17-carboxylate (**5**). To a solution of compound **4** (1.3 g, 3.7 mmol) in benzene:hexanes (40 mL, 1:1, v/v), dibromantin (634 mg, 2.2 mmol, 0.6 equiv.) and 2,2'-azobisisobutyronitrile (12 mg, 0.07 mmol, 0.02 equiv.) were added. The mixture was refluxed for 20 min in a preheated oil bath (100ºC), then cooled to 0ºC and filtered to remove insoluble material. The filtrate was concentrated to a pale-yellow oil. To this oil were added THF (40 mL) and tetrabutylammonium bromide (298 mg, 0.925 mmol, 0.25 equiv.). The mixture was stirred at r.t. for 75 min, then was added tetrabutylammonium fluoride (7.4 mL, 1.0 M solution in THF, 2 equiv.) and stirred for another 50 min in dark. After addition of water (30 mL), the mixture was extracted with ethyl acetate (3 × 30 mL). The organic layer was combined, dried over Na_2SO_4 and concentrated. The residue was subjected to flash chromatography (hexanes:ethyl acetate) to give **5** as a white solid (620 mg, 45%). ^{1}H NMR (400 MHz, Methanol-d_4) δ 5.59 (dd, *J* = 5.8, 2.6 Hz, 1H), 5.48 – 5.41 (m, 1H), 4.66 (tdd, *J* = 11.4, 4.9, 3.9 Hz, 1H), 3.69 (s, 3H), 2.55 – 2.50 (m, 1H), 2.49 (q, *J* = 2.9 Hz, 1H), 2.38 (ddd, *J* = 14.3, 11.9, 2.3 Hz, 1H), 2.24 – 2.15 (m, 1H), 2.12 (ddd, *J* = 12.8, 3.9, 2.5 Hz, 1H), 2.08 – 2.05 (m, 3H), 2.04 (s, 3H), 1.99 – 1.80 (m, 3H), 1.71 (ddt, *J* = 11.4, 9.8, 5.9 Hz, 2H), 1.65 – 1.52 (m, 2H), 1.39 (tt, *J* = 14.6, 5.4 Hz, 2H), 0.97 (s, 3H), 0.63 (s, 3H). MS (ESI) *m/z* 395.4 $[M+Na]^+$.

General procedure for **6a**, **6b**, **6d** and **6e**. To a stirred solution of ester **5** (50-100 mg, 1.0 equiv.) in anhydrous THF (10 mL) was added the corresponding Grignard reagent (0.5-2.0 M in THF, 5 equiv.) at 0ºC protected with argon gas. The reaction mixture was allowed to warm to r.t., stirred overnight, quenched with sat. NH_4Cl and extracted with ethyl acetate (3 × 20 mL). The organic layer was combined and washed with sat. $NaHCO_3$ (20 mL), brine (20 mL) and water (20 mL), dried over anhydrous Na_2SO_4 and concentrated. The crude mixture was subjected to flash chromatography (hexane: ethyl acetate) to give **6a**, **6b**, **6d** and **6e** (yield 55-91%), respectively.

Synthesis of (3S,10R,13S,14R,17S)-17-(2-hydroxypropan-2-yl)-10,13-dimethyl-2,3,4,9,10,11,12,13,14,15,16,17-dodecahydro-1H-cyclopenta[a]phenanthren-3-ol (**6a**). ^{1}H NMR (400 MHz, Chloroform-*d*) δ 5.58 (dd, *J* = 5.7, 2.6 Hz, 1H), 5.40 (dt, *J* = 5.6, 2.8 Hz, 1H), 3.64 (tt, *J* = 11.2, 4.2 Hz, 1H), 2.47 (ddd, *J* = 14.4, 4.8, 2.3 Hz, 1H), 2.28 (dddd, *J* = 18.9, 11.8, 5.9, 3.7 Hz, 1H), 2.18 (ddt, *J* = 10.6, 5.7, 2.9 Hz, 1H), 1.97 (ddt, *J* = 9.4, 7.1, 2.3 Hz, 1H), 1.93 – 1.84 (m, 2H), 1.84 – 1.67 (m, 3H), 1.67 – 1.53 (m, 2H), 1.53 – 1.39 (m, 2H), 1.39 – 1.34 (m, 1H), 1.33 (s, 3H), 1.32 – 1.22 (m, 2H), 1.22 (s, 3H), 1.2 (m, 1H), 0.95 (s, 3H), 0.78 (s, 3H). MS (ESI) *m/z* 353.4 $[M+Na]^+$. Yield 91%. HPLC purity > 98%. HRMS (ESI) *m/z* 313.2521 $[M+H-H_2O]^+$ (error: -3.2 ppm).

Synthesis of (3S,10R,13S,14R,17S)-17-(3-hydroxypentan-3-yl)-10,13-dimethyl-2,3,4,9,10,11,12,13,14,15,16,17-dodecahydro-1H-cyclopenta[a]phenanthren-3-ol (**6b**). ^{1}H NMR (400 MHz, Chloroform-*d*) δ 5.58 (dd, *J* = 5.8, 2.5 Hz, 1H), 5.40 (dt, *J* = 5.6, 2.8 Hz, 1H), 3.64 (tt, *J* = 11.2, 4.1 Hz, 1H), 2.47 (ddd, *J* = 14.4, 4.8, 2.3 Hz, 1H), 2.38 – 2.22 (m, 1H), 2.22 – 2.11 (m, 1H), 2.01 – 1.79 (m, 3H), 1.79 – 1.60 (m, 4H), 1.56 – 1.41 (m, 3H), 1.41 – 1.30 (m, 1H), 1.18 – 0.99 (m, 1H), 0.97 (d, *J* = 6.6 Hz, 2H), 0.95 (s, 3H), 0.90 (m, 2H), 0.88 (s, 2H), 0.88 – 0.85 (m, 3H), 0.81 (s, 3H), 0.79 (t, *J* = 7.6 Hz, 3H). MS (ESI) *m/z* 381.6 $[M+Na]^+$. Yield 85%. HPLC purity > 98%. HRMS (ESI) *m/z* 321.2844 $[M+H-H_2O]^+$ (error: 0.0 ppm).

Synthesis of (3S,10R,13S,14R,17S)-17-(3-hydroxypenta-1,4-dien-3-yl)-10,13-dimethyl-2,3,4,9,10,11,12,13,14,15,16,17-dodecahydro-1H-cyclopenta[a]phenanthren-3-ol (**6c**). To a flame-dried round bottom flask containing anhydrous $CeCl_3$ (782 mg, 3.2 mmol, 13 equiv.) was added anhydrous THF (20 mL). The solution was stirred for 1 h at room temperature under argon protection, and then cooled to -78ºC and stirred for 15 min. Then a 1.0 M vinyl magnesium bromide solution in THF was added (3.2 mmol, 13 equiv.) and stirred for another 1 h at -78 ºC. A THF solution (5 mL) of ester **5** (91 mg, 0.24 mmol, 1.0 equiv.) was then added and stirred for 3 h at -78ºC. The reaction mixture was then allowed to warm to room temperature, stirred for 48 h, quenched with sat. NH_4Cl (25 mL) and extracted with ethyl acetate (3 × 30 mL). The organic layer was combined and washed with sat. $NaHCO_3$ (30 mL), brine (30 mL) and water (30 mL), dried over anhydrous Na_2SO_4 and concentrated. The crude mixture was subjected to flash chromatography (hexane: ethyl acetate) to give **6c** as a white powder (74.6 mg, 0.21 mmol, 86%). [215] ^{1}H NMR (400 MHz, Chloroform-*d*) δ 6.06 (dd, *J* = 17.3, 10.7 Hz, 1H), 5.96 (dd, *J* = 17.3, 10.7 Hz, 1H), 5.57 (dd, *J* = 5.7, 2.5 Hz, 1H), 5.39 (dt, *J* = 5.6, 2.7 Hz, 1H), 5.23 (ddd, *J* = 37.5, 17.3, 1.3 Hz, 2H), 5.06 (ddd, *J* = 27.4, 10.7, 1.3 Hz, 2H), 3.71 – 3.55 (m, 0H), 2.47 (ddd, *J* = 14.3, 4.9, 2.4 Hz, 1H), 2.28 (t, *J* = 12.9 Hz, 1H), 2.18 (ddd, *J* = 12.6, 4.8, 2.5 Hz, 1H), 1.95 (t, *J* = 9.7 Hz, 1H), 1.91 – 1.80 (m, 2H), 1.79 – 1.62 (m, 3H), 1.57 (m, 1H), 1.49 – 1.38 (m, 2H), 1.34 – 1.23 (m, 3H), 1.18 (td, *J* = 13.0, 4.9 Hz, 1H), 0.93 (s, 3H), 0.88 – 0.82 (m, 1H), 0.73 (s, 3H). MS (ESI) *m/z* 377.4 $[M+Na]^+$. HPLC purity > 98%. HRMS (ESI) *m/z* 337.2528 $[M+H-H_2O]^+$ (error: -0.9 ppm).

Synthesis of (3S,10R,13S,14R,17S)-17-(4-hydroxyheptan-4-yl)-10,13-dimethyl-2,3,4,9,10,11,12,13,14,15,16,17-dodecahydro-1H-cyclopenta[a]phenanthren-3-ol (**6d**). ^{1}H NMR (400 MHz, Chloroform-*d*) δ 5.58 (dd, *J* = 5.7, 2.5 Hz, 1H), 5.40 (dt, *J* = 5.6, 2.7 Hz, 1H), 3.64 (tt, *J* = 11.3, 4.1 Hz, 1H), 2.47 (ddd, *J* = 14.3, 4.8, 2.3 Hz, 1H), 2.29 (ddq, *J*

= 13.7, 11.2, 2.1 Hz, 1H), 2.15 (ddd, *J* = 12.6, 4.8, 2.6 Hz, 1H), 2.02 – 1.92 (m, 1H), 1.92 – 1.79 (m, 3H), 1.79 – 1.68 (m, 2H), 1.67 – 1.53 (m, 3H), 1.53 – 1.47 (m, 1H), 1.47 – 1.39 (m, 2H), 1.39 – 1.27 (m, 3H), 1.27 – 1.17 (m, 2H), 0.95 (s, 3H), 0.94 – 0.85 (m, 14H), 0.81 (s, 3H). MS (ESI) *m/z* 409.5 $[M+Na]^+$. Yield 63%. HPLC purity > 98%. HRMS (ESI) *m/z* 369.3157 $[M+H-H_2O]^+$ (error: 0.0 ppm).

*S*ynthesis of (3S,10R,13S,14R,17S)-17-(5-hydroxynonan-5-yl)-10,13-dimethyl-2,3,4,9,10,11,12,13,14,15,16,17-dodecahydro-1H-cyclopenta[a]phenanthren-3-ol (**6e**). ^{1}H NMR (400 MHz, Chloroform-*d*) δ 5.51 (dd, *J* = 5.8, 2.5 Hz, 1H), 5.33 (dt, *J* = 5.6, 2.8 Hz, 1H), 3.57 (tt, *J* = 11.2, 4.0 Hz, 1H), 2.45 – 2.34 (m, 1H), 2.22 (t, *J* = 12.7 Hz, 1H), 2.12 – 2.05 (m, 1H), 1.89 (t, *J* = 9.5 Hz, 1H), 1.85 – 1.72 (m, 3H), 1.72 – 1.61 (m, 2H), 1.61 – 1.47 (m, 6H), 1.46 – 1.31 (m, 3H), 1.31 – 1.16 (m, 6H), 1.16 – 1.09 (m, 1H), 1.08 (s, 2H), 0.88 (s, 3H), 0.87 – 0.76 (m, 14H), 0.74 (s, 3H). MS (ESI) *m/z* 437.5 $[M+Na]^+$. Yield 55%. HPLC purity > 98%. HRMS (ESI) *m/z* 397.3468 $[M+H-H_2O]^+$ (error: -0.5 ppm).

General procedures for **10a-10e**. An ethyl ether solution of compound (2 mg/mL) was subjected to UVB irradiation for 15 min in a quartz tube at 75 °C, using a Rayonet RPR- 100 photochemical reactor (Branford, CT). After removal of ethyl ether, the residue was re-dissolved in ethanol (10 mL) and heated under reflux in dark for 3 h to allow the conversion from the pre-D3 structure (**7**) to the D3 structure (**10**). The mixture was then analyzed by an Agilent 1100 HPLC system (Santa Clara, CA) to optimize the separation conditions using acetonitrile and water as mobile phases. The ethanol solution was then concentrated to minimum volume for HPLC. The separation of D3 compound was carried out on a preparative HPLC system. The reaction mixture (100 μL) was injected onto a 5 μm Phenomenex Luna-PFP column (250 mm × 21.2 mm) (Torrance, CA) with mobile phases of acetonitrile and water at a flow rate of 15 mL/min using linear gradient conditions. Fractions containing D3 compounds were combined and freeze-dried. Yields for 10a-e 10%-18%.

Synthesis of (S,Z)-3-((E)-2-((1S,3aS,7aS)-1-(2-hydroxypropan-2-yl)-7a-methylhexahydro-1H-inden-4(2H)-ylidene)ethylidene)-4-methylenecyclohexanol (**10a**). ^{1}H NMR (400 MHz, Chloroform-*d*) δ 6.15 (d, *J* = 11.3 Hz, 1H), 5.96 (d, *J* = 11.2 Hz, 1H), 4.97 (dt, *J* = 2.6, 1.4 Hz, 1H), 4.74 (d, *J* = 2.5 Hz, 1H), 3.88 (s, 1H), 2.75 (dd, *J* = 12.1, 4.3 Hz, 1H), 2.56 – 2.44 (m, 1H), 2.32 (ddd, *J* = 13.1, 7.9, 4.8 Hz, 1H), 2.21 (dd, *J* = 13.1, 7.5 Hz, 1H), 2.10 (ddd, *J* = 13.6, 8.5, 4.7 Hz, 1H), 2.05 – 1.97 (m, 1H), 1.96 – 1.88 (m, 1H), 1.88 – 1.79 (m, 1H), 1.76 – 1.52 (m, 4H), 1.45 (m, 2H), 1.25 (s, 1H), 1.23 (s, 3H), 1.17 (s, 2H), 1.13 (m, 1H), 1.12 (s, 3H), 0.63 (s, 3H). MS (ESI) *m/z* 353.4 $[M+Na]^+$. HPLC purity > 98%. HRMS (ESI) *m/z* 313.2533 $[M+H-H_2O]^+$ (error: 0.6 ppm).

Synthesis of (S,Z)-3-((E)-2-((1S,3aS,7aS)-1-(3-hydroxypentan-3-yl)-7a-methylhexahydro-1H-inden-4(2H)-ylidene)ethylidene)-4-methylenecyclohexanol (**10b**). ^{1}H NMR (400 MHz, Methanol-d_4) δ 6.24 (d, *J* = 11.2 Hz, 1H), 6.04 (d, *J* = 11.2 Hz, 1H), 5.09 – 5.02 (m, 1H), 4.77 (dd, *J* = 2.8, 1.2 Hz, 1H), 3.78 (tt, *J* = 8.8, 4.0 Hz, 1H), 2.87 (dd, *J* = 11.8, 3.9 Hz, 1H), 2.55 (dd, *J* = 12.9, 4.1 Hz, 1H), 2.43 (dt, *J* = 13.6, 5.0 Hz, 1H),

2.26 – 2.16 (m, 1H), 2.16 – 2.07 (m, 2H), 2.07 – 1.92 (m, 2H), 1.92 – 1.79 (m, 1H), 1.79 – 1.61 (m, 6H), 1.61 – 1.45 (m, 6H), 1.45 – 1.35 (m, 2H), 0.93 – 0.79 (m, 1H), 0.89 (t, *J* = 7.5 Hz, 1H), 0.83 (t, *J* = 7.5 Hz, 3H), 0.74 (s, 3H). MS (ESI) *m/z* 381.6 $[M+Na]^+$. HPLC purity > 98%. HRMS (ESI) *m/z* 321.2842 $[M+H-H_2O]^+$ (error: -0.6 ppm).

Synthesis of (S,Z)-3-((E)-2-((1S,3aS,7aS)-1-(3-hydroxypenta-1,4-dien-3-yl)-7a-methylhexahydro-1H-inden-4(2H)-ylidene)ethylidene)-4-methylenecyclohexanol (**10c**). ^{1}H NMR (400 MHz, Methanol-d_4) δ 6.22 (d, *J* = 11.2 Hz, 1H), 6.12 – 5.96 (m, 3H), 5.22 (ddd, *J* = 32.5, 17.3, 1.7 Hz, 2H), 5.05 (dd, *J* = 2.8, 1.2 Hz, 1H), 5.00 (ddd, *J* = 32.5, 17.3, 1.7 Hz, 2H), 4.76 (dd, *J* = 2.8, 1.2 Hz, 1H), 3.78 (tt, *J* = 9.1, 3.9 Hz, 1H), 2.90 – 2.79 (m, 1H), 2.60 – 2.49 (m, 1H), 2.42 (dt, *J* = 13.6, 5.0 Hz, 1H), 2.27 – 2.19 (m, 1H), 2.14 (dddd, *J* = 13.7, 10.6, 4.6, 1.6 Hz, 2H), 1.99 (q, *J* = 9.2 Hz, 2H), 1.88 – 1.74 (m, 2H), 1.74 – 1.60 (m, 2H), 1.60 – 1.38 (m, 3H), 1.28 (td, *J* = 12.8, 3.9 Hz, 2H), 1.03 – 0.67 (m, 1H), 0.65 (s, 3H). MS (ESI) *m/z* 377.4 $[M+Na]^+$. HPLC purity > 98%. HRMS (ESI) *m/z* 337.2528 $[M+H-H_2O]^+$ (error: -0.9 ppm).

Synthesis of (S,Z)-3-((E)-2-((1S,3aS,7aS)-1-(4-hydroxyheptan-4-yl)-7a-methylhexahydro-1H-inden-4(2H)-ylidene)ethylidene)-4-methylenecyclohexanol (**10d**). ^{1}H NMR (400 MHz, Chloroform-*d*) δ 6.23 (d, *J* = 11.2 Hz, 1H), 6.03 (d, *J* = 11.3 Hz, 1H), 5.05 (dt, *J* = 2.6, 1.4 Hz, 1H), 4.82 (d, *J* = 2.5 Hz, 1H), 3.95 (s, 1H), 2.82 (dd, *J* = 11.7, 4.1 Hz, 1H), 2.57 (dd, *J* = 13.2, 3.8 Hz, 1H), 2.40 (ddd, *J* = 13.1, 7.9, 4.8 Hz, 1H), 2.29 (dd, *J* = 13.2, 7.5 Hz, 1H), 2.18 (ddd, *J* = 13.6, 8.5, 4.7 Hz, 1H), 2.12 – 2.02 (m, 1H), 2.02 – 1.86 (m, 2H), 1.87 – 1.75 (m, 1H), 1.69 (ddd, *J* = 11.6, 9.0, 5.6 Hz, 5H), 1.56 (d, *J* = 9.9 Hz, 3H), 1.45 – 1.27 (m, 5H), 1.27 – 1.15 (m, 2H), 1.09 (s, 1H), 0.90 (dt, *J* = 10.2, 7.1 Hz, 7H), 0.74 (s, 3H). MS (ESI) *m/z* 409.5 $[M+Na]^+$. HPLC purity > 98%. HRMS (ESI) *m/z* 369.3152 $[M+H-H_2O]^+$ (error: -1.4 ppm).

Synthesis of (S,Z)-3-((E)-2-((1S,3aS,7aS)-1-(5-hydroxynonan-5-yl)-7a-methylhexahydro-1H-inden-4(2H)-ylidene)ethylidene)-4-methylenecyclohexanol (**10e**). ^{1}H NMR (500 MHz, Chloroform-d) δ 6.23 (d, J = 11.2 Hz, 1H), 6.03 (d, J = 11.3 Hz, 1H), 5.05 (s, 1H), 4.82 (s, 1H), 3.95 (s, 1H), 2.82 (d, J = 13.1 Hz, 1H), 2.57 (d, J = 13.1 Hz, 1H), 2.39 (dd, J = 13.5, 6.6 Hz, 1H), 2.29 (dd, J = 13.2, 7.5 Hz, 1H), 2.23 – 2.11 (m, 1H), 2.06 (d, J = 15.8 Hz, 1H), 1.99 (t, J = 9.5 Hz, 1H), 1.92 (s, 1H), 1.84 – 1.75 (m, 1H), 1.74 – 1.63 (m, 4H), 1.56 (m, 2H), 1.44 – 1.33 (m, 1H), 1.33 – 1.22 (m, 8H), 1.19 (q, J = 7.2 Hz, 1H), 1.08 (s, 1H), 0.91 (q, J = 6.9 Hz, 10H), 0.74 (s, 3H). MS (ESI) *m/z* 437.5 $[M+Na]^+$. HPLC purity > 98%. HRMS (ESI) *m/z* 397.3469 $[M+H-H_2O]^+$ (error: -0.3 ppm).

HPLC Conditions

An Agilent HPLC 1100 series system consisting of a binary pump, a column oven, a degasser, a diode array detector and an autosampler was used for chromatographic analysis. The purity check of 20S(OH)D3 analogs was carried out on a Phenomenex Luna-PFP C18 column (5 μm, 250 mm × 4.6 mm; Phenomenex) maintained at 25 °C. The flow rate was 1.0 ml/min. The UV absorption at 263 nm was set for

displaying the chromatograms. Isocratic elution using water (A) and acetonitrile (B) was as follows: 60% B for compound **10a**, 70% B for compound **10b**, 70% B for compound **10c**, 80% B for compound **10d** and 90% B for compound **10e**.

Cell Culture

Dulbecco's modified Eagle's medium (DMEM) supplemented with glucose, L-gultamine, pyridoxine hydrochloride, 5% fetal bovine serum (FBS) and 1% penicillin/streptomycin/amphotericin antibiotic solution (Ab) (Sigma-Aldrich, St. Louis, MO, USA) was used to culture immortalized human keratinocytes (HaCaT). Jurkat cells were cultured in RPMI 1640 medium supplemented with 10% FBS and 1% Ab. Eagle's minimal essential medium (EMEM) containing 9% charcoal-stripped FBS, 100 U/ml penicillin and 100 μg/ml streptomycin, non-essential amino acids, 2.5 mM 2-mercaptoethanol and 2.5 mM L-glutamine was used to culture splenocytes from DBA/1 mice. All cells were cultured at 37°C in a humidified atmosphere containing 5% CO_2.

VDRE-luciferase Reporter Assay

Jurkat cells were purchased from American Type Culture Collection (Manassas, VA, USA) and were transduced with lentiviral VDRE luciferase using a Cignal Lenti VDRE Reporter (luc) Kit according to the manufacturer's protocol (QIAGEN, Valencia, CA, USA). The cells then went through 1-week selection under puromycin (1.0 μg/ml) treatment. During the selection, the media were changed every other day. For the biological test, transduced Jurkat cells were washed with PBS (1×) and then seeded in a 96-well plate (10,000 cells/well, 100 μl/well) diluted by FBS-free media. All cells were then synchronized by a 24 h incubation. DMSO solutions (10%; 1.0 μl) of each secosteroid were added to each well of cells with final concentrations of 1000, 300, 100, 30, 10, 3 and 1 nM, which were then incubated for another 24 h. The luciferase signal of the cells was measured by the ONE-Glo™ Luciferase Assay System (Promega, Madison, WI, USA) according to the manufacturer's suggested procedure. DMSO (10%) in water was used as the vehicle control and the final concentration of DMSO in culture media was 0.1% during the activity test. Each concentration of analog was tested in triplicate (n=3).

RT-PCR-based Expression Analysis

HaCaT cells were purchased from Thermo Fisher Scientific (Waltham, MA, USA) and were cultured as described above. The RNA from HaCaT keratinocytes treated with *10a-e*, 1,25(OH)2D3, 22-Oxa-1,25(OH)2D3 or DMSO was isolated using the Absolutely RNA Miniprep Kit (Stratagene, La Jolla, CA, USA). Reverse transcription (100 ng RNA/reaction) was performed with the Transcriptor First Strand cDNA Synthesis Kit (Roche Inc., Mannheim, Germany). Real-time PCR was performed using cDNA diluted 10-fold in sterile water and a SYBR Green PCR Master Mix. The primers for both forward and reverse lines for *VDR*, *CYP24A1* and *TRPV6* genes were designed

based on the mouse and rat sequences using Primer Quest software (Integrated Device Technology, San Jose, CA, USA). Reactions (in triplicate) were performed at 50°C for 2 min, 95°C for 10 min and then 40 cycles of 95°C for 15 s, 60°C for 30 s and 72°C for 30 s. Data were collected and analyzed on a Roche Light Cycler 480. The amount of the final amplified product for each gene was compared and normalized to the amount of β-actin as a housekeeping gene using a comparative Ct method [216].

Antiproliferative Assay

Antiproliferative assay was performed using the (3-(4,5-dimethylthiazol-2-yl)-5-(3-carboxymethoxyphenyl)-2-(4-sulfophenyl)-2H-tetrazolium)/phenazine methosulfate (MTS/PMS) solution (Promega, Madison, WI, USA) as per the manufacturer's instructions [217]. Briefly, SKMEL-188 cells provided as a gift from Dr. Andrzej T. Slominski were plated in on 96-well plates with Ham's F10 media containing 5% charcoal treated FBS (Atlanta Biologicals, Inc. Flowery Branch, GA, USA). After overnight culture, the medium was changed to serum-free medium to synchronize the cells for 24 h. Subsequently, the cells were incubated with compounds **10a-e** for 48 h. Finally, 20 µl of MTS/PMS solution was added to the cells and they were incubated for another 4 h at 37°C then the absorbance was recorded at 490 nm using Cytation 5 Cell Imaging Multi-Mode Reader (Winooski, VT, USA).

IFNγ Inhibition Assay

Compounds **10a-e** and 1,25(OH)2D3 were solubilized in absolute EtOH at 10^{-4} M and diluted to 10^{-6} M by adding EMEM as described above [218]. Splenocytes from DBA/1 mice were isolated, erythrocytes lysed by hypotonic shock, then cells were washed twice with EMEM, and suspended at 2×10^{6}/ml in supplemented EMEM described above. To each well of a 48-well tissue culture plate, 450 µl of the splenocytes were added. Analogs (50 µl of the 10^{-6} M stock), or EtOH diluted 1:100 with the above culture medium as negative control, were added to triplicate wells and then incubated at 37°C in 5% CO_2 in a humidified tissue culture incubator for 2 h, after which 1.0 µg/well of rat anti-mouse cluster of differentiation 3 (CD3) monoclonal antibody was added. After a 72 h incubation, supernatants from each well were harvested and analyzed by the enzyme-linked immunosorbent assay (ELISA) to determine the levels of D-murine IFNγ (R&D Systems, Minneapolis, MN, USA), according to the manufacturer's instructions. The concentration of IFNγ in supernatants from cultures containing analogs were compared with that of EtOH-treated control cultures, by ANOVA. Results are expressed as the mean of triplicate determinations ± SEM.

LAIR1 Assay by Flow Cytometry

Splenocytes from DBA/1 mice were isolated [195] and the level of expression of *LAIR1* was determined following overnight culture with each analog at a concentration of 10^{-7} M (or ethanol as vehicle control) by multi-parameter flow cytometry using an LSRII

flow cytometer (BD Biosciences, San Jose, CA, USA). Cells were labeled with fluorochrome antibodies specific for CD4 (BD Biosciences) and for LAIR1 (eBioscience, San Diego, CA, USA). Gating was performed on $CD4^+$ cells and the data were displayed as mean fluorescence ± standard deviation. A minimum of 10,000 cells were analyzed from each treated sample and the final analysis was performed using Flow software (Tree Star, Ashland, OR, USA). Results are expressed as the mean of duplicate values ± SEM.

Statistical Analysis

The values are reported as the means ± SD (or SE). The significance of the differences between different treatments was estimated by unpaired, two-tailed Student's *t*-test with $p<0.05$ considered as being statistically significant. All statistical analyses were performed and some of the figures were produced using GraphPad Prism 6.0 (Graph-Pad Software, San Diego, CA, USA).

Results

The designed 20S(OH)D3 analogs were synthesized starting from commercially available pregnenolone acetate (**1**). Due to the sensitivity of 5,7-diene structure to light, heat and acidic conditions, we chose to introduce the double bond at the C7 position in later steps [195]. Starting material **1** underwent haloform reaction with high yield (96%) to give the 3-hydroxyl acid **2** following our previously published procedure [214]. To generate the 20-hydroxyl group, the acid of **2** was firstly esterified, with quantitative yield, by methanol in the presence of sulfuric acid, to produce methyl ester **3.** The ester was then ready for the introduction of the same two aliphatic side chains in one Grignard reaction. The 3-hydroxyl group on **3** was then protected to give ester **4,** following our established acetylation procedure [195], for the introduction of C7 double bond. The 5,7-diene structure was then introduced into **4** by free radical reaction under dibromatin/AIBN/TBAB/TBAF conditions to provide the protected methyl ester **5** with acceptable yield (45%). Under dark conditions, the Grignard reaction was carefully carried out using different Grignard reagents in THF to introduce the two side chains to the C20 position where the 20-hydroxyl was formed as a result. Irradiation (15 min) of the 7DHC analogs in ethyl ether by UVB, followed by 3 hours reflux in ethanol gave D3 structures (**10**) together with their parent 7DHC, pre-vitamin D3 (**7**), lumisterol (**8**) and tachysterol (**9**) structures as related impurities. The separation of compounds in the reaction mixture after irradiation was achieved by preparative HPLC using a gradient of acetonitrile in water to afford the final D3 compounds (**10**) with high purity (> 98%) for biological testing.

To evaluate the capability of these analogs to interact with the VDR, a previously established Jurkat cell line transduced with a VDRE luciferase vector construct was used to carry out the reporter assays. We compared the activity of five analogs with that of two positive controls [1,25(OH)2D3 and 22-Oxa-1,25(OH)2D3] to activate the VDR *via* binding to the synthetic VDRE in this construct. In preliminary studies, these analogs lacked the ability to activate the VDR at a concentration of 0.1 μM, however, as shown in

Figure 2-3A, all five analogs significantly activated VDR at a concentration of 1.0 μM. The detected luciferase signal increased 31%, 20%, 27%, 20% and 33% as compared with blank controls for compounds **10a**, **10b**, **10c**, **10d** and **10e**, respectively. Compared with 1,25(OH)2D3 and 22-Oxa-1,25(OH)2D3, these analogs caused weak activation of the VDR causing 33 and 30 times less activation respectively, at 0.1 μM.

We compared the activity of the five synthetic analogs on the expression of *CYP24A1* gene in HaCaT cells to that of 1,25(OH)2D3 and 22-Oxa-1,25(OH)2D3 . As shown in **Figure 2-3B**, after 6 h treatment with 0.1 μM of each analog, relative mRNA levels for *CYP24A1* were 4.7-, 3.2-, 3.4-, 1.9- and 1.6-fold higher than that of the negative control for analogs **10a**, **10b**, **10c**, **10d** and **10e**, respectively. In comparison, cells treated with 0.1 μM 1,25(OH)2D3 or 22-Oxa-1,25(OH)2D3 showed a 366- or 370-fold increase in mRNA for *CYP24A1*, respectively. Following 24 h of treatment (**Figure 2-3C**), the positive controls still caused greater stimulation of *CYP24A1* gene expression than did the Gemini analogs, with the degree of stimulation for all compounds being less than at 6 h. Only **10a** and **10c** significantly stimulated expression over that of the control while 1,25(OH)2D3 and 22-Oxa-1,25(OH)2D3 caused 10- and 78-fold stimulation, respectively.

The ability of the new Gemini analogs to regulate the expression of the *VDR* gene was studied using HaCaT cells. As shown in **Figure 2-3D**, the mRNA expression level was stimulated by 1.4- to 3-fold by the Gemini analogs following 24 h of treatment with 0.1 μM. In addition, the two positive controls, 1,25(OH)2D3 and 22-Oxa-1,25(OH)2D3, also stimulated VDR expression by 1.3- and 1.7-fold, respectively, in comparison with the negative control. Interestingly, compound **10c** and **10e** caused significantly higher stimulation of the expression of the *VDR* gene than did 1,25(OH)2D3 ($p<0.05$), and analogs **10a**, **10b** and **10d** displayed much higher stimulation of VDR expression than both 1,25(OH)2D3 and 22-Oxa-1,25(OH)2D3 ($p<0.01$). These results suggest that the new analogs may increase D3 catabolism, not only by mild stimulation of the expression of the hydroxy-D3-catabolizing enzyme (CYP24A1), but also through increased expression of its own receptor, the VDR.

A well-known target of 1,25(OH)2D3 is the stimulation of the expression of the *TRPV6* gene (encoding an intestinal calcium channel) [219]. Because calcium plays an important role in keratinocytes differentiation, we evaluated the effects of the new Gemini 20S(OH)D3 analogs on the expression of this gene by immortalized human epidermal keratinocytes (HaCaT cells). The mRNA levels of *TRPV6* after a 24 h treatment were increased by 1.4- and 2.6-fold on 1,25(OH)2D3 and 22-Oxa-1,25(OH)2D3 treatment, respectively (**Figure 2-3E**). In contrast, the mRNA level for *TRPV6* was increased by 5.9-fold for analog **10a** relative to the negative control, but only by 1.5- to 2.7-fold for the other Gemini analogs, similarly to that for 1,25(OH)2D3 and 22-Oxa-1,25(OH)2D3 . Interestingly the analog with the shortest side chain (**10a**) caused 4-fold higher expression of the *TRPV6* gene expression than analog **10e** with the longest side chain, indicating that the short aliphatic side chain is most favorable for regulation of the *TRPV6* gene.

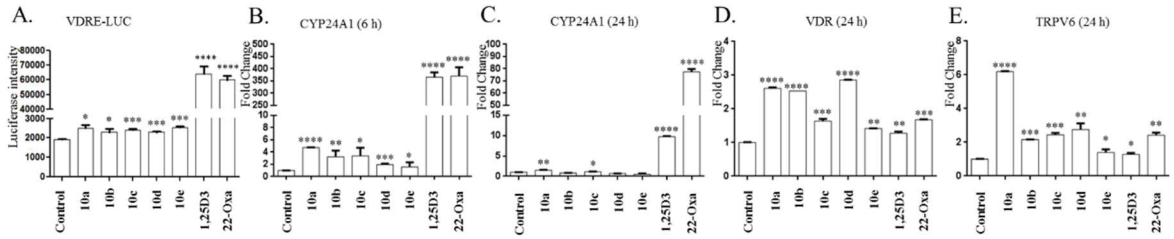

Figure 2-3. Gemini analogs of 20*S*-hydroxyvitamin D3 [20S(OH)D3] activate the VDR in a vitamin D response element-luciferase (VDRE-LUC) reporter assay and regulate cytochrome P450 24A1 (*CYP24A1*), vitamin D receptor (*VDR*) and transient receptor potential cation channel V6 (*TRPV6*) genes.

A: Jurkat cells transduced with a VDRE-LUC reporter construct were treated for 24 h with Gemini analogs (**10a**-**10e**, 1.0 μM), 1α,25-dihydroxyvitamin D3 [1,25(OH)2D3] (0.1 μM), 22-oxa-1,25(OH)2D3 (22-Oxa) (0.1 μM) or 10% dimethyl sulfoxide (DMSO) (final concentration 0.1% DMSO) as a negative control. Gemini 20S(OH)D3 analogs increased mRNA levels for *CYP24A*1 (**B** and **C**), *VDR* (**D**) and *TRPV6* (**E**). HaCaT cells were treated with 100 nM of Gemini analogs, 1,25(OH)2D3, 22-Oxa or DMSO only (solvent) as a control. The mRNA was isolated and the real-time polymerase chain reaction (RT-PCR) was performed using specific primers for *CYP24A1*, *VDR* and *TRPV6* genes. Data are presented as mean ± SE (n = 3). *p<0.05, **p<0.01, ***p<0.005 ****p<0.001 compared with the control.

One of the 20S(OH)D3 analogs, **10e,** inhibited SKMEL-188 melanoma cell proliferation with comparable potency (1.24×10^{-9} M) to that seen for 1,25(OH)2D3 (1.05×10^{-9} M), while analog **10d** had 15-fold lower potency than 1,25(OH)2D3 . Analogs **10a, 10b** and **10c** displayed no significant antiproliferative activity against the growth of SKMEL-188 melanoma cells. These results suggest that a long side chain is required to inhibit proliferation with a potency similarly to that of 1,25(OH)2D3 .

1,25(OH)2D3 acts as an immunomodulatory agent and displays anti-inflammatory activity [195, 196]. Thus many analogs of 1,25(OH)2D3 have been developed with the hope that they can be used as anti-inflammatory agents [196]. To test whether the new Gemini-20S(OH)D3 analogs can exert anti-inflammatory effects, IFNγ concentrations in the medium used to culture mouse splenocytes were measured using our established assay [195]. The Gemini analogs were tested at a concentration of 0.1 μM (**Figure 2-4B**). 1,25(OH)2D3 reduced the IFNγ concentration by 60% compared to the ethanol control. All the analogs significantly reduced IFNγ levels, with the most active compound being **10b**, which caused a 62% reduction in the IFNγ concentration (62%), comparable to that seen for 1,25(OH)2D3 .

Part of the anti-inflammatory activity of 1,25(OH)2D3 is mediated by the up-regulation of *LAIR1*. LAIR1 is a receptor expressed on T-cells and other immune cells believed to down-regulate the immune response [220]. The ability of the new Gemini analogs (100 nM) to up-regulate LAIR1 protein in splenocytes was compared with the EtOH negative control and a 22-Oxa-1,25(OH)2D3 (22-Oxa) positive control (**Figure 2-4C**). All the new Gemini analogs caused a significant increase in LAIR1 levels, generally comparable to that seen for the 22-Oxa positive control, with the highest stimulation being seen for analog **10e** (59%). The data suggest that all the Gemini-20S(OH)D3 analogs are strong anti-inflammatory agents.

Discussion

To completely remove the 3-acetyl group on intermediate **5**, at least four equivalences of Grignard reagents were required to form the desired product **6**. Among these 7DHC analogs, **6c** was not obtained through a normal Grignard reaction in our initial trials due to the formation of an α,β-unsaturated ketone after the first attack of the vinyl side chain. Fortunately, the addition of anhydrous $CeCl_3$ following a reported procedure [214] solved this problem and we ended up with an 86% yield. Grignard reagents with longer side chains (C≥5) were used to produce more 7DHC analogs (**6**), however after UVB irradiation, we were unable to separate the corresponding D3 structures from the mixture.

The Gemini-20S(OH)D3 analogs showed similar ability to activate the VDR and bind to a synthetic VDRE reporter construct, to their parent compound [20S(OH)D3]reported in our previous study [201]. Receptor activation was less than for than classical VDR activators [1,25(OH)2D3 and 22-Oxa-1,25(OH)2D3]. These results

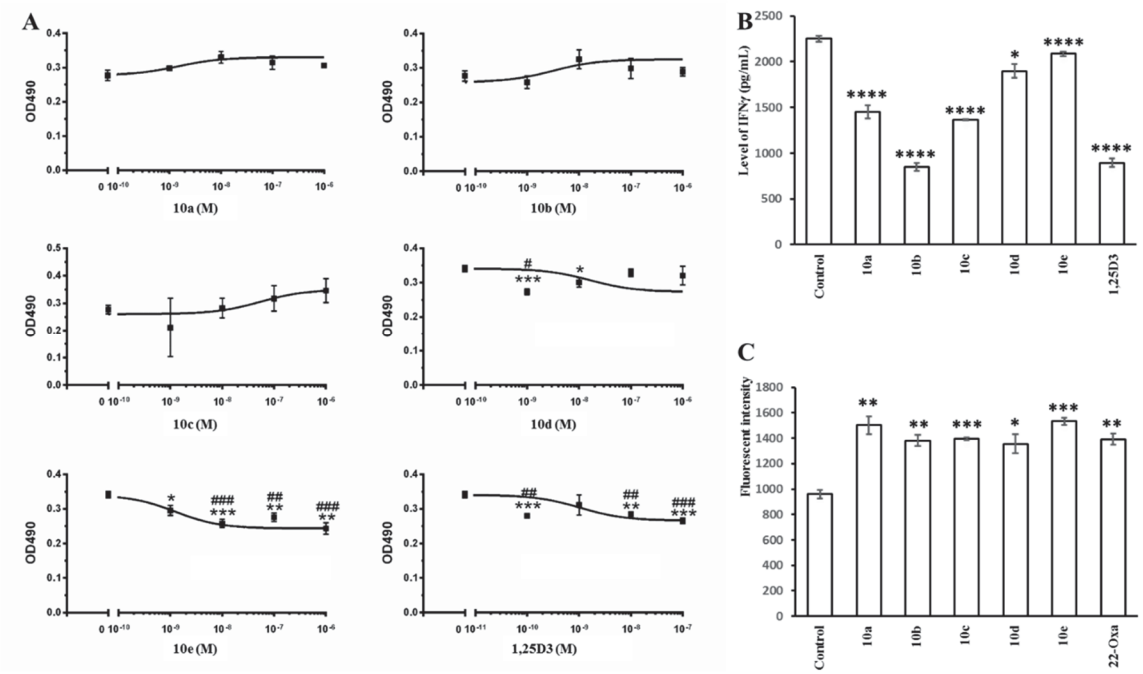

Figure 2-4. Antiproliferative effects of Gemini 20*S*-hydroxyvitamin D3 [20S(OH)D3] analogs on human SKEML-188 melanoma cells and anti-inflammatory effects on splenocytes.

A: SKEML-188 melanoma cells were treated with analogs, 1α,25-dihydroxyvitamin D3 [1,25(OH)2D3] or dimethyl sulfoxide (DMSO) (solvent) as a control to assess their inhibitory effects on cell growth. Gemini 20S(OH)D3 analogs reduced interferon γ (IFNγ) concentration (**B**) and up-regulated leukocyte-associated immunoglobulin-like receptor 1 (*LAIR1*) level (**C**) in mouse splenocytes. Splenic cells were treated by 100 nM of Gemini analogs, 1,25(OH)2D3, 22-Oxa or EtOH only (solvent) as a control. Data are presented as mean ± SE ($n = 3$). *p<0.05, **p<0.01, ***p<0.005, ****p<0.001 compared with the control. IC_{50s}: 1.65×10^{-8} M (**10d**), 1.24×10^{-9} M (**10e**) and 1.05×10^{-9} M [1,25(OH)2D3].

are consistent with these analogs acting as biased agonists on the VDR, similar to 20S(OH)D3 [198], where the ligand can influence the relative binding to different VDREs.

The *CYP24A1* gene has two VDREs and is highly responsive to 1,25(OH)2D3, but poorly responsive to 20S(OH)D3 [198, 201]. CYP24A1 is responsible for the catabolism of 25(OH)D3 and 1,25(OH)2D3 and can act on numerous vitamin D analogs [9, 196]. CYP24A1 initially hydroxylates the vitamin D side chain at C24 converting 1,25(OH)2D3 into 1,24,25(OH)3D3 [9, 195]. The ability of Gemini-20S(OH)D3 analogs to stimulate the expression of the *CYP24A1* gene, although only weakly, supports that they act through the VDR. Their inability to cause the massive induction seen with 1,25(OH)2D3 and 22-Oxa-1,25(OH)2D3 likely results in lower CYP24A1 protein levels and thus lower rates of catabolism, therefore promoting prolonged action. However, the ability of CYP24A1 to metabolize these analogs remains to be determined. Our data show that the Gemini 20S(OH)D3 analogs stimulate the expression of the *VDR* gene in HaCaT cells, suggesting they can up-regulate the basal expression level of their own receptor, the VDR. This might be an alternate way for them to exert their biological activities other than by directly modulating target genes, such as *CYP24A1*. Moreover, Gemini 20S(OH)D3 analogs were able to up-regulate the mRNA level of *TRPV6* which is a membrane calcium channel involved in the first step of calcium absorption in the intestine. The expression of *TRPV6* is reported to be vitamin D-dependent in mice and humans, and is greatly decreased in animals that do not express VDR [221]. In addition, TRPV6 is a direct target of the VDR and positively controls cell proliferation and apoptosis resistance in prostate cancer [222]. Investigating the modulating effects of D3 analogs on *TRPV6* gene is thus very important in order to understand the correlation between vitamin D compounds and their antiproliferative activity.

We have previously reported that 20S(OH)D3 has antiproliferative activity using a colony-forming model. 20S(OH)D3 showed comparable inhibition of colony formation to that by 1,25(OH)2D3 [206, 223], suggesting there is a great potential to use 20S(OH)D3 as a antitumor therapeutic agent, especially given its low calcemic activity. To evaluate the antiproliferative activity of our Gemini analogs, we tested them on the growth of SKMEL-188 cells. Compound **10e,** and to a lesser extent **10d,** had similar IC_{50}s (**Figure 2-4**) to 1,25(OH)2D3 . However, analogs with shorter side chains did not show significant inhibitory effects, indicating that a longer aliphatic side chains is necessary for antiproliferative activity.

IFNγ, or type II interferon, is the only member in the type II class of IFN. It is well known for its immunostimulatory and immunomodulatory effects and is critical for both innate and adaptive immunity [224]. For this reason, IFNγ is treated as a common inflammatory marker. Our previous studies have shown that D3 metabolites down-regulated IFNγ produced by mouse splenocytes [195, 198], inhibited interleukin 17 production by mouse T-lymphocytes [218] and down-regulated nuclear factor kappa-light-chain-enhancer of activated B cells, which is a master regulator of pro-inflammatory actions [225, 226]. The Gemini 20S(OH)D3 analogs caused similar decreases in IFNγ concentrations in cultured splenocytes to that of other D3 metabolites. To further validate their anti-inflammatory effects, flow cytometric measurements of LAIR1 protein levels in

splenocytes were made. LAIR1, also designated as CD305 (cluster of differentiation 305), is encoded by the *LAIR1* gene and is an inhibitory receptor expressed in many peripheral cells in both innate and adaptive immune systems, such as natural killer cells, T-cells and B-cells [227, 228]. It is an important anti-inflammatory marker due to its ability to prevent lysis of cells recognized as self during an immune response. Together with the inhibitory effects on IFNγ, the up-regulation of LAIR1 levels confirms a role for these analogs in the regulation of the immune responses and inflammation.

Summary

To conclude (**Figure 2-5**), the new Gemini 20S(OH)D3 analogs were able to activate the VDR. Analysis of gene expression at the mRNA level showed that the analogs regulated *CYP24A1*, *VDR* and *TRPV6* genes, consistent with their effects being mediated through activation of the VDR [198]. In addition, these analogs displayed antiproliferative and anti-inflammatory activity, which might also correlate with their VDR activation process. This study suggests that Gemini 20S(OH)D3 analogs have great potential as therapeutic agents on the immune system.

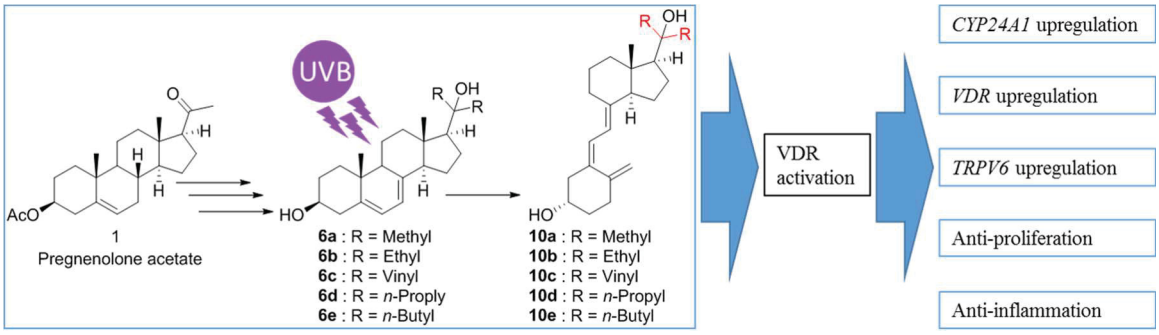

Figure 2-5. Summary of synthesis and biological activities of Gemini 20*S*-hydroxyvitamin D3 [20S(OH)D3] analogs used in this study.
The synthesis starts from pregnenolone acetate to obtain 7-dehydrocholesterol (7DHC) intermediates which were then irradiated by UVB to produce D_3 structures. These analogs likely exert their activities, including gene up-regulation, antiproliferative and anti-inflammatory effects, through activation of the vitamin D receptor (VDR).

CHAPTER 3. CHEMICAL SYNTHESIS AND BIOLOGICAL ACTIVITIES OF 20*S*,24*S*/*R*-DIHYDROXYVITAMIN D3 EPIMERS AND THEIR 1A-HYDROXYL DERIVATIVES*

Bioactive vitamin D3 metabolites 20*S*,24*S*-dihydroxyvitamin D3 [20*S*,24*S*(OH)2D3] and 20*S*,24*R*-dihydroxyvitamin D3 [20*S*,24R(OH)2D3] were chemically synthesized and confirmed to be identical to their enzymatically generated counterparts. The absolute configurations at C24 and its influence on the kinetics of 1α-hydroxylation by CYP27B1 were determined. Their corresponding 1α-hydroxyl derivatives were subsequently produced. Biological comparisons of these products showed different properties with respect to vitamin D3 receptor activation, anti-inflammatory activity, and anti-proliferative activity, with 1α,20S,24R(OH)2D3 being the most potent compound.

Introduction

Vitamin D3 (D3), obtained from either photoconversion of 7-dehydrocholesterol (7DHC) in the skin or dietary sources, plays an important role in the regulation of many physiological processes such as mineralization [229], inflammation [230], and cell proliferation and differentiation [231]. After entering the blood stream, D3 is carried by D3 binding protein (DBP) and is transported to the liver where it undergoes initial hydroxylation at C25 by the microsomal cytochrome P450 (CYP) enzyme 2R1 (CYP2R1) [3] or mitochondrial CYP27A1 [21] to produce 25-hydroxyvitamin D3 [25(OH)D3] (**Figure 3-1**). 25(OH)D3, the major circulating form of D3, is further hydroxylated by 1α-hydroxylase (CYP27B1) in the kidney to yield 1α,25-dihydroxyvitamin D3 [1,25(OH)2D3], the active form of D3. 1,25(OH)2D3 exerts its effects through the vitamin D receptor (VDR) as a native ligand, and modulates the expression of many genes including that encoding CYP24A1. CYP24A1 catalyzes the initial inactivation step of 1,25(OH)2D3 producing 1α,24*R*,25-trihydroxyvitamin D3 [1,24,25(OH)3D3], which is further oxidized by CYP24A1 to calcitroic acid which is excreted [9, 232, 233]. A more recently discovered pathway of D3 activation is catalyzed by CYP11A1, with 20*S*-hydroxyvitamin D3 [20*S*(OH)D3] being the initial and major product [197, 198, 233-236]. Although initially identified from *in vitro* studies, there is mounting evidence that this pathway occurs *in vivo* [237, 238]. 20*S*(OH)D3 acts as a biased agonist on the VDR and thus displays many but not all of the biological activities of 1,25(OH)2D3. Similar properties include promoting the differentiation and suppressing proliferation of keratinocytes, melanocytes, fibroblasts and melanoma cells [198, 216].

In contrast to 1,25(OH)2D3, 20*S*(OH)D3 is a poor inducer of CYP24A1 and is non calcemic in mice up to a dose of 60 μg/kg [206, 223] suggesting that it might be useful as

---

*Adapted with permission. Lin Z, et al. Chemical synthesis and biological activities of 20S,24S/R-dihydroxyvitamin D3 epimers and their 1alpha-hydroxyl derivatives. *J. Med. Chem.* 2015, 58(19), 7881-7. Copyright (2015) American Chemical Society.

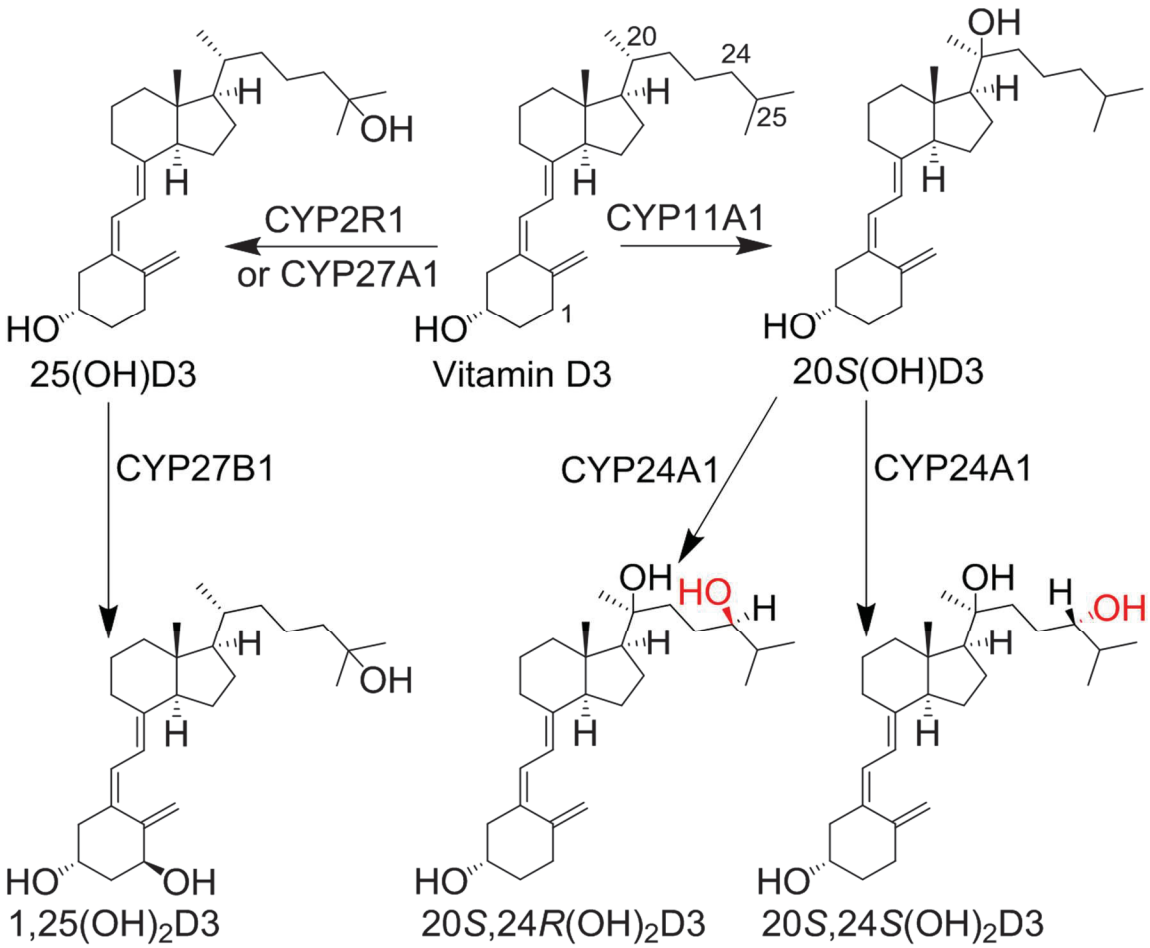

Figure 3-1. D3 conversion to 25(OH)D3, 1,25(OH)$_2$D3, 20*S*(OH)D3, 20*S*,24*R*(OH)$_2$D3 and 20*S*,24*S*(OH)$_2$D3.

a therapeutic agent. In addition, 20*S*(OH)D3 is an antagonist or inverse agonist of RORα and RORγ in skin cells [198]. It can exert anti-inflammatory effects through upregulation of IκB in the NFκB pathway [225, 239] or directly inhibit interleukin-17 (IL-17) production in different cell lines [198]. Rodent models further confirm its anti-inflammatory effects where reduced disease symptoms of scleroderma [240] and rheumatoid arthritis are observed after its administration[198]. Thus, the metabolism of 20*S*(OH)D3 by CYP24A1 and other P450s is of great importance in understanding its actions and fate.

Predictably, both rat and human CYP24A1 are able to hydroxylate 20*S*(OH)D3 producing both 20,24-dihydroxyvitamin D3 [20,24(OH)2D3] isomers [9, 241]. The major isomer made by CYP24A1 is also produced from 20(OH)D3 by a different P450, yet to be identified, in mouse liver microsomes[242]. Activity tests have shown that this isomer and its 1α-hydroxyderivative, are more potent than the parent 20*S*(OH)D3, markedly inhibiting colony formation of SKMEL 188 melanoma cells at low concentrations, suggesting enhanced therapeutic potential as anti-proliferative agents [9]. However, it has not been possible to establish the absolute configurations of these isomers at C24 to determine which is 20*S*,24*S*-dihydroxyvitamin D3 [20*S*,24*S*(OH)2D3] and which is 20*S*,24*R*-dihydroxyvitamin D3 [20*S*,24*R*(OH)2D3], due to the limited amount of these enzymatic products.

Thus, the aim of this study was to unambiguously assign the C24 configurations to the two 20*S*,24(OH)2D3 isomers as well as their 1α-hydroxy derivatives and to more comprehensively evaluate their biological activities. To this end, we made both isomers by chemical synthesis, assigned their structures by NMR and molecular modeling, determined their differential kinetics of 1α-hydroxylation by CYP27B1, and tested their biological activities. In addition, their 1α-hydroxy derivatives were enzymatically synthesized and tested for comparison of their activities with their parent 20,24(OH)2D3 isomers.

Experimental Section

General Methods

All reagents and solvents for the synthesis and separation were purchased from commercial sources and were used as received. Reactions of 5,7-diene structures were all carried out in the dark by wrapping the flasks with aluminum foil. Moisture- or air-sensitive reactions were performed under an argon atmosphere. All reactions were routinely monitored by TLC on silica gel using ethyl acetate and hexane as mobile phases, and visualized by 5% phosphomolybdic acid in ethanol or UV lights. Mass spectra of all compounds were obtained by a Bruker ESQUIRE-LC/MS system equipped with an ESI source. The purities of final D3 compounds, as analyzed by an Agilent 1100 HPLC system (Santa Clara, CA), were above 98%. Ethyl acetate was used for extraction of reaction mixtures and then dried over anhydrous Na2SO4, filtered and removed by rotary evaporator under reduced pressure. For comparison of retention times of

enzymatically [9, 241] and chemically gererated 20*S*,24(OH)2D3 isomers, HPLC was carried out with an acetonitrile in water gradient comprising 45 – 100% acetonitrile for 25 min, then 100% acetonitrile for 15 min, or a methanol in water gradient comprising 64 – 100% methanol for 20 min, then 100% methanol for 25 min, using a flow rate of 0.5 mL/min and a C18 column (Grace Alltima, 25 cm × 4.6 mm, particle size 5 μm).

NMR

A series of 1D and 2D NMR measurements were performed on the two chemically synthesized isomers, 20*S*,24*R*(OH)2D3 (isomer I), and 20*S*,24*S*(OH)2D3 (isomer II), using either a Bruker Avance III 400 MHz, with a BBO 5 mm probe with Z-gradient (Bruker BioSpin, Billerica, MA), or a Varian Unity Inova 500 MHz spectrometer using a 5 mm TXI probe (Agilent Technologies Inc., Santa Clara, CA, USA). Samples (~1.5 mg) were dissolved in 0.3 mL CD3OD using 5 mm Shigemi NMR tubes (Shigemi Inc., Allison Park, PA, USA). NMR data were collected at 25 °C. Chemical shifts were referenced to residual solvent peaks for CD3OD (3.31 ppm for proton and 49.15 ppm for carbon).

Kinetics of Metabolism by Mouse CYP27B1

To measure the kinetics of 1α-hydroxylation by CYP27B1, substrates [20*S*,24*R*(OH)2D3 and 20*S*,24*S*(OH)2D3] were incorporated into phospholipid vesicles prepared from dioleoylphosphatidylcholine and cardiolipin, as before [236]. Mouse CYP27B1 (0.01 μM for isomer I and 0.125 μM for isomer II) was incubated for 2 min with a range of substrate concentrations. Products were extracted with dichloromethane and analyzed by reverse-phase HPLC on a C18 column (Grace Smart, 15 cm × 4.6 mm, particle size 5 μm) with an acetonitrile gradient comprising 45 – 100% acetonitrile for 10 min then 100% acetonitrile for 10 min, at a flow rate of 0.5 mL/min. The Michaelis-Menten equation was fitted to the experimental data with correlation coefficients of 0.991 and 0.993 for isomers I and II, respectively. Data for K_m and k_{cat} are presented as mean ± standard error of the curve fit.

Enzymatic Synthesis of 1α-hydroxy-derivatives Using CYP27B1

These reactions were carried out with the 20*S*,24*R*(OH)2D3 and 20*S*,24*S*(OH)2D3 substrates incorporated into phospholipid vesicles using purified mouse CYP27B1, as reported previously [243], in a scaled up version of the incubations described above. 1α,20*S*,24*R*(OH)2D3 and 1α,20*S*,24*S*(OH)2D3 were purified by HPLC on a C18 column (Grace Alltima, 25 cm × 4.6 mm, particle size 5 μm) using an acetonitrile gradient comprising 45 – 100% acetonitrile for 25 min then 100% acetonitrile for 15 min, at a flow rate of 0.5 mL/min.

Cell Culture

Dulbecco's Modified Eagle Medium (DMEM) supplemented with glucose, *L*-gultamin, pyridoxine hydrochloride, 5% fetal bovine serum (FBS) and 1% penicillin/streptomycin/amphotericin antibiotic solution (Ab) (Sigma-Aldrich, St. Louis, MO) was used to culture immortalized human keratinocytes (HaCaT). The same medium using 10% FBS instead of 5% FBS was used to culture colonic Caco-2 cells. All cells were cultured at 37 °C in a humidified atmosphere containing 5% CO_2.

VDRE Reporter Assays

HaCaT and Caco-2 cells were transduced with lentiviral VDRE luciferase using a Cignal Lenti VDRE Reporter (luc) Kit according to the manufacturer's protocol (QIAGEN, Valencia, CA). After one week selection by puromycin (1 μg/mL), transduced HaCaT and Caco-2 cells were seeded in a 96-well plate (1000 cells/well) using partial media (without FBS) and incubated for 24 h. DMSO solutions of secosteroids to be tested were added to cells, which were then incubated for another 24 h and the luciferase signal measured according to the manufacturer's procedure for the ONE-GloTM Luciferase Assay System (Promega, Madison, WI). The final concentration of DMSO was 0.1% and 0.1% DMSO was used as the vehicle control. All concentrations were tested in triplicate.

Flow Cytometry

Splenocytes from DBA/1 mice were isolated [244] and the expression of LAIR-1 was determined following overnight culture with each secosteroid at a concentration of 10^{-7} M (or vehicle control) by multiparameter flow cytometry using an LSRII flow cytometer (BD Biosciences, San Jose, CA). Cells were labeled with fluorochrome antibodies specific for CD4 (BD Biosciences, San Jose, CA) and for LAIR-1 (eBioscience, San Diego, CA). Gating was performed on CD4 cells and the data was expressed as mean fluorescence ± SD. A minimum of 10,000 cells were analyzed from each sample and the final analysis was performed using Flow software (Tree Star, Ashland, OR). Values represent the mean fluorescence from two separate analyses.

IFNγ Inhibition Assay

Secosteroids were solubilized in absolute EtOH at 10^{-4} M and diluted to 10^{-6} M by adding Eagles Minimal Essential Medium (EMEM) containing 9% charcoal-stripped fetal calf serum, 100 U/mL penicillin and 100 μg/mL streptomycin, non-essential amino acids, 2.5 mM 2-mercaptoethanol, 2.5 mM *L*-glutamine [244]. Splenocytes from mice were isolated, erythrocytes lysed by hypotonic shock, washed twice with EMEM, and suspended at a concentration for 2×10^6/mL in EMEM described above. To each well in a 48-well tissue culture plate, 450 μL of the splenocytes were added. Secosteroids (50 μL of the 10^{-6} M stock) or EtOH diluted 1:100 with the above culture medium were added to

triplicate wells and then incubated at 37 °C in 5% CO_2 in a humidified tissue culture incubator for 2 h, after which 1 μg/well of rat anti-mouse CD3 MOAB was added. After 72 h culture, supernatants from each well were harvested and analyzed by ELISA for levels of D-murine IFNγ (RAD Systems, Minneapolis, MN), according to the manufacturer's instructions. The concentration of IFNγ is supernatants from cultures containing secosteroids were compared to the concentration of IFNγ in the supernatants of EtOH-treated control cultures, by ANOVA. Results are expressed as the mean of triplicate determinations ± SEM.

Results and Discussion

Chemistry

The detailed syntheses and spectral characterization of 20*S*,24*S*(OH)2D3 and 20*S*,24*R*(OH)2D3 are described in the **supporting information** [195]. Briefly, as shown in **Figure 3-2**, we started from commercially available pregnenolone acetate (**1**). We chose to avoid the formation of the C7 double bond in the initial steps, due to the instability of the 5,7-diene under light and acidic conditions. The 3-acetyl of **1** was removed under KOH/MeOH condition and replaced by TBS. The TBS protected silyl ether **3** was treated with allylmagnesium bromide to get the desired 20*S*-homoallylic alcohol **4** as a major product [214], in which the 20*S*-OH was protected with chloromethyl ethyl ether (EOMCl) using diisopropylethylamine in DCM at r.t. Hydroboration of the protected alkene **5** using 9-BBN followed by $NaOH/H_2O_2$ oxidation selectively gave the primary alcohol **6**, which was then oxidized by pyridinium dichromate (PDC) in dichloromethane (DCM) into the aldehyde **7**. This aldehyde was treated with isopropylmagnesium bromide in THF to produce the diastereomeric mixture **8**, which showed two separable spots on TLC (ethyl acetate:hexane) and gave two pure alcohols (**8a**, **8b**) after separation by flash chromatography. The separated alcohols were used for subsequent reactions separately to get both 7DHC diastereomers. Removal of C3 TBS by TBAF followed by reaction with acetic anhydride in pyridine gave the acetylated compounds **10**. To produce the 5,7-diene we used 1,3-dibromo-5,5-dimethylhydantoin (dibromantin)/AIBN/TBAB/TBAF conditions as reported previously [214]. To assure the stereochemistry of C3 and C24 stayed intact, EOM deprotection under acidic condition was carried out before deacetylation. EOM deprotection of **11** by strong acids such as HCl destroys the 5,7-diene structure, thus the weak acid CSA in methanol was chosen to deprotect EOM slowly with 30% yield (61% recovered). Further treatment of aqueous KOH in MeOH gave 20,24-dihydroxyl-7DHC compounds **13**. Irradiation of 7-DHC in ether by UVB light for 15 min, followed by reflux in ethanol produced vitamin D3 compounds **17a** and **17b** which were further separated by preparative HPLC using acetonitrile and water as mobile phases.

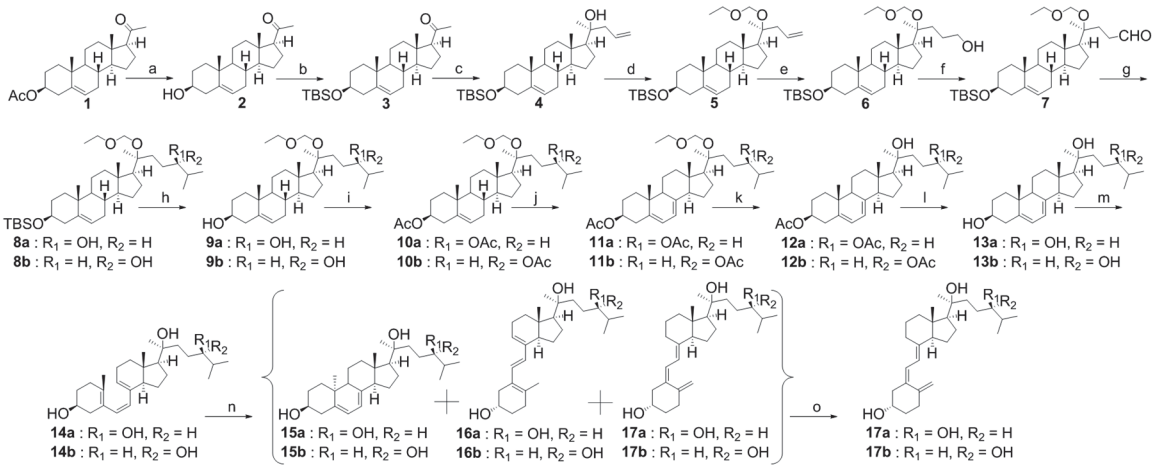

Figure 3-2. Synthesis of compounds 17a and 17b.
Reagents and conditions: (a) aq. KOH, MeOH, r.t., 2 h. 95%. (b) TBSCl, imidazole, DMF, r.t., overnight. 90%. (c) Allylmagnesium bromide, THF, 0 ºC - r.t., overnight. 82%. (d) EOMCl, DIPEA, CH_2Cl_2, r.t., overnight. 89%. (e) 9-BBN, THF, 0 ºC - r.t., 24 h; H_2O, r.t., 0.5 h; NaOH, H_2O_2, -20 ºC - r.t., overnight. 76%. (f) PDC, CH_2Cl_2, r.t., 24 h. 94%. (g) Isopropylmagnesium bromide, THF, 0 ºC - r.t., 6 h. 85%. (h) TBAF, THF, r.t., 12 h. 100%. (i) Ac_2O, pyridine, DMAP, 6 h. 91%. (j) Dibromantin, AIBN, Benzene: Hexane (1:1), reflux 20 min; TBAB, THF, r.t., 75 min, then TBAF, r.t., 50 min. 44%. (k) CSA, MeOH:DCM (1:1), 0 ºC - r.t., 12 h. 30% (61% recovered). (l) aq. KOH, MeOH, 2 h. 90%. (m) UVB, Et_2O, 15 min. (n) Ethanol, reflux, 3 h. (o) HPLC, ACN:H_2O. 13% (steps m, n and o). Overall yield 1.6%. TBSCl: *tert*-butyldimethylsilyl chloride, DMF: dimethylformamide, PDC: pyridinium dichromate, AIBN: azobisisobutyronitrile, ACN: acetonitrile.

HPLC Showed Matched Retention Times between Chemically Synthesized and Enzymatically Generated Counterparts

To confirm the chemically synthesized 20,24(OH)2D3 isomers were identical with enzymatically generated isomers, HPLC was used to compare their retention times. As shown in **Figure 3-3** and **Figure S15** [195], HPLC separation was carried out using two different solvent systems, either an acetonitrile in water gradient or a methanol in water gradient. Under both conditions retention times of each chemically synthesized isomer exactly matched that of the corresponding enzymatic product (see chromatograms of spiked samples in **Figure S15** [195]). Thus, the enzymatically generated isomer originally designated as product B in the original reports of its production by CYP24A1 [9, 241] is isomer I and that designated as product C is isomer II.

Structure Assignments of Isomer I as 17a and Isomer II as 17b

Further confirmation for the same structures between the synthesized and the original enzymatically generated isomers is provided by NMR. The NMR spectra of the chemically synthesized 20*S*,24*S/R*(OH)2D3 isomers are identical to those of the enzymatically generated products (**Figure 3-4A, C** for isomer I and **Figure 3-4B, D** for isomer II) [235, 245]. The distinct splitting patterns of the 26/27 methyl groups served as a fingerprint between isomers I (doublet) and II (pseudo triplet) as clearly indicated in **Figure 3-4A-D**. Full assignments for the ^{1}H and ^{13}C chemical shifts using 2D NMR for both chemically synthesized isomers based on data of several hydroxy-derivatives of vitamin D3 published previously were made [235, 245]. These assignments are summarized in **Table S2** [195], along with previously reported assignments for the enzymatic products for comparison [241].

To determine the absolute configuration at C24, we analyzed the NOESY spectra. In the NOESY spectra the relative integrals are 0.324 (isomer I), and 0.285 (isomer II) for the crosspeaks from 24H to 26/27-Me, using the NOE integral of the geminal 19-CH_2 as the internal reference (**Figure 3-4E**). The average distances from 24H to 26/27-Me are 3.07 Å (average of 3.04 and 3.10 Å), 3.44 Å (average of 2.99, and 3.88 Å), in 24*R* and 24*S*-configurations, respectively, based on the model structures (**Figure 3-4F**). Therefore, isomer I is tentatively assigned the 24*R*-configuration (**17a**), and isomer II to the 24*S*-configuration (**17b**).

In addition, the ^{1}H chemical shift patterns of the two geminal protons at C23 are distinct between isomer I (1.75 ppm and 1.39 ppm, a difference of 0.36 ppm) and isomer II (1.63 ppm and 1.44 ppm, a difference of 0.19 ppm) as shown in **Figure 3-4E** and HSQC spectra in **supporting information** (**Figure S16** [195]). Due to the severe overlap with other protons, reliable NOE integrals cannot be obtained between C24 proton and C23 protons. However, the distances from the oxygen atom of the C24-OH group to the two proton atoms at C23 were 2.62 Å, and 3.32 Å in 20*S*,24*R*(OH)2D3, and 2.57 Å, and 2.62 Å in the 20*S*,24*S*(OH)2D3 model structures (**Figure 3-4F**). Since the ^{1}H chemical shift is sensitive to the chemical environment, it is expected that difference between the

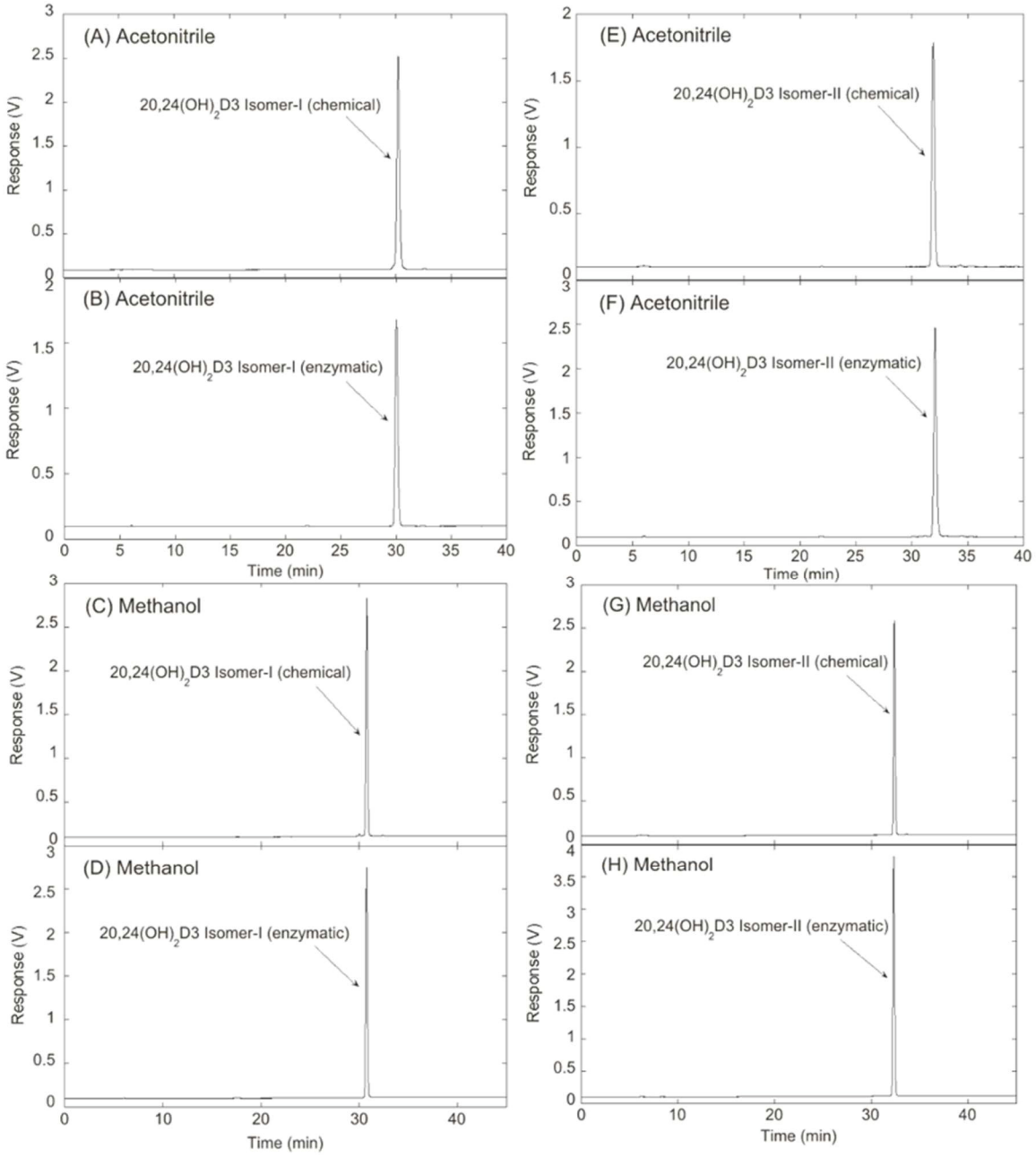

Figure 3-3. Comparison of HPLC retention times of 20,24(OH)$_2$D3 isomers produced enzymatically and chemically.
(**A**, **C**), Isomer I chemical; (**B**, **D**), Isomer I enzymatic; (**E**, **G**), Isomer II chemical; (**F**, **H**), Isomer II enzymatic. Samples were analyzed by reverse phase HPLC utilizing acetonitrile in water (**A**, **B**, **E**, and **F**) or methanol in water (**C**, **D**, **G** and **H**) gradients, as described in the Methods.

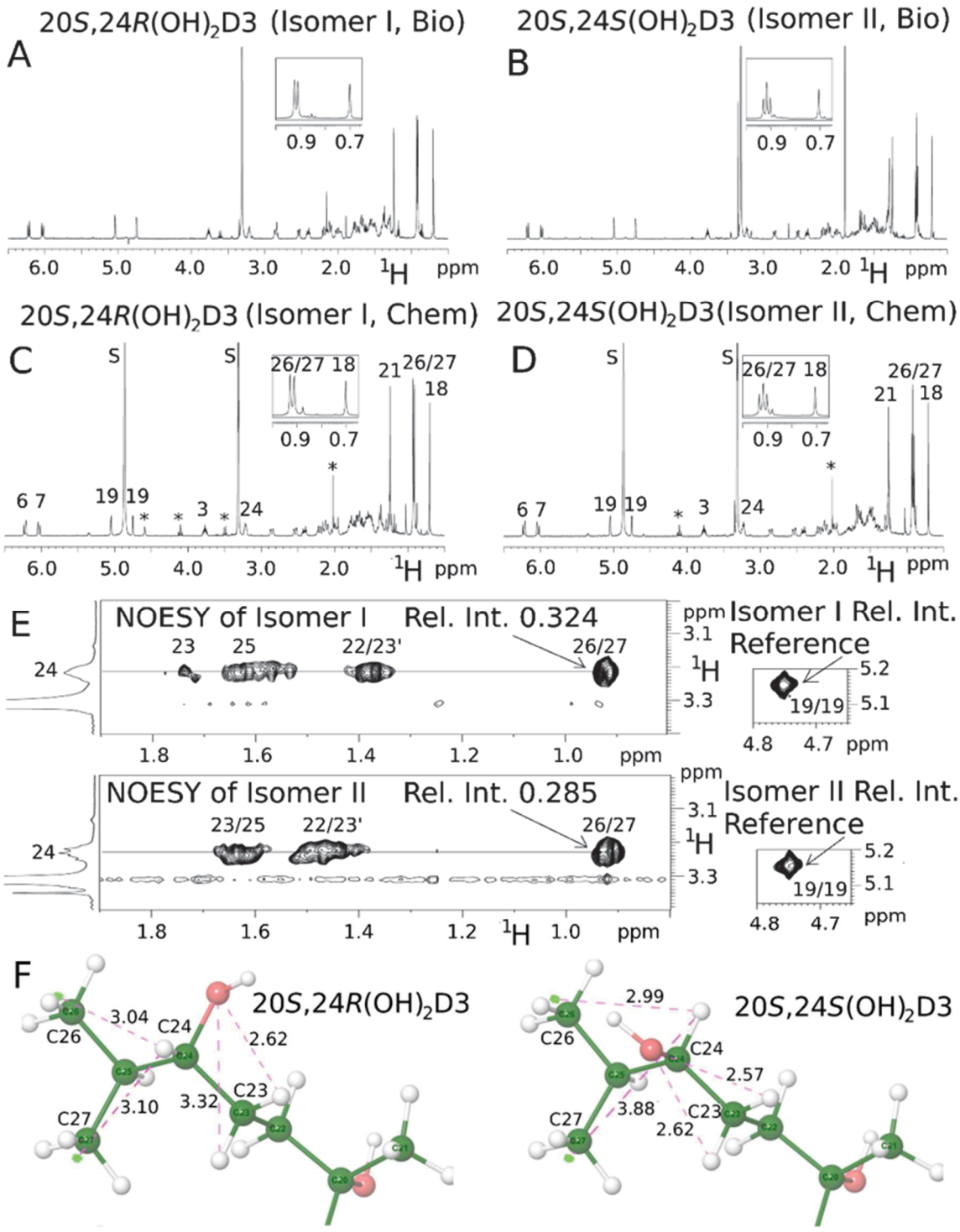

Figure 3-4. **^{1}H NMR spectral comparison between biologically generated (A and B) and chemically synthesized (C and D) 17a/b. ^{1}H-^{1}H NOESY spectra (E) of Isomer I (identified as 17a) and Isomer II (17b) together with their structural models (F).**

^{1}H chemical shifts of the two protons at C23 is larger in the 24*R*-configuration than that in the 24*S*-configuration, consistent with our earlier tentative assignments. Collectively, these NMR results indicate that isomers I and II, regardless of whether they were chemically synthesized as performed in this report or were enzymatically generated as we reported previously [9, 241], are 20*S*,24*R*(OH)2D3 (**17a**), and 20*S*,24*S*(OH)2D3 (**17b**), respectively.

To further confirm the absolute configurations of C24, **8a** and **8b** were chosen to be esterified to *S*- and *R*-Mosher esters separately. Analysis of the ^{1}H-NMR spectra for **8a**, **8b** and their Mosher esters unambiguously supported that isomer I and II had 24*R* and 24*S* configurations, respectively (**Figure S1-S6** and **Table S1**) [195].

Metabolism by Mouse CYP27B1

Previously we have shown that CYP27B1 can hydroxylate both 20*S*(OH)D3 and 20*S*,24*R*(OH)2D3 in the 1α-position [242, 243] and that this modifies their biological activity in a cell-type-dependent manner [9, 204, 246]. We therefore compared the kinetics of the metabolism of 20*S*,24*R*(OH)2D3 and 20*S*,24*S*(OH)2D3 by mouse CYP27B1 (**Table 3-1**). Each isomer was able to be 1α-hydroxylated to produce a single product, previously identified as 1α,20*S*,24*R*-trihydroxyvitamin D3 in the case of 20*S*,24*R*(OH)2D3 [243], and presumed to be the 1α-hydroxy derivative in the case of 20*S*,24*S*-dihydroxyvitamin D3 based on the high specificity for 1α-hydroxylation by CYP27B1[243, 247], 20*S*,24*R*(OH)2D3 was hydroxylated with a k_{cat} 18-fold higher than that for the 24S-isomer. Thus despite its 3.2-fold higher K_m, 20*S*,24*R*(OH)2D3 is metabolized with a 5-fold higher catalytic efficiency (k_{cat}/K_m) than 20*S*,24*S*(OH)2D3. The efficiency of 1α-hydroxylation of 20*S*,24*R*(OH)2D3 by CYP27B1 is comparable to that of 25(OH)D3 [243], so we predict that this hydroxylation does occur *in vivo*.

VDR-induced Transcriptional Activity

To investigate the activation of the vitamin D receptor (VDR) by 20*S*,24*R*(OH)2D3 (**17a**) and 20*S*,24*S*(OH)2D3 (**17b**) together with their 1α-OH derivatives (**18a** and **18b**), two cell lines (HaCaT and Caco-2) were transduced by a lentiviral VDRE luciferase reporter vector. 1,25(OH)2D3 and 22-Oxa were used as positive controls [248]. As seen from **Table 3-2**, both 1,25(OH)2D3 and 22-Oxa-1,25(OH)2D3 (22-Oxa) showed the expected strong activations of VDRE in both cell lines, with the EC50 values showing that 22-Oxa is more potent than 1,25(OH)2D3. Interestingly, **17a** and **17b** were incapable of activating VDRE significantly at concentrations up to 1000 nM, but their 1α-OH derivatives **18a** and **18b** activated VDR. Both **18a** and **18b** showed higher potency than 1,25(OH)2D3 in promoting VDRE-LUC activity, at least with respect to the synthetic promoter construct utilized in these assays. Compound **18a** is about 4~5-fold more potent than **18b** and its potency is comparable with that of 22-Oxa in both of the two cell lines tested. Interestingly, 20*S*,24*R*(OH)2D3

Table 3-1. Kinetics of the metabolism of the 20,24(OH)$_2$D3 isomers by mouse CYP27B1.

Substrate	K_m	k_{cat}	k_{cat}/K_m
20*S*,24*R*(OH)$_2$D3 (**17a**)	7.99 ± 4.01	31.2 ± 10.7	3.90
20*S*,24*S*(OH)$_2$D3 (**17b**)	2.49 ± 0.59	1.76 ± 0.15	0.71

K_m, mmol substrate/mol phospholipid; k_{cat}, nmol/min/nmol P450; k_{cat}/K_m, min^{-1}(mmol/mol phospholipid)$^{-1}$. Data for k_{cat} and K_m are ± SE of the curve fit.

Table 3-2. Biological activities of 20*S*,24*R*/*S*(OH)$_2$D3 and their 1α-hydroxylated derivatives using 1,25(OH)$_2$D3 and 22-oxa-1,25(OH)$_2$D3 as positive controls.

Compound	LAIR (MF)	IFNγ (pg/mL)	VDRE activation (EC_{50}, nM)	
			HaCaT	Caco-2
Vehicle control	973 ± 95	731 ± 15	N/A	N/A
20*S*,24*R*(OH)$_2$D3 (**17a**)	1907 ± 198	465 ± 5	NS	NS
1α,20*S*,24*R*(OH)$_2$D3 (**18a**)	2100 ± 583	291 ± 5	64.9 ± 1.6	66.9 ± 3.6
20*S*,24*S*(OH)$_2$D3 (**17b**)	1537 ± 74	923 ± 10	NS	NS
1α,20*S*,24*S*(OH)$_2$D3 (**18b**)	1819 ± 612	589 ± 6	270.9 ± 2.6	207.9 ± 2.1
1,25(OH)$_2$D3	1642 ± 220	562 ± 5	321.5 ± 14.2	515.2 ± 22.4
22-oxa-1,25(OH)$_2$D3	1511 ± 366	356 ± 6	37.9 ± 1.2	40.8 ± 1.7

N/A: not applicable. NS: no significant activation. MF: mean fluorescence.

(**17a**), which did not cause VDRE activation in these assays, proved to be more potent than 1,25(OH)2D3 with respect to inhibiting colony formation by SKMEL 188 melanoma cells [9] suggesting that there are varied (biased) effects of 20(OH)D3 metabolites towards different promoters containing vitamin D responsive elements, which should be dependent on cofactors activities [198].

Inhibition of IFNγ Production

IFNγ, the only member of type II interferons, is a critical cytokine for both innate and adaptive immunity, and it is also a commonly used inflammation marker. We have previously shown that both 1,25(OH)2D3 and 20*S*(OH)D3 downregulated IFNγ production by mouse spleen cells [198]. To evaluate the activities of the two synthesized 20,24(OH)2D3 isomers **17a/b** and their 1α-OH derivatives, their inhibitory effects on IFNγ production by mouse splenocytes were evaluated. As shown in **Table 3-2**, all secosteroids tested (100 nM) except **17b** significantly reduced production of IFNγ by splenocytes, while **17b** slightly increased production. Interestingly, **17a** decreased IFNγ levels more than than 22-Oxa. With respect to the **17a/b** isomers and their 1α-hydroxyderivatives, isomers with the 24*R* configuration (**17a** and **18a**) caused a greater reduction of IFNγ production, than the 24*S* isomers (**17b** and **18b**), suggesting that the 24*R* configuration is beneficial for anti-inflammatory activity. In addition, the 1α-hydroxy-derivatives caused greater reduction of IFNγ production than their corresponding parent compounds, which may be due to their greater potency for activation of the VDR, as shown in **Table 3-2**.

Upregulation of LAIR-1

Leukocyte associated immunoglobulin-like receptors (LAIR-1) are expressed on T cells and other immune cells and are thought to modulate T cell receptor signaling to down regulate immune responses and autoimmunity [249]. We have recently found that 1,25(OH)2D3 and 20S(OH)D3 can upregulate LAIR-1 expression on T cells which may represent a previously unrecognized mechanism by which vitamin D downregulates autoimmunity (Myers et al., in preparation). To determine whether the anti-inflammatory effects of 20*S*,24*R/S*(OH)2D3 and their 1α-hydroxylation products are mediated, at least partially, through LAIR-1 upregulation, we performed a flow cytometry study on LAIR-1. As shown in **Table 3-2**, all secosteroids tested significantly increased the expression of LAIR-1 compared to the control. The 1α-hydroxyl derivatives of the C24 isomers showed similar stimulation as their parent compounds, while the isomers with the C24R configuration exhibited greater stimulation LAIR-1 levels than their 24S counterparts.

Summary

20*S*,24*S*(OH)2D3 and 20*S*,24*R*(OH)2D3 were chemically synthesized for the first time (**Figure 3-5**). The C24 stereochemistry of the two isomers was unambiguously

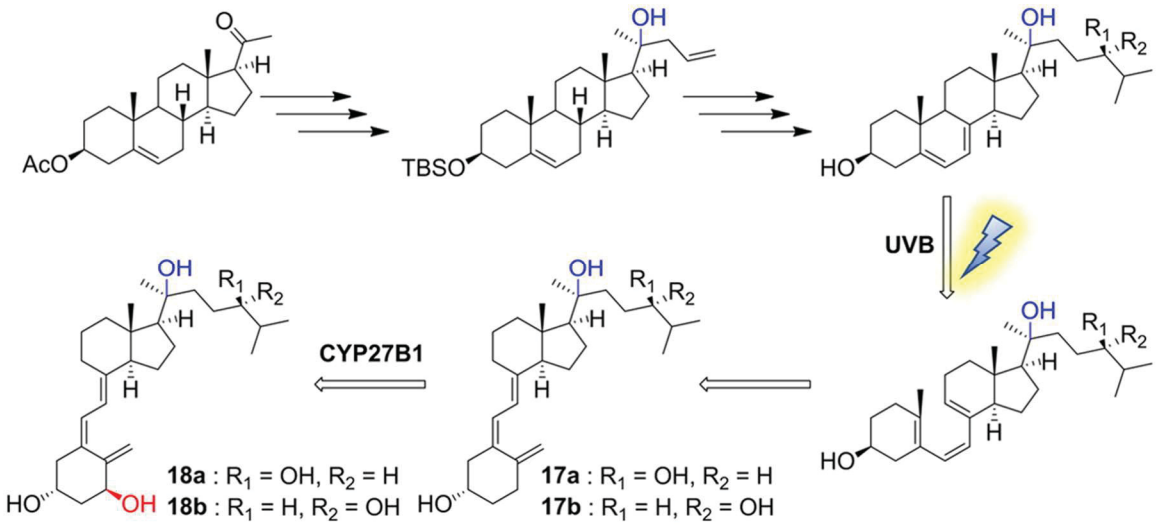

Figure 3-5. Brief synthetic scheme of 20*S*,24*S*/*R*(OH)$_2$D3 and their 1α-OH derivatives.

assigned by NMR analysis. HPLC retention times of chemically synthesized 20*S*,24*S*(OH)2D3 and 20*S*,24*R*(OH)2D3 enabled the identification of the major isomer (I) produced from 20(OH)D3 by CYP24A1 as 20*S*,24*R*(OH)2D3 and the minor isomer (II) as 20*S*,24*S*(OH)2D3 [9, 241]. 20*S*,24*R*(OH)2D3 is also the isomer produced from 20(OH)D3 by an unidentified P450, distinct from CYP24A1 (which is not expressed in liver) in mouse liver microsomes [242]. Biological studies showed that the 24*R*-epimer had stronger or more potent biological activity, regardless of whether the compound was 1α-hydroxylated or not. The 20,24(OH)2D3 isomers lacked the ability to activate VDRE using a synthetic promotor construct, however, their 1α-OH products showed potent VDRE-LUC activation, significantly more potent than that of 1,25(OH)2D3 and comparable with that of or 22-Oxa. In addition, inhibition of IFNγ production by splenocytes and stimulation of LAIR-1 production indicates that that 24*R*-epimer is also more active than 24*S*-epimer with respect to anti-inflammatory activities. The different properties of 20*S*,24*S*(OH)2D3 and 20*S*,24*R*(OH)2D3 are further demonstrated by the ability of CYP27B1 to metabolize 20*S*,24*R*(OH)2D3 with a catalytic efficiency 5.5-fold higher than that for 20*S*,24*S*(OH)2D3, but comparable to 1,25(OH)2D3. In summary, 20*S*,24*R*(OH)2D3 displays greater biological activity than 20*S*,24*S*(OH)2D3, with 1α-hydroxylation enhancing the activities of both epimers. Further investigation on the interaction with the vitamin D receptor and subsequent signal transduction pathways would likely explain their differential biological activities.

CHAPTER 4. SYNTHESIS AND BIOLOGICAL EVALUATION OF VITAMIN D3 METABOLITE 20*S*,23*S*-DIHYDROXYVITAMIN D3 AND ITS 23*R* EPIMER*

The vitamin D3 metabolite, 20*S*,23*S*-dihydroxyvitamin D3, was chemically synthesized for the first time, and identified to be the same as the enzymatically produced metabolite. The C23 absolute configurations of both 20*S*,23*S/R*-dihydroxyvitamin D3 epimers were unambiguously assigned by NMR and Mosher ester analysis. Their kinetics of CYP27B1 metabolism were investigated during the production of their 1α-hydroxylated derivatives. Bioactivities of these products were compared in terms of vitamin D3 receptor activation, anti-inflammatory and anti-proliferative activities.

Introduction

The classical pathway for metabolism (**Figure 4-1**) of vitamin D3 (VD3) starts with hydroxylation at C25 by microsomal cytochrome P450 enzyme, CYP2R1 [250] or the mitochondrial CYP27A1 [251], producing 25-hydroxyvitamin D3 [25(OH)D3], primarily in the liver. 25(OH)D3 then undergoes 1α-hydroxylation in the kidney by CYP27B1 producing the active form of vitamin D3, 1α,25-dihydroxyvitamin D3 [1,25(OH)2D3]. Inactivation of 1,25(OH)2D3 mainly involves CYP24A1-catalyzed hydroxylation and oxidation, ultimately producing calcitroic acid for excretion [252, 253].

An alternatively novel pathway of VD3 metabolism is initiated by CYP11A1 [254-257]. CYP11A1 can metabolize VD3 into several mono-, di- and tri-hydroxylated bioactive metabolites, with 20*S*-hydroxyvitamin D3 [20*S*(OH)D3] and 20*S*,23-dihydroxyvitamin D3 [20*S*,23(OH)2D3] being the most comprehensively studied so far [258]. These two metabolites were initially produced enzymatically *in vitro* by incubating VD3 with bovine CYP11A1 [254, 255]. Subsequent investigations detected the formation of these metabolites from VD3 in keratinocytes, adrenal glands, and human placenta, indicating the occurrence of these CYP11A1-mediated pathways in these cells or tissues [256-258]. Final proof on the occurrence of this pathway *in vivo* was detection of 20*S*(OH)D3, 20*S*,23(OH)2D3 and related hydroxyl derivatives in the human epidermis and serum [259]. Interestingly, the epidermal levels of 20*S*(OH)D3 and 22(OH)D3 were higher than that of 25(OH)D3, but lower in the serum, however, at levels above those required for biological activity as measured *in vitro* [259].

The biological activities of 20*S*(OH)D3 and 20*S*,23(OH)2D3 have been demonstrated in a large number of *in vitro* and *in vivo* systems [258, 260, 261]. They are biased agonists of the vitamin D receptor (VDR) and share many but not all biological actions of 1,25(OH)2D3 [258, 260, 261]. Both of them are inverse agonists on RORα and RORγ [218]. They inhibited the proliferation and stimulated differentiation of epidermal keratinocytes and

---

*Adapted with permission. Lin Z, et al. Synthesis and Biological Evaluation of Vitamin D3 Metabolite 20S,23S-Dihydroxyvitamin D3 and Its 23R Epimer. *J. Med. Chem.* 2016, 59(10), 5102-8. Copyright (2016) American Chemical Society.

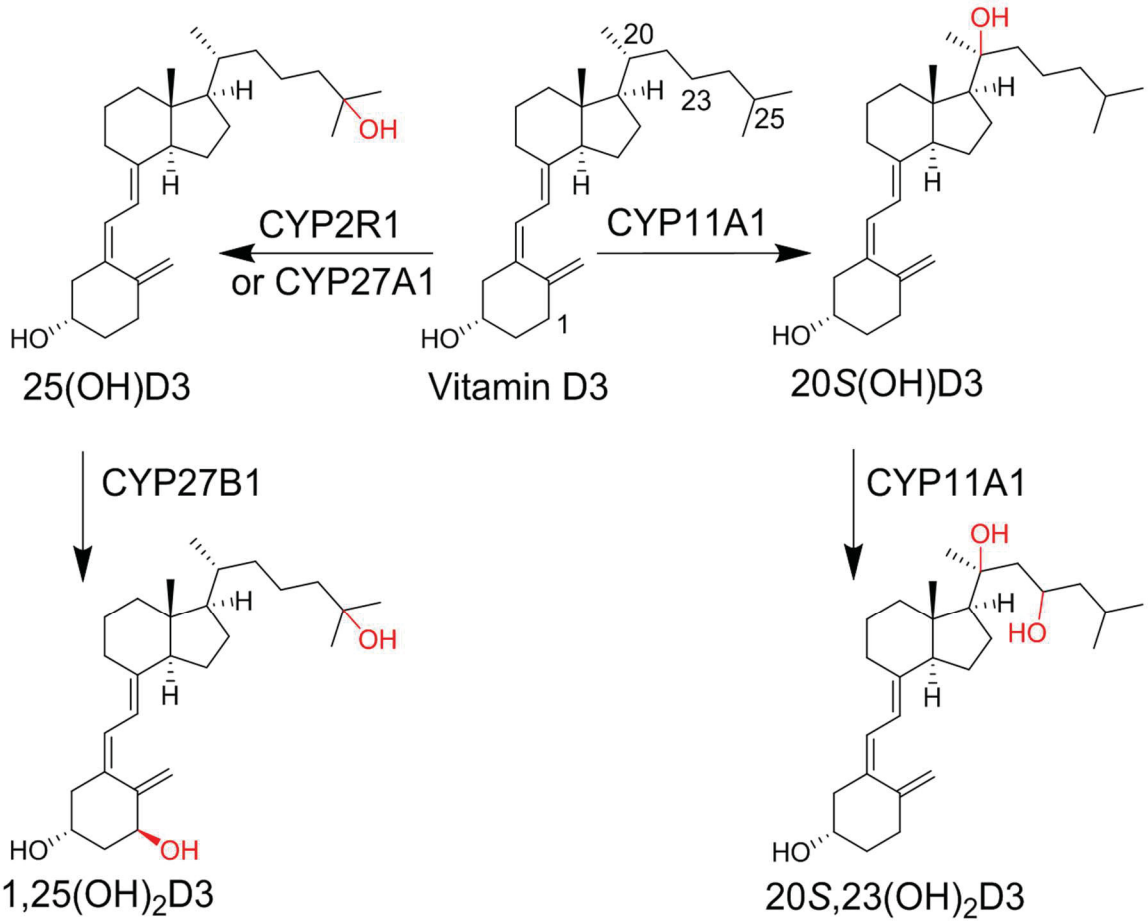

Figure 4-1. VD3 is metabolized to 25(OH)D3 and 1,25(OH)$_2$D3 by the classical pathway or to 20*S*(OH)D3 and 20*S*,23(OH)$_2$D3 by CYP11A1.

leukemia cells from human and mouse [204, 262], and showed anti-melanoma activity [260, 263]. In addition, 20*S*(OH)D3 and 20*S*,23(OH)2D3 exerted their anti-inflammatory activities through downregulation of NFκB activity in normal and immortalized keratinocytes [225, 264, 265], and displayed anti-fibrotic effects on human dermal fibroblasts from scleroderma patients and anti-fibrotic activity in animal models [266]. 1,25(OH)2D3 is a strong inducer of CYP24A1 which catalyzes the inactivation of vitamin D metabolites [201], whereas 20*S*(OH)D3 and 20*S*,23(OH)2D3 are poor stimulators of CYP24A1 expression, suggesting they are less prone to rapid metabolism by this enzyme [258]. Moreover, while 1,25(OH)2D3 causes hypercalcemia in rats and mice, both 20*S*(OH)D3 and 20*S*,23(OH)2D3 are non-calcemic at much higher doses (up to 30 μg/kg in mice) [204, 267]. Thus 20*S*(OH)D3 and 20*S*,23(OH)2D3 have great potential for further development as adjuvant therapeutic agents, especially for a wide variety of immune-driven diseases.

While the structure of enzymatically produced 20*S*,23(OH)2D3 has been elucidated by NMR analysis [255], the absolute configuration at C23 has not been determined unambiguously due to the limited amount of material available. It is well known that the absolute configuration of molecules can have substantial impacts on their biological activities. Therefore, the aim of this study was to: (1) synthesize both epimers of 20*S*,23*R*/*S*(OH)2D3 chemically and determine their absolute configurations by NMR and Mosher ester analyses; (2) identify which epimer corresponds to the enzymatically generated, biologically active 20*S*,23(OH)2D3 metabolite by using HPLC and NMR; (3) evaluate the ability of CYP27B1 to metabolize these two epimers for the production of their 1α-OH derivatives; and (4) assess the differential biological activities for these two epimers as well their 1α-OH derivatives with respect to VDR activation, anti-proliferative and anti-inflammatory effects.

Experimental Section

General Procedures

See **supporting information** [268] for chemistry procedures of intermediates and final products.

HPLC

Purities (**Figures S28-29** [268]) of final VD3 products (**17a** and **17b**) were determined by using an Agilent HPLC 1100 system and a Phenomenex Luna-PFP C18 column (5 μm, 250 mm × 4.6 mm, Torrance, CA) at 25°C and a flow rate of 1.0 mL/min. Acetonitrile and water were used as mobile phases with a gradient comprising 40-70% acetonitrile for 30 min. 263 nm was used to display chromatograms. The purities of **17a** and **17b** were determined as ≥98%.

For identifying which chemically synthesized product was identical to enzymatic product by HPLC, retention times of chemically synthesized isomer I (**17a**) and isomer II (**17b**) were compared with that of enzymatic 20*S*,23(OH)2D3. HPLC was carried out on a C18 column (Grace Alltima, 25 cm × 4.6 mm, 5 μm) with secosteroids being monitored by a UV detector at 265 nm. Two different solvent systems were used, 64 – 100% methanol for 20 min, then 100% methanol for 25 min or 45 – 100% acetonitrile for 25 min, then 100% acetonitrile for 25 min. The flow rate was 0.5 mL/min.

NMR

All NMR data were collected on a Bruker Avance III 400 MHz NMR (Bruker BioSpin, Billerica, MA). Samples were dissolved in 0.5 mL $CDCl_3$ and NMR data were collected at room temperature. TMS was used as an internal standard.

Metabolism of the C23 Epimers by CYP27B1

To measure the kinetics of **17a** and **17b** metabolism by CYP27B1, substrate was incorporated into phospholipid (PL) vesicles at a range of concentrations (0.0025 – 0.07 mol/mol PL) [269-271]. The amount of product after a 3 min incubation with 0.1 μM mouse CYP27B1 was determined by HPLC [270]. Kinetic parameters were determined by fitting the Michaelis-Menten equation to the data with Kaleidagaph 4.1.1. Data for K_m and K_{cat} are presented as mean ± standard error of the curve fit. This procedure was scaled up and the incubation time extended to 1 h to produce μg amounts of the 1α-hydroxy derivatives for biological testing, as described before [270, 271]. After incubation, the product (**18a** or **18b**) was extracted with dichloromethane, dried, and purified by HPLC on a C18 column (Grace Alltima, 25 cm × 4.6 mm, 5 μm) using an acetonitrile in water gradient at a flow rate of 0.5 mL/min: 45 – 100% acetonitrile for 25 min then 100% acetonitrile for 25 min. The two epimers were further purified on the same column using a methanol gradient: 46 - 100% methanol for 15 min then 100% methanol for 25 min, at 0.5 mL/min.

Cell Cultures

HaCat, Caco-2 and Jurkat cells were transduced with a lentiviral VDRE-luciferase reporter vector as before [201, 269]. Cells were grown in media as follows. Caco-2 cells: Dulbecco's Modified Eagle Medium (DMEM) supplemented with 10% fetal bovine serum (FBS) and 1% penicillin/streptomycin/amphotericin antibiotic solution (Ab) (Sigma-Aldrich, St. Louis, MO). HaCaT cells: The same medium used for caco-2 cells with 10% FBS changed into 5% FBS. Jurkat cells: RPMI 1640 medium supplemented with 10% FBS and 1% Ab. Splenocytes from mice: Eagles Minimal Essential Medium (EMEM) supplemented with 9% charcoal-stripped FBS, 100 U/mL penicillin and 100 μg/mL streptomycin, non-essential amino acids, 2.5 mM 2-mercaptoethanol and 2.5 mM *L*-glutamine. SKMEL-188 melanoma cells: Ham's F10 medium supplemented with 5%

FBS and 1% Ab. All cells were cultured at 37 °C in a humidified atmosphere containing 5% CO_2.

VDRE-luciferase Transcriptional Reporter Assay

HaCaT, Caco-2 and Jurkat cells were selected for one week by culturing in medium containing additional 1.0 μg/mL puromycin. Each cell line was then plated in a 96-well plate (10,000 cells/well, 100 μL medium) using FBS-free media and incubated for 24 h to synchronize the cells. Secosteroids at a series of concentrations were added separately to 96-well plate (1.0 μL/well). The final concentration of DMSO was 0.1%. Cells were incubated for another 24 h, and then 100 μL solution of ONE-Glo™ Luciferase Assay System (Promega, Madison, WI) was added to each well. After 5 min reaction at room temperature, the luciferase signal was detected by a BioTek Synergy HT microplate reader (BioTek Instruments, Inc., Winooski, VT, US). All concentrations of secosteroids were tested in triplicate.

Measurement of LAIR1 Concentrations by Flow Cytometry

Splenocytes isolated from DBA/1 mice were used to measure the LAIR1 levels. The cells were treated with each secosteroid at a concentration of 10^{-7} M, ethanol was used as vehicle control. After overnight incubation, cells were labeled with specific fluorochrome antibodies for both CD4 (BD Biosciences, San Jose, CA) and LAIR1 (eBioscience, San Diego, CA). The LAIR1 level was then determined by flow cytometry (multi-parameter) using an LSRII flow cytometer (BD Biosciences, San Jose, CA) when gating was performed on CD4 cells. At least 10,000 cells were analyzed from each sample. Final results were obtained from Flow software (Tree Star, Ashland, OR) analysis. Results are expressed as the mean of quadruplicate values ± standard error (n = 4).

Results and Discussion

Chemistry

The synthetic route to make 20*S*,23*R*(OH)2D3 and 20*S*,23*S*(OH)2D3 is shown in **Figure 4-2**. Detailed synthesis procedures and structural characterizations of intermediates and products are listed in the **supporting information** [268]. Briefly, the 3-acetyl on commercially available pregnenolone acetate (**1**) was first replaced by TBS protection after deacetylation under basic condition [272]. This replacement allowed 3-OTBS to go through later Grignard reactions and hydroboration safely and intact. Addition of vinyl magnesium bromide to 20-ketone (**3**) afforded alcohol **4** with a stereospecific 20*S* configuration as reported in our previous studies [201, 269, 273]. The 20-OH

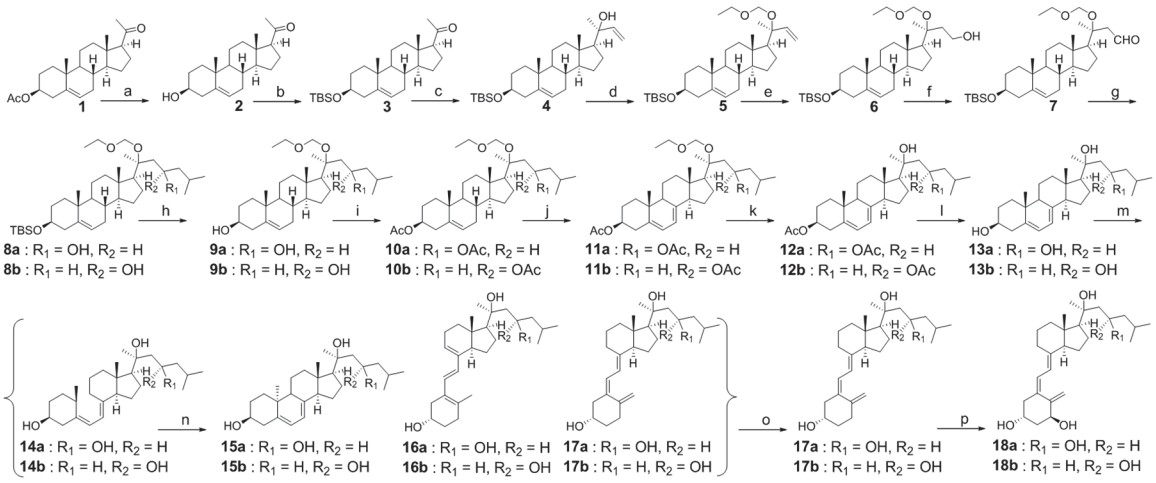

Figure 4-2. Synthesis of compounds 17 and 18.
Reagents and conditions: (a) aq. KOH, MeOH, r.t., 2 h. 94%. (b) TBSCl, imidazole, DMF, r.t., overnight. 92%. (c) Vinylmagnesium bromide, THF, 0 ºC - r.t., overnight. 84%. (d) EOMCl, DIPEA, CH_2Cl_2, r.t., overnight. 92%. (e) 9-BBN, THF, 0 ºC - r.t., 24 h; H_2O, r.t., 0.5 h; NaOH, H_2O_2, -20 ºC - r.t., overnight. 81%. (f) PDC, CH_2Cl_2, r.t., 24 h. 96%. (g) Isobutyl bromide, Mg, THF, I_2, 45 ºC, 1 h; THF, 0 ºC - r.t., 6 h. 85%. (h) TBAF, THF, r.t., 12 h. 100%. (i) Ac_2O, pyridine, DMAP, 12 h. 94%. (j) Dibromantin, AIBN, Benzene: Hexane (1:1), reflux 20 min; TBAB, THF, r.t., 75 min, then TBAF, r.t., 50 min. 39%. (k) Mont. K10, ACN, 0 ºC - r.t., 12 h. 65% (35% recovered). (l) aq. KOH, MeOH, 2 h. 85%. (m) UVB, Et_2O, 15 min. (n) Ethanol, reflux, 3 h. (o) HPLC, ACN:H_2O. 11% (three steps). Overall yield from step (a) to (o) is 1.5%. (p) CYP27B1 enzyme.

was then protected by EOMCl and excess DIPEA in DCM with satisfactory yield (92%). Intermediate **6** was obtained by 9-BBN hydroboration, and went through PDC oxidation to give aldehyde **7**, in which the aldehyde group was utilized to react with isobutylmagnesium bromide to produce two epimers (**8a** and **8b**) with different C23 configuration. Our initial trials to separate **8a** and **8b** using different solvent systems for normal phase TLC failed to obtain pure diastereomers. Fortunately, after being treated with TBAF, mixture **8** gave two separated spots (alcohols **9a** and **9b**) on TLC which were further separated using flash column chromatography for the following reactions. Di-acetylation of 3-OH and 23-OH on **9** afforded protected **10**, which was subsequently transformed into the 5,7-diene 7DHC structure (**11**) by a well-established procedure using dibromantin/AIBN/TBAB/TBAF conditions [274]. EOM protection on C20 was removed to keep the configurations of 3-OH and 23-OH unaffected. In this study, montmorillonite K10 clay was found to be a neat catalyst for the removal of EOM protection at room temperature. Hydrolysis of ester bonds under KOH/MeOH condition rapidly yielded the 7DHC structure (**13**). To get secosteroid structures, B-ring-opening reaction using UVB light irradiation was carried out for **13** dissolved in ethyl ether, followed by heat induced isomerization of pre-vitamin D3 to produce VD3 product (**17a** as isomer I or **17b** as isomer II). Normal phase LC was unable to separate **17** out of the reaction mixture, so HPLC was used for the purification of **17** using acetonitrile (ACN) and water as mobile phases. 1α-Hydroxylated product **18** was produced by enzymatic reaction with CYP27B1 which is highly specific for the 1α-position based on its function [275], and was purified by HPLC.

Isomer II (17b) Showed Matched Retention Times with the CYP11A1 Product in HPLC Chromatograms

To determine which one of the chemically synthesized 20*S*,23(OH)2D3 epimers is identical to the CYP11A1 product, HPLC analysis was carried out to compare their chromatographic behaviors. As shown in **Figure 4-3**, isomer II under different reverse phase HPLC conditions (methanol: water for A and B, and acetonitrile: water for C and D) gave the same retention times as that of enzymatically produced 20*S*,23(OH)2D3, strongly suggesting that isomer II has the same structure as the natural metabolite discovered previously [255, 262].

In addition, our previous study has elucidated the structure of enzymatic 20*S*,23(OH)2D3, and the NMR and UV spectra of synthetic **17b** further confirmed that it was identical to the reported natural product. For comparison, the spectra of **17a** and **17b** are listed in **supporting information** (**Figure S22-30** for spectra and **Table S2** for proton NMR chemical shift assignments) [268]. High-resolution MS spectra obtained using a Waters UPLC coupled to a Xevo G2-S qTof MS system also confirmed their identical structures, using an optimized method [212, 276].

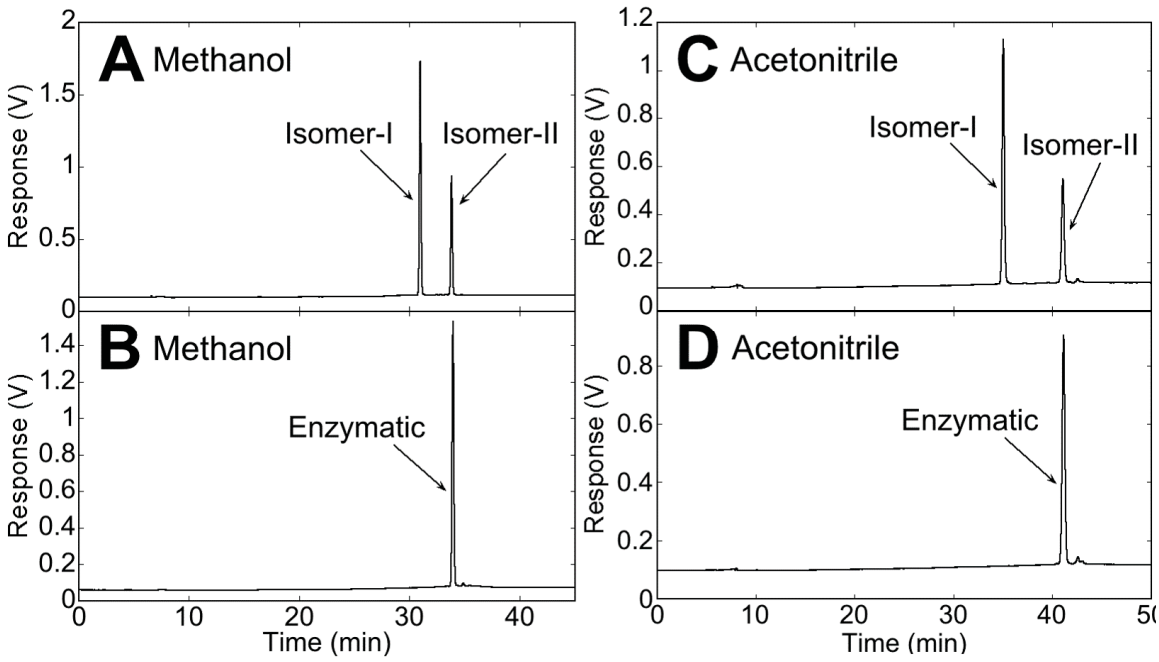

Figure 4-3. Comparison of HPLC retention times of 20*S*,23(OH)$_2$D3 isomers produced chemically and enzymatically.
Chemically synthesized isomer I (2 nmol) and isomer II (1 nmol) were combined (**A** and **C**) and analyzed by HPLC in comparison to 2 nmol enzymatically synthesized 20*S*,23(OH)$_2$D3 (**B** and **D**). Isomer II (**17b**) was found to be the enzymatically produced isomer.

Identification of 9a Having a 23*R* Configuration and 9b Having a 23*S* Configuration by NMR

To determine the C23 configurations of isomer I (**17a**) and isomer II (**17b**), intermediates **9a** and **9b** maintaining the same C23 configurations with **17a** and **17b** were used. Their NMR (1D and 2D) spectra were recorded and compared to assign their C23 configurations with assistance of molecular modeling. Their HSQC, HMBC and NOESY spectra are shown in **Figure 4-4** and **Figure S1-13** [268]. The assignments of their ^{1}H and ^{13}C chemical shifts are listed in **Table S1** [268]. Six methyl signals belonging to the ring system (18-, 19-, 21-, 26- and 27-methyls) and one from EOM protection, CH groups and CH_2 groups were all identified on HSQC (**Figure S11**) [268]. All four quaternary carbons (C5, C10, C13 and C20) were assigned based on their HMBC spectra (**Figure S12**) [268]. The assignment strategy is similar to that of previously reported di- and tri-hydroxyvitamin D3 metabolites [255, 269].

Distances used to distinguish the two epimers are shown in **Figure 4-4**. NOE integrals of 6H to $7H_\beta$ and to $4H_\alpha$ were used as internal references to calibrate other NOE peak integrals (**Figure S13**) [268]. The NOE integrals of reference protons in **9a** and **9b** are comparable as seen in the middle panels of **Figure 4-4B, C** (or **Figure S13**) [268]; however, the NOE peak integral of 23H to the centroid of 21-CH_3 in **9a** (left panel of **Figure 4-4B**) is 2.5 times smaller than that in **9b** (left panel of **Figure 4-4C**). Based on the internal reference distances, the calculated distance between 23H and the centroid of 21-CH_3 in **9a** (3.94 Å) is larger than that in **9b** (2.98 Å) (**Figure 4-4A**). Based on the modelling structures incorporating these NOE distance constraints, we tentatively conclude that **9a** and **9b** have 23*R* and 23*S* configurations, respectively.

Further NMR evidence for the C23 stereochemistry of **9a** and **9b** is provided by the chemical shifts of neighboring C22 protons as shown in the right panels of **Figure 4-4B, C**. In the 23*R* (**9a**) modeled structure, 23-O and 20-O are oriented towards opposite directions, while they are oriented towards similar directions in the 23*S* (**9b**) configuration (**Figure 4-4A**). Consequently, the two germinal protons at C22 experience a relatively similar chemical environment in 23*R* (**9a**) and a very different chemical environment in 23*S* (**9b**). The related distances are shown in **Figure 4-4A**. The two C22 germinal protons showed a similar chemical shift (both are at 1.68 ppm) in **9a**, but very different chemical shifts (1.92 and 1.58 ppm) in **9b** (**Table S1**) [268]. Therefore, the chemical shift patterns of the two protons in 22-CH_2 also suggest that the 23 configuration of **9a** is *R*, and **9b** is *S*.

Confirmation of the 23*R* Configuration of 9a by Mosher Ester Analysis

To confirm our tentative assignments that **9a** has a 23*R* configuration based on the above NMR analysis, we performed the Mosher ester analysis for **9a**. In this intermediate, there are two free OH groups, and two reactions were carried out by transforming **9a** to *S*- and *R*-Mosher 3,23-di-esters, separately (**Figure 4-5**). The 3-OH

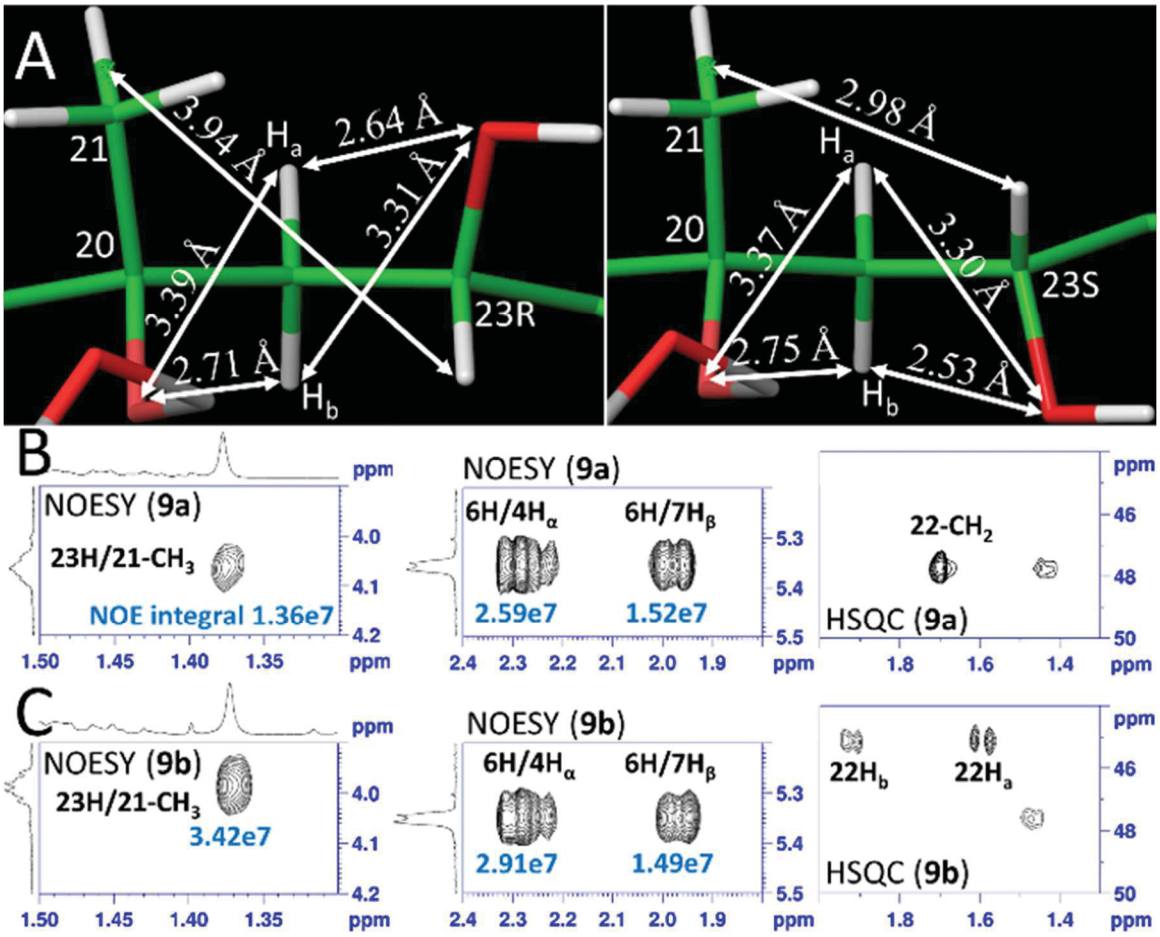

Figure 4-4. Molecular models (A) after energy minimization and the 2D NMR for 9a (23*R*) (B) and 9b (23*S*) (C).

The distance (3.94 Å) between 23H and the centroid of 21-CH_3 in the 23*R*-configuration is longer than that of the 23*S*-configuration based on their NOE peak integrals. The chemical environments for $22H_a$ and $22H_b$ are affected by 23-O and 20-O symmetrically in the 23*R*-configuration, and thus they have similar chemical shifts. In contrast, these two protons are in different environments created by the 23-O and 20-O in 23*S*-configuration, and thus have very different chemical shifts.

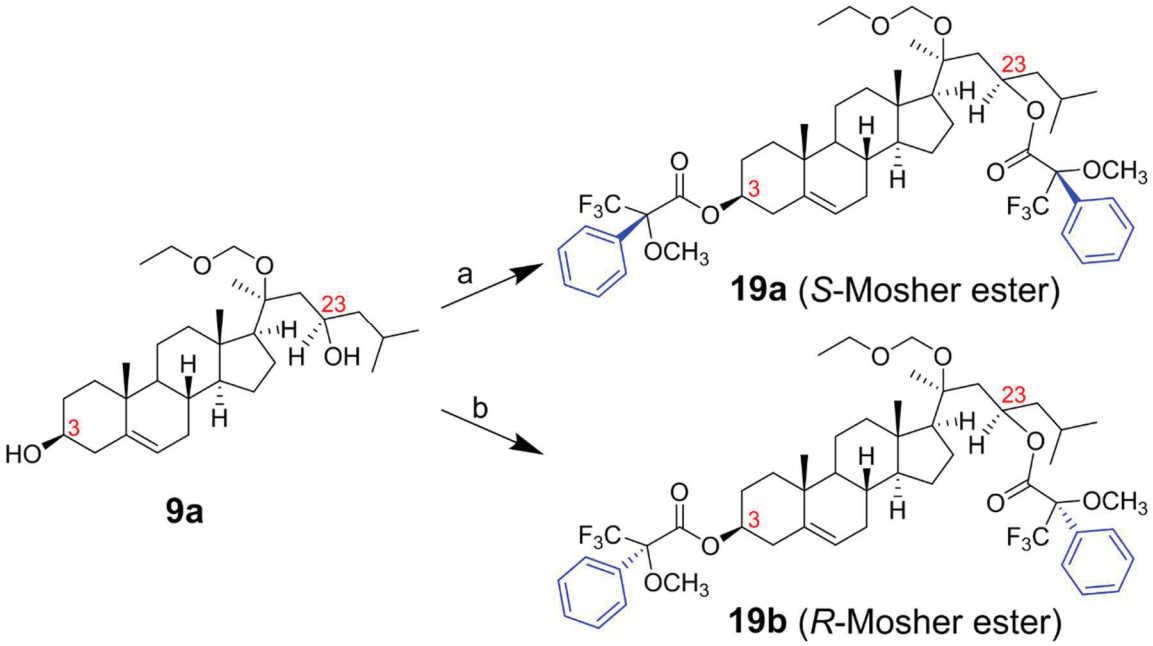

Figure 4-5. Synthesis of Mosher esters 19a and 19b.
Reagents and conditions: (a) (*R*)-Mosher acid chloride, Et_3N, DMAP, DCM, r.t., overnight, 80%. (b) (*S*)-Mosher acid chloride, Et_3N, DMAP, DCM, r.t., overnight, 88%.

has a known β position which makes C3 an *S* configuration, 3*S* is thus used as an internal reference. The ^{1}H-NMR, ^{1}H-^{1}H COSY and ^{19}F-NMR spectra of *S*- and *R*-Mosher esters of **9a** are shown in **Figure S14-19** [268]. The ^{1}H chemical shifts of 2-CH_2 and 4-CH_2 were used to verify the 3*S* configuration, and the ^{1}H chemical shifts of 22-CH_2 and 24-CH_2 were used to determine the C23 configuration. The results of Mosher ester analysis are shown in **Table 4-1**. C23 of **9a** was unambiguously identified as 23*R* according to the chemical shifts of 22-CH_2 and 24-CH_2 in the *S*- and *R*-Mosher esters, **9b** was thus assigned as 23*S*. Since **17a** and **17b** were produced from **9a** and **9b** separately with intact C23 configurations, they were assigned as 20*S*,23*R*(OH)2D3 and 20*S*,23*S*(OH)2D3, respectively. This assignment is consistent with the NMR analyses described earlier.

Kinetics of the Metabolism of 20*S*,23*R*(OH)2D3 (17a) and 20*S*,23*S*(OH)2D3 (17b) by Mouse CYP27B1

CYP27B1 plays a key role in the activation of 25(OH)D3 to 1,25(OH)2D3 and can also 1α-hydroxylate 20*S*,23(OH)2D3 which alters its biological properties [253, 270, 271]. We therefore compared the abilities of mouse CYP27B1 to hydroxylate **17a** and **17b** (**Table 4-2**). CYP27B1 specifically adds a 1α-OH group to a range of VD3 analogs including 25(OH)D3, 20*S*(OH)D3, 20*S*,24*R*(OH)2D3 and 20*S*,24*S*(OH)2D3 [253, 269-271, 275]. Using well established procedures [270, 271], **17b** was converted to **18b** by CYP27B1, as further confirmed by using an authentic, enzymatically produced standard [275]. **17a** was presumably metabolized into its 1α-hydroxylated product based on the hydroxylation specificity of CYP27B1 for this position [253, 271]. **17a** displayed both K_m and K_{cat} values half those for **17b**, therefore the overall catalytic efficiency (K_{cat}/K_m) of CYP27B1 for metabolism of these two epimers is approximately the same. However, the higher K_{cat} value for **17b** indicates that CYP27B1 has a higher capacity to hydroxylate this compound than its unnatural epimer having a 23*R*-configuration when substrate concentrations are high.

The Abilities of 20*S*,23*R*(OH)2D3, 20*S*,23*S*(OH)2D3 and Their 1α-OH Derivatives to Activate the VDR

The VDR is known to mediate many activities of vitamin D compounds, and has been shown to be required for the stimulation of differentiation and CYP24A1 expression in keratinocytes by enzymatically produced **17b** [265]. To test the differential abilities of **17a** and **17b** together with their 1α-hydroxylated derivatives, to activate the VDR, a synthetic VDR transcriptional promoter (VDRE) was transduced into three different cell lines previously used for a lentiviral VDRE-luciferase reporter assay [201, 269]. The three cell lines used were HaCaT cells as a model of normal human keratinocyte, Caco-2 cells as a cancer cell model and Jurkat cells as an immune cell model. Two well-known VDR agonists, 1,25(OH)2D3 and 22-Oxa-1,25(OH)2D3, were used as positive controls in this assay. Both of them showed low EC50 values for VDR activation using the luciferase reporter assay in all three cell lines (**Table 4-3**), with 22-Oxa-1,25(OH)2D3 being more

Table 4-1. **^{1}H-NMR chemical shifts of 9a, *S*- and *R*-Mosher esters ($\Delta\delta = \delta S - \delta R$).**

	^{1}H-NMR chemical shift (ppm)					
Compound	**2H$_\alpha$**	**2H$_\beta$**	**4-CH$_2$**	**22-CH$_2$**	**24H'**	**24H"**
9a	1.84	1.51	2.26	1.68	1.43	1.10
19a (*S*-ester)	1.91	1.61	2.46	1.92	1.63	1.48
19b (*R*-ester)	1.98	1.73	2.36	1.96	1.58	1.44
$\Delta\delta$	-0.07	-0.08	0.10	-0.04	0.05	0.04
	C3 of **9a** is *S*			C23 of **9a** is *R*		

The C3-configuration was used as an internal standard. Chemical shifts of Mosher esters were assigned from ^{1}H-^{1}H COSY spectra.

Table 4-2. **Kinetics of the metabolism of 20*S*,23*R*(OH)$_2$D3 and 17b by CYP27B1.**

Substrate	**K$_m$**	**K$_{cat}$**	**K$_{cat}$/K$_m$**
20*S*,23*R*(OH)$_2$D3 (**17a**)	2.3 ± 0.8	1.17 ± 0.08	5087
20*S*,23*S*(OH)$_2$D3 (**17b**)	5.2 ± 1.8	2.46 ± 0.22	4731

[a] K_m, 10^{-3} mol/mol phospholipid (PL); K_{cat}, min^{-1}; K_{cat}/K_m, $min^{-1}(mmol/mol\ PL)^{-1}$.

Table 4-3. Biological activities of 20*S*,23*R*(OH)$_2$D3, 20*S*,23*S*(OH)$_2$D3 and their 1α-OH derivatives compared to 1,25(OH)$_2$D3 and 22-oxa-1,25(OH)$_2$D3.

Compound	VDRE activation (EC_{50}, nM)			LAIR1 level (MF, AU)
	HaCaT	Caco-2	Jurkat	
Vehicle control	NA	NA	NA	766 ± 22
20*S*,23*R*(OH)$_2$D3 (**17a)**	484 ± 28	562 ± 34	653 ± 61	1481 ± 24
20*S*,23*S*(OH)$_2$D3 (**17b)**	NS	NS	NS	1479 ± 98
1α,20*S*,23*R*(OH)$_3$D3 (**18a)**	116.9 ± 0.21	171.7 ± 3.4	30.64 ± 0.39	1478 ± 78
1α,20*S*,23*S*(OH)$_3$D3 (**18b)**	174.8 ± 8.2	241.4 ± 10	203.0 ± 12.9	1480 ± 53
1,25(OH)$_2$D3	249.7 ± 1.8	223.4 ± 0.8	3.936 ± 0.070	1355 ± 28
22-oxa-1,25(OH)$_2$D3	159.7 ± 3.4	144.5 ± 3.0	0.855 ± 0.036	1479 ± 72

NA: not applicable. NS: no significance. MF: mean fluorescence. LAIR1 levels were measured at 100 nM of compound.

potent than 1,25(OH)2D3. In particular, they gave low nM EC50s in Jurkat cells, suggesting their selectivity among different cell types. Importantly, **17b** was unable to activate VDR at a concentration up to 1,000 nM, while **17a** showed a strong stimulatory effect at this concentration in all three cell lines, indicating that the 23*R* configuration favors VDR activation with the synthetic VDRE used, compared to the 23*S* epimer. Both 1α-OH derivatives (**18a** and **18b**) were more potent than their parent compounds, consistent with 1α-hydroxylation causing activation, as for 25(OH)D3 [253, 275]. Molecular modeling also suggests increased binding interactions of the 1α-OH derivatives (**18a** and **18b**) to the VDR than for **17a** and **17b** (**Figure S32**) [268]. Similarly, **18a** with a 23*R* configuration showed a lower EC50 value than **18b** with a 23*S* configuration, particularly in Jurkat cells, which is consistent with the relative potencies of **17a** and **17b** (parent compounds).

Upregulation of LAIR1 Levels as a Marker of Anti-inflammatory Activity

Leukocyte-associated immunoglobulin-like receptor 1 (LAIR1), also called CD305 (cluster of differentiation 305), is an inhibitory receptor expressed in peripheral mononuclear cells including natural killer cells, T cells and B cells in the immune system [277]. This inhibitory receptor downregulates immune responses and prevents cell lysis, thus it is recognized as an anti-inflammatory protein marker in autoimmunity [277]. Previously, we reported that 20*S*,24*S*/*R*(OH)2D3and their 1αOH-derivatives upregulate the concentration of LAIR1, indicating their anti-inflammatory effects [269]. To test whether 20*S*,23*S*/*R*(OH)2D3 and their 1αOH-derivatives also possess anti-inflammatory activities, we measured LAIR1 levels by flow cytometry in mice splenocytes following treatment with these secosteroids. **Table 4-3** shows that all these compounds including the two positive controls significantly elevated the level of LAIR1 at a concentration of 100 nM. **17a**, **17b**, **18a** and **18b** showed increases comparable with that of 22-Oxa-1,25(OH)2D3, and these effects were stronger than that of 1,25(OH)2D3. In addition, **18a** and **18b** showed similar stimulatory effects to their parent compounds (**17a** and **17b**), indicating that 1α-hydroxylation is not necessary for the anti-inflammatory activity of these secosteroids. These finding are consistent with previously reported inhibitory effects of 20*S*(OH)D3 and 20*S*,23(OH)D3 on production of pro-inflammatory cytokines by mouse and human lymphocytes [218, 258].

Finally, we tested the anti-proliferative activity of these compounds on SKMEL-188 melanoma cells (**Figure S33**) [268]. All D3 derivatives moderately inhibited growth of melanoma cells at concentrations of 0.1-1.0 nM in a dose dependent manner, similar to the classical 1,25(OH)2D3(the effect was statistically significant). The IC_{50} values ranged from 10^{-11} to 10^{-10} M being similar for the 20,23(OH)2D3 isomers, their 1αOH-derivatives (**18a** and **18b) and** 1,25(OH)2D3. However, **18a** and **18b** showed higher maximal inhibition values (**Figure S33**) [268] suggesting that addition of a 1αOH can potentiate the antiproliferative effect.

In this study, the bioactive VD3 metabolite 20*S*,23*S*(OH)2D3 (**17b**) and its non-natural epimer 20*S*,23*R*(OH)2D3 (**17a**) were chemically synthesized, and their C23

configurations were unambiguously assigned by NMR and Mosher ester analyses. **17b** was identified as the enzymatic product of VD3 metabolism by CYP11A1 [255] by HPLC and NMR. Comparison of the kinetics of **17a** and **17b** metabolism by CYP27B1 showed that they have similar catalytic efficiencies for 1α-hydroxylation. This enzymatic 1α-hydroxylation was exploited to make small quantities of **18a** and **18b** for analyzing the effect of the 1α-hydroxyl group on biological activity. Using a synthetic VDRE construct and a luciferase reporter assay we observed that **17a**, but not **17b**, could cause VDR activation. The modest activation of the VDRE by **17a** is consistent with low activation of VDRE of CYP24A1 promoter in our previous study in keratinocytes and leukemia cells, where involvement of the VDR was demonstrated [260, 265]. This is also consistent with our assessment that these compounds act as biased agonists on VDR signaling system [258, 260, 261], and that their biological activity also involves RORs [218]. Both epimers caused VDRE transcriptional activation following 1α-hydroxylation, with the 23*R* epimer being more potent. These results are consistent with our previous observations on the relative potencies of 20*S*,24*R*/*S*(OH)2D3 [269]. 23*R*- and 23*S*-epimers, 1α-hydroxylated or not, showed somewhat different potencies in all three cell lines tested, suggesting an enhanced interaction with the VDR/VDRE complex in immune cells, possibly due to high expression of the VDR or high concentrations of specific coactivators in immune cells that mediate the VDR responses, compared to the other cells tested [253]. Interestingly, the EC50 for **18a** in Jurkat cells was six times lower than that of **18b**. Analysis of the docking of these compounds using the VDR crystal structure, further correlated their potencies to their binding interactions with the VDR, with 1α-hydroxylation markedly increasing the docking score. The anti-inflammatory potential of the C23 epimers was assessed by their ability to increase LAIR1 levels and their anti-proliferative ability from the MTS assay which measures mitochondrial activity. Results reveal that the C23 epimers, both with and without a 1α-hydroxyl group, have potent anti-inflammatory and anti-proliferative activities, better or at least comparable with that of 1,25(OH)2D3 and/or 22-Oxa. The lack of a requirement for 1α-hydroxylation for the anti-inflammatory activity of the novel secosteroids is consistent with the recent discovery that they act as inverse agonists on RORγ, a driver of proinflammatory responses [218]. In contrast, addition of a 1αOH group to the novel secosteroids can increase their affinity towards the VDR [261] leading to improved anti-proliferative activity [258]. The exact mechanisms and structural requirements for these different biological activities remain to be elucidated with further in-depth mechanistic studies.

Summary

In summary (**Figure 4-6**), 20*S*,23*R*/*S*(OH)2D3 (**17a**/**17b**) and their 1α-OH metabolites (**18a**/**18b**) were synthesized for the first time, and 20*S*,23*S*(OH)2D3 (**17b**) was confirmed to be the natural metabolite. These compounds showed different abilities to activate the VDR with **18a** being the most potent. They all showed anti-inflammatory and anti-proliferative activities, although these different biological activities were not linearly correlated, most likely due to distinct mechanisms and structural requirements leading to these biological activities. Further biological studies of the unnatural

metabolite, **18a**, will be necessary to investigate its drug-like properties in comparison to its natural 23*S* counterpart.

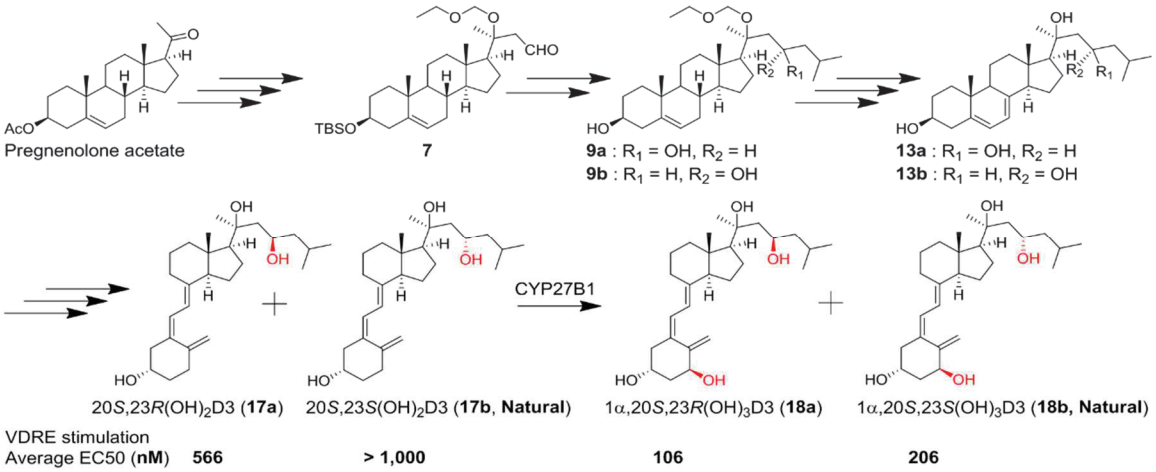

Figure 4-6. Brief synthetic scheme of 20*S*,23*S*/*R*(OH)$_2$D3 and their 1α-OH derivatives.

CHAPTER 5. SYNTHESIS OF 20S-HYDROXYVITAMIN D3 ANALOGS AND THEIR 1A-HYDROXYL DERIVATIVES AS POTENT VITAMIN D RECEPTOR AGONISTS AND ANTI-INFLAMMATORY AGENTS

Natural vitamin D3 metabolite 20S-hydroxyvitamin D3 [20S(OH)D3] is anti-inflammatory at 2 μg/kg and is not hypercalcemic (toxic) up to 60 μg/kg in mice, suggesting its potential as a lead compound. In this study, four analogs (**4**, **13**, **23** and **33**) of 20S(OH)D3 were chemically synthesized and comprehensively tested against different activities together with their 1α-hydroxyl derivatives. Metabolism of 20S(OH)D3 analogs against cytochrome P450 27B1 (CYP27B1, activation enzyme) and CYP24A1 (catabolism enzyme) suggested that they are better substrates of both enzymes than 20S(OH)D3, and can be activated (1α-hydroxylated) by CYP27B1 except 23-amide which is not a substrate but an inhibitor of CYP27B1. Their 1α-OH derivatives were potent vitamin D receptor (VDR) agonists comparable with 1α,25-dihydroxyvitamin D3 [1,25(OH)2D3] although they themselves showed weak or none VDR stimulation activity in three cell lines (Jurkat, HaCaT and Caco2). To understand the molecular interactions between these analog and VDR, two analogs (**4** and **33**) together with 20S(OH)D3 and 1,25(OH)2D3 have been co-crystalized with human VDR, and data will be reported later. These analogs and 1α-OH derivatives significantly upregulated the mRNA expression of VDR target genes (CYP24A1 and VDR), suggesting their actions via VDR, at least partially. In addition, their anti-inflammatory activities have been investigated in aspect of IFNγ inhibition in splenocytes. This study demonstrates the mechanisms of action of 20S(OH)D3 anlogs, is of great importance for future drug development of anti-inflammatory agents.

Introduction

Vitamin D3 (VD3) can be obtained from either dietary sources through intestinal absorption or endogenous production through dermal synthesis. In classical metabolism pathway (**Figure 5-1**), VD3 stays in its inactive form until enzymatic conversion (activation) happens in the liver and kidney [196]. The initial activation involves 25-hydroxylase in the liver to produce 25-hydroxyvitamin D3 [25(OH)D3] as the circulation form of D3. The final activation occurs in the kidney where cytochrome P450 enzyme 27B1 (CYP27B1) specifically hydroxylate 25(OH)D3 at 1α position to give 1α,25-dihydroxyvitamin D3 [1,25(OH)2D3] as the hormonal (active) form of D3 [139, 196]. Through vitamin D receptor (VDR), 1,25(OH)2D3 exerts its effects in mineral homeostasis, anti-inflammation, anti-proliferation, immunomodulation, vitamin D catabolism, pro-apoptosis, anti-pro-differentiation and anti-angiogenesis by modulating expressions of various VDR target genes including catabolism enzyme CYP24A1 [194, 268, 278].

A novel metabolic pathway (**Figure 5-1**) was previously reported by our group for activation and metabolism of VD3 [198, 200], and it starts with CYP11A1 acting on D3 to produce a major hydroxylated product, 20S-hydroxyvitamin D3 [20S(OH)D3].

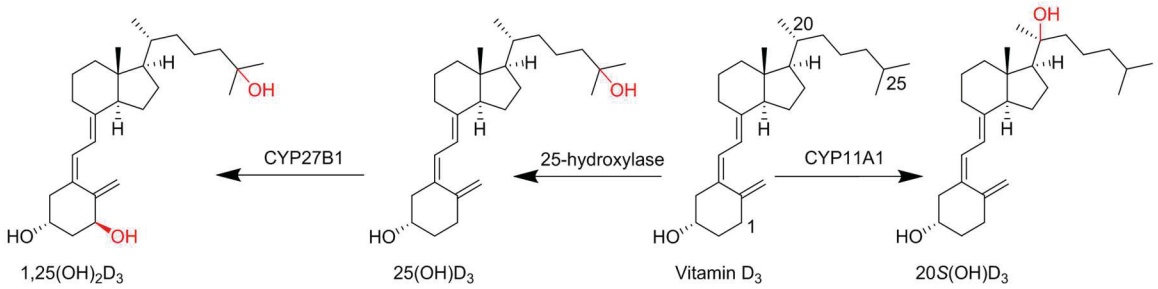

Figure 5-1. Classical metabolism pathway of D3 to circulation form 25(OH)D3 and active form 1,25(OH)2D3 and novel metabolism pathway of D3 to 20S(OH)D3.

20S(OH)D3 displays many similar activities to that of 1,25(OH)2D3 including strong anti-proliferative, anti-leukemic, tumorostatic, anti-fibrotic and differentiation stimulation activities [198, 204, 207, 216, 225, 240] mediated through either VDR activation [198, 279] or inhibition of RORα and RORγ [244]. In addition, 20S(OH)D3 exerted anti-inflammatory activities in vitro through inhibition of NFκB in keratinocytes [225, 265, 279], and in vivo suggested by suppressive effects at a dose as low as 2 μg/kg in collagen-induced arthritis mouse model [280]. More importantly, 20S(OH)D3, acting as a partial agonist of VDR, is not hypercalcemic (toxic). While 1,25(OH)2D3 showed substantial calcemic effect at 2 μg/kg, 20S(OH)D3 did not cause such toxic effect at up to 60 μg/kg in mice [206]. These results suggest that 20S(OH)D3 is a promising lead compound for developing anti-inflammatory agents without hypercalcemic effect.

In this study, a series of 20S(OH)D3 analogs with modified side chains were chemically synthesized. Their abilities to be metabolized by activation enzyme CYP27B1 for biosynthesis of their 1α-OH derivatives, and by catabolism enzyme CYP24A1 were evaluated. Two analogs (**4** and **33**) were chosen to co-crystalize with VDR to decipher their differential modes of recognition in comparison with that of 20S(OH)D3 and 1,25(OH)2D3. 1α-OH derivatives showed much stronger VDR stimulation activity, regulatory activity of VDR target genes, and anti-inflammatory activity than the parent analogs in vitamin D response element (VDRE)-reporter (luciferase), real-time PCR, and IFNγ inhibition assays, respetively.

Experimental

General Methods

All reagents and solvents in synthetic and separation procedure were purchased from commercial sources and were used as received until otherwise noted. Reactions of 5,7-diene structures were all protected by wrapping the flasks with aluminum foil. Moisture- or oxygen-sensitive reactions were performed under an argon atmosphere. All reactions were routinely monitored by TLC on silica gel, and visualized by 5% phosphomolybdic acid in ethanol for non-UV active compounds or UV lights for compounds with absorption at 254 nm. Ethyl acetate was used for extraction of reaction mixtures and then dried over anhydrous Na2SO4, filtered and removed by rotary evaporator under reduced pressure. Mass spectra of all compounds were obtained by a Bruker ESQUIRE-LC/MS system equipped with an ESI source. The purities of final D3 compounds, as analyzed by an Agilent 1100 HPLC system (Santa Clara, CA), were above 98%. High-resolution MS spectra were obtained from Waters UPLC-Q/Tof-MS system with a function of molecular formula prediction. NMR data were collected at 25 °C. Chemical shifts were referenced to residual solvent peaks of CD3OD, MeOD or acetone-d6. NMR measurements were performed on either a Bruker Avance III 400 MHz (Bruker BioSpin, Billerica, MA), or a Varian Unity Inova 500 MHz spectrometer (Agilent Technologies Inc., Santa Clara, CA, USA).

Metabolism of Analogs by CYP24A1 and CYP27B1

Rat CYP24A1, mouse CYP27B1 and adrenodoxin and human adrenodoxin reductase were expressed in *E. coli* and purified as described before [9, 281, 282]. To test metabolism of each analog, they were incorporated into phospholipid vesicles made from dioleoylphosphatidyl choline and cardiolipin by sonication, as before [9, 247]. The substrates in vesicles (510 μM phospholipid) were incubated at 37 °C with either CYP24A1 (0.14 μM) or CYP27B1 (0.8 μM) in a reconstituted system containing adrenodoxin (15 μM) and adrenodoxin reductase (0.4 μM). Samples from incubations with CYP24A1 were extracted with dichloromethane and analysed by HPLC using a Grace Alltima C18 column, as before [9, 241]. Products [except from 23,24-amide-20S(OH)D3 (**33**)] were separated using an acetonitrile on water gradient (45% to 100% for 20 min then 100% acetonitrile for 40 min at a flow rate of 0.5 ml/min). For the more polar 23,24-amide-20S(OH)D3 (**33**), the acetonitrile gradient was 30% to 100% acetonitrile for 30 min then 100% acetonitrile for 20 min, at 0.5 mL/min. Products from incubations with CYP27B1 were similarly extracted with dichloromethane and analysed by reverse phase HPLC using a Grace Smart C18 column and an acetonitrile in water gradient (10 min 45% to 100% acetonitrile then 20 min at 100% acetonitrile, at 0.5 mL/min).

VDRE Reporter Assays

Caco-2, HaCaT and Jurkat cells were cultured as previously [195, 201, 268, 278], and were transduced with lentiviral VDRE luciferase using a Cignal Lenti VDRE Reporter (luc) Kit according to the manufac-turer's protocol (QIAGEN, Valencia, CA). After one week selection by puromycin (1 μg/mL), cells were seeded in a 96-well plate (10000 cells/well/100 μL) using FBS-free medium and synchronized for 24 h. DMSO solutions (1 μL) of secosteroids to be tested were added to cells, which were then incubated for another 24 h. The luciferase signal was then measured according to the manufacturer's procedure for the ONE-GloTM Luciferase Assay System (Promega, Madison, WI). The final concentration of DMSO was 0.1% and 0.1% DMSO was used as the vehicle control. All concentrations were tested in triplicate.

Real Time PCR-based Gene Expression Analysis

HaCaT cells were purchased from Thermo Fisher Scientific (Waltham, MA, USA) and were cultured as VDRE reporter assay. The RNA from HaCaT keratinocytes treated with compounds or DMSO control was isolated using the Absolutely RNA Miniprep Kit (Stratagene, La Jolla, CA, USA). Reverse transcription (100 ng RNA/reaction) was performed with the Transcriptor First Strand cDNA Synthesis Kit (Roche Inc., Mannheim, Germany). Real-time PCR was performed using cDNA diluted 10-fold in sterile water and a SYBR Green PCR Master Mix. The primers for both forward and reverse lines for CYP24A1 and VDR genes were designed based on the mouse and rat sequences using Primer Quest software (Integrated Device Technology,

San Jose, CA, USA). Reactions (in triplicate) were performed at 50 °C for 2 min, 95 °C for 10 min and then 40 cycles of 95 °C for 15 s, 60 °C for 30 s and 72 °C for 30 s. Data were collected and analyzed on a Roche Light Cycler 480. The amount of the final amplified product for each gene was compared and normalized to the amount of β-actin as a housekeeping gene using a comparative Ct method [216].

IFNγ Inhibition Assay

Secosteroids were solubilized in absolute EtOH at 10-4 M and diluted to 10-6 M by adding Eagles Minimal Essential Medium (EMEM) containing 9% charcoal-stripped fetal calf serum, 100 U/mL penicillin and 100 μg/mL streptomycin, non-essential amino acids, 2.5 mM 2-mercaptoethanol, 2.5 mM L-glutamine [244]. The concentrations of 24,24-F_2-20S(OH)D3 and 24,24-F_2-1,20S(OH)2D3 solutions were 10-7 M. Splenocytes from mice were isolated, erythrocytes lysed by hypotonic shock, washed twice with EMEM, and suspended at a concentration for 2 × 106/mL in EMEM described above. To each well in a 48-well tissue culture plate, 450 μL of the splenocytes were added. Secosteroids (50 μL of the 10-6 M stock) or EtOH diluted 1:100 with the above culture medium were added to triplicate wells and then incubated at 37 °C in 5% CO2 in a humidified tissue culture incubator for 2 h, after which 1 μg/well of rat anti-mouse CD3 MOAB was added. After 72 h culture, supernatants from each well were harvested and analyzed by ELISA for levels of D-murine IFNγ (RAD Systems, Minneapolis, MN), according to the manufacturer's instructions. The concentration of IFNγ is supernatants from cultures containing secosteroids were compared to the concentration of IFNγ in the supernatants of EtOH-treated control cultures, by ANOVA.

Results and Discussion

Synthesis of 4 and 5

As shown in **Figure 5-2**, we started from pregnenolone acetate (1) which was transformed into 7-dehydrocholesteral (7DHC) type intermediate (**2**) by a well-established procedure with a 36% yield [195, 268, 278]. Grignard reaction using a self-made Grignard reagent removed 3-acetyl, generated 20S-OH and added the modified side chain in one step to produce **3** with a satisfactory yield (87%). To get D3 structure, **3** dissolved in ethyl ether was irradiated UVB light to open its B-ring, followed by heat induced isomerization to give D3 product **4** [24-DB-20S(OH)D3] with a 12% yield. Preparative HPLC was used to purify **4** from the reaction mixture using acetonitrile (MeCN) and water as mobile phases. 1α-Hydroxylated derivative **5** [24-DB-1,20S(OH)2D3] was produced by CYP27B1 enzyme which specifically added 1α-OH to D3 structures based on its function [247], and was purified by HPLC.

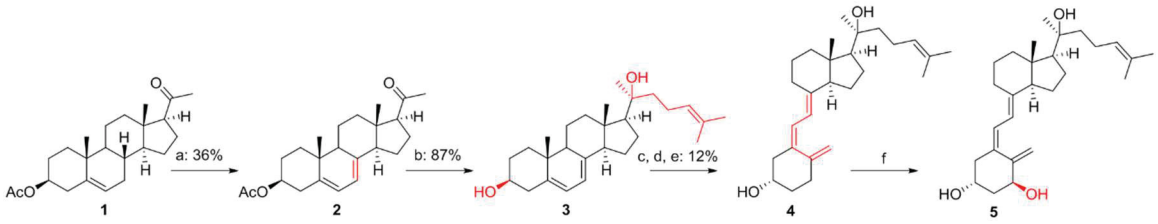

Figure 5-2. Synthesis of 20S(OH)D3 analog 4 and its 1α-OH derivative 5.
Reagents and conditions: (a) Dibromantin, AIBN, Benzene: Hexane (1:1), reflux 20 min; TBAB, THF, r.t., 75 min, then TBAF, r.t., 50 min. (b) 5-Bromo-2-methyl-2-pentene, Mg, THF, 1 h; THF, 0 ºC - r.t., 8 h. (c) UVB, Et2O, 15 min. (d) EtOH, reflux, 3 h. (e) HPLC, MeCN:H2O. (f) CYP27B1.

Synthesis of 13 and 14

The synthetic route starting from 6 reported previously [268] is shown in **Figure 5-3**. Coupling of isopropyl bromine and 6 under basic condition gave 7 with a 92% yield. After replacing 3-OTBS with 3-OAc to afford 9, 7DHC intermediate (10) was produced by the above-mentioned procedure (38% yield). EOM deprotection (81%) and ester hydrolysis (93%) was carried out under acidic condition (CSA) and basic condition (KOH), separately, to afford final 7DHC intermediate 12. Similarly, D3 structure 13 [24-Oxa-20S(OH)D3] and its 1α-OH derivative 14 [24-Oxa-1,20S(OH)2D3] were obtained from B-ring opening reaction and enzymatic transformation, respectively.

Synthesis of 23 and 24

The overall synthetic route starting from previously reported 15 [195] is shown in **Figure 5-4**. PDC oxidation of 15 gave ketone 16 with 95% yield, followed by replacing 3-OTBS with 3-OAc to afford 18 which underwent DAST fluorination to produce 19 with a 30% yield. 7DHC intermediate (20) was produced by the above-mentioned procedure (50% yield), then underwent EOM deprotection (79%) and ester hydrolysis (96%) under acidic condition (CSA) and basic condition (KOH), separately, to afford final 7DHC intermediate 22. Similarly, D3 structure 23 [24,24-F2-20S(OH)D3] and its 1α-OH derivative 24 [24,24-F2-1,20S(OH)2D3] were obtained from B-ring opening reaction and enzymatic transformation, respectively.

Synthesis of 33

The overall synthetic route using intermediate previously reported [268] is shown in **Figure 5-5**. According to a previous procedure [283], 25 was oxidized into acid (26) under mild condition without affecting the acid-sensitive TBS and EOM protection. Amide coupling of 26 and isopropylamine to construct the side chain were catalyzed by PyBOP with a 93% yield. After replacing 3-OTBS with 3-OAc to afford 29, final 7DHC intermediate (32) was produced by the above-mentioned dibromatin/AIBN/TBAB/TBAF reaction, then EOM deprotection and ester hydrolysis, with a 22% yield for three steps. Similarly, D3 structure 33 [23,24-amide-20S(OH)D3] was obtained from the B-ring opening reaction. Its 1α-OH derivative 34, however, was not obtained during enzymatic transformation.

Metabolism of 20S(OH)D3 Analogs by CYP24A1

Figure 5-6 shows HPLC analysis of the products resulting from a 10 min incubation of 20S(OH)D3, 24-DB-20S(OH)D3 (4), 24-Oxa-20S(OH)D3 (13), 24,24-F_2-20S(OH)D3 (23) and 23,24-amide-20S(OH)D3 (33) with rat CYP24A1 and reveals that the enzyme is capable of metabolizing all five of these compounds, despite the structural

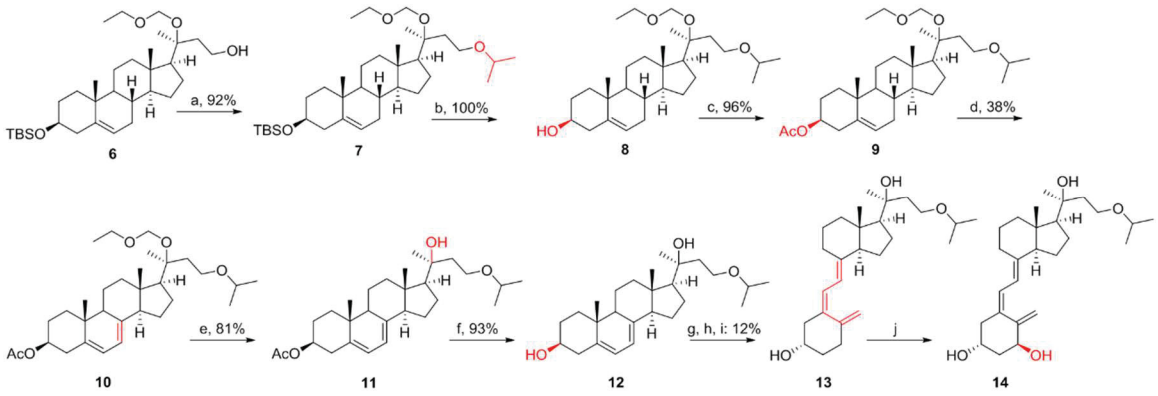

Figure 5-3. Synthesis of 20S(OH)D3 analog 16 and its 1α-OH derivative 17. Reagents and conditions: (a) Isopropyl bromine, NaH, THF, r.t., overnight. (b) TBAF, THF, r.t., 12 h. (c) Ac2O, pyridine, DMAP, 6 h. (d) Dibromantin, AIBN, Benzene: Hexane (1:1), reflux 20 min; TBAB, THF, r.t., 75 min, then TBAF, r.t., 50 min. (e) CSA, MeOH:DCM (1:1), 0 ºC - r.t., 12 h. (f) aq. KOH, MeOH, 2 h. (g) UVB, Et2O, 15 min. (h) EtOH, reflux, 3 h. (i) HPLC, MeCN:H2O. (j) CYP27B1.

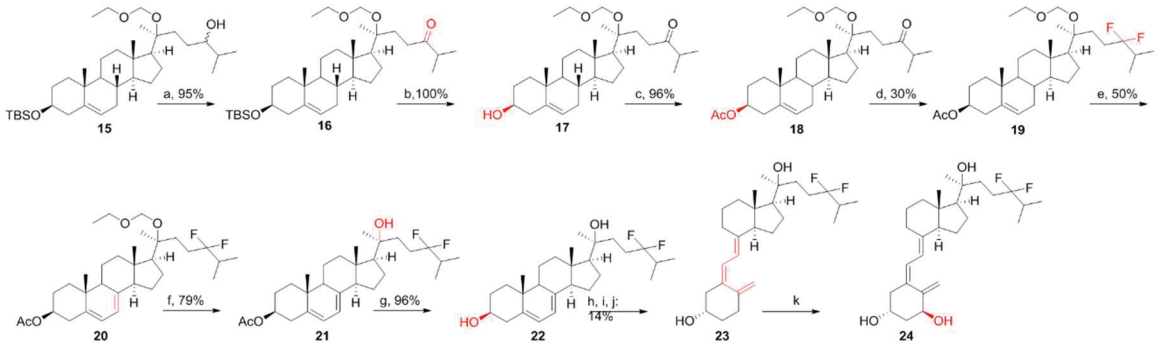

Figure 5-4. Synthesis of 20S(OH)D3 analog 23 and its 1α-OH derivative 24. Reagents and conditions: (a) PDC, CH2Cl2, r.t., 24 h. (b) TBAF, THF, r.t., 12 h. (c) Ac_2O, pyridine, DMAP, 6 h. (d) DAST, DCM, r.t. – 40 ºC (e) Dibromantin, AIBN, Benzene: Hexane (1:1), reflux 20 min; TBAB, THF, r.t., 75 min, then TBAF, r.t., 50 min. (f) CSA, MeOH:DCM (1:1), 0 ºC - r.t., 12 h. (g) aq. KOH, MeOH, 2 h. (h) UVB, Et_2O, 15 min. (i) EtOH, reflux, 3 h. (j) HPLC, ACN:H_2O. (k) CYP27B1.

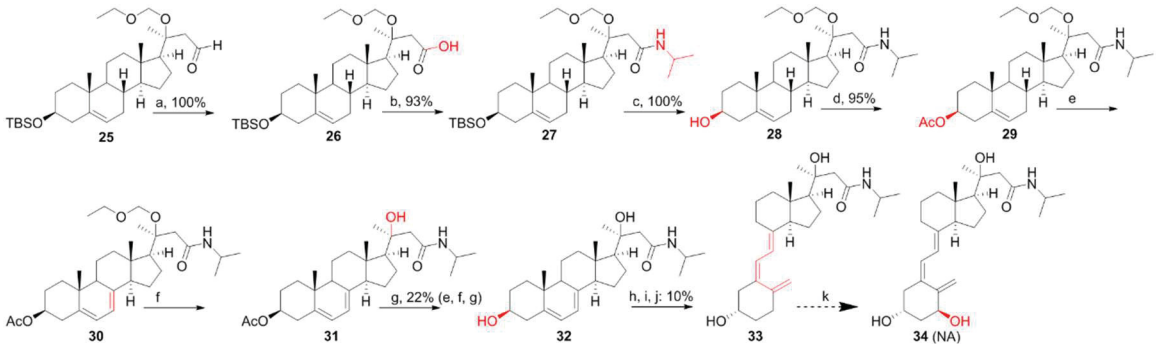

Figure 5-5. Synthesis of 20S(OH)D3 analog 33.
Reagents and conditions: (a) NaIO4, NaH2PO4, H2O2, MeCN:THF (10:1), 0 ºC - r.t., 2 h. (b) PyBOP, isopropylamine, pyridine, 0 ºC - r.t., 12 h. (c) TBAF, THF, r.t., 12 h. (d) Ac_2O, Et3N, DMAP, DCM, 12 h. (e) Dibromantin, AIBN, Benzene: Hexane (1:1), reflux 20 min; TBAB, THF, r.t., 75 min, then TBAF, r.t., 50 min. (f) CSA, MeOH:DCM (1:1), 0 ºC - r.t., 12 h. (g) aq. K2CO3, MeOH, 12 h; HPLC. (h) UVB, Et_2O, 15 min. (i) EtOH, reflux, 3 h. (j) HPLC, MeCN:H_2O. (k) CYP27B1. NA, not applicable.

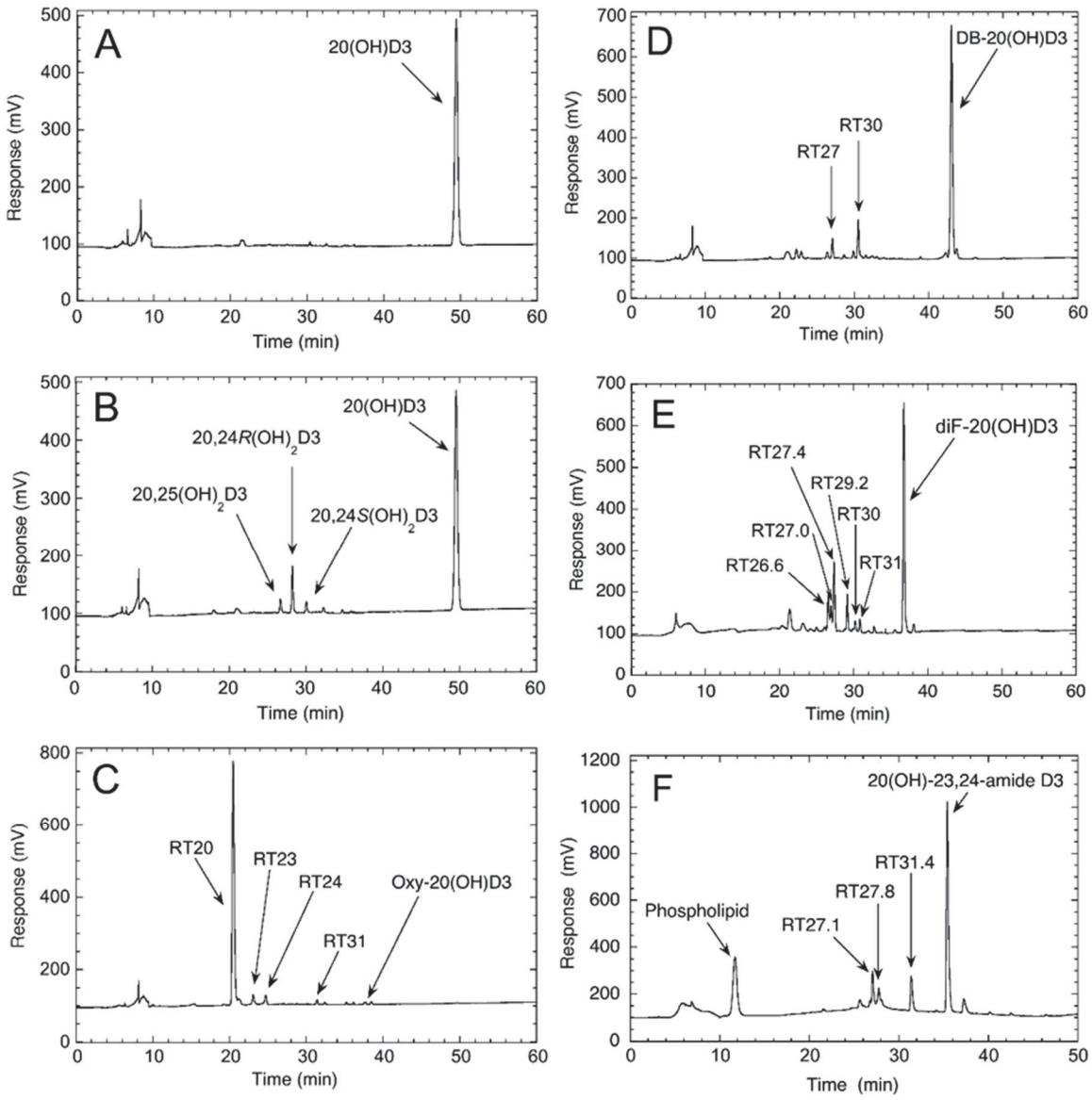

Figure 5-6. Metabolism of 20-hydroxyvitamin D3 analogues in phospholipid vesicles by rat CYP24A1.

Analogues were incorporated into phospholipid vesicles at a ratio of 0.018 mol/mol phospholipid and incubated with rat CYP24A1 (0.14 μM) for 10 min at 37˚C. Samples were analysed by reverse-phase HPLC using an acetonitrile in water gradient as described in the Methods. (**A**) Chromatogram for control incubation of 20S(OH)D3 where human adrenodoxin was omitted from the reaction. (**B**) Test reaction for 20S(OH)D3; (**C**) test reaction for 24-Oxa-20S(OH)D3 (**13**); (**D**) test reaction for 24-DB-20S(OH)D3 (**4**); (**E**) test reaction for 24,24-F_2-20S(OH)D3 (**23**); (**F**) test reaction for 23,24-amide-20S(OH)D3 (**33**). Arrows indicate major products not present in control chromatograms where adrenodoxin was excluded. RT, retention time in min.

differences. Three major products were observed with 20S(OH)D3 as substrate (**Figure 5-6B**) that were not present in the control (**Figure 5-6A**), as reported before [9, 241]. These were identified from authentic standards as 20S,25(OH)2D3, and the two C24 enantiomers of 20S,24(OH)2D3 [195, 241]. One of the C24 enantiomers, 20S,24R(OH)2D3 is the major product and accounts for almost 70% of the total products. The action of CYP24A1 on 24-DB-20S(OH)D3 (4) resulted in at least nine products (**Figure 5-6D**), suggesting a complex pathway of metabolism. There were two major products formed from this analog, RT27 and RT30 (indicated by arrows), which accounted for approximately 20% and 30% of the total products, respectively. 24,24-F_2-20S(OH)D3 (23) (**Figure 5-6E**) was converted to at least 6 different products by incubation with CYP24A1. In contrast, 24-Oxa-20S(OH)D3 (13) tested under identical conditions generated only one major product with a retention time of 20 min (RT20) and three minor products (**Figure 5-6D**). By 10 min of incubation, almost all of 24-Oxa-20S(OH)D3 (13) had been metabolised by CYP24A1. Three major products (indicated by arrows) and at least three minor ones were observed for the metabolism of 23,24-amide-20S(OH)D3 (33) by CYP24A1 (**Figure 5-6F**).

The time courses for the metabolism of each analog by CYP24A1 revealed that by 20 min there was 6-fold greater metabolism of 24-Oxa-20S(OH)D3 (13) than for 20S(OH)D3 (**Figure 5-7**). The major product of 24-Oxa-20S(OH)D3 (13) (RT20), accounted for 71% of the total secosteroids (products and substrate) at one min and by 20 min it was 95% of all secosteroids. 24,24-F2-20S(OH)D3 (23) was initially metabolized at a faster rate than 24-DB-20S(OH)D3 (4), 20S(OH)D3 and 23,24-amide-20S(OH)D3 (33) but the amounts of product from 24,24-F2-20S(OH)D3 (23) and 24-DB-20S(OH)D3 (4) were similar by 10 min. For the first two min, 24-DB-20S(OH)D3 (4) appears to be metabolised at almost the same rate as 20S(OH)D3. The time course for 20S(OH)D3 in comparison to 24-DB-20S(OH)D3 (4) and 23,24-amide-20S(OH)D3 (33), plateaued early, with the amount of product at the end of the incubation being only 2.2-fold higher than at one min. By 20 min, less than 15% of the 20S(OH)D3 had been metabolised. While initially being metabolized at the lowest rate of any of the analogs, 23,24-amide-20S(OH)D3 (33) maintained its initial rate longer with more product being present at the end of the 20 min incubation for than any of the other analogs except 24-Oxa-20S(OH)D3 (13) (**Figure 5-7**).

To determine the kinetic parameters of CYP24A1 for the metabolism of the 20-hydroxy analogues, an incubation time of one min was chosen to obtain the initial rate based on the time courses (**Figure 5-7**) and previous studies [9, 284]. K_m values varied greatly between the 20-hydroxy analogues (**Table 5-1**). 24-DB-20S(OH)D3 (**4**) had the lowest K_m value for CYP24A1, whereas 20S(OH)D3 displayed the highest which is over 17-fold higher than for 24-DB-20S(OH)D3 (**4**). 24-Oxa-20S(OH)D3 (**13**) and 24,24-F_2-20S(OH)D3 (**23**) displayed similar K_m values, 3-4 fold lower than that for 20S(OH)D3, while 23,24-amide-20S(OH)D3 (**33**) gave a K_m half that of 20S(OH)D3. There was also variation in the k_{cat} values for the metabolism of these analogues. The highest k_{cat} value was observed for 24-Oxa-20S(OH)D3 (**13**) and the lowest were for 24-DB-20S(OH)D3 (**4**) and 23,24-amide-20S(OH)D3 (**33**). The resulting k_{cat}/K_m values show that 24-Oxa-

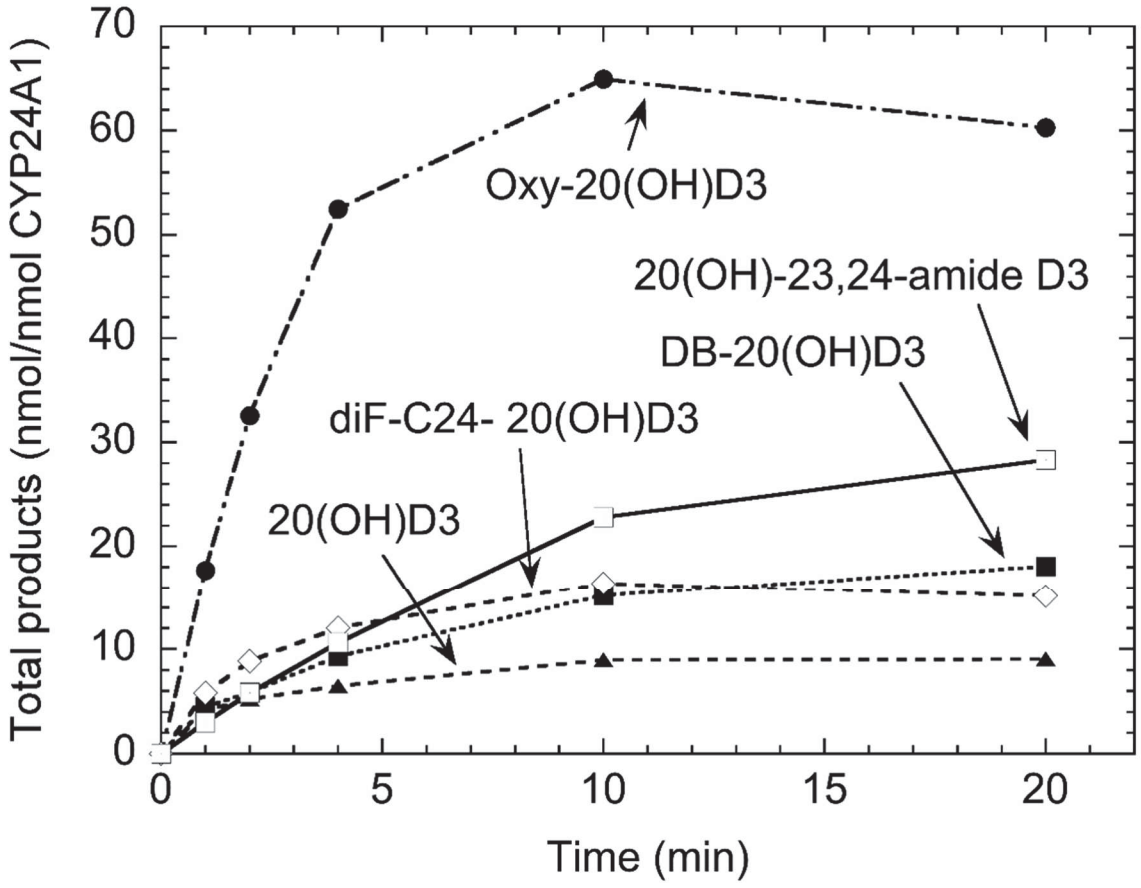

Figure 5-7. Time courses for metabolism of 20-hydroxyvitamin D3 analogs in phospholipid vesicles by rat CYP24A1.
20S(OH)D3, 24-DB-20S(OH)D3 (**4**), 24-Oxa-20S(OH)D3 (**13**), 24,24-F_2-20S(OH)D3 (**23**) and 23,24-amide-20S(OH)D3 (**33**) were incorporated into phospholipid vesicles at a ratio of 0.018 mol/mol phospholipid and incubated with 0.14 μM rat CYP24A1 at 37 °C. Products were analysed by HPLC.

Table 5-1. Kinetic data for the metabolism of the 20S-hydroxyvitamin D3 analogues by rat CYP24A1.

Substrate	K_m	k_{cat}	k_{cat}/K_m
20S(OH)D3	34.8 ± 9.4	10.1 ± 1.2	0.29
24-DB-20S(OH)D3 (**4**)	2.0 ± 1.7	4.2 ± 0.7	2.16
24-Oxa-20S(OH)D3 (**13**)	7.9 ± 1.5	29.2 ± 1.5	3.72
24,24-F_2-20S(OH)D3 (**23**)	11.6 ± 3.1	7.8 ± 0.6	0.67
23,24-amide-20S(OH)D3 (**33**)	15.4 ± 1.7	4.8 ± 0.2	0.31

K_m: mmol/mol PL, k_{cat}: min^{-1}. 20S-hydroxyvitamin D3 analogues were incorporated into phospholipid vesicles and incubated for one min in a reconstituted system with rat CYP24A1 (0.14 μM) and a range of substrate concentrations. Kinetic parameters were determined by fitting hyperbolic curves to the data using KaleidaGraph version 4.1. Data for K_m and k_{cat} are shown ± SE from the curve fit.

20S(OH)D3 (**13**) is most efficiently metabolised by rat CYP24A1 with a value 72% higher than for the next best analog, 24-DB-20S(OH)D3 (**4**). 20S(OH)D3 and 23,24-amide-20S(OH)D3 (**33**) displayed similar catalytic efficiencies which were the lowest of the analogs tested and 13-fold lower than for 24-Oxa-20S(OH)D3 (**13**). Thus, the modification at C24 that were introduced to reduce the rate of their metabolism by CYP24A1 generally had the opposite effect to increase the efficiency of their metabolism. This can be explained in part by the presence of additional functional groups on the side chain increasing the interaction with CYP24A1 active site, thus lowering the K_m. The known ability of CYP24A1 to hydroxylate the vitamin D side chain from C23 to C27 depending on what prior functional groups are present [241, 284] provides an explanation as to why blocking of one of two carbons on the side chain from hydroxylation does not prevent hydroxylation at neighbouring carbons.

Metabolism of 20S(OH)D3 Analogs by CYP27B1

In order to make the 1α-hydroxy-derivatives of the 20S(OH)D3 enzymatically, the ability of mouse CYP27B1 to hydroxylate these metabolites was examined. 20S(OH)D3 analogs were incorporated into phospholipid vesicles and incubated with CYP27B1, then the extent of their metabolism was determined by HPLC (**Table 5-2**). All analogs tested except 23,24-amide-20S(OH)D3 (**33**) were metabolized by CYP24A1. In each case only a single metabolite was produced, assumed to be the 1α-hydroxy-derivative based on the known high specificity of the enzyme for the 1α-position [243, 247, 281]. 24-Oxa-20S(OH)D3 (**13**) showed the highest conversion to product in the 20 min incubation, with greater than 90% conversion which was 4.3 fold higher than that observed with 20S(OH)D3. Metabolism of 24-DB-20S(OH)D3 (**4**) was almost twice that of 20S(OH)D3 and metabolism of 24,24-F_2-20S(OH)D3 (**23**) almost three fold. Thus, the modifications to C24 and/or C25 seen in 24-Oxa-20S(OH)D3 (**13**), 24-DB-20S(OH)D3 (**4**) and 24,24-F_2-20S(OH)D3 (**23**) enhanced their ability to be metabolized by CYP27B1. The replacement of carbon 24 with an oxygen atom had a similar effect to adding a hydroxyl group at C24 which we previously showed increased the catalytic efficiency of 1α-hydroxylation by both increasing the k_{cat} and decreasing the K_m relative to the values seen for 20S(OH)D3 [243]. In contrast, the introduction of an amide linkage into the side chain, as in 23,24-amide-20S(OH)D3 (**33**), prevented its hydroxylation by CYP27B1. In a separate experiment we found that when present with an equal concentration 25(OH)D3, 23,24-amide-20S(OH)D3 (**33**) was able to reduce the metabolism of 25(OH)D3 from 82% to 56% in a 20 min incubation, suggesting that it can compete for binding to the active site of CYP24A1 with 25(OH)D3 but binds in an unfavourable position for hydroxylation.

VDRE Stimulation Activity

Using our previous established VDRE-Luciferase reporter models [195, 201, 268, 278], the VDR-induced transcriptional activity of the analogs and their 1αOH derivatives were

Table 5-2. Metabolism of the 20S-hydroxyvitamin D3 analogues by mouse CYP27B1.

Substrate	Product (% total secosteroids)
20S(OH)D3	21.1
24-DB-20S(OH)D3 (**4**)	40.6
24-Oxa-20S(OH)D3 (**13**)	91.3
24,24-F_2-20S(OH)D3 (**23**)	57.1
23,24-amide-20S(OH)D3 (**33**)	0
25(OH)D3	86.0
25(OH)D3+23,24-amide-20S(OH)D3 (**33**) (1:1)	53.0

20S-hydroxyvitamin D3 analogues were incorporated into phospholipid vesicles at a ratio of 0.018 mol/mol phospholipid and incubated with 0.8 μM mouse CYP27B1 for 20 min at 37 ˚C. Products were analysed by reverse phase HPLC using an acetonitrile in water gradient.

investigated in three different cell lines (Caco-2, HaCaT and Jurkat). As shown in **Table 5-3**, both positive controls, 1,25(OH)2D3 and 22-Oxa-1,25(OH)2D3, showed strong activity for VDR activation in all three cell lines, with 22-Oxa-1,25(OH)2D3 being the most active one among all tested compounds. 20S(OH)D3 analogs were unable to significantly activate VDR except 24-DB-20S(OH)D3 (**4**) showing mild activity. All 1αOH derivatives displayed potent activities which were better than or comparable with that of 1,25(OH)2D3, the native ligand of VDR, suggesting that these analogs were also strong VDR agonists. The better activities of 1αOH derivatives than their parent analogs suggested the importance of 1αOH for VDR activation, which was consistent with our previous studies on 20S,23S/R(OH)2D3 [268] and 20S,24S/R(OH)2D3 [195]. One thing noteworthy is that 24-DB-20S(OH)D3 (**4**) and 24-DB-1,20S(OH)2D3 (**5**) having relatively better activities stood out of the 20S(OH)D3 analogs and their 1α-OH derivatives, respectively. Such superiority might be associated with the role of 24,25-double bond inside the VDR binding pocket.

RT-PCR-based Expression Analysis

We compared the activity of the synthetic analogs on the expression of *CYP24A1* gene in HaCaT cells to that of 1,25(OH)2D3 and 22-Oxa-1,25(OH)2D3. As shown in **Figure 5-8**, after 24 h treatment with 0.1 μM of each analog, 20S(OH)D3 analogs lack the ability to affect the mRNA levels for *CYP24A1*, except 24-DB-20S(OH)D3 which showed 39.1-fold change of the control. In comparison, all three 1,20(OH)2D3 analogs significantly increased the expression level of *CYP24A1*, being stronger than their parent 20S(OH)D3 analog, respectively. The cells treated with 0.1 μM 1,25(OH)2D3 or 22-Oxa-1,25(OH)2D3 showed a 10.4- or 82.3-fold increase in mRNA for *CYP24A1*, respectively.

The ability of the analogs to regulate the expression of the *VDR* gene was studied using HaCaT cells. In general, the mRNA expression level was only slightly stimulated by both 20S(OH)D3 analogs and 1,20(OH)2D3 analogs, with 23,24-amide-20S(OH)D3 being the most potent giving a 2.8-fold change among 20S(OH)D3 analogs, and with 24,24-F2-1,20S(OH)2D3 being the most potent analog giving a 3.8-fold change among 1,20(OH)2D3 analogs following 24 h of treatment with 0.1 μM. In addition, the two positive controls, 1,25(OH)2D3 and 22-Oxa-1,25(OH)2D3, also stimulated VDR expression by 1.2- and 1.6-fold, respectively, in comparison with the negative control. These results suggest that the new analogs may increase D3 catabolism, not only by mild stimulation of the expression of the hydroxy-D3-catabolizing enzyme (CYP24A1), but also through increased expression of its own receptor, the VDR.

Inhibitory Activity of IFNγ Production

1,25(OH)2D3 and some of its analogs can act as immunomodulatory agents and have anti-inflammatory activities [78, 196]. IFNγ as an important cytokine of immune system is a common inflammation marker. To test whether these analogs are anti-inflammatory

Table 5-3. VDRE stimulation and anti-inflammatory activities of 20S(OH)D3 analogs and their 1α-OH derivatives.

Compound	VDRE stimulation (EC_{50} ± SD, nM)			IFNγ (ratio ± SD)
	Caco-2	HaCaT	Jurkat	
24-DB-20S(OH)D3 (**4**)	580.2 ± 19.2	460.4 ± 36.5	439.3 ± 25.7	1.335±0.022
24-Oxa-20S(OH)D3 (**13**)	NS	NS	NS	0.824±0.031
24,24-F_2-20S(OH)D3 (**23**)	NS	NS	NS	0.698±0.031
23,24-amide-20S(OH)D3 (**33**)	NS	NS	NS	0.628±0.014
24-DB-1,20S(OH)2D3 (**5**)	181.6 ± 6.1	197.8 ± 8.1	237.4 ± 5.5	0.381±0.017
24-Oxa-1,20S(OH)2D3 (**14**)	188.0 ± 1.9	226.5 ± 3.5	248.4 ± 5.0	0.628±0.008
24,24-F_2-1,20S(OH)2D3 (**24**)	235.7 ± 4.1	254.1 ± 7.9	605.0 ± 4.5	0.560±0.010
23,24-amide-1,20S(OH)2D3 (**34**)	NA	NA	NA	NA
1,25(OH)2D3	465.3±20.9	305.2±12.4	31.8±4.5	0.397±0.049
22-Oxa-1,25(OH)2D3	42.5±1.6	40.1±1.5	2.9±0.3	0.487±0.017
Control	NA	NA	NA	1.000±0.015

SD: standard deviation, NS: no significance, NA: not applicable.

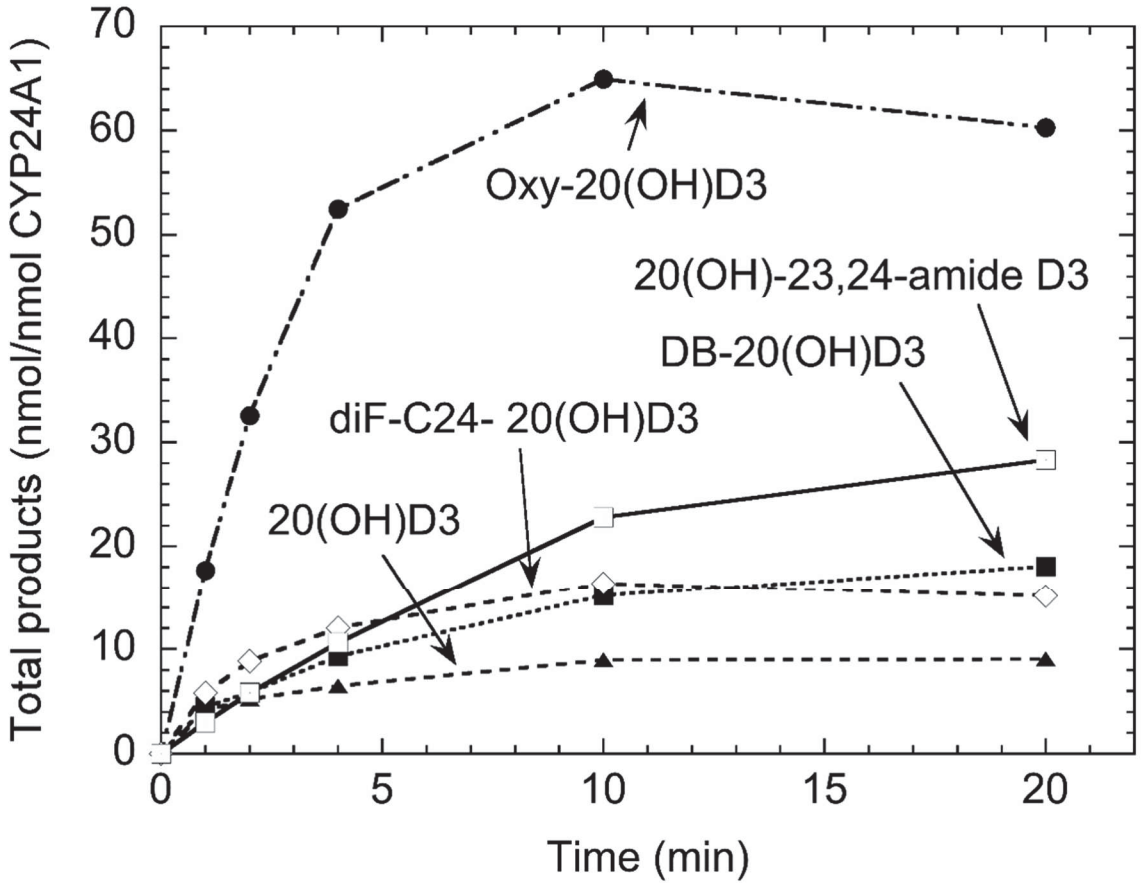

Figure 5-8. Time courses for metabolism of 20-hydroxyvitamin D3 analogs in phospholipid vesicles by rat CYP24A1.
20S(OH)D3, 24-DB-20S(OH)D3 (**4**), 24-Oxa-20S(OH)D3 (**13**), 24,24-F_2-20S(OH)D3 (**23**) and 23,24-amide-20S(OH)D3 (**33**) were incorporated into phospholipid vesicles at a ratio of 0.018 mol/mol phospholipid and incubated with 0.14 μM rat CYP24A1 at 37 °C. Products were analysed by HPLC.

agents, IFNγ inhibition assay was performed using our established assay [195, 268, 278]. As shown in **Table 5-2**, positive controls 1,25(OH)2D3 and 22-Oxa-1,25(OH)2D3 decreased IFNγ production by 60% and 51% at 100 nM, respectively. Except 24-DB-20S(OH)D3 (4), other 20S(OH)D3 analogs significantly reduced IFNγ concentrations, however less potent than 1,25(OH)2D3 and 22-Oxa-1,25(OH)2D3. After 1α-hydroxylation, the anti-inflammatory activities of all 1α-OH derivatives (37% to 62% inhibition) were significantly improved as compared with their parent analogs (-34% to 30% inhibition). Among these compounds, 24-DB-1,20S(OH)2D3 (5) was the most active one which showed better activity than both 1,25(OH)2D3 and 22-Oxa-1,25(OH)2D3. These results suggested that 20S(OH)D3 analogs have good anti-inflammatory effects, and such activities can be potentiated 1α-hydroxylation.

Summary

In this study, four 20S(OH)D3 analogs with side chain modifications were chemically synthesized, and their 1α-OH derivatives [except that of 23,24-amide-1,20S(OH)2D3 (**34**)] were produced from biosynthesis of CYP27B1. Enzymatic studies showed that CYP27B1 can activate (1α-hydroxylate) 20S(OH)D3 analogs [except 23,24-amide-20S(OH)D3 (**33**)], and CYP24A1 can metabolize all analogs, with faster rates than 20S(OH)D3 itself for both CYP27B1 activation and CYP24A1 catabolism. 20S(OH)D3 analogs showed mild to moderate VDR stimulatory, VDR downstream gene regulatory and anti-inflammatory activities, and these activities can be significantly improved by 1α-hydroxylation. Co-crystal structures of VDR in complex with 20S(OH)D3, 24-DB-20S(OH)D3 (**4**), and 23,24-amide-20S(OH)D3 (**33**) are under investigation, which can reveal their molecular interactions in the binding pocket of VDR, and in turn will be insightful for developing novel VDR agonists as anti-inflammatory agents.

CHAPTER 6. SYNTHESIS OF NATURAL 1A,20*S*-DIHYDROXYVITAMIN D3 AS A POTENT VITAMIN D RECEPTOR AGONIST

1α,20*S*-Dihydroxyvitamin D3 [1,20*S*(OH)2D3], a natural and bioactive vitamin D3 metabolite, was chemically synthesized for the first time using a 17-step scheme designed by retrosysnthesis. A semi-reduced intermediate (**14a**) of the Birch reduction for 1α-OH formation was obtained for the first time, and thus was used to propose the reaction mechanism. X-ray crystallography analysis of intermediate **15** confirmed the formation of 1α-OH. 1,20*S*(OH)2D3 binds efficiently in vitamin D receptor (VDR), being similar with its native ligand 1α,25-dihydroxyvitamin D3 [1,25(OH)2D3]. However, their co-crystal structures revealed differential molecular interactions of 20*S*-OH and 25-OH in VDR, which may help understand their biological activities. In addition, 1,20*S*(OH)2D3 functions as a VDR agonist with stronger/comparable activities than/with 1,25(OH)2D3 in aspects of VDR stimulation, regulating VDR downstream genes (*VDR*, *CYP24A1*, *TRPV6* and *CYP27B1*), inhibiting inflammatory marker IFNγ. This study offers a convenient synthetic route using a novel intermediate 1α,3β-diacetoxypregn-5-en-20-one (**3**), and provides molecular basis of design for drug development of 1,20*S*(OH)2D3 and its analogs.

Introduction

The classical activation pathway of vitamin D3 (VD3) includes two key steps: 25-hydroxylation to produce 25-hydroxyvitamin D3 [25(OH)D3], and the following 1α-hydroxylation by cytochrome P450 27B1 (CYP27B1) to produce the active 1α,25-dihydroxyvitamin D3 [1,25(OH)2D3] (**Figure 6-1**). [196] This natural ligand of vitamin D receptor (VDR), regulates expressions of various genes (such as its catabolism enzyme CYP24A1) and exerts its activities through VDR. These activities include anti-inflammation, anti-proliferation, pro-differentiation, pro-apoptosis, immunomodulation, mineral homeostasis, anti-angiogenesis and vitamin D catabolism. [20, 194, 285] In addition, D3 can also be activated by a novel metabolic pathway, which is initiated by CYP11A1 (P450scc) metabolizing D3 to 20*S*-hydroxyvitamin D3 [20S(OH)D3] as a major product. [237] As an activation enzyme, CYP27B1 is able to hydroxylate 20*S*(OH)D3 producing the natural metabolite 1α,20*S*-dihydroxyvitamin D3 [1,20*S*(OH)2D3] in μg scale. [246, 273] Alternative biosynthesis using CYP11A1 acting against commercially available 1α-hydroxyvitamin D3 [1(OH)D3] brought up the production of 1,20*S*(OH)2D3 to 0.5-1 mg. [246]

1,20*S*(OH)2D3 was found to upregulate the mRNA expression of CYP24, suggesting a role in modulating VDR downstream genes probably via VDR. [246] It also inhibited cell growth and showed potent anti-leukemic and anti-melanoma effects, while displaying less calcemic (toxic) effect than 1,25(OH)2D3. [198, 204, 207, 246] The lack of molecular interactions between 1,20*S*(OH)2D3 and VDR makes it difficult to understand the mechanism of action of 1,20*S*(OH)2D3, however, or to explain the differential effects

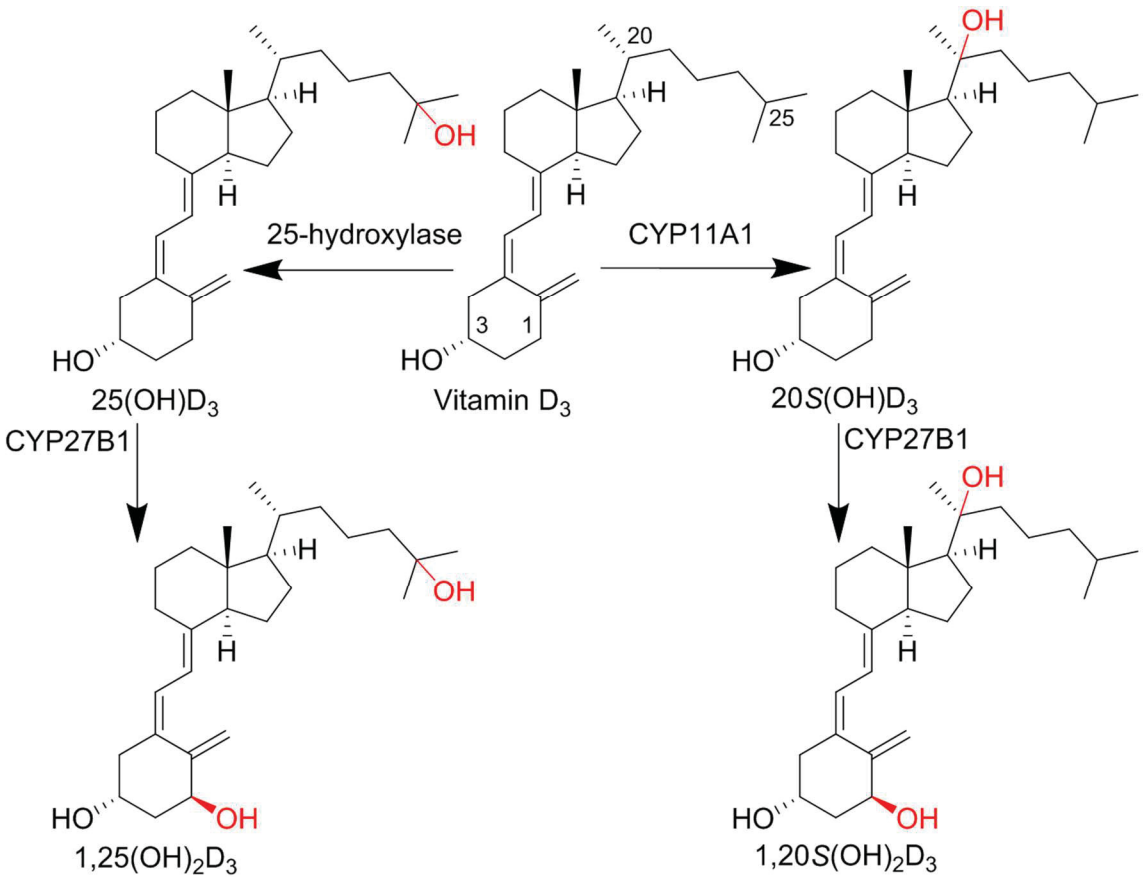

Figure 6-1. Classical and novel metabolic pathways of vitamin D3.

of 1,20*S*(OH)2D3 and 1,25(OH)2D3. The great promise of 1,20*S*(OH)2D3 has attracted us to investigate it further as a therapeutic agent, but the productions of 1,20*S*(OH)2D3[246, 273] and its analogs[195, 268] have been limited by the enzymatic reactions using either CYP27B1 or CYP11A1. The limited availability of these compounds has greatly impeded further in-depth biological investigations, and it is thus urgent to develop a practical synthetic scheme for 1,20*S*(OH)2D3 and its analogs.

Experimental

Chemistry

General procedures. Reagents and solvents for the synthesis were anhydrous (purchased or self-dried) to ensure good product yield. Solvents used for separations were ACS chemical grade, purchased from commercial sources and used upon arrival. NH_4Cl was sublimed in our lab for Birch reduction. Reactions for light sensitive compounds (7DHC or D3 structures) were protected from light by wrapping flasks with aluminum foil, and were monitored under UV lights. Moisture-sensitive reactions were carried out under argon gas in flame-dried flasks. Reactions for non-UV active compounds were visualized on TLC by 5% phosphomolybdic acid in ethanol. All NMR data were collected on a Bruker Avance III 400 MHz NMR or Varian Inova 500 MHz NMR. Samples were dissolved in 0.5 mL $CDCl_3$, MeOD, DMSO-d6 or actone-d6, and NMR data were collected at r.t. TMS was sometimes used as an internal standard. Mass spectra of compounds were provided by a Bruker LC-IT-MS system with an ESI source. High-resolution MS spectra and extracted ion chromatogram (EIC) were provided by a Waters UPLC Xevo G2-S QTof MS system based on our previous conditions. [206, 212, 278] Ethyl acetate, DCM, hexanes were used for extraction of reaction mixtures, washed with aqueous Na_2CO_3, brine, and water, and then dried over anhydrous Na_2SO_4. The solution was transferred to round-bottom flask and dried by rotary evaporator.

Synthesis of **5**. 1-((3S,8S,10R,13S,14S,17S)-3-hydroxy-10,13-dimethyl-2,3,4,7,8,9,10,11,12,13,14,15,16,17-tetradecahydro-1H-cyclopenta[a]phenanthren-17-yl)ethan-1-one. To a stirred mixture of pregnenolone acetate (**4**) (10.3 g, 28.8 mmol) in methanol (150 mL) was added K_2CO_3 (19.8 g, 143.8 mmol, 5 equiv.). The reaction mixture was stirred overnight at room temperature. Ice water (1.9 L) was added, and the reaction mixture was stirred for 30 min, filtered, and washed by distilled water (500 mL) to give **5** as a white solid (8.9 g, 28.2 mmol, 98%). ^{1}H NMR (400 MHz, Chloroform-*d*) δ 5.35 (dt, *J* = 5.4, 2.0 Hz, 1H), 3.52 (td, *J* = 11.0, 5.5 Hz, 1H), 2.54 (t, *J* = 9.0 Hz, 1H), 2.38 – 2.15 (m, 4H), 2.13 (s, 3H), 2.09 – 1.95 (m, 2H), 1.94 – 1.78 (m, 2H), 1.77 – 1.38 (m, 8H), 1.36 – 1.04 (m, 3H), 1.01 (s, 3H), 0.63 (s, 3H). MS (ESI) m/z 339.3 $[M + Na]^+$.

Synthesis of **6**. 1-((3S,8S,10R,13S,14S,17S)-3-((tert-butyldimethylsilyl)oxy)-10,13-dimethyl-2,3,4,7,8,9,10,11,12,13,14,15,16,17-tetradecahydro-1H-cyclopenta[a]phenanthren-17-yl)ethan-1-one. To a stirred mixture of **5** (8.9 g, 28.2 mmol) in DMF (freshly distilled over CaH_2, 200 mL) was added *tert*-butyldimethylsilyl chloride (8.5 g, 56.3 mmol, 2 equiv.) and imidazole (7.7 g, 112.6 mmol, 4 equiv.). The above mixture was stirred at r.t. overnight until completion as monitored by TLC (20% EA in

hexane). The reaction was quenched by addition of ice water (1.8 L), the precipitate was filtered, washed with water (400 mL), and dried under vacuum to give **6** (11.9 g, 27.9 mmol, 99%) as a white solid. ^{1}H NMR (400 MHz, Chloroform-*d*) δ 5.26 (dq, *J* = 5.8, 1.7 Hz, 1H), 3.42 (tt, *J* = 11.0, 4.8 Hz, 1H), 2.47 (t, *J* = 8.9 Hz, 1H), 2.20 (dddd, *J* = 14.4, 8.7, 6.2, 5.8, 3.0 Hz, 1H), 2.15 – 2.08 (m, 1H), 2.06 (s, 3H), 2.03 – 1.86 (m, 2H), 1.76 (dt, *J* = 13.2, 3.5 Hz, 1H), 1.71 – 1.31 (m, 9H), 1.26 – 0.95 (m, 4H), 0.94 (s, 3H), 0.93 – 0.87 (m, 1H), 0.83 (s, 9H), 0.57 (s, 3H), 0.00 (s, 6H). MS (ESI) m/z 453.4 $[M + Na]^+$.

Synthesis of **7**. (1R)-1-((3S,8S,10R,13S,14S,17S)-3-((tert-butyldimethylsilyl)oxy)-10,13-dimethyl-2,3,4,7,8,9,10,11,12,13,14,15,16,17-tetradecahydro-1H-cyclopenta[a]phenanthren-17-yl)ethan-1-ol. To a stirred solution of **6** (11.9 g, 27.9 mmol) in 100 mL DCM:MeOH (1:1), $NaBH_4$ (1060 mg, 27.9, 1.0 equiv.) was added at 0 ºC. The reaction was allowed to reach r.t. and stirred until completion monitored by TLC (20% EA in hexane). The mixture was added sat. Na_2CO_3 (300 mL) and stirred for 30 min, extracted with DCM (3 × 100 mL). The organic layer was combined, washed with brine (100 mL) and water (2 × 100 mL), dried over anhydrous Na_2SO_4. The crude mixture was subjected to flash chromatography (10% ethyl acetate in hexanes) to give **7** (11.6 g, 26.8 mmol, 96%) as a white solid. ^{1}H NMR (400 MHz, Chloroform-*d*) δ 5.26 (dt, *J* = 5.5, 1.9 Hz, 1H), 3.68 (dt, *J* = 9.7, 5.8 Hz, 1H), 3.42 (tt, *J* = 11.0, 4.7 Hz, 1H), 2.29 – 2.15 (m, 1H), 2.11 (ddd, *J* = 13.1, 5.1, 2.3 Hz, 1H), 2.01 (dt, *J* = 12.5, 3.5 Hz, 1H), 1.97 – 1.85 (m, 1H), 1.76 (dt, *J* = 13.3, 3.6 Hz, 1H), 1.70 – 1.33 (m, 9H), 1.33 – 1.15 (m, 2H), 1.12 (d, *J* = 5.5 Hz, 1H), 1.08 (d, *J* = 6.1 Hz, 3H), 1.04 – 0.97 (m, 2H), 0.95 (s, 3H), 0.89 (td, *J* = 11.1, 5.5 Hz, 1H), 0.83 (s, 9H), 0.71 (s, 3H), 0.00 (s, 6H). MS (ESI) m/z 455.4 $[M + Na]^+$.

Synthesis of **8**. (1R)-1-((3S,8S,10R,13S,14S,17S)-3-((tert-butyldimethylsilyl)oxy)-10,13-dimethyl-2,3,4,7,8,9,10,11,12,13,14,15,16,17-tetradecahydro-1H-cyclopenta[a]phenanthren-17-yl)ethyl acetate. To a solution of alcohol **7** (10.1 g, 23.4 mmol) in DCM (100 mL) was added acetic anhydride (11.9 g, 117.0 mmol, 5 equiv.), Et_3N (24.3 g, 234 mmol, 10 equiv.) and catalytic DMAP (0.05 equiv.). The reaction mixture was stirred at r.t. overnight. The solvents were removed under reduced pressure, and the resulting mixture was subjected to flash chromatography (10% EtOAc in hexane) to give **8** (11.0 g, 23.2 mmol, 99%) as a white solid. ^{1}H NMR (400 MHz, Chloroform-*d*) δ 5.32 (dt, *J* = 4.9, 1.8 Hz, 1H), 4.85 (dq, *J* = 10.4, 6.1 Hz, 1H), 3.48 (tt, *J* = 11.0, 4.7 Hz, 1H), 2.27 (ddd, *J* = 13.7, 10.9, 2.8 Hz, 1H), 2.17 (ddd, *J* = 13.4, 5.0, 2.2 Hz, 1H), 2.02 (d, *J* = 7.3 Hz, 3H), 1.96 (q, *J* = 3.7, 2.4 Hz, 1H), 1.92 – 1.34 (m, 12H), 1.25 (ddq, *J* = 14.7, 12.9, 8.7, 7.3 Hz, 2H), 1.16 (d, *J* = 6.1 Hz, 3H), 1.13 – 1.01 (m, 2H), 1.01 (s, 3H), 0.95 (dt, *J* = 11.2, 5.8 Hz, 1H), 0.90 (s, 9H), 0.65 (s, 3H), 0.06 (s, 6H). ^{13}C NMR (101 MHz, $CDCl_3$) δ 170.44, 141.63, 120.95, 77.21, 72.88, 72.61, 56.17, 55.00, 50.26, 42.82, 42.18, 39.22, 37.40, 36.61, 32.10, 31.93, 31.77, 25.94, 24.32, 21.54, 20.97, 19.95, 19.44, 18.27, 12.37, -4.57. MS (ESI) m/z 497.4 $[M + Na]^+$.

Synthesis of **9**. (1R)-1-((3S,8S,10R,13S,14S,17S)-3-hydroxy-10,13-dimethyl-2,3,4,7,8,9,10,11,12,13,14,15,16,17-tetradecahydro-1H-cyclopenta[a]phenanthren-17-yl)ethyl acetate. To a solution of ester **8** (10.4 g, 22.0 mmol) in THF (100 mL) was added tetrabutylammonium fluoride (1.0 M in THF, 43.9 mL, 2.0 equiv.), and the mixture was

stirred at room temperature for 12 h. The reaction mixture was quenched with sat. $NaHCO_3$ (400 mL), then extracted with ethyl acetate (3 × 200 mL). The combined organic layer was washed with brine (200 mL) and H_2O (200 mL), and dried over Na_2SO_4. The crude mixture resulting from removing solvents under reduced pressure was subjected to flash chromatography (30% ethyl acetate in hexane) to give an alcohol with quantitative yield. ^{1}H NMR (400 MHz, Chloroform-*d*) δ 5.35 (dt, *J* = 5.3, 1.9 Hz, 1H), 4.84 (dq, *J* = 10.3, 6.1 Hz, 1H), 3.52 (q, *J* = 8.8, 6.1 Hz, 1H), 2.38 – 2.13 (m, 2H), 2.02 (s, 3H), 1.96 (td, *J* = 4.9, 2.4 Hz, 1H), 1.89 – 1.78 (m, 3H), 1.78 – 1.33 (m, 9H), 1.33 – 1.18 (m, 3H), 1.16 (d, *J* = 6.1 Hz, 3H), 1.14 – 1.02 (m, 2H), 1.01 (d, *J* = 2.0 Hz, 3H), 0.96 (ddd, *J* = 12.0, 10.7, 5.0 Hz, 1H), 0.65 (s, 3H). ^{13}C NMR (101 MHz, $CDCl_3$) δ 170.46, 140.83, 121.48, 72.88, 71.75, 56.12, 54.98, 50.16, 42.29, 42.17, 39.18, 37.26, 36.52, 31.89, 31.76, 31.66, 25.46, 24.32, 21.54, 20.98, 19.94, 19.40, 12.38. MS (ESI) m/z 383.4 $[M + Na]^+$.

Synthesis of **10**. (1R)-1-((8S,10R,13S,14S,17S)-10,13-dimethyl-3-oxo-8,9,10,11,12,13,14,15,16,17-decahydro-3H-cyclopenta[a]phenanthren-17-yl)ethyl acetate. A solution of **9** (5.0 g, 13.9 mmol) and DDQ (12.6 g, 55.6 mmol) in 1,4-dioxane (250 mL) freshly dried over NaH was refluxed for 4 hours. The reaction mixture was cooled to r.t., 40% ethyl acetate in hexane (250 mL) was added, and the mixture was stirred for 3 min and filtered. The filtrate was dried and subjected to flash chromatography twice (15% ethyl acetate in hexane and 15% ethyl acetate in DCM) to afford **10** (3.7 g, 10.4 mmol, 75%) as white crystals. ^{1}H NMR (400 MHz, Chloroform-*d*) δ 6.99 (d, *J* = 10.1 Hz, 1H), 6.17 (ddd, *J* = 9.8, 6.1, 2.3 Hz, 2H), 5.95 (dd, *J* = 11.5, 2.0 Hz, 2H), 4.81 (dq, *J* = 10.5, 6.1 Hz, 1H), 2.21 (t, *J* = 10.3 Hz, 1H), 1.96 (s, 3H), 1.90 – 1.64 (m, 3H), 1.57 (ddd, *J* = 16.8, 9.4, 3.8 Hz, 2H), 1.38 (ddd, *J* = 13.0, 9.9, 3.7 Hz, 1H), 1.34 – 1.14 (m, 4H), 1.12 (s, 3H), 1.10 (d, *J* = 6.1 Hz, 3H), 0.92 – 0.75 (m, 1H), 0.69 (s, 3H). ^{13}C NMR (101 MHz, $CDCl_3$) δ 186.35, 170.37, 162.54, 152.90, 138.23, 128.13, 127.72, 123.81, 72.59, 54.69, 53.03, 48.40, 42.81, 41.20, 38.82, 38.01, 25.36, 23.69, 21.76, 21.52, 20.73, 19.88, 12.50. MS (ESI) m/z 377.5 $[M + Na]^+$.

Synthesis of **11**. (8S,10R,13S,14S,17S)-17-((R)-1-hydroxyethyl)-10,13-dimethyl-8,9,10,11,12,13,14,15,16,17-decahydro-3H-cyclopenta[a]phenanthren-3-one. To a stirred mixture of **10** (3.0 g, 8.5 mmol) in methanol (100 mL) was added KOH (2.4 g, 42.4 mmol, 5 equiv.). The reaction mixture was stirred for 3 h at room temperature. Sat. $NaHCO_3$ (900 mL) was added, the mixture was extracted with DCM (3 × 200 mL). The organic layer was combined, washed with brine (200 mL) and water (200 mL), and dried under reduced pressure. The crude mixture was subjected to flash chromatography (30% ethyl acetate in hexane) to give **11** as a white solid (2.6 g, 8.3 mmol, 98%). ^{1}H NMR (400 MHz, Chloroform-*d*) δ 7.09 (d, *J* = 10.1 Hz, 1H), 6.25 (ddd, *J* = 10.0, 7.8, 2.4 Hz, 2H), 6.08 – 5.93 (m, 2H), 3.77 (dq, *J* = 9.8, 6.1 Hz, 1H), 2.43 – 2.15 (m, 2H), 2.03 – 1.56 (m, 4H), 1.53 – 1.24 (m, 6H), 1.22 (s, 3H), 1.18 (d, *J* = 6.1 Hz, 3H), 0.89 (s, 3H). ^{13}C NMR (101 MHz, $CDCl_3$) δ 186.35, 162.65, 153.01, 138.46, 128.08, 127.62, 123.75, 70.37, 58.08, 53.15, 48.46, 43.01, 41.25, 39.45, 38.04, 25.54, 23.96, 23.86, 21.74, 20.74, 12.39. MS (ESI) m/z 335.4 $[M + Na]^+$.

Synthesis of **12**. (8S,10R,13S,14S,17S)-17-((R)-1-((tert-butyldimethylsilyl)oxy)ethyl)-10,13-dimethyl-8,9,10,11,12,13,14,15,16,17-decahydro-3H-cyclopenta[a]phenanthren-3-one. To a stirred solution of **11** (2.4 g, 7.7 mmol) in DMF (freshly distilled over CaH_2, 50 mL) was added *tert*-butyldimethylsilyl chloride (2.3 g, 15.4 mmol, 2 equiv.) and imidazole (2.1 g, 3.1 mmol, 4 equiv.). The above mixture was stirred at r.t. overnight. The reaction was quenched by addition of ice water (150 mL), and extracted with DCM (3 × 100 mL). The organic layer was combined, washed with brine (100 mL) and water (100 mL), and dried under reduced pressure. The crude mixture was subjected to flash chromatography (15% ethyl acetate in hexane) to give **12** as a colorless sticky solid (3.3 g, 7.5 mmol, 97%). ^{1}H NMR (400 MHz, Chloroform-*d*) δ 7.10 (d, *J* = 10.1 Hz, 1H), 6.24 (ddd, *J* = 9.6, 7.4, 2.4 Hz, 2H), 6.11 – 5.99 (m, 2H), 3.91 – 3.66 (m, 1H), 2.37 – 2.16 (m, 2H), 1.90 – 1.51 (m, 3H), 1.45 (tq, *J* = 8.8, 4.4, 4.0 Hz, 2H), 1.39 – 1.23 (m, 2H), 1.21 (s, 3H), 1.11 (d, *J* = 5.9 Hz, 3H), 0.93 (d, *J* = 0.9 Hz, 3H), 0.91 (d, *J* = 0.9 Hz, 9H), 0.83 (s, 3H), 0.10 (s, 6H). ^{13}C NMR (101 MHz, $CDCl_3$) δ 186.39, 162.81, 153.14, 138.72, 128.01, 127.53, 123.68, 70.97, 58.04, 53.33, 48.58, 42.76, 41.30, 39.10, 38.11, 26.07, 25.68, 25.65, 23.81, 23.73, 21.69, 20.72, 18.08, 12.13, -3.43, -3.99. MS (ESI) m/z 449.5 $[M + Na]^+$.

Synthesis of **13**. (2aR,3aR,3bR,5aS,6S,8aS,8bS)-6-((R)-1-((tert-butyldimethylsilyl)oxy)ethyl)-3b,5a-dimethyl-2a,3a,3b,3c,4,5,5a,6,7,8,8a,8b-dodecahydro-2H-cyclopenta[7,8]phenanthro[3,4-b]oxiren-2-one. To a solution of **12** (2.1 g, 4.9 mmol) in methanol (44.1 mL) was added 7% methanolic KOH solution (1.47 mL) and 30% H_2O_2 solution (4.9 mL) at -40 ºC. The mixture was allowed to warm up to 0 ºC and stirred at the same temperature for 12 h. The excess H_2O_2 was quenched by adding saturated Na_2SO_3 (100 mL). The mixture was extracted with EtOAc (3 × 100 mL). The combined organic layers were washed with brine (100 mL), dried over Na_2SO_4, and concentrated. The crude mixture was subjected to flash chromatography (15% ethyl acetate in hexane) to provide the epoxide **13** (1.6 g, 3.6 mmol, 73%) as colorless sticky oil. ^{1}H NMR (400 MHz, Chloroform-*d*) δ 6.26 – 5.99 (m, 2H), 5.66 (d, *J* = 1.9 Hz, 1H), 3.79 (dq, *J* = 9.1, 5.9 Hz, 1H), 3.62 (d, *J* = 4.1 Hz, 1H), 3.55 – 3.36 (m, 1H), 2.39 – 2.14 (m, 2H), 2.03 – 1.39 (m, 6H), 1.38 – 1.22 (m, 4H), 1.20 (s, 3H), 1.12 (d, *J* = 5.9 Hz, 3H), 0.91 (d, *J* = 0.9 Hz, 9H), 0.82 (s, 3H), 0.10 (s, 6H). ^{13}C NMR (101 MHz, $CDCl_3$) δ 194.79, 158.98, 140.62, 127.75, 119.39, 77.20, 70.95, 59.49, 58.04, 54.74, 53.00, 46.23, 42.74, 38.92, 37.45, 26.06, 25.64, 23.85, 23.73, 21.03, 18.49, 18.08, 12.00, -3.41, -3.99. MS (ESI) m/z 465.4 $[M + Na]^+$.

Synthesis of **14a**. (1S,8S,10R,13S,14S,17S)-17-((R)-1-((tert-butyldimethylsilyl)oxy)ethyl)-1-hydroxy-10,13-dimethyl-1,2,4,7,8,9,10,11,12,13,14,15,16,17-tetradecahydro-3H-cyclopenta[a]phenanthren-3-one. A four-necked flask was equipped with a powder addition funnel, a liquid dropping funnel, a cold-finger filled with dry ice-acetone and connected to an anhydrous NH_3 source. Anhydrous N_2 was swept through the system for 10 min, and then ammonia (10 mL) was trapped in the flask cooled to -80 ºC. Lithium wire (350 mg, 6.7 mmol, 50 equiv.) was added to the reaction mixture. After stirring for 30 min, the epoxide **13** (50 mg, 0.14 mmol) in THF (2 mL) was added drop-wise over 2 h. The cooling bath of the flask was changed to dry ice-MeCN (-40 ºC) to allow the reaction to warm up to -40 ºC

for 1 h. The flask was dipped in a -80 ºC cooling bath, and sublimed NH_4Cl (361 mg, 6.7 mmol, 50 equiv.) was added over 5 min. The mixture turned white and pasty. Liquid NH_3 was removed via a stream of nitrogen, and the resulting residue was added to H_2O (20 mL) and extracted with EtOAc (3 × 20 mL). The organic layer was washed with brine (10 mL), dried over Na_2SO_4, and concentrated. The residue was subjected to flash chromatography (20% EtOAc in hexane) to give the **14a** (major product, 39 mg, 0.09 mmol, 65%) as a colorless solid. ^{1}H NMR (500 MHz, Chloroform-*d*) δ 5.50 (dd, *J* = 5.5, 2.8 Hz, 1H), 4.03 (s, 1H), 3.67 (dt, *J* = 10.0, 6.0 Hz, 1H), 3.30 – 3.12 (m, 1H), 2.88 (dd, *J* = 17.5, 2.4 Hz, 1H), 2.70 (dd, *J* = 15.6, 2.8 Hz, 1H), 2.45 (dt, *J* = 15.4, 3.0 Hz, 1H), 2.13 (dt, *J* = 13.1, 3.5 Hz, 1H), 2.01 – 1.88 (m, 1H), 1.62 – 1.28 (m, 10H), 1.28 – 1.13 (m, 2H), 1.11 (s, 3H), 1.01 (d, *J* = 6.0 Hz, 3H), 0.81 (d, *J* = 2.0 Hz, 9H), 0.67 (s, 3H), 0.00 (s, 6H). HRMS (ESI+) m/z 447.3289 [M + H]+ (error: -1.1 ppm).

Synthesis of **14**. (1S,3R,8S,10R,13S,14S,17S)-17-((R)-1-((tert-butyldimethylsilyl)oxy)ethyl)-10,13-dimethyl-2,3,4,7,8,9,10,11,12,13,14,15,16,17-tetradecahydro-1H-cyclopenta[a]phenanthrene-1,3-diol. A four-necked flask was equipped with a powder addition funnel, a liquid dropping funnel, a cold-finger filled with dry ice-acetone and connected to an anhydrous NH_3 source. Anhydrous N_2 was swept through the system for 10 min, and then ammonia (150 mL) was trapped in the flask cooled to -80 ºC. Lithium wire (1.1 g, 177.6 mmol, 50 equiv.) was added to the reaction mixture. After stirring for 30 min, the epoxide **13** (1.6 g, 3.6 mmol) in THF (40 mL) was added drop-wise over 2 h. The cooling bath of the flask was changed to dry ice-MeCN (-40 ºC) to allow the reaction to warm up to -40 ºC for 1 h. The flask was dipped in a -80 ºC cooling bath, and sublimed NH_4Cl (9.5 g, 177.6 mmol, 50 equiv.) was added over at least 2 h. After the mixture turned white and pasty, liquid NH_3 was removed via a stream of nitrogen. The resulting residue was added H_2O (300 mL) and extracted with EtOAc (3 × 100 mL). The organic layer was washed with brine (100 mL), dried over Na_2SO_4, and concentrated. The residue was subjected to flash chromatography (60% EtOAc in hexane) to give **14** (970 mg, 2.2 mmol, 61%) as a colorless solid. ^{1}H NMR (400 MHz, Chloroform-*d*) δ 5.60 – 5.39 (m, 1H), 3.92 (tt, *J* = 11.2, 5.1 Hz, 1H), 3.79 (s, 1H), 3.73 – 3.55 (m, 1H), 2.41 – 2.16 (m, 2H), 2.16 – 2.06 (m, 1H), 2.06 – 1.99 (m, 1H), 1.96 – 1.83 (m, 1H), 1.73 – 1.61 (m, 1H), 1.61 – 1.25 (m, 8H), 1.25 – 1.16 (m, 1H), 1.16 – 1.04 (m, 2H), 1.01 (dd, *J* = 6.1, 1.4 Hz, 4H), 0.97 (d, *J* = 1.4 Hz, 3H), 0.82 (d, *J* = 1.5 Hz, 9H), 0.64 (d, *J* = 1.4 Hz, 3H), 0.00 (d, *J* = 1.7 Hz, 6H). ^{13}C NMR (101 MHz, $CDCl_3$) δ 137.39, 125.56, 72.98, 70.99, 66.47, 58.26, 56.30, 42.05, 41.84, 41.76, 41.41, 39.02, 38.22, 31.85, 31.78, 26.09, 25.74, 24.48, 23.78, 20.08, 19.50, 18.09, 12.05, -3.41, -4.02. HRMS (ESI+) m/z 471.3273 [M + Na]+ (error: 0.6 ppm).

Synthesis of **15**. (1S,3R,8S,10R,13S,14S,17S)-17-((R)-1-((tert-butyldimethylsilyl)oxy)ethyl)-10,13-dimethyl-2,3,4,7,8,9,10,11,12,13,14,15,16,17-tetradecahydro-1H-cyclopenta[a]phenanthrene-1,3-diyl diacetate. To a solution of alcohol **14** (725 mg, 1.6 mmol) in DCM (20 mL) was added Ac_2O (1.6 g, 16.2 mmol, 10 equiv.), Et_3N (3.4 g, 32.4 mmol, 20 equiv.) and catalytic DMAP (0.05 equiv.). The reaction mixture was stirred at r.t. for overnight. The solvents were removed under reduced pressure, the resulting mixture was subjected to flash chromatography (10% EtOAc in hexane) to give **15** (843.7 mg, 1.6 mmol, 98%) as a white solid, which was further

crystalized in hexane to determine its absolute structure. ^{1}H NMR (400 MHz, Chloroform-*d*) δ 5.58 – 5.49 (m, 1H), 5.06 (d, *J* = 3.0 Hz, 1H), 4.92 (tt, *J* = 11.2, 4.9 Hz, 1H), 3.72 (dt, *J* = 11.8, 5.9 Hz, 1H), 2.48 (dd, *J* = 13.7, 5.2 Hz, 1H), 2.42 – 2.28 (m, 1H), 2.21 – 2.08 (m, 3H), 2.06 (s, 3H), 2.03 (s, 3H), 2.01 – 1.91 (m, 2H), 1.91 – 1.75 (m, 1H), 1.62 (s, 3H), 1.57 – 1.23 (m, 6H), 1.23 – 1.11 (m, 1H), 1.11 (s, 3H), 1.08 (d, *J* = 5.7 Hz, 3H), 0.89 (s, 9H), 0.70 (s, 3H), 0.06 (s, 6H). ^{13}C NMR (101 MHz, $CDCl_3$) δ 170.64, 170.59, 136.39, 125.35, 77.43, 74.91, 71.27, 69.66, 58.40, 56.55, 42.35, 42.26, 40.66, 39.23, 37.55, 32.09, 31.96, 31.82, 26.33, 26.04, 24.65, 24.06, 21.55, 21.35, 20.35, 19.66, 18.31, 12.22, -3.31, -3.81. MS (ESI) m/z 555.4 $[M + Na]^+$.

Synthesis of **16**. (1S,3R,8S,10R,13S,14S,17S)-17-((R)-1-hydroxyethyl)-10,13-dimethyl-2,3,4,7,8,9,10,11,12,13,14,15,16,17-tetradecahydro-1H-cyclopenta[a]phenanthrene-1,3-diyl diacetate. To a solution of ester **15** (437 mg, 0.8 mmol) in THF (5 mL) was added TBAF (1.0 M in THF, 1.6 mL, 2.0 equiv.) and stirred at room temperature for 48 h. The reaction mixture was quenched with sat. $NaHCO_3$ (100 mL), then extracted with ethyl acetate (3 × 20 mL). The combined organic layer was washed with brine (20 mL) and H_2O (20 mL), dried over Na_2SO_4. The crude mixture after removing solvents under reduced pressure was subjected to flash chromatography (30% ethyl acetate in hexane) to give an alcohol with quantitative yield. ^{1}H NMR (400 MHz, Chloroform-*d*) δ 5.47 (dd, *J* = 5.5, 2.4 Hz, 1H), 4.99 (d, *J* = 3.1 Hz, 1H), 4.85 (tt, *J* = 11.4, 5.2 Hz, 1H), 3.66 (s, 1H), 2.49 – 2.36 (m, 1H), 2.28 (t, *J* = 13.0 Hz, 1H), 2.08 – 2.00 (m, 2H), 1.99 (d, *J* = 2.0 Hz, 3H), 1.96 (d, *J* = 2.0 Hz, 3H), 1.94 – 1.85 (m, 1H), 1.77 (t, *J* = 12.8 Hz, 1H), 1.70 – 1.37 (m, 5H), 1.37 – 1.10 (m, 5H), 1.07 (dd, *J* = 6.3, 1.9 Hz, 3H), 1.03 (d, *J* = 2.0 Hz, 3H), 1.01 – 0.93 (m, 1H), 0.82 (d, *J* = 2.1 Hz, 1H), 0.70 (s, 3H). ^{13}C NMR (101 MHz, $CDCl_3$) δ 170.38, 170.31, 136.15, 125.03, 74.61, 70.46, 69.40, 58.46, 56.16, 42.25, 42.14, 40.42, 39.68, 37.33, 31.91, 31.67, 31.54, 25.58, 24.52, 23.72, 21.34, 21.10, 20.24, 19.44, 12.37. MS (ESI) m/z 441.4 $[M + Na]^+$.

Synthesis of **3**. (1S,3R,8S,10R,13S,14S,17S)-17-acetyl-10,13-dimethyl-2,3,4,7,8,9,10,11,12,13,14,15,16,17-tetradecahydro-1H-cyclopenta[a]phenanthrene-1,3-diyl diacetate. To a DCM (10 mL) solution of **16** (200 mg, 0.5 mmol) was added dess–martin periodinane (811 mg, 1.9 mmol, 4.0 equiv.) and stirred at room temperature for 12 h. The reaction mixture was quenched with sat. $NaHCO_3$ (30 mL) and stirred for 1 h, then extracted with DCM (3 × 20 mL). The combined organic layer was washed with brine (10 mL) and H2O (10 mL), dried over Na_2SO_4. The crude mixture after removing solvents under reduced pressure was subjected to flash chromatography (30% EtOAc in hexane) to give **3** (189 mg, 0.45 mmol, 95%) as a white solid. ^{1}H NMR (400 MHz, Chloroform-*d*) δ 5.47 (dd, *J* = 5.4, 2.4 Hz, 1H), 5.01 (d, *J* = 3.2 Hz, 1H), 4.86 (tt, *J* = 11.6, 5.1 Hz, 1H), 2.52 – 2.35 (m, 2H), 2.28 (t, *J* = 12.6 Hz, 1H), 2.12 (q, *J* = 11.4, 10.9 Hz, 1H), 2.04 (s, 3H), 2.00 (s, 3H), 1.96 (s, 3H), 1.92 (d, *J* = 2.8 Hz, 2H), 1.77 (t, *J* = 12.8 Hz, 1H), 1.69 – 1.04 (m, 10H), 1.02 (s, 3H), 0.92 – 0.72 (m, 1H), 0.55 (s, 3H). ^{13}C NMR (101 MHz, $CDCl_3$) δ 209.34, 170.39, 170.34, 136.03, 124.91, 74.52, 69.30, 63.60, 56.85, 43.94, 42.03, 40.43, 38.69, 37.25, 31.92, 31.67, 31.56, 31.50, 24.45, 22.75, 21.33, 21.15, 20.43, 19.41, 13.25. MS (ESI) m/z 439.5 $[M + Na]^+$.

Synthesis of **17**. (1S,3R,10R,13S,14R,17S)-17-acetyl-10,13-dimethyl-2,3,4,9,10,11,12,13,14,15,16,17-dodecahydro-1H-cyclopenta[a]phenanthrene-1,3-diyl diacetate. To a solution of compound **3** (170 mg, 0.41 mmol) in sodium-dried benzene–hexane (10 mL, 1:1) was added dibromantin (70 mg, 0.25 mmol, 0.6 equiv.) and AIBN (2.7 mg, 0.02 mmol, 0.04 equiv.). The mixture was refluxed for 20 min in a preheated oil bath (100 ºC) and then placed in an ice bath to cool. Insoluble material was removed by filtration and the filtrate was concentrated to yield a white solid. To a solution of this solid in tetrahydrofuran (10 mL) was added tetrabutylammonium bromide (33 mg, 0.1 mmol, 0.25 equiv.) and stirred for 75 min at r.t. To this reaction mixture was added tetrabutylammonium fluoride (0.8 mL of 1.0 M solution in THF, 2 equiv.) and the resulting solution was stirred for 50 min in the dark. Sat. Na_2CO_3 solution (30 mL) was added and stirred for 30 min. The mixture was extracted by ethyl acetate (3 × 30 mL). The organic layer was dried and concentrated. The residual was subjected to flash chromatography (20% EtOAc in hexane) to give **17** (88 mg, 0.21 mmol, 52%) as a white solid. ^{1}H NMR (400 MHz, Methanol-d_4) δ 5.73 – 5.66 (m, 1H), 5.44 (dd, J = 5.7, 2.8 Hz, 1H), 5.03 – 4.99 (m, 1H), 4.96 (q, J = 6.0 Hz, 1H), 2.73 (t, J = 8.9 Hz, 1H), 2.63 (dd, J = 14.7, 5.0 Hz, 1H), 2.57 – 2.35 (m, 2H), 2.21 (t, J = 9.8 Hz, 1H), 2.16 (s, 3H), 2.11 (s, 3H), 2.04 (s, 3H), 2.01 – 1.63 (m, 4H), 1.54 (q, J = 12.0, 8.9 Hz, 3H), 1.46 – 1.06 (m, 2H), 1.03 (s, 3H), 1.01 – 0.79 (m, 1H), 0.58 (s, 3H). ^{13}C NMR (101 MHz, MeOD) δ 212.25, 172.51, 172.14, 140.91, 136.82, 122.81, 117.73, 75.91, 69.96, 64.34, 55.72, 45.52, 42.39, 39.24, 39.16, 36.83, 33.09, 32.12, 24.41, 23.89, 21.78, 21.70, 21.52, 16.83, 14.02. MS (ESI) m/z 437.5 $[M + Na]^+$.

Synthesis of **18**. 1-((1S,3R,10R,13S,14R,17S)-1,3-dihydroxy-10,13-dimethyl-2,3,4,9,10,11,12,13,14,15,16,17-dodecahydro-1H-cyclopenta[a]phenanthren-17-yl)ethan-1-one. To a stirred solution of **17** (20 mg, 0.048 mmol) in methanol (2 mL) was added K_2CO_3 (33 mg, 0.24 mmol, 5 equiv.). The reaction mixture was stirred overnight at r.t. The reaction mixture was dried and subjected to flash chromatography directly (hexane:EtOAc:MeOH=60:35:5) to give **18** as a white solid (16 mg, 0.047 mmol, 98%). ^{1}H NMR (400 MHz, Methanol-d_4) δ 5.68 – 5.63 (m, 1H), 5.41 (dd, J = 5.7, 2.8 Hz, 1H), 3.99 (dq, J = 11.2, 5.8, 4.9 Hz, 1H), 3.75 (d, J = 3.2 Hz, 1H), 2.89 (t, J = 9.7 Hz, 1H), 2.78 (t, J = 8.8 Hz, 1H), 2.54 – 2.41 (m, 1H), 2.38 – 2.20 (m, 1H), 2.17 (s, 3H), 2.15 – 2.05 (m, 2H), 1.96 – 1.66 (m, 4H), 1.66 – 1.48 (m, 2H), 1.31 (s, 3H), 0.94 (s, 3H), 0.60 (s, 3H). ^{13}C NMR (101 MHz, MeOD) δ 212.11, 141.09, 139.17, 122.04, 117.30, 73.09, 65.79, 64.25, 55.72, 45.51, 43.29, 40.94, 39.41, 39.31, 38.70, 31.60, 24.37, 23.74, 21.44, 16.74, 13.56. MS (ESI) m/z 353.4 $[M + Na]^+$.

Synthesis of **2**. (1S,3R,10R,13S,14R,17S)-17-(2-hydroxy-6-methylheptan-2-yl)-10,13-dimethyl-2,3,4,9,10,11,12,13,14,15,16,17-dodecahydro-1H-cyclopenta[a]phenanthrene-1,3-diol. To a flame dried flask (25 mL) containing Mg (324 mg, 135.5 mmol, 2 equiv.) and catalytic I2 was added sodium dried THF (10 mL) and 1-bromo-4-methylpentane (1.1 g, 6.7 mmol, 1 equiv.). Under argon protection, the reaction mixture was stirred under reflux for 1 h, and cooled to 0 ºC. Then the self-made Grignard reagent (0.35 mL, 0.235 mmol, 5 equiv.) was added to **18** (16 mg, 0.047 mmol, 1.0 equiv.) pre-dissolved in anhydrous THF (3 mL) under 0 ºC. The reaction mixture was allowed to warm to r.t., stirred overnight, quenched with sat. NH_4Cl (10 mL), and

extracted with ethyl acetate (3 × 5 mL). The organic layer was combined and washed with sat. $NaHCO_3$ (3 mL), brine (3 mL) and water (3 mL), dried over anhydrous Na_2SO_4, and concentrated. The crude mixture was subjected to flash chromatography (hexane:EtOAc:MeOH=60:35:5) to give product **2** (17 mg, 0.041 mmol, 87%) as a colorless sticky solid. ^{1}H NMR (400 MHz, Acetone-d_6) δ 5.60 (d, J = 5.7 Hz, 1H), 5.35 (dd, J = 5.9, 2.9 Hz, 1H), 4.03 (d, J = 6.1 Hz, 1H), 3.76 (s, 1H), 3.72 (d, J = 2.5 Hz, 1H), 3.58 – 3.49 (m, 1H), 2.92 (s, 2H), 2.44 (dd, J = 15.2, 5.1 Hz, 1H), 2.24 (dt, J = 38.5, 11.7 Hz, 2H), 2.02 – 1.84 (m, 2H), 1.84 – 1.51 (m, 7H), 1.51 – 1.30 (m, 5H), 1.28 (s, 3H), 1.17 (td, J = 11.3, 9.3, 4.6 Hz, 4H), 0.92 (s, 3H), 0.89 (dd, J = 6.9, 2.5 Hz, 6H), 0.85 (s, 3H). ^{13}C NMR (101 MHz, Acetone) δ 141.86, 139.37, 121.14, 116.21, 74.60, 72.59, 65.01, 58.67, 55.84, 45.16, 43.94, 42.88, 41.44, 40.59, 40.53, 40.02, 38.16, 28.67, 26.96, 23.47, 23.04, 23.00, 22.89, 22.73, 21.05, 16.63, 14.07. HRMS (ESI+) m/z 399.3265 [M + Na - H2O]+ (error: 0.5 ppm).

Synthesis of **1**. (1R,3S,Z)-5-(2-((1S,3aS,7aS,E)-1-(2-hydroxy-6-methylheptan-2-yl)-7a-methyloctahydro-4H-inden-4-ylidene)ethylidene)-4-methylenecyclohexane-1,3-diol. A ethyl ether solution of **2** (17 mg, 1 mg/mL) was purged with argon gas for 10 min and subjected to UVB irradiation for 15 min in a quartz tube with a temperature below 50 °C, using a Rayonet RPR-100 photochemical reactor (Branford, CT). The compound was protected from light and sit in the dart at r.t. for 10 days to allow the conversion from pre-VD3 to VD3. The mixture was dried, dissolved in EtOH, and analyzed by an Agilent 1100 HPLC system (Santa Clara, CA) to obtain an optimized the analytical condition (50-100% MeCN, 0-30 min). The separation was carried out using a preparative HPLC system. The reaction mixture (500 μL) was injected by an autosampler onto a 5 μm Phenomenex Luna-PFP column (250 mm × 21.2 mm) (Torrance, CA) with mobile phase following the gradient (0-30 min, 40-70% MeCN) at a flow rate of 15 mL/min. Fractions containing product was monitored by UV absorbance, collected, and dried by lyophilizer (2.2 mg, 13%). ^{1}H NMR (400 MHz, Methanol-d_4) δ 6.34 (d, J = 11.1 Hz, 1H), 6.10 (d, J = 11.2 Hz, 1H), 5.31 (s, 1H), 4.92 (s, 3H), 4.38 (d, J = 6.3 Hz, 1H), 4.15 (s, 1H), 2.88 (d, J = 12.7 Hz, 1H), 2.59 – 2.46 (m, 1H), 2.28 (dd, J = 13.4, 6.7 Hz, 1H), 2.17 – 1.96 (m, 2H), 1.90 (d, J = 6.1 Hz, 2H), 1.85 – 1.28 (m, 11H), 1.26 (s, 3H), 1.19 (t, J = 7.2 Hz, 3H), 0.91 (dd, J = 6.6, 2.0 Hz, 6H), 0.73 (s, 3H). HRMS (ESI+) m/z 399.3260 [M + Na - H2O]+ (error: -0.7 ppm).

Crystal Structure Analysis of 15

Crystallization procedure. To a clean test tube (13 × 100 mm), 18 mg of compound **15** powder and 3 mL anhydrous n-hexane were added. The tube was shaken until the solid was completely dissolved, then sealed with 5 layers of sealing film (Parafilm) membrane. The resulting solution was allowed to stand in a quiet environment for 10 days, by which time the hexane had evaporated, leaving crystals of **15**.

X-ray analysis. A colorless, needle-like specimen of **15**, approximate dimensions 0.438 mm x 0.050 mm x 0.015 mm, was cleaved from a longer needle. The selected

crystal was affixed to a MiTeGen sample support with low-viscosity cryo oil, and flash cooled to 100K for x-ray analysis on a Bruker X8 κ diffractometer.

The crystal was illuminated with the X-ray beam from a Bruker IμSCu microfocus sealed tube, and the diffraction data were measured with a Bruker Photon-100 detector. The resulting images were integrated with the SAINT software package using a narrow-frame algorithm. Integration of the data based on a monoclinic unit cell yielded a total of 22378 reflections to a maximum θ angle of 68.716° (0.83 Å resolution), of which 5512 were independent and 4649 (84.3%) were considered observed. The data were complete (100.0%) to a θ angle of 67.679° (0.83 Å). A numerical absorption correction was applied, and data were corrected for inter-frame scaling differences, via program SADABS.

The structure was solved and refined via SHELXT and SHELXL-2014, using the space group $P2_1$, with $Z = 2$ for the formula unit, $C_{31}H_{52}O_5Si$ (one molecule of **15**). Hydrogen atoms were placed in idealized positions, and refined according to a riding model. The final anisotropic full-matrix least-squares refinement converged at R1 = 5.96% for the observed data and wR2 = 12.80% for all data. The largest peak in the final difference electron density synthesis was 0.381 $e^-/Å^3$ and the deepest hole was −0.299 $e^-/Å^3$, with an RMS deviation of 0.052 $e^-/Å^3$.

The structure contains one unique molecule per unit cell, with nine distinct stereocenters. The data support high confidence in the reported absolute structure, as judged by a refined Flack parameter value of 0.02(5).

Theoretical Calculations

The calculations were performed with Gaussian 09 program. [286] Structures **A** and **B** (**Figure 6-2**) were optimized at B3LYP/6-31+G(d) theoretical level, [287, 288] then frequency calculation were performed at the same theoretical level at 195.15K. Due to convergence problem at B3LYP/6-31+G(d), structural optimization and frequency calculation were carried out at B3LYP/6-31G(d) theoretical level at 298.15 K for structures **A** and **B**. Single point calculations were then performed at a higher theoretical level with B3LYP/6-311++G(d,p) method in THF using SMD solvation model. [288] Free energies were given by adding the solvation energy changes to the computed gas-phase free energies. Computed structures are illustrated using CYLView. [289]

The stability difference of **A** and **B** is similar to that of equatorial and axial substituents at chair cyclohexane. The repulsion between the axial oxygen atoms decrease the stability of conformer **B**.

Crystallization and Structural Analysis of 1,20S(OH)2D3–VDR Complex

cDNA encoding zVDR LBD (156-453 AA) was subcloned into pET28b vector to generate N-terminal His-tag fusion proteins. Purification was carried out as previously

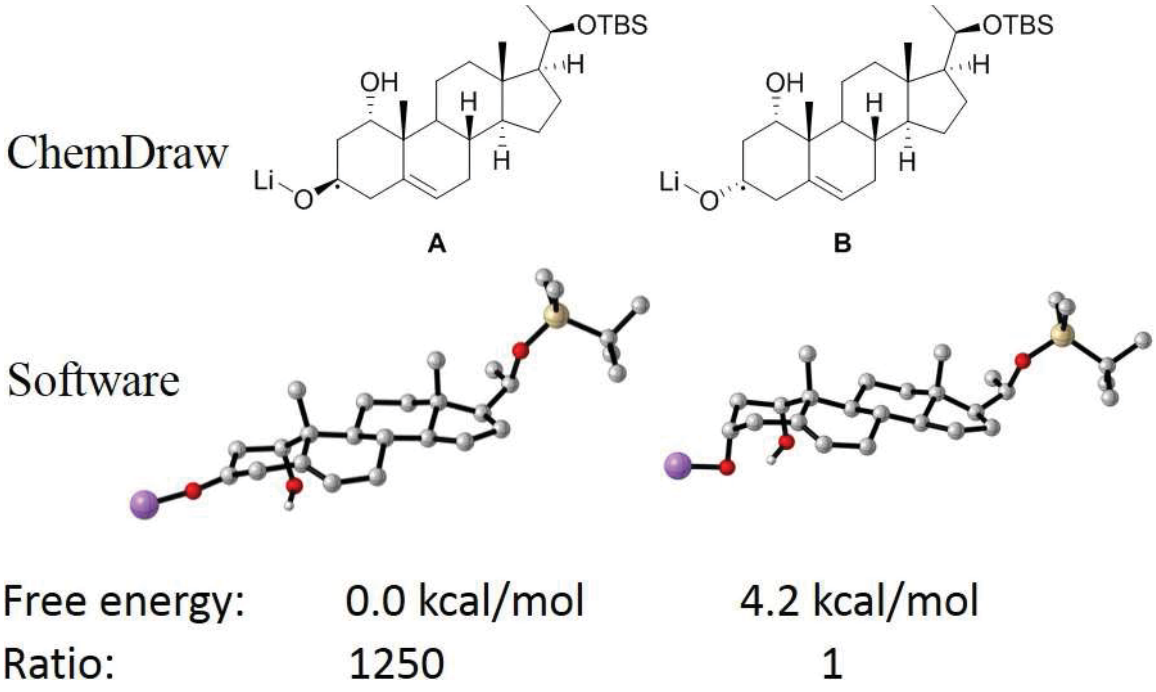

Figure 6-2. Structures used for calculation.

described, including metal affinity chromatography and gel filtration [290].The protein was concentrated using Amicon ultra-30 (Millipore) to 3-7 mg/ml and incubated with a two-fold excess of ligand and a three-fold excess of the coactivator SRC-1 peptide (686-RHKILHRLLQEGSPS-698). Crystals were obtained in 50 mM Bis–Tris pH 6.5, 1.6 M lithium sulfate and 50 mM magnesium sulfate. Protein crystals were mounted in a fiber loop and flash-cooled under a nitrogen flux after cryo-protection with 20% glycerol. Data collection from a single frozen crystal was performed at 100 K on the ID23-1 beamline at ESRF (France). The raw data were processed and scaled with the HKL2000 program suite [291]. The crystals belong to the space group $P6_522$, with one LBD complex per asymmetric unit. The structure was solved and refined using BUSTER [292], Phenix [293] and iterative model building using COOT [294]. Crystallographic refinement statistics are presented in **Table 6-1**. All structural figures were prepared using PyMOL (www.pymol.org/).

VDRE Stimulation Assay

HaCat, Caco-2 and Jurkat cells were transduced by lentiviral VDRE-reporter (luciferase) vector. [195, 268, 278] Caco-2 cells were grown in Dulbecco's Modified Eagle Medium (DMEM) containing 10% fetal bovine serum (FBS) and 1% penicillin/streptomycin/amphotericin antibiotic solution (Ab) (Sigma-Aldrich, St. Louis, MO). HaCaT cells were grown in DMEM supplemented with 5% FBS and 1% Ab. Jurkat cells were grown in RPMI 1640 medium containing 10% FBS and 1% Ab. All cells were cultured at 37 °C in a humidified atmos-phere containing 5% CO2. All cell lines were selected for at least one week by medium containing additional 1.0 μg/mL puromycin before compound treatment. Each cell line was then plated in a 96-well plate (10,000 cells/100 μL medium/well) using FBS-free media and incubated for 24 h. 1,20S(OH)2D3, 1,25(OH)2D3 and 22-Oxa-1,25(OH)2D3 at a series of concentrations in 10% DMSO were added separately to 96-well plate (1.0 μL/well), while 10% DMSO was used as control. After 24 h incubation, 100 μL of ONE-GloTM Luciferase Assay System (Promega, Madison, WI) was added to each well. After 5 min at r.t., the signal was recorded by a BioTek Synergy HT microplate reader (BioTek Instruments, Inc., Winooski, VT, US). All concentrations of secosteroids were tested in triplicate.

VDR Translocation

The effects of 1,20S(OH)2D3 on VDR translocation from the cytoplasm to the nucleus were tested on previous SKMEL-188 cells model, [295] which was stably transduced with pLenti-CMV-VDREGFP-pgk-puro (VDR and EGFP expressed as fusion protein). [296, 297] Cells were treated with secosteroids (up to 100 nM) for 16 h followed by fixing with 4% paraformaldehyde (PFA). Fixed cells were mounted with fluorescent-mounting media (Dako, Carpinteria, CA, USA) and analyzed with a fluorescence microscope. Translocation to the nucleus was determined by counting cells with a fluorescent nucleus and the results are presented as the percentage of the total cells that

Table 6-1. Crystallographic data collection and refinement statistics for zVDR LBD in complex with 1,20S(OH)$_2$D$_3$

Data processing	Parameter
Beamline	ID23-1
X-ray source detector	PILATUS 6M
λ (Å)	1.000000
Resolution (Å)	47.85 - 1.98 (2.051 - 1.98)
Crystal space group	P $6_5$22
Cell parameters (Å)	a = b = 65.936; c = 262.97
Unique reflections	24360 (2364)
Mean redundancy	2.0 (2.0)
Rsym (%)	1.54 (27.11)
Mean I/σ(I)	14.92 (2.32)
completeness (%)	98 (100)
Refinement	
rmsd bond length (Å)	0.003
rmsd bond angles (deg)	0.62
Rcryst (%)	20.01
Rfree (%)	22.50
no. of non-H atoms	
protein	1992
ligands	30
water	58
average B factor	
protein	71.72
ligands	59.89
water	71.70
Ramachandran plots	
favored (%)	99
allowed (%)	1.2

displayed nuclear staining, as described previously. [296] The data were obtained from at least two separate experiments, with images taken randomly from at least six different fields and counted as described. [296, 297]

Real-time PCR Assay

HaCaT cells were seeded in 60 mm dishes (1 million/dish) in 10 mL DMEM supplemented with 5% FBS and 1% Ab. After overnight they were cultured in FBS-free medium for another 12 h to synchronize the cells. The media were then removed, and compounds in DMEM (5% FBS and 1% Ab) with a concentration of 100 nM were added to the dishes. After 24 h incubation, media were removed, and 10 mL PBS was used to wash the dish. Cells were then detached by trypsin, centrifuged in Eppendorf tube, washed with PBS (5 mL), and stored at -80 °C. Absolutely RNA Miniprep Kit (Stratagene, La Jolla, CA, USA) was used to isolate the RNA, and Transcriptor First Strand cDNA Synthesis Kit (Roche Inc., Mannheim, Germany) was used for reverse transcription (100 ng RNA/reaction). Real-time PCR was carried out using cDNA which was diluted 10-fold in sterile water and a SYBR Green PCR Master Mix. The forward reverse primers for VDR, CYP24A1, TRPV6 and CYP27B1 genes were designed based on the rat and mouse sequences using Primer Quest software (Integrated Device Technology, San Jose, CA, USA). Reactions (n=3) were performed at 50 °C for 2 min, 95 °C for 10 min and then 40 cycles of 95 °C for 15 s, 60 °C for 30 s and 72 °C for 30 s. Data were collected and analyzed on a Roche Light Cycler 480. Using a comparative Ct method, [216] the amount of the final amplified product was normalized to the amount of β-actin as a housekeeping gene.

IFNγ Inhibition Assay.

Secosteroids were solubilized in absolute EtOH at 10^{-4} M and diluted to 10^{-6} M by adding Eagles Minimal Essential Medium (EMEM) containing 9% charcoal-stripped fetal calf serum, 100 U/mL penicillin and 100 μg/mL streptomycin, non-essential amino acids, 2.5 mM 2-mercaptoethanol, 2.5 mM L-glutamine [244]. Splenocytes were isolated from 7-week old C57BL/6 female mice, erythrocytes lysed by hypotonic shock, washed twice with EMEM, suspended and cultured at a concentration for 2×10^6/mL (500 μL/well) for 72 h in EMEM described above. To each well in a 48-well tissue culture plate, 450 μL of the splenocytes were added. Secosteroids (50 μL of the 10-6 M stock) or EtOH diluted 1:100 with the above culture medium were added to triplicate wells and then incubated at 37 °C in 5% CO2 in a humidified tissue culture incubator for 2 h, after which 1 μg/well of rat anti-mouse CD3 MOAB was added. After 72 h culture, supernatants from each well were harvested and analyzed by ELISA for levels (pg/mL) of D-murine IFNγ (RAD Systems, Minneapolis, MN), according to the manufacturer's instructions. The concentration of IFNγ is supernatants from cultures containing secosteroids were compared to the concentration of IFNγ in the supernatants of EtOH-treated control cultures, by ANOVA.

Results and Discussion

Retrosynthesis of 1,20S(OH)2D3

A retrosynthetic strategy including a common 1α-OH intermediate (**3**) was proposed (**Figure 6-3**). The D3 structure could be obtained from UVB transformation of **2**, [195, 268, 278] of which the 20*S*-OH and side chain could be achieved by Grignard reaction of **3**. [195, 201, 268, 278] Introduction of 1α-OH to **4** could be carried out by a multi-step conversion similar to androstenolone. [298]

Synthesis of 1,20*S*(OH)2D3

The synthesis (**Figure 6-4**) started with deacetylation and TBS protection of pregnenolone acetate (**4**) to give intermediate **6**. $NaBH_4$ treatment of **6** selectively afforded 20*R* epimer as a major product which was then protected by acetyl to go through the DDQ oxidation safely (75% yield) to produce intermediate **10**. After replacing 20-OAc with 20-OTBS, a 1α,2α-epoxide group was introduced by adding KOH and H_2O_2 solution to afford intermediate **13** (73%), followed by Birch reduction to give 1α,3β-diol **14** (61%) as a major product. [298-300] To confirm 1α-OH formation, **14** was protected with acetyl to produce **15**, which was characterized by 1D and 2D NMR spectrometry and crystalized from hexane for X-ray analysis (Cambridge Crystallographic Data Center, code: CCDC 1527430). After removal of 20-OTBS, intermediate **16** was oxidized by DMP to 1α,3β-diacetoxypregn-5-en-20-one (**3**, 95%), which was then transformed into the 5,7-diene 7DHC intermediate (**17**, 52%) by a well-established procedure. [195, 268, 278] To avoid potential separation problems caused by acetyl protection during Grignard reaction, ester hydrolysis was carried out prior to Grignard reaction (87%) to afford 1α,20*S*-7DHC (**2**). UVB irradiation of **2** in ether followed by vitamin D3 isomerization afforded the desired product (**1**, 13% yield), which was compared with its enzymatic counterpart after HPLC separation.

Pregnenolone acetate (**4**) has often been used as the starting material for 20*S*(OH)D3 analogs, [195, 268, 278] in which 1α-hydroxylation was necessary to display potent VDR stimulation activities. [195, 268] Previously, the production of 1α-OH derivatives of 20*S*(OH)D3 analogs was completely relying on CYP27B1 biosynthesis, owing to the lack of appropriate 1α-OH intermediates. The limited amount of 1α-OH derivatives remains a big hurdle for biological testing. Fortunately, the discovery of 1α,3β-diacetoxypregn-5-en-20-one (**3**) opens a possible avenue for large scale production of various 1,20*S*(OH)2D3 analogs in the near future.

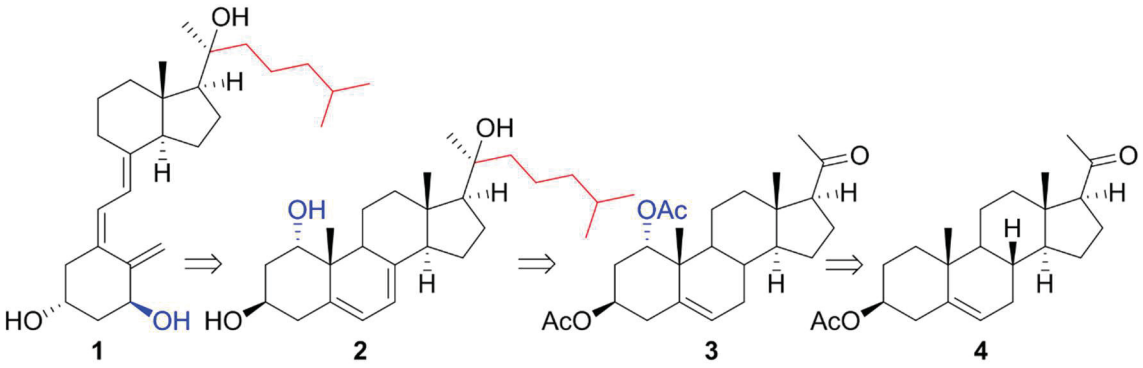

Figure 6-3. Retrosynthesis of 1,20*S*$(OH)_2D_3$.

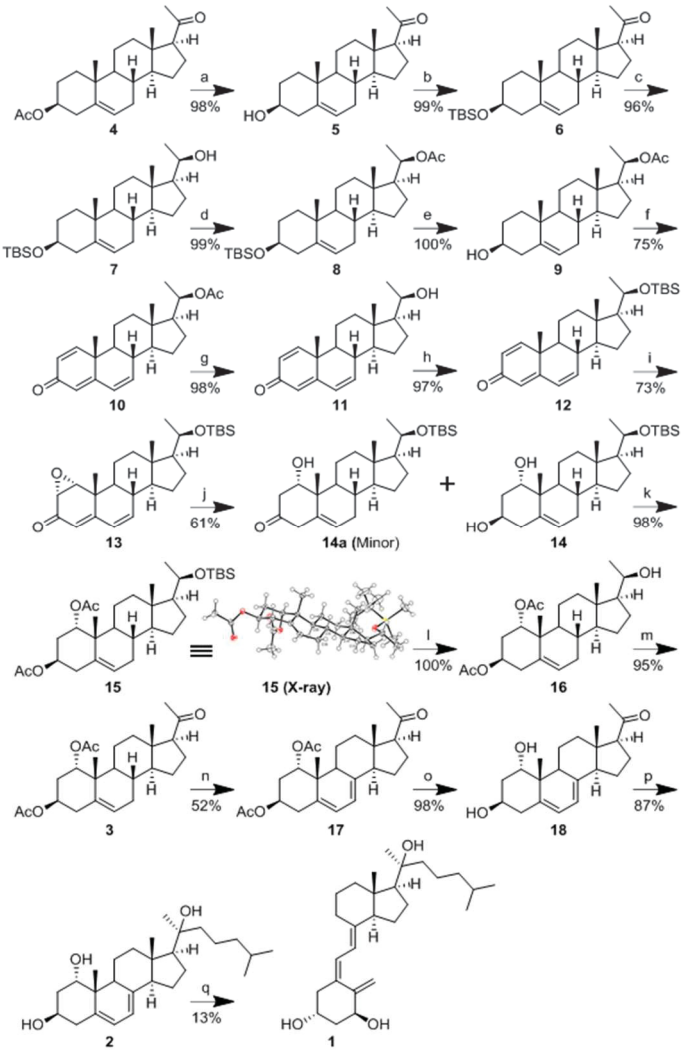

Figure 6-4. Synthesis of 1α,20*S*-dihydroxyvitamin D_3.
Reagents and conditions: (a) K_2CO_3, MeOH, r.t., overnight. (b) TBSCl, imidazole, DMF, r.t., overnight. (c) $NaBH_4$, DCM: MeOH (1:1), 0 ºC - r.t., overnight. (d) Ac_2O, Et_3N, DMAP, DCM, r.t., overnight. (e) TBAF, THF, r.t., 12 h. (f) DDQ, 1,4-dioxane, reflux, 4 h. (g) KOH, MeOH, r.t., 3 h. (h) TBSCl, imidazole, DMF, r.t., overnight. (i) KOH in MeOH, 30% H_2O_2, MeOH, -40 ºC – 0 ºC, 12 h. (j) Li, NH_3 (l), -80 ºC, 30 min; addition of starting material in THF, -80 ºC, 2 h; -40 ºC, 1 h; NH_4Cl, -80 ºC, 2 h. (k) Ac_2O, Et_3N, DMAP, DCM, r.t., overnight. (l) TBAF, THF, r.t., 48 h. (m) DMP, DCM, r.t., 12 h. (n) Dibromantin, AIBN, benzene: hexane (1:1), reflux 20 min; TBAB, THF, r.t., 75 min; TBAF, r.t., 50 min. (o) K_2CO_3, MeOH, r.t., overnight. (p) Mg, I_2, 1-bromo-4-methylpentane, THF, reflux, 1 h; addition of self-made Grignard reagent, THF, 0 ºC – r.t., overnight. (q) UVB light, Et_2O, 50 ºC, 15 min; r.t., 10 d; HPLC, MeCN:H_2O. TBSCl = *tert*-butyldimethylsilyl chloride, DMAP = 4-dimethylaminopyridine, TBAF = tetra-*n*-butylammonium fluoride, DDQ = 2,3-dichloro-5,6-dicyanobenzoquinone, DMP = Dess–Martin periodinane, AIBN = azobisisobutyronitrile, TBAB = tetra-*n*-butylammonium bromide.

Proposed Mechanism for Birch Reduction of 13

In **Figure 6-4**, the critical step is the Birch reduction of epoxide **13**. Inconsistent yields of similar reactions were reported ranging from poor to moderate yields for this modified version of Birch reduction, probably due to difference in synthetic procedure.[298-300] We experienced the same challenge in initial trials. Our efforts to obtain a consistent yield at this step have shown us that the addition of NH_4Cl (quenching step) is the key to the success of this reaction. Quick addition (< 10 min) of NH_4Cl gave predominantly intermediate **14a**, whereas slow addition (> 2 h) afforded mainly the desired product **14**. **14a** as a semi-reduced intermediate was obtained and characterized for the first time, and sheds some light on the possible mechanisms of this stepwise reaction (**Figure 6-5**).

The solvated electrons from Lithium in liquid ammonia add to the double bond to give a radical anion. The addition of NH_4Cl provides a proton to the radical anion and also to the penultimate carbanion. Quick addition of NH_4Cl will totally consume electrons and mainly form the intermediate **14a**. However, slow addition of NH_4Cl afforded mainly the desired product **14** since the remaining electrons will further reduce ketone **14a**. Gaussian calculations were carried out to compare the formation of 3α- and 3β-OH, which as a result have a ratio of 1/1250 (3α-/3β-OH) in polar solvent, being consistent with our synthetic results. Understanding the mechanism helps in optimizing the yields of this and similar reactions.

Transcriptional Activity

The ability of 1,20*S*(OH)2D3 to activate VDR was analysed in three cell lines (HaCaT, Caco-2 and Jurkat) transduced with lentiviral vitamin D response elements (VDRE) reporter (luciferase).[195, 201, 268, 278] Compared with 1,25(OH)2D3 and 22-Oxa-1,25(OH)2D3, two known VDR agonists, 1,20*S*(OH)2D3 showed potent transcriptional activity with EC50s of 450.4 nM in HaCaT cells, 284.8 nM in Caco-2 cells and 19.1 nM in Jurkat cells. Although less active than 22-Oxa-1,25(OH)2D3 in all three cell lines, 1,20*S*(OH)2D3 is equally potent to (HaCaT and Caco-2 cells) or less potent than (Jurkat cells) 1,25(OH)2D3, the native ligand of VDR (**Table 6-2**).

X-ray Crystallographic Analysis of the zVDR Ligand Binding Domain in Complex with 1,20*S*(OH)2D3

The overall structure of VDR-1,20*S*(OH)2D3 (Protein Data Bank, code: 5MX7) is highly homologous to the VDR-1,25(OH)2D3 structure, adopting the canonical active conformation. When compared to the zVDR LBD-1,25(OH)2D3 structure [301], the Cα atoms of the zVDR LBD–1,20*S*(OH)2D3 complex have a root mean square deviation of 0.25 Å over 238 residues. The ligand binds similarly as 1,25(OH)2D3 (**Figure 6-6** and **Figure 6-7**). The 1-OH and 3-OH form similar H-bonds while the 20S-OH forms a weak

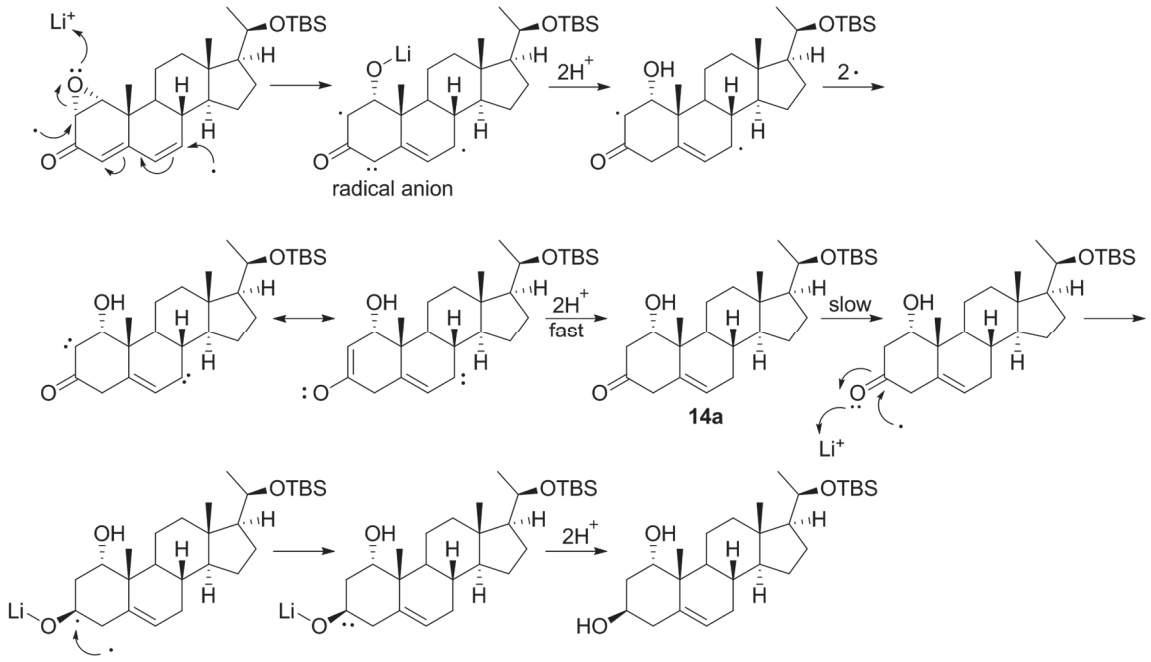

Figure 6-5. Proposed reaction mechanisms for Birch reduction of 13.

Table 6-2. VDRE stimulation effect of 1,20*S*(OH)$_2$D$_3$.

Compound	VDRE stimulation (EC_{50}, nM)			IFNγ production (pg/mL)
	HaCaT	Caco-2	Jurkat	
Control	NA	NA	NA	710±9
1,20*S*(OH)$_2$D$_3$	450.4±14.9	284.8±13.2	19.1±0.9	383±3
1,25(OH)$_2$D$_3$	421.9±3.1	300.2±9.2	2.1±0.1	353±11
22-Oxa-1,25(OH)$_2$D$_3$	10.5.±2.6	154.5±0.8	1.2±0.1	258±2

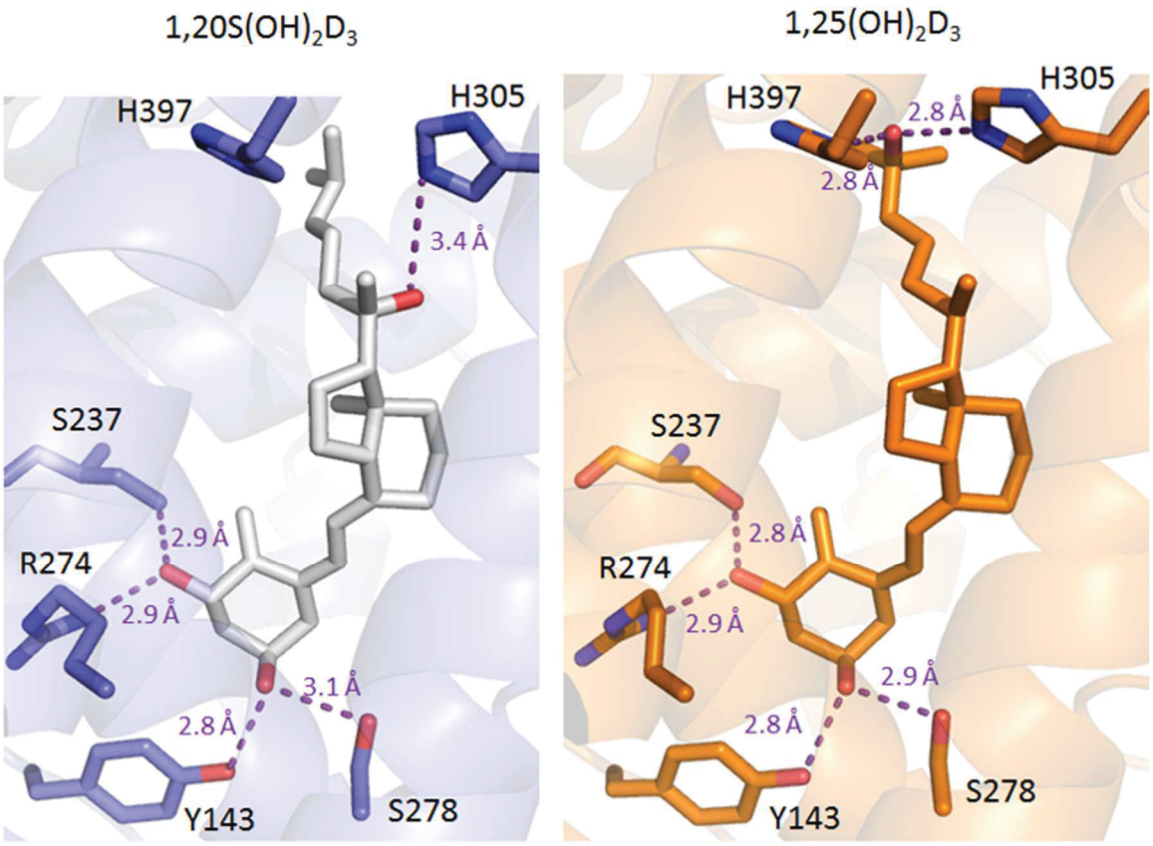

Figure 6-6. X-ray crystal structures of 1,20*S*$(OH)_2D_3$ and 1,25$(OH)_2D_3$ in complex with zVDR LBD.
Hydrogen bonds are shown by dashed lines and hydrogen-bonding residues are labelled.

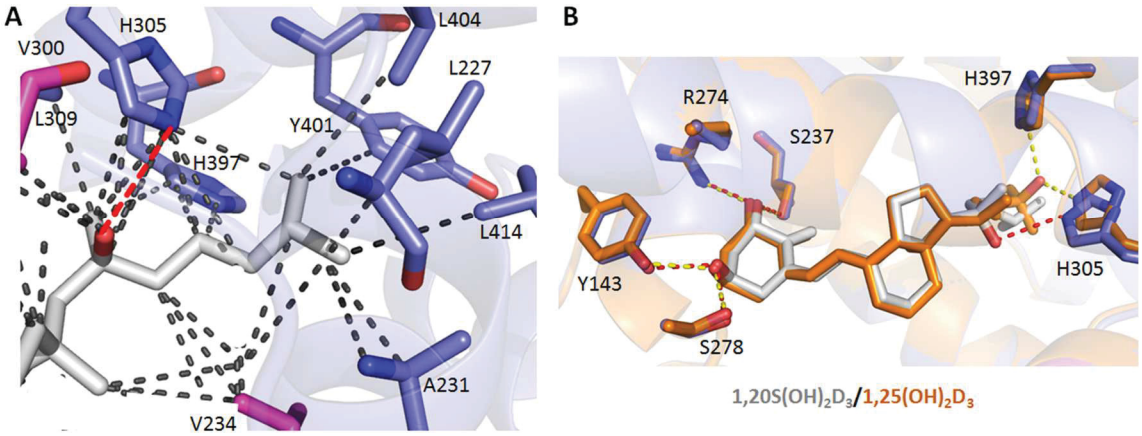

Figure 6-7. Molecular interactions of VDR LBD in the presence of 1,20S(OH)2D3 or 1,25(OH)2D3.

A) Details of the interactions mediated by the side chain of 1,20S$(OH)_2D_3$ with residues of the zVDR LBD at a 4 Å distance cutoff. The residues numbers correspond to hVDR. (B) Overlay of 1,25$(OH)_2D_3$ (carbon atoms in orange and oxygen atoms in red) with 1,20S$(OH)_2D_3$ (grey) within zVDR LBD complexes with the indication of the hydrogen bonds formed by the ligands. The Hydrogen bonds are shown by red or yellow dashed lines and Van Der Waals interactions by grey dashed lines.

H-bond with His305 (3.42 Å) and does not interact with His397. (Note that the residues numbers correspond to hVDR). His305 (loop6-7) is slightly shifted to maintain this interaction. In addition, the 20*S*-OH forms a Van der Waals interaction with Val300. While most of the Van der Waals interactions are maintained, the side chain and terminal methyl groups that are differently positioned interact differently with some of the residues (**Figure 6-7**). Weaker interactions are formed with Leu227 (4.1 Å instead of 3.8 Å with C26) and Tyr399 (4.1 Å instead of 3.8 Å with C27), interactions compensated by stronger interactions with Val234 (3.9 Å instead of 4.2 Å with C22), and Leu412 (3.9 Å instead of 4.2 Å with C27). Overall, the efficient H-bond interaction of 20*S*-OH with His305 and hydrophobic contacts formed by the ligand explains its agonist activity, however, less potent than or comparable to 1,25(OH)2D3.

VDR Translocation Activity

1,25(OH)2D3 stays inactive until it binds to cytosolic or membrane VDR.[20] Translocation of 1,25(OH)2D3-bound VDR from cytoplasm to nucleus is a key step to exert its regulatory effects. [20, 196] In SKMEL-188 melanoma cells transduced with pLenti-CMVVDR-EGFP-pgk-puro, [279] both 1,20*S*(OH)2D3 and 1,25(OH)2D3 showed stimulatory effect with EC_{50} values of 2.14×10^{-9} and 7.87×10^{-9} nM (**Figure 6-8**), respectively. The results indicate that 1,20S(OH)2D3 induces VDR translocation in a similar fashion with 1,25(OH)2D3.

Regulatory Activity of VDR Downstream Genes

To investigate how 1,20*S*(OH)2D3 affects VDR target genes through VDR activation, the expression levels of *VDR*, *CYP24A1*, *TRPV6* and *CYP27B1* genes were studied in HaCaT cells (**Figure 6-8**). 1,20*S*(OH)2D3 was capable of mildly upregulating the expression (1.6-fold) of its own receptor, the VDR, while being moderately stronger than 1,25(OH)2D3 (1.3-fold) and comparable to 22-Oxa-1,25(OH)2D3 (1.7-fold). 1,25(OH)2D3 is known to induce expression of vitamin D catabolism enzyme CYP24A1. [7, 278] Similarly, 1,20*S*(OH)2D3 strongly stimulates *CYP24A1* mRNA levels 34-fold, as compared with 10-fold for 1,25(OH)2D3 and 78-fold for 22-Oxa-1,25(OH)2D3. In addition, *TRPV6* encoding an intestinal calcium channel is also a well-known target of VDR for mineral homeostasis. [278, 302] The mRNA levels of *TRPV6* were increased by 1.4-, 1.4- and 2.6-fold for 1,20*S*(OH)2D3, 1,25(OH)2D3 and 22-Oxa-1,25(OH)2D3, respectively. Moreover, VDR activation induced by its agonist inhibits the expression of vitamin D activation enzyme CYP27B1. [216, 303] As shown in **Figure 6-8** although weaker than 1,25(OH)2D3 and 22-Oxa-1,25(OH)2D3, 1,20*S*(OH)2D3 slightly inhibited the expression of *CYP27B1*. These results indicate that 1,20*S*(OH)2D3 is able to activate VDR, and exert its effects through regulating VDR target genes in a similar manner to 1,25(OH)2D3.

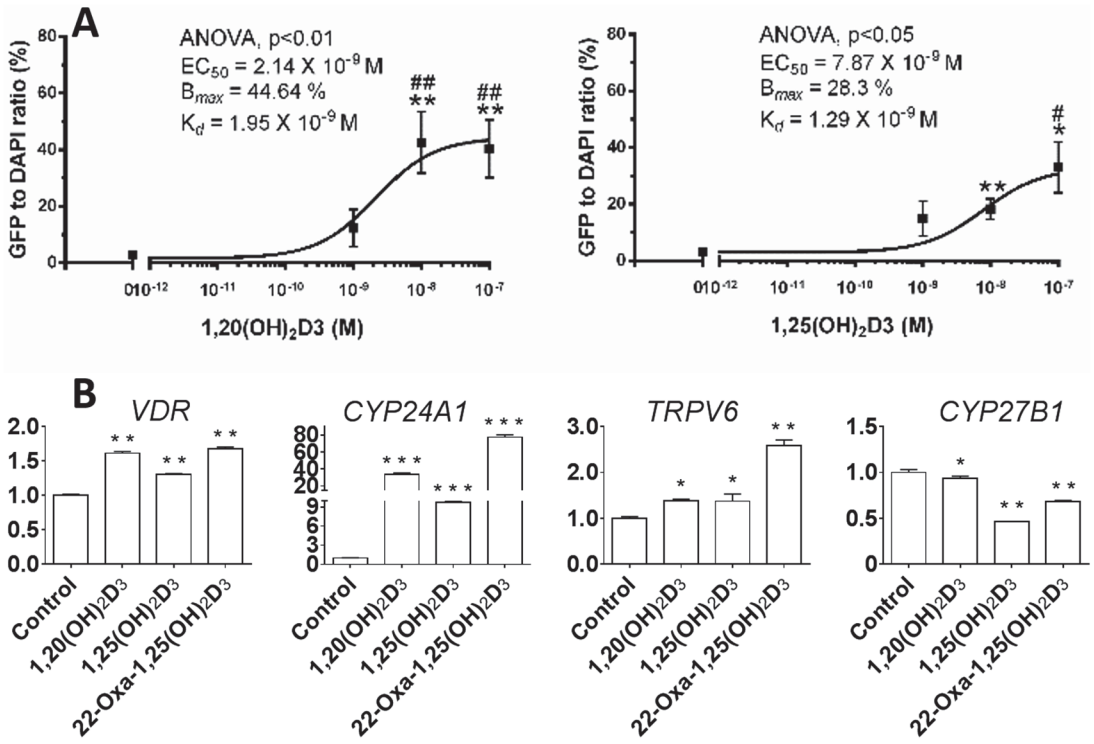

Figure 6-8. Biological activities of 1,20S(OH)$_2$D$_3$.
(**A**) The effect on vitamin D receptor (VDR) translocation from cytoplasm to nucleus. Data are mean ± SEM ($n \geq 6$). The dose-dependent stimulation of VDR translocation was analysed by one-way ANOVA with #p<0.05 and ##p<0.01. The differences between control and treatment were analyzed with Student's t-test, where *p<0.05 and **p<0.01. (**B**) 1,20S(OH)$_2$D$_3$ regulates mRNA expression of genes *VDR*, *CYP24A1*, *TRPV6* and *CYP27B1* in HaCaT cells at 100 nM after 24 h treatment (n = 3). *p< 0.05, **p<0.01 and ***p<0.001.

Anti-inflammatory Activity

As shown in **Table 6-2**, positive controls 1,25(OH)2D3 and 22-Oxa-1,25(OH)2D3 decreased IFNγ production by 50% and 64% at 1.0 nM, respectively. 1,20(OH)2D3 significantly reduced IFNγ concentrations (56% reduction), being comparable with 1,25(OH)2D3 however less potent than 22-Oxa-1,25(OH)2D3. The results suggested that 1,20(OH)2D3 have good anti-inflammatory effect, and could serve as a lead compound for development of 1,20(OH)2D3 analogs.

Summary

The natural vitamin D3 metabolite, 1,20*S*(OH)2D3 was chemically synthesized for the first time and biologically tested. The mechanism of the critical Birch reduction in the 1α-OH synthesis was proposed for the first time; understanding this mechanism will help optimize synthetic yields of similar 1α-OH intermediates. 1α,3β-diacetoxypregn-5-en-20-one can serve as a common intermediate for production of other 1,20S(OH)2D3 analogs. 1,20*S*(OH)2D3 strongly binds to and activates VDR leading to regulatory effects similar to those of 1,25(OH)2D3 on VDR downstream genes including, but not limited to, *VDR*, *CYP24A1*, *TRPV6* and *CYP27B1*. The crystal structure of 1,20*S*(OH)2D3 in VDR reveals differences from 1,25(OH)2D3, with respect to their interactions, including the important role of the efficient, H-bond mediated interaction between 20*S*-OH and His305. This study provides a basis for rational design and practical synthesis of novel 1,20*S*(OH)2D3 analogs for future drug development.

CHAPTER 7. CONCLUSION

To conclude, the new Gemini 20S(OH)D3 analogs were able to activate the VDR. Analysis of gene expression at the mRNA level showed that the analogs regulated *CYP24A1*, *VDR* and *TRPV6* genes, consistent with their effects being mediated through activation of the VDR. In addition, these analogs displayed anti-proliferative and anti-inflammatory activity, which might also correlate with their VDR activation process. This study suggests that Gemini 20S(OH)D3 analogs have great potential as therapeutic agents on the immune system.

20S,24S(OH)2D3 and 20S,24R(OH)2D3 were chemically synthesized for the first time. The C24 stereochemistry of the two isomers was unambiguously assigned by NMR analysis. HPLC retention times of chemically synthesized 20S,24S(OH)2D3 and 20S,24R(OH)2D3 enabled the identification of the major isomer produced from 20(OH)D3 by CYP24A1 as 20S,24R(OH)2D3 and the minor isomer as 20S,24S(OH)2D3. 20S,24R(OH)2D3 is also the isomer produced from 20(OH)D3 by an unidentified P450, distinct from CYP24A1 (which is not expressed in liver) in mouse liver microsomes. Biological studies showed that the 24R-epimer had stronger or more potent biological activity, regardless of whether the compound was 1α-hydroxylated or not. The 20,24(OH)2D3 isomers lacked the ability to activate VDRE using a synthetic promotor construct, however, their 1α-OH products showed potent VDRE-LUC activation, significantly more potent than that of 1,25(OH)2D3 and comparable with that of or 22-Oxa. In addition, inhibition of IFNγ production by splenocytes and stimulation of LAIR-1 production indicates that that 24R-epimer is also more active than 24S-epimer with respect to anti-inflammatory activities. The different properties of 20S,24S(OH)2D3 and 20S,24R(OH)2D3 are further demonstrated by the ability of CYP27B1 to metabolize 20S,24R(OH)2D3 with a catalytic efficiency 5.5-fold higher than that for 20S,24S(OH)2D3, but comparable to 1,25(OH)2D3. In summary, 20S,24R(OH)2D3 displays greater biological activity than 20S,24S(OH)2D3, with 1α-hydroxylation enhancing the activities of both epimers. Further investigation on the interaction with the vitamin D receptor and subsequent signal transduction pathways would likely explain their differential biological activities.

20*S*,23*R*/*S*(OH)2D3 and their 1α-OH metabolites were synthesized for the first time, and 20*S*,23*S*(OH)2D3 was confirmed to be the natural metabolite. These compounds showed different abilities to activate the VDR with 1α,20*S*,23*R*/*S*(OH)3D3 being the most potent. They all showed anti-inflammatory and anti-proliferative activities, although these different biological activities were not linearly correlated, most likely due to distinct mechanisms and structural requirements leading to these biological activities. Further biological studies of the unnatural metabolite, 1α,20*S*,23*R*/*S*(OH)3D3, will be necessary to investigate its drug-like properties in comparison to its natural 23*S* counterpart.

Four 20S(OH)D3 analogs with side chain modifications on C24 were chemically synthesized, and their 1α-OH derivatives [except that of 23,24-amide-1,20S(OH)2D3]

were produced from biosynthesis of CYP27B1. Enzymatic studies showed that CYP27B1 can activate (1α-hydroxylate) 20S(OH)D3 analogs [except 23,24-amide-20S(OH)D3], and CYP24A1 can metabolize all analogs, with faster rates than 20S(OH)D3 itself for both CYP27B1 activation and CYP24A1 catabolism. 20S(OH)D3 analogs showed mild to moderate VDR stimulatory, VDR downstream gene regulatory and anti-inflammatory activities, and these activities can be significantly improved by 1α-hydroxylation. Co-crystal structures of VDR in complex with 20S(OH)D3, 24-DB-20S(OH)D3, and 23,24-amide-20S(OH)D3 will reveal their molecular interactions in the binding pocket of VDR, and in turn will be insightful for developing novel VDR agonists as anti-inflammatory agents.

The natural vitamin D3 metabolite, 1,20*S*(OH)2D3 was chemically synthesized for the first time and biologically tested. The mechanism of the critical Birch reduction in the 1α-OH synthesis was proposed for the first time; understanding this mechanism will help optimize synthetic yields of similar 1α-OH intermediates. 1α,3β-diacetoxypregn-5-en-20-one can serve as a common intermediate for production of other 1,20S(OH)2D3 analogs. 1,20*S*(OH)2D3 strongly binds to and activates VDR leading to regulatory effects similar to those of 1,25(OH)2D3 on VDR downstream genes including, but not limited to, *VDR*, *CYP24A1*, *TRPV6* and *CYP27B1*. The crystal structure of 1,20*S*(OH)2D3 in VDR reveals differences from 1,25(OH)2D3, with respect to their interactions, including the important role of the efficient, H-bond mediated interaction between 20*S*-OH and His305. This study provides a basis for rational design and practical synthesis of novel 1,20*S*(OH)2D3 analogs for future drug development.

In summary, different series of 20S(OH)D3 analogs have been synthesized in this study. Biological tests suggest that these analogs were substrates of CYP27B1 and CYP24A1, were able to activate VDR, regulate VDR downstream genes, and exert their anti-inflammatory effects. Crystallography analysis of 1,20(OH)2D3 and 20S(OH)D3 analogs (will report later) showed that they are ligands of VDR, and show different interactions in the VDR binding domain compared with 1,25(OH)D3, the native ligand of VDR. Together with the investigations of 1,20(OH)2D3, this study provides molecular basis of design, practical synthetic strategies, and insightful mechanisms of actions for future development of 20S(OH)D3 and 1,20(OH)2D3 analogs as VDR agonists and anti-inflammatory agents.

LIST OF REFERENCES

1. Simon, R. R.; Borzelleca, J. F.; DeLuca, H. F.; Weaver, C. M. Safety assessment of the post-harvest treatment of button mushrooms (Agaricus bisporus) using ultraviolet light. *Food Chem Toxicol* **2013,** *56*, 278-289.
2. MacLaughlin, J. A.; Anderson, R. R.; Holick, M. F. Spectral character of sunlight modulates photosynthesis of previtamin D3 and its photoisomers in human skin. *Science* **1982,** *216*, 1001-1003.
3. Zhu, J. G.; Ochalek, J. T.; Kaufmann, M.; Jones, G.; Deluca, H. F. CYP2R1 is a major, but not exclusive, contributor to 25-hydroxyvitamin D production in vivo. *Proc Natl Acad Sci U S A* **2013,** *110*, 15650-15655.
4. Goltzman, D.; Hendy, G. N.; White, J. H. Vitamin D and its receptor during late development. *Biochim Biophys Acta* **2015,** *1849*, 171-180.
5. Bosse, Y.; Lemire, M.; Poon, A. H.; Daley, D.; He, J. Q.; Sandford, A.; White, J. H.; James, A. L.; Musk, A. W.; Palmer, L. J.; Raby, B. A.; Weiss, S. T.; Kozyrskyj, A. L.; Becker, A.; Hudson, T. J.; Laprise, C. Asthma and genes encoding components of the vitamin D pathway. *Respir Res* **2009,** *10*, 98.
6. Brunette, M. G.; Chan, M.; Ferriere, C.; Roberts, K. D. Site of 1,25(OH)2 vitamin D3 synthesis in the kidney. *Nature* **1978,** *276*, 287-289.
7. St-Arnaud, R. CYP24A1-deficient mice as a tool to uncover a biological activity for vitamin D metabolites hydroxylated at position 24. *J Steroid Biochem Mol Biol* **2010,** *121*, 254-256.
8. Fukumoto, S. Physiological regulation and disorders of phosphate metabolism--pivotal role of fibroblast growth factor 23. *Intern Med* **2008,** *47*, 337-343.
9. Tieu, E. W.; Tang, E. K.; Chen, J.; Li, W.; Nguyen, M. N.; Janjetovic, Z.; Slominski, A.; Tuckey, R. C. Rat CYP24A1 acts on 20-hydroxyvitamin D(3) producing hydroxylated products with increased biological activity. *Biochem Pharmacol* **2012,** *84*, 1696-1704.
10. Zhu, J.; DeLuca, H. F. Vitamin D 25-hydroxylase - Four decades of searching, are we there yet? *Arch Biochem Biophys* **2012,** *523*, 30-36.
11. Brenza, H. L.; DeLuca, H. F. Regulation of 25-hydroxyvitamin D3 1alpha-hydroxylase gene expression by parathyroid hormone and 1,25-dihydroxyvitamin D3. *Arch Biochem Biophys* **2000,** *381*, 143-152.
12. Murayama, A.; Takeyama, K.; Kitanaka, S.; Kodera, Y.; Kawaguchi, Y.; Hosoya, T.; Kato, S. Positive and negative regulations of the renal 25-hydroxyvitamin D3 1alpha-hydroxylase gene by parathyroid hormone, calcitonin, and 1alpha,25(OH)2D3 in intact animals. *Endocrinology* **1999,** *140*, 2224-2231.
13. Quarles, L. D. Endocrine functions of bone in mineral metabolism regulation. *J Clin Invest* **2008,** *118*, 3820-3828.
14. Juppner, H. Phosphate and FGF-23. *Kidney Int Suppl* **2011**, S24-27.
15. Abrahamsen, B.; Harvey, N. C. The role of vitamin D supplementation in patients with rheumatic diseases. *Nat Rev Rheumatol* **2013,** *9*, 411-422.
16. Holick, M. F.; Kleiner-Bossaller, A.; Schnoes, H. K.; Kasten, P. M.; Boyle, I. T.; DeLuca, H. F. 1,24,25-Trihydroxyvitamin D3. A metabolite of vitamin D3 effective on intestine. *J Biol Chem* **1973,** *248*, 6691-6696.

17. Boyle, I. T.; Omdahl, J. L.; Gray, R. W.; DeLuca, H. F. The biological activity and metabolism of 24,25-dihydroxyvitamin D 3. *J Biol Chem* **1973,** *248*, 4174-4180.
18. Moore, D. D.; Kato, S.; Xie, W.; Mangelsdorf, D. J.; Schmidt, D. R.; Xiao, R.; Kliewer, S. A. International Union of Pharmacology. LXII. The NR1H and NR1I receptors: constitutive androstane receptor, pregnene X receptor, farnesoid X receptor alpha, farnesoid X receptor beta, liver X receptor alpha, liver X receptor beta, and vitamin D receptor. *Pharmacol Rev* **2006,** *58*, 742-759.
19. Deeb, K. K.; Trump, D. L.; Johnson, C. S. Vitamin D signalling pathways in cancer: potential for anticancer therapeutics. *Nat Rev Cancer* **2007,** *7*, 684-700.
20. Haussler, M. R.; Haussler, C. A.; Bartik, L.; Whitfield, G. K.; Hsieh, J. C.; Slater, S.; Jurutka, P. W. Vitamin D receptor: molecular signaling and actions of nutritional ligands in disease prevention. *Nutr Rev* **2008,** *66*, S98-112.
21. Haussler, M. R.; Whitfield, G. K.; Haussler, C. A.; Hsieh, J. C.; Thompson, P. D.; Selznick, S. H.; Dominguez, C. E.; Jurutka, P. W. The nuclear vitamin D receptor: biological and molecular regulatory properties revealed. *J Bone Miner Res* **1998,** *13*, 325-349.
22. Bhalla, A. K.; Amento, E. P.; Clemens, T. L.; Holick, M. F.; Krane, S. M. Specific high-affinity receptors for 1,25-dihydroxyvitamin D3 in human peripheral blood mononuclear cells: presence in monocytes and induction in T lymphocytes following activation. *J Clin Endocrinol Metab* **1983,** *57*, 1308-1310.
23. Provvedini, D. M.; Tsoukas, C. D.; Deftos, L. J.; Manolagas, S. C. 1,25-dihydroxyvitamin D3 receptors in human leukocytes. *Science* **1983,** *221*, 1181-1183.
24. Takahashi, K.; Nakayama, Y.; Horiuchi, H.; Ohta, T.; Komoriya, K.; Ohmori, H.; Kamimura, T. Human neutrophils express messenger RNA of vitamin D receptor and respond to 1alpha,25-dihydroxyvitamin D3. *Immunopharmacol Immunotoxicol* **2002,** *24*, 335-347.
25. Xu, H.; Soruri, A.; Gieseler, R. K.; Peters, J. H. 1,25-Dihydroxyvitamin D3 exerts opposing effects to IL-4 on MHC class-II antigen expression, accessory activity, and phagocytosis of human monocytes. *Scand J Immunol* **1993,** *38*, 535-540.
26. Rigby, W. F.; Shen, L.; Ball, E. D.; Guyre, P. M.; Fanger, M. W. Differentiation of a human monocytic cell line by 1,25-dihydroxyvitamin D3 (calcitriol): a morphologic, phenotypic, and functional analysis. *Blood* **1984,** *64*, 1110-1115.
27. Adams, J. S.; Gacad, M. A. Characterization of 1 alpha-hydroxylation of vitamin D3 sterols by cultured alveolar macrophages from patients with sarcoidosis. *J Exp Med* **1985,** *161*, 755-765.
28. Barnes, P. F.; Modlin, R. L.; Bikle, D. D.; Adams, J. S. Transpleural gradient of 1,25-dihydroxyvitamin D in tuberculous pleuritis. *J Clin Invest* **1989,** *83*, 1527-1532.
29. Helming, L.; Bose, J.; Ehrchen, J.; Schiebe, S.; Frahm, T.; Geffers, R.; Probst-Kepper, M.; Balling, R.; Lengeling, A. 1alpha,25-Dihydroxyvitamin D3 is a potent suppressor of interferon gamma-mediated macrophage activation. *Blood* **2005,** *106*, 4351-4358.
30. Towers, T. L.; Staeva, T. P.; Freedman, L. P. A two-hit mechanism for vitamin D3-mediated transcriptional repression of the granulocyte-macrophage colony-

stimulating factor gene: vitamin D receptor competes for DNA binding with NFAT1 and stabilizes c-Jun. *Mol Cell Biol* **1999,** *19*, 4191-4199.
31. Cannell, J. J.; Vieth, R.; Umhau, J. C.; Holick, M. F.; Grant, W. B.; Madronich, S.; Garland, C. F.; Giovannucci, E. Epidemic influenza and vitamin D. *Epidemiol Infect* **2006,** *134*, 1129-1140.
32. Koeffler, H. P.; Amatruda, T.; Ikekawa, N.; Kobayashi, Y.; DeLuca, H. F. Induction of macrophage differentiation of human normal and leukemic myeloid stem cells by 1,25-dihydroxyvitamin D3 and its fluorinated analogues. *Cancer Res* **1984,** *44*, 5624-5628.
33. Dickie, L. J.; Church, L. D.; Coulthard, L. R.; Mathews, R. J.; Emery, P.; McDermott, M. F. Vitamin D3 down-regulates intracellular Toll-like receptor 9 expression and Toll-like receptor 9-induced IL-6 production in human monocytes. *Rheumatology (Oxford)* **2010,** *49*, 1466-1471.
34. Liu, P. T.; Stenger, S.; Li, H.; Wenzel, L.; Tan, B. H.; Krutzik, S. R.; Ochoa, M. T.; Schauber, J.; Wu, K.; Meinken, C.; Kamen, D. L.; Wagner, M.; Bals, R.; Steinmeyer, A.; Zugel, U.; Gallo, R. L.; Eisenberg, D.; Hewison, M.; Hollis, B. W.; Adams, J. S.; Bloom, B. R.; Modlin, R. L. Toll-like receptor triggering of a vitamin D-mediated human antimicrobial response. *Science* **2006,** *311*, 1770-1773.
35. Nguyen, T. M.; Pavlovitch, J.; Papiernik, M.; Guillozo, H.; Walrant-Debray, O.; Pontoux, C.; Garabedian, M. Changes in 1,25-(OH)2D3 synthesis and its receptor expression in spleen cell subpopulations of mice infected with LPBM5 retrovirus. *Endocrinology* **1997,** *138*, 5505-5510.
36. Overbergh, L.; Decallonne, B.; Valckx, D.; Verstuyf, A.; Depovere, J.; Laureys, J.; Rutgeerts, O.; Saint-Arnaud, R.; Bouillon, R.; Mathieu, C. Identification and immune regulation of 25-hydroxyvitamin D-1-alpha-hydroxylase in murine macrophages. *Clin Exp Immunol* **2000,** *120*, 139-146.
37. Guillot, X.; Semerano, L.; Saidenberg-Kermanac'h, N.; Falgarone, G.; Boissier, M. C. Vitamin D and inflammation. *Joint Bone Spine* **2010,** *77*, 552-557.
38. Van Belle, T. L.; Gysemans, C.; Mathieu, C. Vitamin D in autoimmune, infectious and allergic diseases: a vital player? *Best Pract Res Clin Endocrinol Metab* **2011,** *25*, 617-632.
39. Almerighi, C.; Sinistro, A.; Cavazza, A.; Ciaprini, C.; Rocchi, G.; Bergamini, A. 1Alpha,25-dihydroxyvitamin D3 inhibits CD40L-induced pro-inflammatory and immunomodulatory activity in human monocytes. *Cytokine* **2009,** *45*, 190-197.
40. Gauzzi, M. C.; Purificato, C.; Donato, K.; Jin, Y.; Wang, L.; Daniel, K. C.; Maghazachi, A. A.; Belardelli, F.; Adorini, L.; Gessani, S. Suppressive effect of 1alpha,25-dihydroxyvitamin D3 on type I IFN-mediated monocyte differentiation into dendritic cells: impairment of functional activities and chemotaxis. *J Immunol* **2005,** *174*, 270-276.
41. Penna, G.; Adorini, L. 1 Alpha,25-dihydroxyvitamin D3 inhibits differentiation, maturation, activation, and survival of dendritic cells leading to impaired alloreactive T cell activation. *J Immunol* **2000,** *164*, 2405-2411.
42. Piemonti, L.; Monti, P.; Sironi, M.; Fraticelli, P.; Leone, B. E.; Dal Cin, E.; Allavena, P.; Di Carlo, V. Vitamin D3 affects differentiation, maturation, and

function of human monocyte-derived dendritic cells. *J Immunol* **2000,** *164*, 4443-4451.
43. Adorini, L.; Penna, G.; Giarratana, N.; Roncari, A.; Amuchastegui, S.; Daniel, K. C.; Uskokovic, M. Dendritic cells as key targets for immunomodulation by Vitamin D receptor ligands. *J Steroid Biochem Mol Biol* **2004,** *89-90*, 437-441.
44. Chang, C. C.; Ciubotariu, R.; Manavalan, J. S.; Yuan, J.; Colovai, A. I.; Piazza, F.; Lederman, S.; Colonna, M.; Cortesini, R.; Dalla-Favera, R.; Suciu-Foca, N. Tolerization of dendritic cells by T(S) cells: the crucial role of inhibitory receptors ILT3 and ILT4. *Nat Immunol* **2002,** *3*, 237-243.
45. Griffin, M. D.; Lutz, W.; Phan, V. A.; Bachman, L. A.; McKean, D. J.; Kumar, R. Dendritic cell modulation by 1alpha,25 dihydroxyvitamin D3 and its analogs: a vitamin D receptor-dependent pathway that promotes a persistent state of immaturity in vitro and in vivo. *Proc Natl Acad Sci U S A* **2001,** *98*, 6800-6805.
46. Hewison, M.; Freeman, L.; Hughes, S. V.; Evans, K. N.; Bland, R.; Eliopoulos, A. G.; Kilby, M. D.; Moss, P. A.; Chakraverty, R. Differential regulation of vitamin D receptor and its ligand in human monocyte-derived dendritic cells. *J Immunol* **2003,** *170*, 5382-5390.
47. Mahon, B. D.; Wittke, A.; Weaver, V.; Cantorna, M. T. The targets of vitamin D depend on the differentiation and activation status of CD4 positive T cells. *J Cell Biochem* **2003,** *89*, 922-932.
48. Lemire, J. M.; Adams, J. S.; Kermani-Arab, V.; Bakke, A. C.; Sakai, R.; Jordan, S. C. 1,25-Dihydroxyvitamin D3 suppresses human T helper/inducer lymphocyte activity in vitro. *J Immunol* **1985,** *134*, 3032-3035.
49. Lemire, J. M.; Archer, D. C.; Beck, L.; Spiegelberg, H. L. Immunosuppressive actions of 1,25-dihydroxyvitamin D3: preferential inhibition of Th1 functions. *J Nutr* **1995,** *125*, 1704S-1708S.
50. Boonstra, A.; Barrat, F. J.; Crain, C.; Heath, V. L.; Savelkoul, H. F.; O'Garra, A. 1alpha,25-Dihydroxyvitamin d3 has a direct effect on naive CD4(+) T cells to enhance the development of Th2 cells. *J Immunol* **2001,** *167*, 4974-4980.
51. Penna, G.; Amuchastegui, S.; Cossetti, C.; Aquilano, F.; Mariani, R.; Sanvito, F.; Doglioni, C.; Adorini, L. Treatment of experimental autoimmune prostatitis in nonobese diabetic mice by the vitamin D receptor agonist elocalcitol. *J Immunol* **2006,** *177*, 8504-8511.
52. Daniel, C.; Sartory, N. A.; Zahn, N.; Radeke, H. H.; Stein, J. M. Immune modulatory treatment of trinitrobenzene sulfonic acid colitis with calcitriol is associated with a change of a T helper (Th) 1/Th17 to a Th2 and regulatory T cell profile. *J Pharmacol Exp Ther* **2008,** *324*, 23-33.
53. Tang, J.; Zhou, R.; Luger, D.; Zhu, W.; Silver, P. B.; Grajewski, R. S.; Su, S. B.; Chan, C. C.; Adorini, L.; Caspi, R. R. Calcitriol suppresses antiretinal autoimmunity through inhibitory effects on the Th17 effector response. *J Immunol* **2009,** *182*, 4624-4632.
54. Veldman, C. M.; Cantorna, M. T.; DeLuca, H. F. Expression of 1,25-dihydroxyvitamin D(3) receptor in the immune system. *Arch Biochem Biophys* **2000,** *374*, 334-338.

55. Ooi, J. H.; McDaniel, K. L.; Weaver, V.; Cantorna, M. T. Murine CD8+ T cells but not macrophages express the vitamin D 1alpha-hydroxylase. *J Nutr Biochem* **2014,** *25*, 58-65.
56. Meehan, T. F.; DeLuca, H. F. CD8(+) T cells are not necessary for 1 alpha,25-dihydroxyvitamin D(3) to suppress experimental autoimmune encephalomyelitis in mice. *Proc Natl Acad Sci U S A* **2002,** *99*, 5557-5560.
57. Lysandropoulos, A. P.; Jaquiery, E.; Jilek, S.; Pantaleo, G.; Schluep, M.; Du Pasquier, R. A. Vitamin D has a direct immunomodulatory effect on CD8+ T cells of patients with early multiple sclerosis and healthy control subjects. *J Neuroimmunol* **2011,** *233*, 240-244.
58. Yu, S.; Bruce, D.; Froicu, M.; Weaver, V.; Cantorna, M. T. Failure of T cell homing, reduced CD4/CD8alphaalpha intraepithelial lymphocytes, and inflammation in the gut of vitamin D receptor KO mice. *Proc Natl Acad Sci U S A* **2008,** *105*, 20834-20839.
59. Boissier, M. C.; Assier, E.; Biton, J.; Denys, A.; Falgarone, G.; Bessis, N. Regulatory T cells (Treg) in rheumatoid arthritis. *Joint Bone Spine* **2009,** *76*, 10-14.
60. Jeffery, L. E.; Burke, F.; Mura, M.; Zheng, Y.; Qureshi, O. S.; Hewison, M.; Walker, L. S.; Lammas, D. A.; Raza, K.; Sansom, D. M. 1,25-Dihydroxyvitamin D3 and IL-2 combine to inhibit T cell production of inflammatory cytokines and promote development of regulatory T cells expressing CTLA-4 and FoxP3. *J Immunol* **2009,** *183*, 5458-5467.
61. Ardalan, M. R.; Maljaei, H.; Shoja, M. M.; Piri, A. R.; Khosroshahi, H. T.; Noshad, H.; Argani, H. Calcitriol started in the donor, expands the population of CD4+CD25+ T cells in renal transplant recipients. *Transplant Proc* **2007,** *39*, 951-953.
62. Ghoreishi, M.; Bach, P.; Obst, J.; Komba, M.; Fleet, J. C.; Dutz, J. P. Expansion of antigen-specific regulatory T cells with the topical vitamin d analog calcipotriol. *J Immunol* **2009,** *182*, 6071-6078.
63. Jeffery, L. E.; Wood, A. M.; Qureshi, O. S.; Hou, T. Z.; Gardner, D.; Briggs, Z.; Kaur, S.; Raza, K.; Sansom, D. M. Availability of 25-hydroxyvitamin D(3) to APCs controls the balance between regulatory and inflammatory T cell responses. *J Immunol* **2012,** *189*, 5155-5164.
64. Chen, L.; Cencioni, M. T.; Angelini, D. F.; Borsellino, G.; Battistini, L.; Brosnan, C. F. Transcriptional profiling of gamma delta T cells identifies a role for vitamin D in the immunoregulation of the V gamma 9V delta 2 response to phosphate-containing ligands. *J Immunol* **2005,** *174*, 6144-6152.
65. Colin, E. M.; Asmawidjaja, P. S.; van Hamburg, J. P.; Mus, A. M.; van Driel, M.; Hazes, J. M.; van Leeuwen, J. P.; Lubberts, E. 1,25-dihydroxyvitamin D3 modulates Th17 polarization and interleukin-22 expression by memory T cells from patients with early rheumatoid arthritis. *Arthritis Rheum* **2010,** *62*, 132-142.
66. Merino, F.; Alvarez-Mon, M.; de la Hera, A.; Ales, J. E.; Bonilla, F.; Durantez, A. Regulation of natural killer cytotoxicity by 1,25-dihydroxyvitamin D3. *Cell Immunol* **1989,** *118*, 328-336.

67. Balogh, G.; de Boland, A. R.; Boland, R.; Barja, P. Effect of 1,25(OH)(2)-vitamin D(3) on the activation of natural killer cells: role of protein kinase C and extracellular calcium. *Exp Mol Pathol* **1999,** *67*, 63-74.
68. Yang, S.; Smith, C.; DeLuca, H. F. 1 alpha, 25-Dihydroxyvitamin D3 and 19-nor-1 alpha, 25-dihydroxyvitamin D2 suppress immunoglobulin production and thymic lymphocyte proliferation in vivo. *Biochim Biophys Acta* **1993,** *1158*, 279-286.
69. Chen, S.; Sims, G. P.; Chen, X. X.; Gu, Y. Y.; Chen, S.; Lipsky, P. E. Modulatory effects of 1,25-dihydroxyvitamin D3 on human B cell differentiation. *J Immunol* **2007,** *179*, 1634-1647.
70. Heine, G.; Niesner, U.; Chang, H. D.; Steinmeyer, A.; Zugel, U.; Zuberbier, T.; Radbruch, A.; Worm, M. 1,25-dihydroxyvitamin D(3) promotes IL-10 production in human B cells. *Eur J Immunol* **2008,** *38*, 2210-2218.
71. Shirakawa, A. K.; Nagakubo, D.; Hieshima, K.; Nakayama, T.; Jin, Z.; Yoshie, O. 1,25-dihydroxyvitamin D3 induces CCR10 expression in terminally differentiating human B cells. *J Immunol* **2008,** *180*, 2786-2795.
72. Feldman, D.; Krishnan, A. V.; Swami, S.; Giovannucci, E.; Feldman, B. J. The role of vitamin D in reducing cancer risk and progression. *Nat Rev Cancer* **2014,** *14*, 342-357.
73. Krishnan, A. V.; Feldman, D. Molecular pathways mediating the anti-inflammatory effects of calcitriol: implications for prostate cancer chemoprevention and treatment. *Endocr Relat Cancer* **2010,** *17*, R19-38.
74. Krishnan, A. V.; Swami, S.; Peng, L.; Wang, J.; Moreno, J.; Feldman, D. Tissue-selective regulation of aromatase expression by calcitriol: implications for breast cancer therapy. *Endocrinology* **2010,** *151*, 32-42.
75. Moreno, J.; Krishnan, A. V.; Swami, S.; Nonn, L.; Peehl, D. M.; Feldman, D. Regulation of prostaglandin metabolism by calcitriol attenuates growth stimulation in prostate cancer cells. *Cancer Res* **2005,** *65*, 7917-7925.
76. Nonn, L.; Peng, L.; Feldman, D.; Peehl, D. M. Inhibition of p38 by vitamin D reduces interleukin-6 production in normal prostate cells via mitogen-activated protein kinase phosphatase 5: implications for prostate cancer prevention by vitamin D. *Cancer Res* **2006,** *66*, 4516-4524.
77. Krishnan, A. V.; Moreno, J.; Nonn, L.; Swami, S.; Peehl, D. M.; Feldman, D. Calcitriol as a chemopreventive and therapeutic agent in prostate cancer: role of anti-inflammatory activity. *J Bone Miner Res* **2007,** *22 Suppl 2*, V74-80.
78. Krishnan, A. V.; Feldman, D. Mechanisms of the anti-cancer and anti-inflammatory actions of vitamin D. *Annu Rev Pharmacol Toxicol* **2011,** *51*, 311-336.
79. Cohen-Lahav, M.; Shany, S.; Tobvin, D.; Chaimovitz, C.; Douvdevani, A. Vitamin D decreases NFkappaB activity by increasing IkappaBalpha levels. *Nephrol Dial Transplant* **2006,** *21*, 889-897.
80. Karin, M.; Lin, A. NF-kappaB at the crossroads of life and death. *Nat Immunol* **2002,** *3*, 221-227.
81. Stio, M.; Martinesi, M.; Bruni, S.; Treves, C.; Mathieu, C.; Verstuyf, A.; d'Albasio, G.; Bagnoli, S.; Bonanomi, A. G. The Vitamin D analogue TX 527

blocks NF-kappaB activation in peripheral blood mononuclear cells of patients with Crohn's disease. *J Steroid Biochem Mol Biol* **2007,** *103*, 51-60.
82. Maeda, S.; Omata, M. Inflammation and cancer: role of nuclear factor-kappaB activation. *Cancer Sci* **2008,** *99*, 836-842.
83. Bao, B. Y.; Yao, J.; Lee, Y. F. 1alpha, 25-dihydroxyvitamin D3 suppresses interleukin-8-mediated prostate cancer cell angiogenesis. *Carcinogenesis* **2006,** *27*, 1883-1893.
84. Ferrero-Miliani, L.; Nielsen, O. H.; Andersen, P. S.; Girardin, S. E. Chronic inflammation: importance of NOD2 and NALP3 in interleukin-1beta generation. *Clin Exp Immunol* **2007,** *147*, 227-235.
85. Foersch, S.; Waldner, M. J.; Neurath, M. F. Innate and adaptive immunity in inflammatory bowel diseases. *Dig Dis* **2013,** *31*, 317-320.
86. Geremia, A.; Biancheri, P.; Allan, P.; Corazza, G. R.; Di Sabatino, A. Innate and adaptive immunity in inflammatory bowel disease. *Autoimmun Rev* **2014,** *13*, 3-10.
87. Cutolo, M.; Otsa, K.; Paolino, S.; Yprus, M.; Veldi, T.; Seriolo, B. Vitamin D involvement in rheumatoid arthritis and systemic lupus erythaematosus. *Ann Rheum Dis* **2009,** *68*, 446-447.
88. Gomez-Vaquero, C.; Fiter, J.; Enjuanes, A.; Nogues, X.; Diez-Perez, A.; Nolla, J. M. Influence of the BsmI polymorphism of the vitamin D receptor gene on rheumatoid arthritis clinical activity. *J Rheumatol* **2007,** *34*, 1823-1826.
89. Cutolo, M.; Otsa, K.; Laas, K.; Yprus, M.; Lehtme, R.; Secchi, M. E.; Sulli, A.; Paolino, S.; Seriolo, B. Circannual vitamin d serum levels and disease activity in rheumatoid arthritis: Northern versus Southern Europe. *Clin Exp Rheumatol* **2006,** *24*, 702-704.
90. Rossini, M.; Bagnato, G.; Frediani, B.; Iagnocco, A.; G, L. A. M.; Minisola, G.; Caminiti, M.; Varenna, M.; Adami, S. Relationship of focal erosions, bone mineral density, and parathyroid hormone in rheumatoid arthritis. *J Rheumatol* **2011,** *38*, 997-1002.
91. Merlino, L. A.; Curtis, J.; Mikuls, T. R.; Cerhan, J. R.; Criswell, L. A.; Saag, K. G.; Iowa Women's Health, S. Vitamin D intake is inversely associated with rheumatoid arthritis: results from the Iowa Women's Health Study. *Arthritis Rheum* **2004,** *50*, 72-77.
92. Costenbader, K. H.; Feskanich, D.; Holmes, M.; Karlson, E. W.; Benito-Garcia, E. Vitamin D intake and risks of systemic lupus erythematosus and rheumatoid arthritis in women. *Ann Rheum Dis* **2008,** *67*, 530-535.
93. Nielen, M. M.; van Schaardenburg, D.; Lems, W. F.; van de Stadt, R. J.; de Koning, M. H.; Reesink, H. W.; Habibuw, M. R.; van der Horst-Bruinsma, I. E.; Twisk, J. W.; Dijkmans, B. A. Vitamin D deficiency does not increase the risk of rheumatoid arthritis: comment on the article by Merlino et al. *Arthritis Rheum* **2006,** *54*, 3719-3720.
94. Patel, S.; Farragher, T.; Berry, J.; Bunn, D.; Silman, A.; Symmons, D. Association between serum vitamin D metabolite levels and disease activity in patients with early inflammatory polyarthritis. *Arthritis Rheum* **2007,** *56*, 2143-2149.
95. Hein, G.; Oelzner, P. [Vitamin D metabolites in rheumatoid arthritis: findings--hypotheses--consequences]. *Z Rheumatol* **2000,** *59 Suppl 1*, 28-32.

96. Andjelkovic, Z.; Vojinovic, J.; Pejnovic, N.; Popovic, M.; Dujic, A.; Mitrovic, D.; Pavlica, L.; Stefanovic, D. Disease modifying and immunomodulatory effects of high dose 1 alpha (OH) D3 in rheumatoid arthritis patients. *Clin Exp Rheumatol* **1999,** *17*, 453-456.
97. Grazio, S.; Naglic, D. B.; Anic, B.; Grubisic, F.; Bobek, D.; Bakula, M.; Kavanagh, H. S.; Kuna, A. T.; Cvijetic, S. Vitamin D serum level, disease activity and functional ability in different rheumatic patients. *Am J Med Sci* **2015,** *349*, 46-49.
98. Park, Y. E.; Kim, B. H.; Lee, S. G.; Park, E. K.; Park, J. H.; Lee, S. H.; Kim, G. T. Vitamin D status of patients with early inflammatory arthritis. *Clin Rheumatol* **2015,** *34*, 239-246.
99. Abourazzak, F. E.; Talbi, S.; Aradoini, N.; Berrada, K.; Keita, S.; Hazry, T. 25-hydroxy vitamin D and its relationship with clinical and laboratory parameters in patients with rheumatoid arthritis. *Clin Rheumatol* **2015,** *34*, 353-357.
100. Harries, A. D.; Brown, R.; Heatley, R. V.; Williams, L. A.; Woodhead, S.; Rhodes, J. Vitamin D status in Crohn's disease: association with nutrition and disease activity. *Gut* **1985,** *26*, 1197-1203.
101. Levin, A. D.; Wadhera, V.; Leach, S. T.; Woodhead, H. J.; Lemberg, D. A.; Mendoza-Cruz, A. C.; Day, A. S. Vitamin D deficiency in children with inflammatory bowel disease. *Dig Dis Sci* **2011,** *56*, 830-836.
102. Gilman, J.; Shanahan, F.; Cashman, K. D. Determinants of vitamin D status in adult Crohn's disease patients, with particular emphasis on supplemental vitamin D use. *Eur J Clin Nutr* **2006,** *60*, 889-896.
103. Pappa, H. M.; Gordon, C. M.; Saslowsky, T. M.; Zholudev, A.; Horr, B.; Shih, M. C.; Grand, R. J. Vitamin D status in children and young adults with inflammatory bowel disease. *Pediatrics* **2006,** *118*, 1950-1961.
104. Lamb, E. J.; Wong, T.; Smith, D. J.; Simpson, D. E.; Coakley, A. J.; Moniz, C.; Muller, A. F. Metabolic bone disease is present at diagnosis in patients with inflammatory bowel disease. *Aliment Pharmacol Ther* **2002,** *16*, 1895-1902.
105. Hlavaty, T.; Krajcovicova, A.; Koller, T.; Toth, J.; Nevidanska, M.; Huorka, M.; Payer, J. Higher vitamin D serum concentration increases health related quality of life in patients with inflammatory bowel diseases. *World J Gastroenterol* **2014,** *20*, 15787-15796.
106. Froicu, M.; Weaver, V.; Wynn, T. A.; McDowell, M. A.; Welsh, J. E.; Cantorna, M. T. A crucial role for the vitamin D receptor in experimental inflammatory bowel diseases. *Mol Endocrinol* **2003,** *17*, 2386-2392.
107. Compston, A.; Coles, A. Multiple sclerosis. *Lancet* **2002,** *359*, 1221-1231.
108. Goverman, J. Autoimmune T cell responses in the central nervous system. *Nat Rev Immunol* **2009,** *9*, 393-407.
109. Mayne, C. G.; Spanier, J. A.; Relland, L. M.; Williams, C. B.; Hayes, C. E. 1,25-Dihydroxyvitamin D3 acts directly on the T lymphocyte vitamin D receptor to inhibit experimental autoimmune encephalomyelitis. *Eur J Immunol* **2011,** *41*, 822-832.
110. Chang, J. H.; Cha, H. R.; Lee, D. S.; Seo, K. Y.; Kweon, M. N. 1,25-Dihydroxyvitamin D3 inhibits the differentiation and migration of T(H)17 cells to

protect against experimental autoimmune encephalomyelitis. *PLoS One* **2010,** *5*, e12925.
111. Munger, K. L.; Levin, L. I.; Hollis, B. W.; Howard, N. S.; Ascherio, A. Serum 25-hydroxyvitamin D levels and risk of multiple sclerosis. *JAMA* **2006,** *296*, 2832-2838.
112. Islam, T.; Gauderman, W. J.; Cozen, W.; Mack, T. M. Childhood sun exposure influences risk of multiple sclerosis in monozygotic twins. *Neurology* **2007,** *69*, 381-388.
113. Kampman, M. T.; Wilsgaard, T.; Mellgren, S. I. Outdoor activities and diet in childhood and adolescence relate to MS risk above the Arctic Circle. *J Neurol* **2007,** *254*, 471-477.
114. van der Mei, I. A.; Ponsonby, A. L.; Dwyer, T.; Blizzard, L.; Taylor, B. V.; Kilpatrick, T.; Butzkueven, H.; McMichael, A. J. Vitamin D levels in people with multiple sclerosis and community controls in Tasmania, Australia. *J Neurol* **2007,** *254*, 581-590.
115. Nieves, J.; Cosman, F.; Herbert, J.; Shen, V.; Lindsay, R. High prevalence of vitamin D deficiency and reduced bone mass in multiple sclerosis. *Neurology* **1994,** *44*, 1687-1692.
116. Smolders, J.; Menheere, P.; Kessels, A.; Damoiseaux, J.; Hupperts, R. Association of vitamin D metabolite levels with relapse rate and disability in multiple sclerosis. *Mult Scler* **2008,** *14*, 1220-1224.
117. Munger, K. L.; Zhang, S. M.; O'Reilly, E.; Hernan, M. A.; Olek, M. J.; Willett, W. C.; Ascherio, A. Vitamin D intake and incidence of multiple sclerosis. *Neurology* **2004,** *62*, 60-65.
118. Hammad, H.; Lambrecht, B. N. Dendritic cells and epithelial cells: linking innate and adaptive immunity in asthma. *Nat Rev Immunol* **2008,** *8*, 193-204.
119. Brehm, J. M.; Celedon, J. C.; Soto-Quiros, M. E.; Avila, L.; Hunninghake, G. M.; Forno, E.; Laskey, D.; Sylvia, J. S.; Hollis, B. W.; Weiss, S. T.; Litonjua, A. A. Serum vitamin D levels and markers of severity of childhood asthma in Costa Rica. *Am J Respir Crit Care Med* **2009,** *179*, 765-771.
120. Brehm, J. M.; Schuemann, B.; Fuhlbrigge, A. L.; Hollis, B. W.; Strunk, R. C.; Zeiger, R. S.; Weiss, S. T.; Litonjua, A. A.; Childhood Asthma Management Program Research, G. Serum vitamin D levels and severe asthma exacerbations in the Childhood Asthma Management Program study. *J Allergy Clin Immunol* **2010,** *126*, 52-58 e55.
121. Rosser, F.; Brehm, J. M.; Forno, E.; Acosta-Perez, E.; Kurland, K.; Canino, G.; Celedon, J. C. Proximity to a major road, vitamin D insufficiency, and severe asthma exacerbations in Puerto Rican children. *Am J Respir Crit Care Med* **2014,** *190*, 1190-1193.
122. Somashekar, A. R.; Prithvi, A. B.; Gowda, M. N. Vitamin d levels in children with bronchial asthma. *J Clin Diagn Res* **2014,** *8*, PC04-07.
123. Bener, A.; Ehlayel, M. S.; Bener, H. Z.; Hamid, Q. The impact of Vitamin D deficiency on asthma, allergic rhinitis and wheezing in children: An emerging public health problem. *J Family Community Med* **2014,** *21*, 154-161.
124. Awasthi, S.; Vikram, K. Serum 25 hydroxy vitamin D insufficiency associated with bronchial asthma in Lucknow, India. *Indian J Pediatr* **2014,** *81*, 644-649.

125. Bose, S.; Breysse, P. N.; McCormack, M. C.; Hansel, N. N.; Rusher, R. R.; Matsui, E.; Peng, R.; Curtin-Brosnan, J.; Diette, G. B.; Center for Childhood Asthma in the Urban, E. Outdoor exposure and vitamin D levels in urban children with asthma. *Nutr J* **2013,** *12*, 81.
126. Kolokotroni, O.; Papadopoulou, A.; Middleton, N.; Kouta, C.; Raftopoulos, V.; Nicolaidou, P.; Yiallouros, P. K. Vitamin D levels and status amongst asthmatic and non-asthmatic adolescents in Cyprus: a comparative cross-sectional study. *BMC Public Health* **2015,** *15*, 48.
127. Niruban, S. J.; Alagiakrishnan, K.; Beach, J.; Senthilselvan, A. Association between vitamin D and respiratory outcomes in Canadian adolescents and adults. *J Asthma* **2015**, 1-33.
128. Confino-Cohen, R.; Brufman, I.; Goldberg, A.; Feldman, B. S. Vitamin D, asthma prevalence and asthma exacerbations: a large adult population-based study. *Allergy* **2014,** *69*, 1673-1680.
129. Li, F.; Peng, M.; Jiang, L.; Sun, Q.; Zhang, K.; Lian, F.; Litonjua, A. A.; Gao, J.; Gao, X. Vitamin D deficiency is associated with decreased lung function in Chinese adults with asthma. *Respiration* **2011,** *81*, 469-475.
130. Carraro, S.; Giordano, G.; Reniero, F.; Carpi, D.; Stocchero, M.; Sterk, P. J.; Baraldi, E. Asthma severity in childhood and metabolomic profiling of breath condensate. *Allergy* **2013,** *68*, 110-117.
131. van Oeffelen, A. A.; Bekkers, M. B.; Smit, H. A.; Kerkhof, M.; Koppelman, G. H.; Haveman-Nies, A.; van der, A. D.; Jansen, E. H.; Wijga, A. H. Serum micronutrient concentrations and childhood asthma: the PIAMA birth cohort study. *Pediatr Allergy Immunol* **2011,** *22*, 784-793.
132. Iqbal, S. F.; Freishtat, R. J. Mechanism of action of vitamin D in the asthmatic lung. *J Investig Med* **2011,** *59*, 1200-1202.
133. Brehm, J. M.; Acosta-Perez, E.; Klei, L.; Roeder, K.; Barmada, M.; Boutaoui, N.; Forno, E.; Kelly, R.; Paul, K.; Sylvia, J.; Litonjua, A. A.; Cabana, M.; Alvarez, M.; Colon-Semidey, A.; Canino, G.; Celedon, J. C. Vitamin D insufficiency and severe asthma exacerbations in Puerto Rican children. *Am J Respir Crit Care Med* **2012,** *186*, 140-146.
134. Dogru, M.; Kirmizibekmez, H.; Yesiltepe Mutlu, R. G.; Aktas, A.; Ozturkmen, S. Clinical effects of vitamin D in children with asthma. *Int Arch Allergy Immunol* **2014,** *164*, 319-325.
135. Larose, T. L.; Langhammer, A.; Chen, Y.; Camargo, C. A., Jr.; Romundstad, P.; Mai, X. M. Serum 25-hydroxyvitamin D levels and lung function in adults with asthma: the HUNT Study. *Eur Respir J* **2014**.
136. Hypponen, E.; Sovio, U.; Wjst, M.; Patel, S.; Pekkanen, J.; Hartikainen, A. L.; Jarvelinb, M. R. Infant vitamin d supplementation and allergic conditions in adulthood: northern Finland birth cohort 1966. *Ann N Y Acad Sci* **2004,** *1037*, 84-95.
137. Tolppanen, A. M.; Sayers, A.; Granell, R.; Fraser, W. D.; Henderson, J.; Lawlor, D. A. Prospective association of 25-hydroxyvitamin d3 and d2 with childhood lung function, asthma, wheezing, and flexural dermatitis. *Epidemiology* **2013,** *24*, 310-319.

138. Griz, L. H.; Bandeira, F.; Gabbay, M. A.; Dib, S. A.; Carvalho, E. F. Vitamin D and diabetes mellitus: an update 2013. *Arq Bras Endocrinol Metabol* **2014,** *58*, 1-8.
139. Plum, L. A.; DeLuca, H. F. Vitamin D, disease and therapeutic opportunities. *Nat Rev Drug Discov* **2010,** *9*, 941-955.
140. Litchfield, A. B.; Hayes, R. M.; Shuler, F. D.; Flesher, S. L. Type I diabetes in children and vitamin D. *W V Med J* **2015,** *111*, 32-37.
141. Mitri, J.; Pittas, A. G. Vitamin D and diabetes. *Endocrinol Metab Clin North Am* **2014,** *43*, 205-232.
142. Makinen, M.; Simell, V.; Mykkanen, J.; Ilonen, J.; Veijola, R.; Hyoty, H.; Knip, M.; Simell, O.; Toppari, J.; Hermann, R. An increase in serum 25-hydroxyvitamin D concentrations preceded a plateau in type 1 diabetes incidence in Finnish children. *J Clin Endocrinol Metab* **2014,** *99*, E2353-2356.
143. Serra-Planas, E.; Aguilera, E.; Granada, M. L.; Soldevila, B.; Salinas, I.; Reverter, J. L.; Pizarro, E.; Pellitero, S.; Alonso, N.; Mauricio, D.; Puig-Domingo, M. High prevalence of vitamin D deficiency and lack of association with subclinical atherosclerosis in asymptomatic patients with Type 1 Diabetes Mellitus from a Mediterranean area. *Acta Diabetol* **2015**.
144. Shih, E. M.; Mittelman, S.; Pitukcheewanont, P.; Azen, C. G.; Monzavi, R. Effects of vitamin D repletion on glycemic control and inflammatory cytokines in adolescents with type 1 diabetes. *Pediatr Diabetes* **2014**.
145. Skaaby, T.; Husemoen, L. L.; Thuesen, B. H.; Linneberg, A. Prospective population-based study of the association between vitamin D status and incidence of autoimmune disease. *Endocrine* **2015**.
146. Cadario, F.; Prodam, F.; Savastio, S.; Monzani, A.; Balafrej, A.; Bellomo, G.; Bona, G. Vitamin D status and Type 1 diabetes in children: evaluation according to latitude and skin colour. *Minerva Pediatr* **2015**.
147. Gregori, S.; Giarratana, N.; Smiroldo, S.; Uskokovic, M.; Adorini, L. A 1alpha,25-dihydroxyvitamin D(3) analog enhances regulatory T-cells and arrests autoimmune diabetes in NOD mice. *Diabetes* **2002,** *51*, 1367-1374.
148. Mao, L.; Ji, F.; Liu, Y.; Zhang, W.; Ma, X. Calcitriol plays a protective role in diabetic nephropathy through anti-inflammatory effects. *Int J Clin Exp Med* **2014,** *7*, 5437-5444.
149. Garcia-Carrasco, M.; Mendoza-Pinto, C.; Munguia-Realpozo, P.; Rodriguez-Gallegos, A.; Vallejo-Ruiz, V.; Munoz-Guarneros, M.; Mendez-Martinez, S.; Soto-Santillan, P.; Pezzat-Said, E.; Reyes-Leyva, J.; Lopez-Colombo, A.; Ruiz-Arguelles, A.; Cervera, R. Lack of association between serum 25-hydroxyvitamin D levels and cervical human papillomavirus infection in systemic lupus erythematosus. *Lupus* **2014**.
150. de Souza, V. A.; Bastos, M. G.; Fernandes, N. M.; Mansur, H. N.; Raposo, N. R.; de Souza, D. M.; de Andrade, L. C. Association of hypovitaminosis D with Systemic Lupus Erythematosus and inflammation. *J Bras Nefrol* **2014,** *36*, 430-436.
151. Yap, K. S.; Morand, E. F. Vitamin D and systemic lupus erythematosus: continued evolution. *Int J Rheum Dis* **2014**.

152. Petri, M.; Bello, K. J.; Fang, H.; Magder, L. S. Vitamin D in systemic lupus erythematosus: modest association with disease activity and the urine protein-to-creatinine ratio. *Arthritis Rheum* **2013,** *65*, 1865-1871.
153. Lertratanakul, A.; Wu, P.; Dyer, A. R.; Kondos, G.; Edmundowicz, D.; Carr, J.; Ramsey-Goldman, R. Risk Factors in the Progression of Subclinical Atherosclerosis in Women With Systemic Lupus Erythematosus. *Arthritis Care & Research* **2014,** *66*, 1177-1185.
154. Mao, S.; Huang, S. Association between vitamin D receptor gene BsmI, FokI, ApaI and TaqI polymorphisms and the risk of systemic lupus erythematosus: a meta-analysis. *Rheumatol Int* **2014,** *34*, 381-388.
155. Carvalho, C.; Marinho, A.; Leal, B.; Bettencourt, A.; Boleixa, D.; Almeida, I.; Farinha, F.; Costa, P. P.; Vasconcelos, C.; Silva, B. M. Association between vitamin D receptor (VDR) gene polymorphisms and systemic lupus erythematosus in Portuguese patients. *Lupus* **2015**.
156. Laverny, G.; Penna, G.; Vetrano, S.; Correale, C.; Nebuloni, M.; Danese, S.; Adorini, L. Efficacy of a potent and safe vitamin D receptor agonist for the treatment of inflammatory bowel disease. *Immunol Lett* **2010,** *131*, 49-58.
157. Laverny, G.; Penna, G.; Uskokovic, M.; Marczak, S.; Maehr, H.; Jankowski, P.; Ceailles, C.; Vouros, P.; Smith, B.; Robinson, M.; Reddy, G. S.; Adorini, L. Synthesis and anti-inflammatory properties of 1alpha,25-dihydroxy-16-ene-20-cyclopropyl-24-oxo-vitamin D3, a hypocalcemic, stable metabolite of 1alpha,25-dihydroxy-16-ene-20-cyclopropyl-vitamin D3. *J Med Chem* **2009,** *52*, 2204-2213.
158. Uskokovic, M. R.; Manchand, P.; Marczak, S.; Maehr, H.; Jankowski, P.; Adorini, L.; Reddy, G. S. C-20 cyclopropyl vitamin D3 analogs. *Curr Top Med Chem* **2006,** *6*, 1289-1296.
159. Siu-Caldera, M. L.; Clark, J. W.; Santos-Moore, A.; Peleg, S.; Liu, Y. Y.; Uskokovic, M. R.; Sharma, S.; Reddy, G. S. 1alpha,25-dihydroxy-24-oxo-16-ene vitamin D3, a metabolite of a synthetic vitamin D3 analog, 1alpha,25-dihydroxy-16-ene vitamin D3, is equipotent to its parent in modulating growth and differentiation of human leukemic cells. *J Steroid Biochem Mol Biol* **1996,** *59*, 405-412.
160. Daniel, C.; Schlauch, T.; Zugel, U.; Steinmeyer, A.; Radeke, H. H.; Steinhilber, D.; Stein, J. 22-ene-25-oxa-vitamin D: a new vitamin D analogue with profound immunosuppressive capacities. *Eur J Clin Invest* **2005,** *35*, 343-349.
161. Martinesi, M.; Treves, C.; Bonanomi, A. G.; Milla, M.; Bagnoli, S.; Zuegel, U.; Steinmeyer, A.; Stio, M. Down-regulation of adhesion molecules and matrix metalloproteinases by ZK 156979 in inflammatory bowel diseases. *Clin Immunol* **2010,** *136*, 51-60.
162. Daniel, C.; Radeke, H. H.; Sartory, N. A.; Zahn, N.; Zuegel, U.; Steinmeyer, A.; Stein, J. The new low calcemic vitamin D analog 22-ene-25-oxa-vitamin D prominently ameliorates T helper cell type 1-mediated colitis in mice. *J Pharmacol Exp Ther* **2006,** *319*, 622-631.
163. Verlinden, L.; Verstuyf, A.; Van Camp, M.; Marcelis, S.; Sabbe, K.; Zhao, X. Y.; De Clercq, P.; Vandewalle, M.; Bouillon, R. Two novel 14-Epi-analogues of 1,25-dihydroxyvitamin D3 inhibit the growth of human breast cancer cells in vitro and in vivo. *Cancer Res* **2000,** *60*, 2673-2679.

164. van Etten, E.; Gysemans, C.; Verstuyf, A.; Bouillon, R.; Mathieu, C. Immunomodulatory properties of a 1,25(OH)(2) vitamin D(3) analog combined with IFNbeta in an animal model of syngeneic islet transplantation. *Transplant Proc* **2001,** *33*, 2319.
165. Gysemans, C.; Van Etten, E.; Overbergh, L.; Verstuyf, A.; Waer, M.; Bouillon, R.; Mathieu, C. Treatment of autoimmune diabetes recurrence in non-obese diabetic mice by mouse interferon-beta in combination with an analogue of 1alpha,25-dihydroxyvitamin-D3. *Clin Exp Immunol* **2002,** *128*, 213-220.
166. van Halteren, A. G.; van Etten, E.; de Jong, E. C.; Bouillon, R.; Roep, B. O.; Mathieu, C. Redirection of human autoreactive T-cells Upon interaction with dendritic cells modulated by TX527, an analog of 1,25 dihydroxyvitamin D(3). *Diabetes* **2002,** *51*, 2119-2125.
167. Van Etten, E.; Decallonne, B.; Verlinden, L.; Verstuyf, A.; Bouillon, R.; Mathieu, C. Analogs of 1alpha,25-dihydroxyvitamin D3 as pluripotent immunomodulators. *J Cell Biochem* **2003,** *88*, 223-226.
168. van Etten, E.; Decallonne, B.; Bouillon, R.; Mathieu, C. NOD bone marrow-derived dendritic cells are modulated by analogs of 1,25-dihydroxyvitamin D3. *J Steroid Biochem Mol Biol* **2004,** *89-90*, 457-459.
169. Ferreira, G. B.; Overbergh, L.; Verstuyf, A.; Mathieu, C. 1alpha,25-Dihydroxyvitamin D3 and its analogs as modulators of human dendritic cells: a comparison dose-titration study. *J Steroid Biochem Mol Biol* **2013,** *136*, 160-165.
170. Baeke, F.; Korf, H.; Overbergh, L.; Verstuyf, A.; Thorrez, L.; Van Lommel, L.; Waer, M.; Schuit, F.; Gysemans, C.; Mathieu, C. The vitamin D analog, TX527, promotes a human CD4+CD25highCD127low regulatory T cell profile and induces a migratory signature specific for homing to sites of inflammation. *J Immunol* **2011,** *186*, 132-142.
171. Ferreira, G. B.; Baeke, F.; Verstuyf, A.; De Clercq, P.; Waelkens, E.; Mathieu, C.; Overbergh, L. A proteomic approach on the effects of TX527, a 1alpha,25-dihydroxyvitamin D3 analog, in human T lymphocytes. *J Steroid Biochem Mol Biol* **2014,** *144 Pt A*, 96-101.
172. Baeke, F.; Van Belle, T. L.; Takiishi, T.; Ding, L.; Korf, H.; Laureys, J.; Gysemans, C.; Mathieu, C. Low doses of anti-CD3, ciclosporin A and the vitamin D analogue, TX527, synergise to delay recurrence of autoimmune diabetes in an islet-transplanted NOD mouse model of diabetes. *Diabetologia* **2012,** *55*, 2723-2732.
173. Verlinden, L.; Leyssens, C.; Beullens, I.; Marcelis, S.; Mathieu, C.; De Clercq, P.; Verstuyf, A. The vitamin D analog TX527 ameliorates disease symptoms in a chemically induced model of inflammatory bowel disease. *J Steroid Biochem Mol Biol* **2013,** *136*, 107-111.
174. Hirata, M.; Kato, H.; Debuchi, H.; Ikesue, A.; Mitamura, M.; Nakagawa, H. Anti-inflammatory effect of 22-oxa-1 alpha,25-dihydroxyvitamin D3 on carrageenin-induced inflammation in rats. *Biol Pharm Bull* **1994,** *17*, 1130-1131.
175. Komine, M.; Watabe, Y.; Shimaoka, S.; Sato, F.; Kake, K.; Nishina, H.; Ohtsuki, M.; Nakagawa, H.; Tamaki, K. The action of a novel vitamin D3 analogue, OCT, on immunomodulatory function of keratinocytes and lymphocytes. *Arch Dermatol Res* **1999,** *291*, 500-506.

176. Hirose, M.; Nishino, T.; Obata, Y.; Nakazawa, M.; Nakazawa, Y.; Furusu, A.; Abe, K.; Miyazaki, M.; Koji, T.; Kohno, S. 22-Oxacalcitriol prevents progression of peritoneal fibrosis in a mouse model. *Perit Dial Int* **2013,** *33*, 132-142.
177. Nakagawa, K.; Sasaki, Y.; Kato, S.; Kubodera, N.; Okano, T. 22-Oxa-1alpha,25-dihydroxyvitamin D3 inhibits metastasis and angiogenesis in lung cancer. *Carcinogenesis* **2005,** *26*, 1044-1054.
178. Aparna, R.; Subhashini, J.; Roy, K. R.; Reddy, G. S.; Robinson, M.; Uskokovic, M. R.; Venkateswara Reddy, G.; Reddanna, P. Selective inhibition of cyclooxygenase-2 (COX-2) by 1alpha,25-dihydroxy-16-ene-23-yne-vitamin D3, a less calcemic vitamin D analog. *J Cell Biochem* **2008,** *104*, 1832-1842.
179. Bischof, M. G.; Redlich, K.; Schiller, C.; Chirayath, M. V.; Uskokovic, M.; Peterlik, M.; Cross, H. S. Growth inhibitory effects on human colon adenocarcinoma-derived Caco-2 cells and calcemic potential of 1 alpha,25-dihydroxyvitamin D3 analogs: structure-function relationships. *J Pharmacol Exp Ther* **1995,** *275*, 1254-1260.
180. Wieder, R.; Novick, S. C.; Hollis, B. W.; Bryan, M.; Chanel, S. M.; Owusu, K.; Camastra, D.; Saunders, T.; Pliner, L.; Harrison, J.; Bonate, P.; Williams, T.; Soignet, S. Pharmacokinetics and safety of ILX23-7553, a non-calcemic-vitamin D3 analogue, in a phase I study of patients with advanced malignancies. *Invest New Drugs* **2003,** *21*, 445-452.
181. Zugel, U.; Steinmeyer, A.; Giesen, C.; Asadullah, K. A novel immunosuppressive 1alpha,25-dihydroxyvitamin D3 analog with reduced hypercalcemic activity. *J Invest Dermatol* **2002,** *119*, 1434-1442.
182. Strauch, U. G.; Obermeier, F.; Grunwald, N.; Dunger, N.; Rath, H. C.; Scholmerich, J.; Steinmeyer, A.; Zugel, U.; Herfarth, H. H. Calcitriol analog ZK191784 ameliorates acute and chronic dextran sodium sulfate-induced colitis by modulation of intestinal dendritic cell numbers and phenotype. *World J Gastroenterol* **2007,** *13*, 6529-6537.
183. Martinesi, M.; Ambrosini, S.; Treves, C.; Zuegel, U.; Steinmeyer, A.; Vito, A.; Milla, M.; Bonanomi, A. G.; Stio, M. Role of vitamin D derivatives in intestinal tissue of patients with inflammatory bowel diseases. *J Crohns Colitis* **2014,** *8*, 1062-1071.
184. Johnsson, C.; Tufveson, G. MC 1288--a vitamin D analogue with immunosuppressive effects on heart and small bowel grafts. *Transpl Int* **1994,** *7*, 392-397.
185. Johnsson, C.; Binderup, L.; Tufveson, G. The effects of combined treatment with the novel vitamin D analogue MC 1288 and cyclosporine A on cardiac allograft survival. *Transpl Immunol* **1995,** *3*, 245-250.
186. Pakkala, I.; Taskinen, E.; Pakkala, S.; Raisanen-Sokolowski, A. MC1288, a vitamin D analog, prevents acute graft-versus-host disease in rat bone marrow transplantation. *Bone Marrow Transplant* **2001,** *27*, 863-867.
187. Raisanen-Sokolowski, A. K.; Pakkala, I. S.; Samila, S. P.; Binderup, L.; Hayry, P. J.; Pakkala, S. T. A vitamin D analog, MC1288, inhibits adventitial inflammation and suppresses intimal lesions in rat aortic allografts. *Transplantation* **1997,** *63*, 936-941.

188. Johnsson, C.; Tufveson, G.; Binderup, L.; Karlsson‐Parra, A. Synergistic actions of the vitamin D analogue MC 1288 and 15‐deoxyspergualin in xenotransplantation. *Xenotransplantation* **1997,** *4*, 186-193.
189. Griffin, M. D.; Lutz, W. H.; Phan, V. A.; Bachman, L. A.; McKean, D. J.; Kumar, R. Potent inhibition of dendritic cell differentiation and maturation by vitamin D analogs. *Biochem Biophys Res Commun* **2000,** *270*, 701-708.
190. Lillevang, S. T.; Rosenkvist, J.; Andersen, C. B.; Larsen, S.; Kemp, E.; Kristensen, T. Single and combined effects of the vitamin D analogue KH1060 and cyclosporin A on mercuric-chloride-induced autoimmune disease in the BN rat. *Clin Exp Immunol* **1992,** *88*, 301-306.
191. Stio, M.; Bonanomi, A. G.; d'Albasio, G.; Treves, C. Suppressive effect of 1,25-dihydroxyvitamin D3 and its analogues EB 1089 and KH 1060 on T lymphocyte proliferation in active ulcerative colitis. *Biochem Pharmacol* **2001,** *61*, 365-371.
192. Mathieu, C.; Waer, M.; Casteels, K.; Laureys, J.; Bouillon, R. Prevention of type I diabetes in NOD mice by nonhypercalcemic doses of a new structural analog of 1,25-dihydroxyvitamin D3, KH1060. *Endocrinology* **1995,** *136*, 866-872.
193. Binderup, L.; Latini, S.; Binderup, E.; Bretting, C.; Calverley, M.; Hansen, K. 20-epi-vitamin D3 analogues: a novel class of potent regulators of cell growth and immune responses. *Biochem Pharmacol* **1991,** *42*, 1569-1575.
194. Wierzbicka, J.; Piotrowska, A.; Zmijewski, M. A. The renaissance of vitamin D. *Acta Biochim Pol* **2014,** *61*, 679-686.
195. Lin, Z.; Marepally, S. R.; Ma, D.; Myers, L. K.; Postlethwaite, A. E.; Tuckey, R. C.; Cheng, C. Y.; Kim, T. K.; Yue, J.; Slominski, A. T.; Miller, D. D.; Li, W. Chemical synthesis and biological activities of 20S,24S/R-dihydroxyvitamin D3 epimers and their 1alpha-hydroxyl derivatives. *J Med Chem* **2015,** *58*, 7881-7887.
196. Lin, Z.; Li, W. The roles of vitamin D and its analogs in inflammatory diseases. *Curr Top Med Chem* **2016,** *16*, 1242-1261.
197. Slominski, A.; Semak, I.; Zjawiony, J.; Wortsman, J.; Li, W.; Szczesniewski, A.; Tuckey, R. C. The cytochrome P450scc system opens an alternate pathway of vitamin D3 metabolism. *FEBS J* **2005,** *272*, 4080-4090.
198. Slominski, A. T.; Kim, T. K.; Li, W.; Yi, A. K.; Postlethwaite, A.; Tuckey, R. C. The role of CYP11A1 in the production of vitamin D metabolites and their role in the regulation of epidermal functions. *J Steroid Biochem Mol Biol* **2014,** *144 Pt A*, 28-39.
199. Slominski, A. T.; Kim, T. K.; Shehabi, H. Z.; Tang, E. K.; Benson, H. A.; Semak, I.; Lin, Z.; Yates, C. R.; Wang, J.; Li, W.; Tuckey, R. C. In vivo production of novel vitamin D2 hydroxy-derivatives by human placentas, epidermal keratinocytes, Caco-2 colon cells and the adrenal gland. *Mol Cell Endocrinol* **2014,** *383*, 181-192.
200. Slominski, A. T.; Li, W.; Kim, T. K.; Semak, I.; Wang, J.; Zjawiony, J. K.; Tuckey, R. C. Novel activities of CYP11A1 and their potential physiological significance. *J Steroid Biochem Mol Biol* **2015,** *151*, 25-37.
201. Wang, Q.; Lin, Z.; Kim, T. K.; Slominski, A. T.; Miller, D. D.; Li, W. Total synthesis of biologically active 20S-hydroxyvitamin D3. *Steroids* **2015,** *104*, 153-162.

202. Slominski, A. T.; Kim, T. K.; Li, W.; Postlethwaite, A.; Tieu, E. W.; Tang, E. K.; Tuckey, R. C. Detection of novel CYP11A1-derived secosteroids in the human epidermis and serum and pig adrenal gland. *Sci Rep* **2015,** *5*, 14875.
203. Slominski, A. T.; Zmijewski, M. A.; Semak, I.; Sweatman, T.; Janjetovic, Z.; Li, W.; Zjawiony, J. K.; Tuckey, R. C. Sequential metabolism of 7-dehydrocholesterol to steroidal 5,7-dienes in adrenal glands and its biological implication in the skin. *PLoS One* **2009,** *4*, e4309.
204. Slominski, A. T.; Janjetovic, Z.; Fuller, B. E.; Zmijewski, M. A.; Tuckey, R. C.; Nguyen, M. N.; Sweatman, T.; Li, W.; Zjawiony, J.; Miller, D.; Chen, T. C.; Lozanski, G.; Holick, M. F. Products of vitamin D3 or 7-dehydrocholesterol metabolism by cytochrome P450scc show anti-leukemia effects, having low or absent calcemic activity. *PLoS One* **2010,** *5*, e9907.
205. Slominski, A.; Kim, T. K.; Zmijewski, M. A.; Janjetovic, Z.; Li, W.; Chen, J.; Kusniatsova, E. I.; Semak, I.; Postlethwaite, A.; Miller, D. D.; Zjawiony, J. K.; Tuckey, R. C. Novel vitamin D photoproducts and their precursors in the skin. *Dermatoendocrinol* **2013,** *5*, 7-19.
206. Chen, J.; Wang, J.; Kim, T. K.; Tieu, E. W.; Tang, E. K.; Lin, Z.; Kovacic, D.; Miller, D. D.; Postlethwaite, A.; Tuckey, R. C.; Slominski, A. T.; Li, W. Novel vitamin D analogs as potential therapeutics: metabolism, toxicity profiling, and antiproliferative activity. *Anticancer Res* **2014,** *34*, 2153-2163.
207. Slominski, A. T.; Janjetovic, Z.; Kim, T. K.; Wright, A. C.; Grese, L. N.; Riney, S. J.; Nguyen, M. N.; Tuckey, R. C. Novel vitamin D hydroxyderivatives inhibit melanoma growth and show differential effects on normal melanocytes. *Anticancer Res* **2012,** *32*, 3733-3742.
208. Slominski, A. T.; Li, W.; Bhattacharya, S. K.; Smith, R. A.; Johnson, P. L.; Chen, J.; Nelson, K. E.; Tuckey, R. C.; Miller, D.; Jiao, Y.; Gu, W.; Postlethwaite, A. E. Vitamin D analogs 17,20S(OH)2pD and 17,20R(OH)2pD are noncalcemic and exhibit antifibrotic activity. *J Invest Dermatol* **2011,** *131*, 1167-1169.
209. Slominski, A.; Janjetovic, Z.; Tuckey, R. C.; Nguyen, M. N.; Bhattacharya, K. G.; Wang, J.; Li, W.; Jiao, Y.; Gu, W.; Brown, M.; Postlethwaite, A. E. 20S-hydroxyvitamin D3, noncalcemic product of CYP11A1 action on vitamin D3, exhibits potent antifibrogenic activity in vivo. *J Clin Endocrinol Metab.* **2013,** *98*, E298-303.
210. Pazos, G.; Rivadulla, M. L.; Perez-Garcia, X.; Gandara, Z.; Perez, M. Gemini analogs of vitamin D. *Curr Top Med Chem* **2014,** *14*, 2388-2397.
211. Okamoto, R.; Gery, S.; Kuwayama, Y.; Borregaard, N.; Ho, Q.; Alvarez, R.; Akagi, T.; Liu, G. Y.; Uskokovic, M. R.; Koeffler, H. P. Novel Gemini vitamin D3 analogs: large structure/function analysis and ability to induce antimicrobial peptide. *Int J Cancer* **2014,** *134*, 207-217.
212. Pingili, A. K.; Kara, M.; Khan, N. S.; Estes, A. M.; Lin, Z.; Li, W.; Gonzalez, F. J.; Malik, K. U. 6beta-hydroxytestosterone, a cytochrome P450 1B1 metabolite of testosterone, contributes to angiotensin II-induced hypertension and its pathogenesis in male mice. *Hypertension* **2015,** *65*, 1279-1287.
213. Lin, Z.; Yang, R.; Guan, Z.; Chen, A.; Li, W. Ultra-performance LC separation and quadrupole time-of-flight MS identification of major alkaloids in Plumula Nelumbinis. *Phytochem Anal* **2014,** *25*, 485-494.

214. Lu, Y.; Chen, J.; Janjetovic, Z.; Michaels, P.; Tang, E. K.; Wang, J.; Tuckey, R. C.; Slominski, A. T.; Li, W.; Miller, D. D. Design, synthesis, and biological action of 20R-hydroxyvitamin D3. *J Med Chem* **2012,** *55*, 3573-3577.
215. Li, F.; Calabrese, D.; Brichacek, M.; Lin, I.; Njardarson, J. T. Efficient synthesis of thiopyrans using a sulfur-enabled anionic cascade. *Angew Chem Int Ed Engl* **2012,** *51*, 1938-1941.
216. Zbytek, B.; Janjetovic, Z.; Tuckey, R. C.; Zmijewski, M. A.; Sweatman, T. W.; Jones, E.; Nguyen, M. N.; Slominski, A. T. 20-Hydroxyvitamin D3, a product of vitamin D3 hydroxylation by cytochrome P450scc, stimulates keratinocyte differentiation. *J Invest Dermatol* **2008,** *128*, 2271-2280.
217. Sittampalam, G. S.; Gal-Edd, N.; Arkin, M.; Auld, D.; Austin, C.; Bejcek, B.; Glicksman, M.; Inglese, J.; Lemmon, V.; Li, Z. Cell Viability Assays. **2013**.
218. Slominski, A. T.; Kim, T. K.; Takeda, Y.; Janjetovic, Z.; Brozyna, A. A.; Skobowiat, C.; Wang, J.; Postlethwaite, A.; Li, W.; Tuckey, R. C.; Jetten, A. M. RORalpha and ROR gamma are expressed in human skin and serve as receptors for endogenously produced noncalcemic 20-hydroxy- and 20,23-dihydroxyvitamin D. *FASEB J.* **2014,** *28*, 2775-2789.
219. Clapham, D. E.; Julius, D.; Montell, C.; Schultz, G. International Union of Pharmacology. XLIX. Nomenclature and structure-function relationships of transient receptor potential channels. *Pharmacol Rev.* **2005,** *57*, 427-450.
220. Meyaard, L.; Adema, G. J.; Chang, C.; Woollatt, E.; Sutherland, G. R.; Lanier, L. L.; Phillips, J. H. LAIR-1, a novel inhibitory receptor expressed on human mononuclear leukocytes. *Immunity* **1997,** *7*, 283-290.
221. Van Cromphaut, S. J.; Dewerchin, M.; Hoenderop, J. G.; Stockmans, I.; Van Herck, E.; Kato, S.; Bindels, R. J.; Collen, D.; Carmeliet, P.; Bouillon, R.; Carmeliet, G. Duodenal calcium absorption in vitamin D receptor-knockout mice: functional and molecular aspects. *Proc Natl Acad Sci U S A* **2001,** *98*, 13324-13329.
222. Lehen'kyi, V.; Flourakis, M.; Skryma, R.; Prevarskaya, N. TRPV6 channel controls prostate cancer cell proliferation via Ca(2+)/NFAT-dependent pathways. *Oncogene* **2007,** *26*, 7380-7385.
223. Wang, J.; Slominski, A.; Tuckey, R. C.; Janjetovic, Z.; Kulkarni, A.; Chen, J.; Postlethwaite, A. E.; Miller, D.; Li, W. 20-hydroxyvitamin D(3) inhibits proliferation of cancer cells with high efficacy while being non-toxic. *Anticancer Res* **2012,** *32*, 739-746.
224. Schoenborn, J. R.; Wilson, C. B. Regulation of interferon-gamma during innate and adaptive immune responses. *Adv Immunol* **2007,** *96*, 41-101.
225. Janjetovic, Z.; Zmijewski, M. A.; Tuckey, R. C.; DeLeon, D. A.; Nguyen, M. N.; Pfeffer, L. M.; Slominski, A. T. 20-Hydroxycholecalciferol, product of vitamin D3 hydroxylation by P450scc, decreases NF-kappaB activity by increasing IkappaB alpha levels in human keratinocytes. *PLoS One* **2009,** *4*, e5988.
226. Janjetovic, Z.; Tuckey, R. C.; Nguyen, M. N.; Thorpe, E. M., Jr.; Slominski, A. T. 20,23-dihydroxyvitamin D3, novel P450scc product, stimulates differentiation and inhibits proliferation and NF-kappaB activity in human keratinocytes. *J Cell Physiol.* **2010,** *223*, 36-48.

227. Kang, X.; Lu, Z.; Cui, C.; Deng, M.; Fan, Y.; Dong, B.; Han, X.; Xie, F.; Tyner, J. W.; Coligan, J. E.; Collins, R. H.; Xiao, X.; You, M. J.; Zhang, C. C. The ITIM-containing receptor LAIR1 is essential for acute myeloid leukaemia development. *Nat Cell Biol* **2015,** *17*, 665-677.
228. Perbellini, O.; Falisi, E.; Giaretta, I.; Boscaro, E.; Novella, E.; Facco, M.; Fortuna, S.; Finotto, S.; Amati, E.; Maniscalco, F.; Montaldi, A.; Alghisi, A.; Aprili, F.; Bonaldi, L.; Paolini, R.; Scupoli, M. T.; Trentin, L.; Ambrosetti, A.; Semenzato, G.; Pizzolo, G.; Rodeghiero, F.; Visco, C. Clinical significance of LAIR1 (CD305) as assessed by flow cytometry in a prospective series of patients with chronic lymphocytic leukemia. *Haematologica* **2014,** *99*, 881-887.
229. Hagino, H. Vitamin D analogs for the treatment of osteoporosis. *Can J Physiol Pharmacol* **2015**, 1-6.
230. Ferronato, M. J.; Salomon, D. G.; Fermento, M. E.; Gandini, N. A.; Lopez Romero, A.; Rivadulla, M. L.; Perez-Garcia, X.; Gomez, G.; Perez, M.; Fall, Y.; Facchinetti, M. M.; Curino, A. C. Vitamin D Analogue: Potent Antiproliferative Effects on Cancer Cell Lines and Lack of Hypercalcemic Activity. *Arch Pharm (Weinheim)* **2015**.
231. Thill, M.; Reichert, K.; Woeste, A.; Polack, S.; Fischer, D.; Hoellen, F.; Rody, A.; Friedrich, M.; Koster, F. Combined treatment of breast cancer cell lines with vitamin D and COX-2 inhibitors. *Anticancer Res* **2015,** *35*, 1189-1195.
232. Schuster, I. Cytochromes P450 are essential players in the vitamin D signaling system. *Biochim Biophys Acta* **2011,** *1814*, 186-199.
233. Jones, G.; Prosser, D. E.; Kaufmann, M. 25-Hydroxyvitamin D-24-hydroxylase (CYP24A1): its important role in the degradation of vitamin D. *Arch Biochem Biophys* **2012,** *523*, 9-18.
234. Guryev, O.; Carvalho, R. A.; Usanov, S.; Gilep, A.; Estabrook, R. W. A pathway for the metabolism of vitamin D3: unique hydroxylated metabolites formed during catalysis with cytochrome P450scc (CYP11A1). *Proc Natl Acad Sci U S A* **2003,** *100*, 14754-14759.
235. Tuckey, R. C.; Li, W.; Shehabi, H. Z.; Janjetovic, Z.; Nguyen, M. N.; Kim, T. K.; Chen, J.; Howell, D. E.; Benson, H. A. E.; Sweatman, T.; Baldisseri, D. M.; Slominski, A. Production of 22-Hydroxy Metabolites of Vitamin D-3 by Cytochrome P450scc (CYP11A1) and Analysis of Their Biological Activities on Skin Cells. *Drug Metabolism and Disposition* **2011,** *39*, 1577-1588.
236. Tuckey, R. C.; Nguyen, M. N.; Slominski, A. Kinetics of vitamin D3 metabolism by cytochrome P450scc (CYP11A1) in phospholipid vesicles and cyclodextrin. *Int J Biochem Cell Biol* **2008,** *40*, 2619-2626.
237. Slominski, A. T.; Kim, T. K.; Shehabi, H. Z.; Semak, I.; Tang, E. K.; Nguyen, M. N.; Benson, H. A.; Korik, E.; Janjetovic, Z.; Chen, J.; Yates, C. R.; Postlethwaite, A.; Li, W.; Tuckey, R. C. In vivo evidence for a novel pathway of vitamin D(3) metabolism initiated by P450scc and modified by CYP27B1. *FASEB J* **2012,** *26*, 3901-3915.
238. Slominski, A. T.; Janjetovic, Z.; Kim, T. K.; Wasilewski, P.; Rosas, S.; Hanna, S.; Sayre, R. M.; Dowdy, J. C.; Li, W.; Tuckey, R. C. Novel non-calcemic secosteroids that are produced by human epidermal keratinocytes protect against solar radiation. *J Steroid Biochem Mol Biol* **2015,** *148*, 52-63.

239. Janjetovic, Z.; Tuckey, R. C.; Nguyen, M. N.; Thorpe, E. M., Jr.; Slominski, A. T. 20,23-dihydroxyvitamin D3, novel P450scc product, stimulates differentiation and inhibits proliferation and NF-kappaB activity in human keratinocytes. *J Cell Physiol* **2010,** *223*, 36-48.
240. Slominski, A.; Janjetovic, Z.; Tuckey, R. C.; Nguyen, M. N.; Bhattacharya, K. G.; Wang, J.; Li, W.; Jiao, Y.; Gu, W.; Brown, M.; Postlethwaite, A. E. 20S-hydroxyvitamin D3, noncalcemic product of CYP11A1 action on vitamin D3, exhibits potent antifibrogenic activity in vivo. *J Clin Endocrinol Metab* **2013,** *98*, E298-303.
241. Tieu, E. W.; Li, W.; Chen, J.; Kim, T. K.; Ma, D.; Slominski, A. T.; Tuckey, R. C. Metabolism of 20-hydroxyvitamin D3 and 20,23-dihydroxyvitamin D3 by rat and human CYP24A1. *J Steroid Biochem Mol Biol* **2015,** *149*, 153-165.
242. Cheng, C. Y.; Slominski, A. T.; Tuckey, R. C. Metabolism of 20-hydroxyvitamin D3 by mouse liver microsomes. *J Steroid Biochem Mol Biol* **2014,** *144 Pt B*, 286-293.
243. Tang, E. K.; Chen, J.; Janjetovic, Z.; Tieu, E. W.; Slominski, A. T.; Li, W.; Tuckey, R. C. Hydroxylation of CYP11A1-derived products of vitamin D3 metabolism by human and mouse CYP27B1. *Drug Metab Dispos* **2013,** *41*, 1112-1124.
244. Slominski, A. T.; Kim, T. K.; Takeda, Y.; Janjetovic, Z.; Brozyna, A. A.; Skobowiat, C.; Wang, J.; Postlethwaite, A.; Li, W.; Tuckey, R. C.; Jetten, A. M. RORalpha and ROR gamma are expressed in human skin and serve as receptors for endogenously produced noncalcemic 20-hydroxy- and 20,23-dihydroxyvitamin D. *FASEB J* **2014,** *28*, 2775-2789.
245. Li, W.; Chen, J. J.; Janjetovic, Z.; Kim, T. K.; Sweatman, T.; Lu, Y.; Zjawiony, J.; Tuckey, R. C.; Miller, D.; Slominski, A. Chemical synthesis of 20S-hydroxyvitamin D3, which shows antiproliferative activity. *Steroids* **2010,** *75*, 926-935.
246. Tuckey, R. C.; Janjetovic, Z.; Li, W.; Nguyen, M. N.; Zmijewski, M. A.; Zjawiony, J.; Slominski, A. Metabolism of 1alpha-hydroxyvitamin D3 by cytochrome P450scc to biologically active 1alpha,20-dihydroxyvitamin D3. *J Steroid Biochem Mol Biol* **2008,** *112*, 213-219.
247. Tang, E. K.; Li, W.; Janjetovic, Z.; Nguyen, M. N.; Wang, Z.; Slominski, A.; Tuckey, R. C. Purified mouse CYP27B1 can hydroxylate 20,23-dihydroxyvitamin D3, producing 1alpha,20,23-trihydroxyvitamin D3, which has altered biological activity. *Drug Metab Dispos* **2010,** *38*, 1553-1559.
248. Falzon, M. The noncalcemic vitamin D analogues EB1089 and 22-oxacalcitriol interact with the vitamin D receptor and suppress parathyroid hormone-related peptide gene expression. *Mol Cell Endocrinol* **1997,** *127*, 99-108.
249. Meyaard, L. The inhibitory collagen receptor LAIR-1 (CD305). *J Leukoc Biol* **2008,** *83*, 799-803.
250. Zhu, J. G.; Ochalek, J. T.; Kaufmann, M.; Jones, G.; Deluca, H. F. CYP2R1 is a major, but not exclusive, contributor to 25-hydroxyvitamin D production in vivo. *Proc. Natl. Acad. Sci. U. S. A.* **2013,** *110*, 15650-15655.
251. Haussler, M. R.; Whitfield, G. K.; Haussler, C. A.; Hsieh, J. C.; Thompson, P. D.; Selznick, S. H.; Dominguez, C. E.; Jurutka, P. W. The nuclear vitamin D receptor:

biological and molecular regulatory properties revealed. *J. Bone Miner. Res.* **1998,** *13*, 325-349.
252. Tieu, E. W.; Tang, E. K.; Chen, J.; Li, W.; Nguyen, M. N.; Janjetovic, Z.; Slominski, A.; Tuckey, R. C. Rat CYP24A1 acts on 20-hydroxyvitamin D(3) producing hydroxylated products with increased biological activity. *Biochem. Pharmacol.* **2012,** *84*, 1696-1704.
253. Lin, Z.; Li, W. The roles of vitamin D and its analogs in inflammatory diseases. *Curr. Top. Med. Chem.* **2016,** *16*, 1-20.
254. Slominski, A.; Semak, I.; Zjawiony, J.; Wortsman, J.; Li, W.; Szczesniewski, A.; Tuckey, R. C. The cytochrome P450scc system opens an alternate pathway of vitamin D3 metabolism. *FEBS J.* **2005,** *272*, 4080-4090.
255. Tuckey, R. C.; Li, W.; Zjawiony, J. K.; Zmijewski, M. A.; Nguyen, M. N.; Sweatman, T.; Miller, D.; Slominski, A. Pathways and products for the metabolism of vitamin D3 by cytochrome P450scc. *FEBS J.* **2008,** *275*, 2585-2596.
256. Slominski, A. T.; Kim, T. K.; Shehabi, H. Z.; Semak, I.; Tang, E. K.; Nguyen, M. N.; Benson, H. A.; Korik, E.; Janjetovic, Z.; Chen, J.; Yates, C. R.; Postlethwaite, A.; Li, W.; Tuckey, R. C. In vivo evidence for a novel pathway of vitamin D(3) metabolism initiated by P450scc and modified by CYP27B1. *FASEB J.* **2012,** *26*, 3901-3915.
257. Slominski, A. T.; Li, W.; Kim, T. K.; Semak, I.; Wang, J.; Zjawiony, J. K.; Tuckey, R. C. Novel activities of CYP11A1 and their potential physiological significance. *J. Steroid Biochem. Mol. Biol.* **2015,** *151*, 25-37.
258. Slominski, A. T.; Kim, T. K.; Li, W.; Yi, A. K.; Postlethwaite, A.; Tuckey, R. C. The role of CYP11A1 in the production of vitamin D metabolites and their role in the regulation of epidermal functions. *J. Steroid Biochem. Mol. Biol.* **2014,** *144 Pt A*, 28-39.
259. Slominski, A. T.; Kim, T. K.; Li, W.; Postlethwaite, A.; Tieu, E. W.; Tang, E. K.; Tuckey, R. C. Detection of novel CYP11A1-derived secosteroids in the human epidermis and serum and pig adrenal gland. *Sci. Rep.* **2015,** *5*, 14875.
260. Slominski, A. T.; Kim, T. K.; Janjetovic, Z.; Tuckey, R. C.; Bieniek, R.; Yue, J.; Li, W.; Chen, J.; Nguyen, M. N.; Tang, E. K.; Miller, D.; Chen, T. C.; Holick, M. 20-Hydroxyvitamin D2 is a noncalcemic analog of vitamin D with potent antiproliferative and prodifferentiation activities in normal and malignant cells. *Am. J. Physiol. Cell Physiol.* **2011,** *300*, C526-541.
261. Kim, T. K.; Wang, J.; Janjetovic, Z.; Chen, J.; Tuckey, R. C.; Nguyen, M. N.; Tang, E. K.; Miller, D.; Li, W.; Slominski, A. T. Correlation between secosteroid-induced vitamin D receptor activity in melanoma cells and computer-modeled receptor binding strength. *Mol. Cell. Endocrinol.* **2012,** *361*, 143-152.
262. Tuckey, R. C.; Li, W.; Shehabi, H. Z.; Janjetovic, Z.; Nguyen, M. N.; Kim, T. K.; Chen, J.; Howell, D. E.; Benson, H. A. E.; Sweatman, T.; Baldisseri, D. M.; Slominski, A. Production of 22-hydroxy metabolites of vitamin D-3 by cytochrome P450scc (CYP11A1) and analysis of their biological activities on skin cells. *Drug Metab. Dispos.* **2011,** *39*, 1577-1588.
263. Slominski, A. T.; Janjetovic, Z.; Kim, T. K.; Wright, A. C.; Grese, L. N.; Riney, S. J.; Nguyen, M. N.; Tuckey, R. C. Novel vitamin D hydroxyderivatives inhibit

melanoma growth and show differential effects on normal melanocytes. *Anticancer Res.* **2012,** *32*, 3733-3742.
264. Janjetovic, Z.; Brozyna, A. A.; Tuckey, R. C.; Kim, T. K.; Nguyen, M. N.; Jozwicki, W.; Pfeffer, S. R.; Pfeffer, L. M.; Slominski, A. T. High basal NF-kappaB activity in nonpigmented melanoma cells is associated with an enhanced sensitivity to vitamin D3 derivatives. *Br. J. Cancer* **2011,** *105*, 1874-1884.
265. Janjetovic, Z.; Tuckey, R. C.; Nguyen, M. N.; Thorpe, E. M., Jr.; Slominski, A. T. 20,23-dihydroxyvitamin D3, novel P450scc product, stimulates differentiation and inhibits proliferation and NF-kappaB activity in human keratinocytes. *J. Cell. Physiol.* **2010,** *223*, 36-48.
266. Slominski, A.; Janjetovic, Z.; Tuckey, R. C.; Nguyen, M. N.; Bhattacharya, K. G.; Wang, J.; Li, W.; Jiao, Y.; Gu, W.; Brown, M.; Postlethwaite, A. E. 20S-hydroxyvitamin D3, noncalcemic product of CYP11A1 action on vitamin D3, exhibits potent antifibrogenic activity in vivo. *J. Clin. Endocrinol. Metab.* **2013,** *98*, E298-303.
267. Chen, J.; Wang, J.; Kim, T. K.; Tieu, E. W.; Tang, E. K.; Lin, Z.; Kovacic, D.; Miller, D. D.; Postlethwaite, A.; Tuckey, R. C.; Slominski, A. T.; Li, W. Novel vitamin D analogs as potential therapeutics: metabolism, toxicity profiling, and antiproliferative activity. *Anticancer Res.* **2014,** *34*, 2153-2163.
268. Lin, Z.; Marepally, S. R.; Ma, D.; Kim, T. K.; Oak, A. S.; Myers, L. K.; Tuckey, R. C.; Slominski, A. T.; Miller, D. D.; Li, W. Synthesis and Biological Evaluation of Vitamin D3 Metabolite 20S,23S-Dihydroxyvitamin D3 and Its 23R Epimer. *J Med Chem* **2016,** *59*, 5102-5108.
269. Lin, Z.; Marepally, S. R.; Ma, D.; Myers, L. K.; Postlethwaite, A. E.; Tuckey, R. C.; Cheng, C. Y.; Kim, T. K.; Yue, J.; Slominski, A. T.; Miller, D. D.; Li, W. Chemical synthesis and biological activities of 20S,24S/R-dihydroxyvitamin D3 epimers and their 1alpha-hydroxyl derivatives. *J. Med. Chem.* **2015,** *58*, 7881-7887.
270. Cheng, C. Y.; Slominski, A. T.; Tuckey, R. C. Metabolism of 20-hydroxyvitamin D3 by mouse liver microsomes. *J. Steroid Biochem. Mol. Biol.* **2014,** *144 Pt B*, 286-293.
271. Tang, E. K.; Chen, J.; Janjetovic, Z.; Tieu, E. W.; Slominski, A. T.; Li, W.; Tuckey, R. C. Hydroxylation of CYP11A1-derived products of vitamin D3 metabolism by human and mouse CYP27B1. *Drug Metab. Dispos.* **2013,** *41*, 1112-1124.
272. Xiao, M.; Wang, J.; Lin, Z.; Lu, Y.; Li, Z.; White, S. W.; Miller, D. D.; Li, W. Design, synthesis and structure-activity relationship studies of novel survivin inhibitors with potent anti-proliferative properties. *PLoS One* **2015,** *10*, e0129807.
273. Li, W.; Chen, J.; Janjetovic, Z.; Kim, T. K.; Sweatman, T.; Lu, Y.; Zjawiony, J.; Tuckey, R. C.; Miller, D.; Slominski, A. Chemical synthesis of 20S-hydroxyvitamin D3, which shows antiproliferative activity. *Steroids* **2010,** *75*, 926-935.
274. Lu, Y.; Chen, J.; Janjetovic, Z.; Michaels, P.; Tang, E. K.; Wang, J.; Tuckey, R. C.; Slominski, A. T.; Li, W.; Miller, D. D. Design, synthesis, and biological action of 20R-hydroxyvitamin D3. *J. Med. Chem.* **2012,** *55*, 3573-3577.

275. Tang, E. K.; Li, W.; Janjetovic, Z.; Nguyen, M. N.; Wang, Z.; Slominski, A.; Tuckey, R. C. Purified mouse CYP27B1 can hydroxylate 20,23-dihydroxyvitamin D3, producing 1alpha,20,23-trihydroxyvitamin D3, which has altered biological activity. *Drug Metab. Dispos.* **2010,** *38*, 1553-1559.
276. Lin, Z.; Yang, R.; Guan, Z.; Chen, A.; Li, W. Ultra-performance LC separation and quadrupole time-of-flight MS identification of major alkaloids in Plumula Nelumbinis. *Phytochem. Anal.* **2014,** *25*, 485-494.
277. Meyaard, L. The inhibitory collagen receptor LAIR-1 (CD305). *J. Leukoc. Biol.* **2008,** *83*, 799-803.
278. Lin, Z.; Marepally, S. R.; Kim, T. K.; Janjetovic, Z.; Oak, A. S.; Postlethwaite, A. E.; Myers, L. K.; Tuckey, R. C.; Slominski, A. T.; Miller, D. D.; Li, W. Design, Synthesis and Biological Activities of Novel Gemini 20S-Hydroxyvitamin D3 Analogs. *Anticancer Res* **2016,** *36*, 877-886.
279. Slominski, A. T.; Kim, T. K.; Janjetovic, Z.; Tuckey, R. C.; Bieniek, R.; Yue, J.; Li, W.; Chen, J.; Nguyen, M. N.; Tang, E. K.; Miller, D.; Chen, T. C.; Holick, M. 20-Hydroxyvitamin D2 is a noncalcemic analog of vitamin D with potent antiproliferative and prodifferentiation activities in normal and malignant cells. *Am J Physiol Cell Physiol* **2011,** *300*, C526-541.
280. Slominski, A. T.; Tuckey, R. C.; Zbytek, B.; Zmijewski, M. A.; Nguyen, M. N.; Janjetovic, Z.; Chen, J.; Li, W.; Miller, D. D.; Zjawiony, J. K. Enzymatic Production or Chemical Synthesis and Uses for 5,7-Dienes and UVB Conversion Products Thereof. In Google Patents: 2014.
281. Tang, E. K.; Voo, K. J.; Nguyen, M. N.; Tuckey, R. C. Metabolism of substrates incorporated into phospholipid vesicles by mouse 25-hydroxyvitamin D3 1alpha-hydroxylase (CYP27B1). *J Steroid Biochem Mol Biol* **2010,** *119*, 171-179.
282. Tuckey, R. C.; Li, W.; Shehabi, H. Z.; Janjetovic, Z.; Nguyen, M. N.; Kim, T. K.; Chen, J.; Howell, D. E.; Benson, H. A.; Sweatman, T.; Baldisseri, D. M.; Slominski, A. Production of 22-hydroxy metabolites of vitamin d3 by cytochrome p450scc (CYP11A1) and analysis of their biological activities on skin cells. *Drug Metab Dispos* **2011,** *39*, 1577-1588.
283. Chandrasekhar, S.; Rao, C. L.; Reddy, M. S.; Sharma, G. D.; Kiran, M. U.; Naresh, P.; Chaitanya, G. K.; Bhanuprakash, K.; Jagadeesh, B. Beta-sugar aminoxy peptides as rigid secondary structural scaffolds. *J Org Chem* **2008,** *73*, 9443-9446.
284. Tieu, E. W.; Tang, E. K.; Tuckey, R. C. Kinetic analysis of human CYP24A1 metabolism of vitamin D via the C24-oxidation pathway. *FEBS J* **2014,** *281*, 3280-3296.
285. Christakos, S.; Dhawan, P.; Verstuyf, A.; Verlinden, L.; Carmeliet, G. Vitamin D: Metabolism, Molecular Mechanism of Action, and Pleiotropic Effects. *Physiol Rev* **2016,** *96*, 365-408.
286. Frisch, M.; Trucks, G.; Schlegel, H.; Scuseria, G.; Robb, M.; Cheeseman, J.; Scalmani, G.; Barone, V.; Mennucci, B.; Petersson, G. Gaussian 09. Wallingford, CT, USA: Gaussian. In Inc: 2009.
287. Becke, A. D. Density‐functional thermochemistry. III. The role of exact exchange. *The Journal of chemical physics* **1993,** *98*, 5648-5652.

288. Lee, C.; Yang, W.; Parr, R. G. Development of the Colle-Salvetti correlation-energy formula into a functional of the electron density. *Physical review B* **1988,** *37*, 785.
289. Legault, C. CYLview, 1.0 b. *Université de Sherbrooke* **2009**.
290. Huet, T.; Maehr, H.; Lee, H. J.; Uskokovic, M. R.; Suh, N.; Moras, D.; Rochel, N. Structure–function study of gemini derivatives with two different side chains at C-20, Gemini-0072 and Gemini-0097. *MedChemComm* **2011,** *2*, 424-429.
291. Otwinowski, Z.; Minor, W. Processing of X-ray diffraction data collected in oscillation mode. *Methods in enzymology* **1997,** *276*, 307-326.
292. Bricogne, G.; Blanc, E.; Brandl, M.; Flensburg, C.; Keller, P.; Paciorek, W.; Roversi, P.; Sharff, A.; Smart, O.; Vonrhein, C. BUSTER version 2.11. 2. *Cambridge, United Kingdom: Global Phasing Ltd* **2011**.
293. Adams, P. D.; Afonine, P. V.; Bunkóczi, G.; Chen, V. B.; Davis, I. W.; Echols, N.; Headd, J. J.; Hung, L.-W.; Kapral, G. J.; Grosse-Kunstleve, R. W. PHENIX: a comprehensive Python-based system for macromolecular structure solution. *Acta Crystallographica Section D: Biological Crystallography* **2010,** *66*, 213-221.
294. Emsley, P.; Cowtan, K. Coot: model-building tools for molecular graphics. *Acta Crystallographica Section D: Biological Crystallography* **2004,** *60*, 2126-2132.
295. Slominski, A.; Zbytek, B.; Slominski, R. Inhibitors of melanogenesis increase toxicity of cyclophosphamide and lymphocytes against melanoma cells. *International journal of cancer* **2009,** *124*, 1470-1477.
296. Slominski, A. T.; Kim, T.-K.; Janjetovic, Z.; Tuckey, R. C.; Bieniek, R.; Yue, J.; Li, W.; Chen, J.; Nguyen, M. N.; Tang, E. K. 20-Hydroxyvitamin D2 is a noncalcemic analog of vitamin D with potent antiproliferative and prodifferentiation activities in normal and malignant cells. In Am Physiological Soc: 2011.
297. Kim, T.-K.; Wang, J.; Janjetovic, Z.; Chen, J.; Tuckey, R. C.; Nguyen, M. N.; Tang, E. K.; Miller, D.; Li, W.; Slominski, A. T. Correlation between secosteroid-induced vitamin D receptor activity in melanoma cells and computer-modeled receptor binding strength. *Molecular and cellular endocrinology* **2012,** *361*, 143-152.
298. Yin, Y. Z.; Liu, C.; Tang, L. Q.; Liu, Z. P. Recoverable Pd/C catalyst mediated dehydrogenation of sterols and an improved synthesis of 1alpha-hydroxydehydroepiandrosterone. *Steroids* **2012,** *77*, 1419-1422.
299. Poza, J.; Rega, M.; Paz, V.; Alonso, B.; Rodriguez, J.; Salvador, N.; Fernandez, A.; Jimenez, C. Synthesis and evaluation of new 6-hydroximinosteroid analogs as cytotoxic agents. *Bioorg Med Chem* **2007,** *15*, 4722-4740.
300. Mouriño, A. An improved synthesis of 1α, 3β-dihydroxycholesta-5, 7-diene. *Synth Commun* **1978,** *8*, 117-125.
301. Otero, R.; Seoane, S.; Sigüeiro, R.; Belorusova, A. Y.; Maestro, M. A.; Pérez-Fernández, R.; Rochel, N.; Mouriño, A. Carborane-based design of a potent vitamin D receptor agonist. *Chemical Science* **2016,** *7*, 1033-1037.
302. Clapham, D. E.; Julius, D.; Montell, C.; Schultz, G. International Union of Pharmacology. XLIX. Nomenclature and structure-function relationships of transient receptor potential channels. *Pharmacol Rev* **2005,** *57*, 427-450.

303. Holick, M. F. Resurrection of vitamin D deficiency and rickets. *J Clin Invest* **2006,** *116*, 2062-2072.

VITA

Zongtao Lin was born in Henan Province, China, in 1987. He received his B.S. degree in Pharmacy in 2009 at Zhengzhou University, and M.S. degree in Pharmacognosy in 2012 at Peking University. Then he joined Dr. Wei Li's group in the Department of Pharmaceutical Sciences at the University of Tennessee Health Science Center in 2012, expects to oomplete his Ph.D. degree with a concentration of Medicinal Chemistry in 2017.